ELUCIDATING FACTORS THAT IMPACT THE REMOVAL OF ORGANIC MICROCONSTITUENTS BY AMMONIA OXIDIZING AND HETEROTROPHIC BACTERIA

Wendell O'Neil Khunjar

Dissertation submitted to the faculty of the Virginia Polytechnic Institute and State University in partial fulfillment of the requirements for the degree of

Doctor of Philosophy
In
Civil Engineering

Nancy G. Love, Chair
Diana S. Aga
Willie F. Harper Jr.
John C. Little
Ann M. Stevens
Peter J. Vikesland

December 17, 2009

Blacksburg, VA

Keywords: Carbamazepine, Iopromide, 17α-ethinylestradiol, Trimethoprim, Sorption, Exopolymeric Substances, *Nitrosomonas europaea*, Trace organic contaminants.

ELUCIDATING FACTORS THAT IMPACT THE REMOVAL OF ORGANIC MICROCONSTITUENTS BY AMMONIA OXIDIZING AND HETEROTROPHIC BACTERIA

Wendell O'Neil Khunjar

ABSTRACT

Although wastewater treatment plants are a line of defense in minimizing indiscriminate output of microconstituents to natural waters, we do not possess a fundamental understanding of the mechanisms involved in microconstituent removal during wastewater treatment. With this in mind, experiments were designed to investigate the factors that can influence the fate of four microconstituents, carbamazepine (CBZ), 17α-ethinylestradiol (EE2), iopromide (IOP), and trimethoprim (TMP), during biological suspended culture treatment. Specifically, the role that various ecological members of biological treatment systems play in biotransforming these compounds was evaluated.

Sorption assays were performed with inactivated biomass samples (ammonia oxidizing bacteria (AOB), laboratory enriched heterotrophic cultures free of active nitrifiers with low (Ox^-) or high (Ox^+) oxygenase activity, and a nitrifying activated sludge (NAS) from a full-scale wastewater treatment plant) to determine whether partitioning dictates removal of individual microconstituents. No microconstituents sorbed to the AOB culture. Neither CBZ nor IOP sorbed to Ox^-, Ox^+ and NAS cultures; however, EE2 and TMP sorbed to the Ox^-, Ox^+ and NAS biomass. Sorption was positively influenced by the presence of exopolymeric substances (EPS) associated with the cultures. The protein content of EPS affected EE2 and TMP sorption more appreciably than the polysaccharide content of EPS.

Further experiments were performed to investigate microconstituent biodegradation by AOBs, Ox^- and Ox^+ cultures. The influence of growth state and oxygenase activity on biotransformation by each culture was also evaluated. Results indicate that EE2 was the only microconstituent that was amenable to biotransformation by batch cultured AOB and heterotrophic cultures. EE2 was biotransformed but not mineralized by AOB chemostat and batch cultures. TMP was not transformed by AOB batch or chemostat cultures; however both EE2 and TMP were transformed by Ox^- and Ox^+ chemostat cultures. Radiolabeled studies showed that EE2 was mineralized by this culture. Kinetically, AOBs dominated EE2 transformation to monohydroxylated metabolites; however, both Ox^- and Ox^+ cultures further degraded and mineralized EE2 and metabolites generated by AOBs. These results indicate that biotransformation of EE2 by NAS may be limited by heterotrophic activity whereas TMP fate may be a function of heterotrophic activity only. Oxygenase activity did not limit EE2 or TMP biotransformation in chemostat cultures.

Subsequent experiments that were performed to identify the factors that influence heterotrophic degradation of EE2 and TMP indicated that the presence of readily biodegradable substrates slows EE2 and TMP biotransformation. The impact of slowly biodegradable substrates like EPS on EE2 and TMP degradation was unclear. These results suggest that EE2 and TMP are most amenable to biodegradation in bioreactors where endogenous conditions dominate.

ACKNOWLEDGEMENTS

There are many people who have crossed paths with me and influenced my decisions over the last 27 years. While I can try to voice my appreciation, there are no words that can adequately capture the essence of this support. Nevertheless, I will endeavor to do so.

I would like to acknowledge my funding sources, Charles E. Via Jr. Department of Civil and Environmental Engineering MS and PhD Fellowships, US. Department of Education GAANN Fellowship and the National Science Foundation, Grant No. 0504477. Without these financial contributions, my graduate work would not have been possible.

I would also like to thank my PhD committee for all the support and kind words that have helped keep me on track over the past 5 years. Scheduling meetings across seven of a busiest people in the world was always a challenge but I have definitely benefitted from your contributions to my professional development. You have treated me not as a student, but as an equal and for that, I am greatly appreciative.

Drs. Aga and Harper - I have thoroughly enjoyed our collaboration. You have shown me what true mutual respect involves and have allowed me freedom to develop my ideas into this dissertation. There must have been times where you were tired seeing emails from me beginning with "I apologize…" but you stuck with me and for that, I am grateful.

Dr. Little - I thank you for your patience, piercing questions and most importantly, your humorous interjections during committee meetings.

Dr. Stevens - I also thank you for your patience and support. As my project morphed into a different monster, we did not end up working as closely as I had anticipated. Nevertheless, you provided words of wisdom and beneficial insight when needed.

Dr. Vikesland - I thank you for helping develop my own pedagogical style over the past few years. Our conversations, especially during the latter part of my tenure at VT, have reinforced my desire to continue along the path that circumstance has chosen for me.

Dr. Love – Thank you for everything. Your support over the last 5 years has been invaluable. I have learned a tremendous amount from you and am deeply grateful for having the opportunity to be your student and colleague.

My time at VT would not have been the same without the fellowship of past and present Love Research Group members, Rick Kelly, Joy Muller, Kartik Chandran, Paul Sweetman, Mert Muftugil, KaMan Chan, Anna Zaklikowski, Kaoru Ikuma, Shoko Miwa, Phil Saunders, Kevin Gilmore, Ameet Pinto, Jeremy 'Jerry/Jason' Guest, Jason 'Jeremy' Beck, Komgrit 'K2' Kotcharaksa, Sam Hardin and Lindsay Tayloe. I also want to acknowledge fellow Sludge Puppies, Chris Muller, Lauren Zuransky, Chris 'C-dub' Wilson, Archibald 'Fuzzy B' Wilson, Krista Rule, Lashun King, Rob Rebodos, Heather Rectanus, Chris Strock for helping to make life outside of lab as enjoyable as it was inside.

Dr. Henriques - I thank you for your kind words and support that you provided as Ines, senior PhD candidate and subsequently as Dr. Henriques. Our conversations in the breakroom and via skype helped me limp along to the finish line. Hopefully, you finally received your picture frame in the mail.

I also need to thank the Aga research group at SUNY Buffalo. Tony, Dawn, Susie, Jola – Without your expertise, this work would not have been possible. Hopefully, our collaborations can continue as we move on to different phases in life.

Jody and Julie - A thousand thanks for all your help. I could go on and on but I hope you understand that I would not be writing this without your help.

Betty and Beth - I can safely say that without your help pushing through my late paperwork, I would not be here today. Thank you!

EHSS (Doug, Joey and Kenny) – Your help (radioactive protocols/pickups, dry ice shipments) is greatly appreciated.

I would like to thank Drs. David L. Kirchman and Hila Elifantz (Graduate Student at time of collaboration) from the University of Delaware, Marine Biosciences division for introducing me to the marvelous world of microautoradiography.

Drs. Glass and Jones – I am glad to have worked with you at Howard. Without your guidance and encouragement during undergrad, I don't think I would have been as prepared as I was for graduate school. Thank you!

Family – What can I say? Thanks for the love, the patience, the understanding, the visits, the phone calls, the patience, the food, the support, the encouragement, the patience. I love you all and dedicate this to you.

Jen – Thank you. I am grateful that you came into my life when you did. You helped me to keep going during the difficult phases of this process and always helped to define a new perspective on what is truly important in life. You are my best friend and I love you.

ATTRIBUTION

Christine Klein, *PhD*, Former Graduate Research Assistant, Department of Chemistry, University at Buffalo, State University of New York, Buffalo, NY, 14260.

Jolanta Skotnicka-Pitak, *MS*, Former Graduate Research Assistant, Department of Chemistry, University at Buffalo, State University of New York, Buffalo, NY, 14260.

Mary Celiz Dawn, *MS*, Current Graduate Research Assistant, Department of Chemistry, University at Buffalo, State University of New York, Buffalo, NY, 14260.

Seuyung Baik, *MS*, Current Graduate Research Assistant, Department of Chemistry, University at Buffalo, State University of New York, Buffalo, NY, 14260.

Susie Mackintosh, *MS*, Current Graduate Research Assistant, Department of Chemistry, University at Buffalo, State University of New York, Buffalo, NY, 14260.

Dr. Diana S. Aga, *PhD*., Associate Professor, Department of Chemistry, University at Buffalo, State University of New York, Buffalo, NY, 14260.

Dr. Willie F. Harper Jr., *PhD*, Associate Professor, Department of Civil and Environmental Engineering, University of Pittsburgh, Pittsburgh, PA, 15260.

Ms. Klein, Ms. Skotnicka-Pitak, Ms. Celiz, Ms. Mackintosh and Mr. Baik are credited with performing LC-MS (MS), NMR and X-ray crystallography analyses on samples derived from experiments outlined in **Chapter 3** of this work. Future publications based on material from this dissertation will reflect individual contribution.

Drs. Love, Aga and Harper served as Co-Principal Investigators for the research described throughout this dissertation as funded by the National Science Foundation, Grant No. 0504477.

TABLE OF CONTENTS

LIST OF FIGURES

LIST OF TABLES

LIST OF ABBREVIATIONS

AOB	Ammonia Oxidizing Bacteria
AOP	Advanced Oxidation Process
AMO	Ammonia Monooxygenase
ARISA	Automated Approach for Ribosomal Intergenic Spacer Analyses
AS	Activated Sludge
ATU	Allythiourea
BAP	Biomass-Associated Products
Bardenpho	**Bar**nard **Den**itrification **Pho**sphorous
BOD	Biochemical Oxygen Demand
BNR	Biological Nutrient Removal
C12O	Catechol 1,2 Dioxygenase
C23O	Catechol 2,3 Dioxygenase
CAS	Conventional Activated Sludge
CBZ	Carbamazepine
CER	Cation Exchange Resin
Chemostat	**Chem**ical Environment Is **Stat**ic
CMAS	Completely Mixed Activated Sludge
CMP	Chloramphenicol
COD	Chemical Oxygen Demand
CSTR	Continuous Stirred Tank Reactor
C_W	Concentration of Microconstituent in Aqueous Phase
C_S	Concentration of Microconstituent in Solid Phase
DAPI	4',6-Diamidino-2-phenylindole
DGGE	Denaturing Gradient Gel Electrophoresis
DNA	Deoxyribonucleic Acid
DWTP	Drinking Water Treatment Plant
EAAS	Extended Aeration Activated Sludge
E1	Estrone
E2	17β-estradiol
EE2	17α-ethinylestradiol
DO	Dissolved Oxygen
EPS	Extracellular Polymeric Substances
ESI	Electrospray Ionization
ESI-TOF-MS	Electrospray Ionization – Time of Flight – Mass Spectrometry
FISH	Fluorescence In-Situ Hybridization
FISH-MAR	Fluorescence In-Situ Hybridization- Microautoradiography
f_{OM}	Organic matter fraction
GC	Gas Chromatography
GC-MS	Gas Chromatography – Mass Spectrometry
HPLC	High Performance Liquid Chromatography
HRT	Hydraulic Retention Time
IOP	Iopromide

K_D	Solid/Water Partition Coefficient
K_F	Freundlich Coefficient
K_H	Henry's constant
K_{OM}	Organic Matter Sorption Coefficient
K_{OW}	Octanol/Water Partition Coefficient
K_S	Half Saturation/Affinity Contstant
LC	Liquid Chromatography
LC-ESI-MS	Liquid Chromatography – Electrospray Ionization – Mass Spectrometry
LC-MS	Liquid Chromatography – Mass Spectrometry
***m/z* ratio**	Mass to Charge Ratio
MLE	Modified Ludzack-Ettinger
MLSS	Mixed Liquor Suspended Solids
MLVSS	Mixed Liquor Volatile Suspended Solids
MS	Mass Spectrometry
MW	Molecular Weight
n	Dimensionless Freundlich coefficient
NAD(P)H	Nicotinamide Adenine Dinucleotide (Phosphate)
NAS	Nitrifying Activated Sludge
NEM	N-Ethyl-Maleimide
NGR	Nitrite Generation Rate
NMR	Nuclear Magnetic Resonance
OLR	Organic Loading Rate
OUR	Oxygen Uptake Rate
Ox^-	Lab-scale Heterotrophic Culture with Minimal Oxygenase Activity
Ox^+	Lab-scale Heterotrophic Culture with High Oxygenase Activity
PPCP	Pharmaceutical and Personal Care Products
PSD	Particle Size Distribution
rbCOD	Readily Biodegradable Substrate
RNA	Ribonucleic Acid
SBR	Sequencing Batch Reactor
SIP	Stable Isotope Probing
SOC	Synthetic Organic Carbon
sOUR	Specific Oxygen Uptake Rate
sNGR	Specific Nitrite Generation Rate
SMP	Soluble Microbial Products
SRT	Solids Retention Time
TGGE	Temperature Gradient Gel Electrophoresis
TMP	Trimethoprim
Tod	Toluene Dioxygenase
TrOC	Trace Organic Compounds
T-RFLP	Terminal restriction length polymorphism
TSS	Total Suspended Solids
UAP	Utilization-Associated Products
VSS	Volatile Suspended Solids
WWTP	Wastewater Treatment Plant
YES	Yeast Estrogen Screen

CHAPTER 1 - EXECUTIVE SUMMARY

1.1 Introduction

Contamination of water systems with industrial and anthropogenic compounds is a worldwide phenomenon that contributes to a lack of basic access to potable water and sanitary conditions by over one fifth of the world's population [1]. Traditionally, studies on rehabilitation of polluted environments have focused on priority contaminants resulting in the promulgation of regulations mandating maximum acceptable contaminant levels [2]. Little emphasis has been placed on determining the fate of microconstituents within the environment despite decades of use. Recent surveys of aquatic environments have yielded extensive data characterizing incidence and to a lesser extent, the ecological impact of microconstituents [1, 3-7]. These compounds have been identified at ng/L to μg/L levels [6-9] in natural water bodies as well as wastewater treatment plants (WWTPs). Detrimental effects on aquatic life like feminization of water body fauna [10-12] and increased selectivity for antibiotic resistant bacterial strains [13, 14] have been linked to the presence and recalcitrance of estrogens such as 17α-ethinylestradiol (EE2) and antibiotics like trimethoprim (TMP) respectively. Conflicting reports regarding the ecotoxicological effects of carbamazepine (CBZ) on aquatic microfauna exist [15, 16] while it is generally accepted that iopromide (IOP) poses no negative influence on aquatic life [17, 18]. The anthropogenic nature of these microconstituents dictates that our industry develop a coherent framework that describes fate in water and wastewater treatment systems with a view to achieving total elimination of microconstituents from aquatic environments.

WWTPs can be considered as the last line of defense in minimizing indiscriminate output of point source contaminants to the natural water cycle. A fundamental understanding of the mechanisms involved in microconstituent removal during wastewater treatment is needed to optimize processes designed to achieve elimination of these compounds. Similar to other synthetic organic compounds (SOCs), microconstituents are removed via several mechanisms including volatilization, abiotic transformations, biotransformation and sorption to solids [4, 19]. For the purposes of this work, volatilization is defined as the mass transfer of a liquid phase constituent to the gas phase [20]; abiotic transformation is used to define all chemical and

photochemical reactions that are not catalyzed by microorganisms [21]; sorption is used to describe the combination of adsorption and absorption [21]; and biotransformation defines the conversion of parent organic microconstituent to less complex intermediates by microorganisms. If further biodegradation of these microconstituents and intermediates yields carbon dioxide, this process is referred to as mineralization. The physical nature and chemical structure of each compound (**Outlined in Table 2.1**) will influence the primary mechanisms of removal. Correspondingly, care must be taken when extrapolating findings across multiple classes of compounds [1].

It needs to be acknowledged that we do not possess a comprehensive and fundamental knowledge of factors that drive removal of microconstituents in WWTPs. To develop best management practices that address microconstituent removal, current and future studies need to move past blackbox surveys of treatment facilities. These studies need to address the microbiological and molecular basis of microconstituent removal. This study was performed with this rationale in mind. The influence of microbial ecology and microbial physiology of organisms found in nitrifying activated sludge (NAS) on microconstituent biodegradation was addressed.

1.2 Investigating the Partitioning Behavior of Carbamazepine, 17α-ethinylestradiol, Iopromide and Trimethoprim in the presence of Ammonia Oxidizing and Heterotrophic Cultures

In this (**Section 4.1**), experiments were designed to investigate sorption of four model microconstituents, carbamazepine (CBZ), 17α-ethinylestradiol (EE2), iopromide (IOP) and trimethoprim (TMP) to biomass used in biotransformation experiments. Sorption assays were performed with a pure culture of ammonia oxidizing bacteria (AOB), laboratory enriched heterotrophic cultures with no nitrifying activity and low (Ox^-) or high (Ox^+) oxygenase activity and a NAS from a full-scale domestic wastewater treatment plant. Each culture was inactivated with an optimized concentration of sodium azide, a potent inhibitor of terminal oxidases, and supplemented with radiolabeled and non-radiolabeled compounds. Mass balances on aqueous phase concentrations were performed to determine the mass of microconstituents sorbed to biomass.

No microconstituent sorbed to the AOB culture. Only EE2 and TMP sorbed to the Ox^-, Ox^+ and NAS biomass. There was no clear correlation between the octanol/water coefficients (K_{OW}) and microconstituent sorption (**Table 1.1**). It was hypothesized that sorption of EE2 and TMP was influenced by the exopolymeric substance (EPS) content of each culture. Subsequent experiments were performed to evaluate the relative importance of EPS in enabling sorption of EE2 and TMP. Biomass devoid of cation-linked EPS was used as sorbent and results were compared to sorption by undisrupted biomass. Sorption of EE2 and TMP was greatly reduced in the absence of EPS. Additionally, EE2 sorption to various types of biomass lacking cation-linked EPS was homogenous whereas TMP sorption was variable. These results clearly indicate that EE2 and TMP sorption are affected by the presence of EPS, although in different manners.

Table 1.1. Summary of sorption results for biomass cultures with EPS.

	AOB	**Ox^-**	**Ox^+**	**NAS**
CBZ (log K_{OW} = 2.45)	No	No	No	No
EE2 (log K_{OW} = 3.90)	No	Yes	Yes	Yes
IOP (log K_{OW} = -2.33)	No	No	No	No
TMP (log K_{OW} = 0.91)	N/P	Yes	Yes	Yes

N/P – sorption assays were not performed with AOB and TMP.

Attempts to correlate sorption of EE2 and TMP with the protein and polysaccharide content of biomass EPS yielded mildly positive relationships. Furthermore, data show that sorption of microconstituents is a function of the organic matter fraction of mixed liquor and the physical-chemical characteristics of the microconstituent. CBZ and IOP did not sorb to any of the biomass types while EE2 and TMP bound to EPS containing Ox^-, Ox^+ and NAS biomass. To account for these losses, sorption controls were included during all biotransformation experiments.

1.3 Elucidating the Role of Ammonia Oxidizing Bacteria versus Heterotrophic Bacteria during the Biotransformation of Microconstituents

The specific objective during this phase of the study (**Section 4.2**) was to investigate the impact that the two primary ecological groups (AOBs and heterotrophs) in nitrifying activated sludge can have on microconstituent biodegradation. Experiments were performed with batch and continuous flow AOB, Ox^- and Ox^+ cultures. These experiments were designed to facilitate

further understanding of the individual impact that each of these cultures has on microconstituent fate.

CBZ, IOP and TMP were not transformed by batch cultured AOBs. Neither CBZ nor TMP were transformed by Ox^- and Ox^+ batch cultures. EE2 was transformed by Ox^+ batch cultures only but Ox^- cultures may have started to show biodegradation as the primary substrate was consumed. Collectively, these results suggested that EE2 was the only microconstituent under consideration that was amenable to biotransformation by batch cultured cells.

Further studies with chemostat cultures indicated that EE2 was biotransformed but not mineralized by AOBs. TMP was not transformed by AOB continuous flow cultures; however both EE2 and TMP were transformed by Ox^- and Ox^+ chemostat cultures. Changes in oxygenase activity did not affect the extent or rate of EE2 or TMP degradation. These results showed that batch and chemostat growth conditions produced different biodegradation responses for EE2 and TMP for heterotrophic cultures. AOBs were kinetically superior in EE2 biotransformation compared to Ox^- and Ox^+ cultures; furthermore, mineralization of EE2 and its AOB-derived metabolites is performed by heterotrophs. Therefore, it is concluded that while EE2 is capable of being biotransformed by both AOBs and heterotrophs, its heterotrophic biodegradation is slower than AOB transformation. In contrast to EE2, TMP was only biotransformed by heterotrophic bacteria. Translated to activated sludge, these results suggest that heterotrophic bacteria play an important role in the transformation of EE2, TMP and possibly other microconstituents. Furthermore, activated sludge AOBs may initially biotransform EE2 into byproducts that can be used by heterotrophs. Specifically, the data presented here definitely show that AOBs are capable of biotransforming EE2 and have the potential to play a significant role in EE2 fate in partnership with heterotrophic bacteria in activated sludge communities; however, the definitive experiment showing their role in situ has not yet been done by us or others.

Table 1.2. Summary of results from biotransformation experiments.

	CBZ	EE2	IOP	TMP
	AOBs (Monooxygenase)			
Batch	No	Yes	No	No
Chemostat	N/P	Yes	N/P	No
	Ox^- (Minimal oxygenases)			
Batch	No	No	N/P	No
Chemostat	N/P	Yes	N/P	Yes
	Ox^+ (High mono/di-oxygenases)			
Batch	No	Yes	N/P	No
Chemostat	N/P	Yes	N/P	Yes

N/P – experiments were not performed.

1.4 Investigating the Role of Readily Biodegradable Substrates and Physiological State in Biotransforming 17α-Ethinylestradiol and Trimethoprim

Since the mineralization of EE2 and possibly TMP was shown to be primarily dependent on heterotrophs, attempts were made to elucidate factors that can influence heterotrophic degradation of EE2 and TMP in NAS (**Section 4.3**). These experiments were performed with Ox^- chemostat cultures and were designed to study the effect that readily biodegradable substrates and EPS have on EE2 and TMP degradation.

The results showed that the short-term presence of readily biodegradable carbon slowed EE2 and TMP removal. It was postulated that the slowdown in metabolism was a manifestation of physiological adaptation to the exogenously added readily biodegradable carbon source. Experiments also confirmed that EE2 could be metabolized as a growth substrate in the absence of readily biodegradable organic carbon. These results are significant as they suggest that microconstituents like EE2 and TMP are amenable to degradation in bioreactors where endogenous conditions dominate.

A simple conceptual model describing microconstituent degradation by heterotrophs was developed. Simulations from this model matched experimental data well and suggest that EE2 and TMP fate in heterotrophic chemostats was most sensitive to pseudo-first order reaction rate constants. Surprisingly, sorption did not have a substantial effect on EE2 and TMP removal from bioreactors. This was a manifestation of the low biomass and EPS content of the heterotrophic

cultures used in this study, and sorption would be more likely to have a significant impact for EE2 and TMP in a full-scale NAS.

1.5 Summary and Concluding Remarks

Microconstituent fate in NAS can be affected by sorption and biotransformation; however the relative contribution of either phenomenon on overall fate varies by compound. CBZ did not sorb and was highly recalcitrant to biotransformation. As a result, advanced oxidation processes are likely to be suitable for partial treatment of this compound. IOP is also resistant to sorption and is not transformed by AOBs under batch conditions. Further experiments with IOP and heterotrophic cultures were not performed due to time and resource constraints. EE2 and TMP both sorbed to biomass. This sorption appears to be correlated with the EPS content of the culture. EE2 was also biotransformed by AOBs and heterotrophs, but its ultimate fate in NAS will probably be limited by heterotrophic activity based on the results from this study. TMP was not biotransformed by AOBs; instead TMP degradation was driven by heterotrophic activity.

Results from this study confirm that biotransformation of certain microconstituents is feasible; however, we still lack a fundamental understanding of reaction cascades that are involved. This work shows that heterotrophic organisms can play an important yet underappreciated role in the biodegradation of these microconstituents. Further work is needed to elucidate these degradation pathways, particularly since most transformation products are yet to be identified. Future work should also focus on strategies that allow efficient coupling of nutrient removal and microconstituent degradation processes.

1.6 References

1. Schwarzenbach, R. P., Escher, B.I., Fenner, K., Hofstetter, T.B., Johnson, C.A.,von Gunten, U., Wehrli, B., The Challenge of Micropollutants in Aquatic Systems. *Science* **2006,** *313*, 1072-1077.
2. Agency, E. P., National Primary Drinking Water Regulations. In Vol. 40 CFR part 141
3. Daughton, C. G. In *Non-Regulated Contaminants: Emerging Research - Existing and Future Pollutants in Water Supplies, Old Pollutants, New Concerns, New Pollutants,Unknown issues*, Roundtable on Environmental Health Sciences, Research and Medicine, Washington D.C., 2003; National Acadamies, Institute of Medicine: Washington D.C., 2003.
4. Joss, A., Zabczynski, Z., Gobel, A., Hoffmann, B., Loffler, D., McArdell, C.S., Ternes, T.A., Thomsen, A., Siegrist H., Biological Degradation of Pharmaceuticals in Municipal

Wastewater Treatment: Proposing a Classification Scheme. *Water Research* **2006,** *40*, 1686-1696.
5. Loffler, D., Rombke, J., Meller, M., Ternes, T.A., Environmental Fate of Pharmaceuticals in Water/Sediment Systems. *Environmental Science Technology* **2005,** *39*, 5209-5218.
6. Ternes, T. A., P. Keckel, Mueller, J. Behaviour and Occurrence of Estrogens in Municipal Sewage Treatment Plants. 1. Investigations in Germany, Canada and Brazil. *Science Total Environment* **1999,** *225*, 91-99.
7. Ternes, T. A., P. Keckel, Mueller, J., Behaviour and Occurrence of Estrogens in Municipal Sewage Treatment Plants. II. Aerobic Batch Experiments With Activated Sludge. *Science Total Environment* **1999,** *225*.
8. Gobel, A., Thomsen, A., McArdell, C.S., Joss, A., Giger, W. , Occurrence and Sorption Behavior of Sulfonamides, Macrolides, and Trimethoprim in Activated Sludge Treatment *Environmental Science and Technology* **2005,** *39*, (11), 3981 -3989.
9. Kolpin, D. W., Furlong, E.T., Meyer, M.T., Thurman, E.M., Zaugg, S.D., Barber, L.B., Buxton, H.T., Pharmaceuticals, Hormones, and Other Organic Wastewater Contaminants in U.S. Streams, 1999-2000: A National Reconnaissance. *Environmental Science Technology* **2000,** *36*, 1202-1211.
10. Irwin, L. K., Gray, S., Oberdorster, E., Vitellogenin Induction in Painted Turtle, *Chrysemys picta*, as a Biomarker of Exposure to Environmental Levels of Estradiol. *Aquatic Toxicology* **2001,** *55*, (49-60).
11. Khanal, S. K., Xie, B., Thompson, M. L., Sung, S., Ong, S.K., Van Leeuwen, J. H., Fate, Transport, and Biodegradation of Natural Estrogens in the Environment and Engineered Systems. *Environmental Science and Technology* **2006,** *40*, (21), 6537-6546.
12. Lavado, R., Thibaut, R., Raldua, D., Martın, R., Porte, C., First Evidence of Endocrine Disruption in Feral Carp from the Ebro River. *Toxicology and Applied Pharmacology* **2004,** *196*, 247-257.
13. Ohlsen, K., Ternes, T., Werner, G., Wallner, U., Loffler, D., Ziebuhr, W., Witte, W., Hacker, J., Impact of Antibiotics on Conjugational Resistance Gene Transfer in *Staphylococcus aureus* in Sewage. *Environmental Microbiology* **2003,** *5*, 711-716.
14. Levy, S. B. In *Antibiotic Resistance: an Ecological Imbalance.*, Antibiotic Resistance: Origins, Evolution, Selection and Spread., West Sussex, England,, 1997; Chadwick, D. J., Goode, J., Ed. Wiley.: West Sussex, England,, 1997; pp 1-14.
15. Jos, A.; Repetto, G.; Rios, J. C.; Hazen, M. J.; Molero, M. L.; Peso, A. d.; Salguero, M.; Fernández-Freire, P.; Pérez-Martín, J. M.; Cameán, A., Ecotoxicological Evaluation of Carbamazepine using Six Different Model Systems with Eighteen Endpoints. *Toxicology in Vitro* **2003,** *17*, (5-6), 525-532.
16. Kim, Y.; Choi, K.; Jung, J.; Park, S.; Kim, P.-G.; Park, J., Aquatic Toxicity of Acetaminophen, Carbamazepine, Cimetidine, Diltiazem and Six Major Sulfonamides, and their Potential Ecological Risks in Korea. *Environmental International* **2007,** *33*, (3), 37-375.
17. Hartmann, T. S., Lange, R., Schweinfurth, H., Environmental Risk Assessment for the Widely Used Iodinated X-Ray Contrast Agent Iopromide (Ultravist). *Ecotoxicology and Environmental Safety* **1999,** *42*, 274-281.
18. Steger-Hartmann, T., Lange, R., Schweinfurth,H., Tschampel, M., Rehman, I., Investigations into the Environmental Fate and Effects of Iopromide (Ultravist),a Widely Used Iodinated X-ray Contrast Medium. *Water Research* **2002,** *36*, 266-274.

19. Andersen, H. R., Hansen, M., Kjolholt, J., Stuer-Lauridsen, F., Ternes, T.A., Halling-Sorensen, B., Assessment of the Importance of Sorption for Steroid Estrogens Removal During Activated Sludge Treatment. *Chemosphere* **2005,** *61*, 139-146.
20. Grady Jr., C. P. L., Daigger, G.T., and Lim, H.C., *Biological Wastewater Treatment,* Second ed.; Marcel Dekker, Inc.: New York, NY., 1999.
21. Schwarzenbach, R. P., Gschwend, P.M., Imboden, D.M., *Environmental Organic Chemistry*. 2nd Edition ed.; Wiley Interscience: Hoboken, N.J, 2003.

CHAPTER 2 - LITERATURE REVIEW

NUTRIENT REMOVAL AND MICROCONSTITUENT DEGRADATION: TWO PEAS IN THE SAME POD?

2.1 Current knowledge on the occurrence and fate of microconstituents during activated sludge treatment is inadequate

Data currently available for organic microconstituents including anti-seizure, steroidal estrogens, x-ray contrast agents and antibiotics suggest variable treatment in WWTPs [1-3]. Biotransformation experiments performed with microconstituents at full scale wastewater treatment facilities [4, 5], lab-scale batch [6] and continuous flow systems [7, 8] indicated varying degrees of treatment of parent compounds, ranging from no removal of carbamazepine (CBZ) [9], 10 to 90% removal of 17α-ethinylestradiol (EE2) [4],0 to 85% removal for iopromide (IOP) [3] and 0 to 45% removal of trimethoprim (TMP) [7, 9]. Increased degradation of some microconstituents, like estrogens, has been suggested to correlate with long solids retention time (SRT > 7 days) [10]. Consequently, some researchers have attributed this microconstituent biotransformation to co-metabolic processes performed by nitrifiers [11, 12]. Little consideration has been placed on heterotrophic contribution despite heterotrophs possessing greater catabolic flexibility. That such an important aspect of the literature is missing is surprising since there are studies that indirectly show transformation of natural estrogens like estrone (E1) and 17β-estradiol (E2) by heterotrophic organisms in the presence of allylthiourea, a potent inhibitor of AOBs [13, 14]. This implies that heterotrophic activity in nitrifying activated sludge (NAS) should not be discounted.

The absence of metabolite data associated with microconstituent degradation in NAS precludes development of a comprehensive model that describes microconstituent fate. This lack of understanding about the mechanisms that drive biotransformation of microconstituents prevents use of process controls to achieve simultaneous degradation of readily biodegradable substrates, nutrients and recalcitrant organics like microconstituents. There is also a dearth of kinetic information that describes biotransformation during activated sludge treatment. Within this context, this chapter seeks to address the current knowledge of microconstituent fate in NAS by:

1. Reviewing literature on the specific fate of the organic microconstituents CBZ, EE2, IOP and TMP (**Table 2.1**) in NAS,
2. Discussing how co-oxidation, co-metabolism and mixed substrate utilization applies to microconstituent degradation and,
3. Interpreting how operating conditions during NAS treatment affect the metabolism of microconstituents amenable to biotransformation.

Table 2.1. Chemical properties of model organic microconstituents.

	Carbamazepine (CBZ) $C_{15}H_{12}N_2O$ [15, 16]	**17α-Ethinylestradiol** (EE2) $C_{20}H_{24}O_2$ [15-17]	**Iopromide** (IOP) $C_{18}H_{24}I_3N_3O_8$ [15, 16]	**Trimethoprim** (TMP) $C_{14}H_{18}N_4O_3$ [15, 18]
Structure	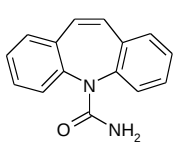	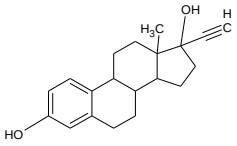	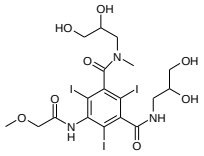	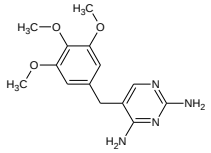
Use	Anti-seizure drug	Oral Contraceptive	X-ray contrast agent	Antibiotic
Log K_{OW}	2.45	3.90	-2.33	0.91
Log K_D (L/kg)	0.09	2.5 -3.0	1	2.32
K_H (atm-m^3/mole)	1.08 x 10^{-10}	7.94 x 10^{-12}	1.00 x 10^{-28}	2.39 x 10^{-14}
pK_A (20^{0}C)	14.0	10.4	10.6	7.40
Solubility in water (mg/L)	17.7 (25^{0}C)	11.3 (27^{0}C)	23.8 (25^{0}C)	400 (25^{0}C)

2.2 Microconstituent fate in activated sludge is variable

2.2.1 Carbamezepine is recalcitrant to biotransformation

CBZ is an anti-convulsant widely prescribed to treat epilepsy and trigeminal neuralgia [19]. This compound can be metabolized by liver microsomes to form gluconuride and hydroxylated metabolites that are excreted in urine [19, 20]. Upon excretion, CBZ and its metabolites have been noted for their recalcitrance to biotransformation in wastewater treatment plants [21, 22]. This recalcitrance is surprising since CBZ metabolism in humans is known to proceed via hydroxlation and epoxidation reactions typically associated with aromatic compound degradation

[19]. Nevertheless, findings of this nature explain the presence of CBZ in receiving water bodies [23]. Effective CBZ removal can be achieved through use of advanced oxidation processes (AOPs) including UV/ H_2O_2 (35% transformation of CBZ [24]) and O_3 (30% mineralization of CBZ [25]). CBZ transformation by AOPs can result in the formation of byproducts like 1-(2-benzaldehyde)-(1H,3H)-quinazoline-2,4-dione (BQD), 1-(2-benzaldehyde)-4-hydro-(1H,3H)-quinazoline-2-one (BQM) and 1-(2-benzoic acid)-(1H,3H)- quinazoline-2,4-dione (BaQD) [26]. Biofilter reactors may then be used to polish water quality before discharge to the environment. At present, combinations of AOPs and biofiltration have not been studied in great detail. As a result, the efficacy of this proposed treatment scheme is still unknown.

2.2.2 IOP transformation in activated sludge is hypothesized to be limited by de-iodination

IOP is an iodinated X-ray contrast agent that is widely detected in surface waters throughout North America and Europe [27]. This compound experiences variable treatment in WWTPs ranging from no removal to 85% removal [21]. No correlation has been found between IOP removal efficiency and SRT [28]. Further, transformation products that have been identified are stable and do not undergo mineralization [27, 29]. This lack of mineralization corresponds with the stability of carbon-iodine bonds in IOP and its transformation products. Dehalogenation can occur under aerobic conditions when the halogen ion is eliminated from an unstable halohydrin formed after monooxygenation or by spontaneous re-aromatization of dihydrodiols formed from dioxygenation [30, 31]. In both cases, the reactions yield oxygenated metabolites that can be subject to ring cleavage. At present, it does not appear that oxidative de-iodination of IOP occurs during aerobic activated sludge treatment since all carbon-iodine bonds remain intact and the proposed transformations involve side chain modifications [3]. Despite its widespread distribution and recalcitrance, IOP has no apparent detrimental ecotoxicological impact on aquatic species [32]. Correspondingly, it may be prudent to use IOP presence as an indicator compound to identify water bodies that might be contaminated with other microconstituents [33].

2.2.3 EE2 degradation involves both ammonia oxidizing bacteria and heterotrophic bacteria

EE2 is a synthetic hormone component of oral contraceptives [34] that has been identified as an environmentally relevant endocrine disruptor [35]. In humans, EE2 is metabolized to a biologically inactive form via hydroxylation and methylation by liver microsomes prior to conjugation with glucuronic acid and/or sulfate [5, 36, 37]. Conjugated EE2 can be reconverted

to the free estrogen form via glucuronidase/sulfatase activity of fecal bacteria [36]. These glucorunidase/sulfatase transformations are important since the free estrogen form possesses endocrine disrupting activity [5] that is undesirable [38]. Recent work by Gomes et al. has confirmed the importance of conjugation/deconjugation reactions in sewage and suggested that deconjugation of glucuronides occurs more rapidly than that of sulfate conjugates [39].

EE2 is transformed to different degrees by nitrifying activated sludges (NAS) [2, 3, 11, 40], pure culture *Nitrosomonas europaea* [13], various species of microalgae [41, 42] and pure culture *Sphingobacterium sp.* JCR5 [43] (**Table 2.2** and **Table 2.3**). The biotransformation of EE2 in NAS is hypothesized to be governed by the activity of ammonia oxidizing bacteria [11, 44]. Yi et al. postulated that electrophilic action by the oxygenated binuclear copper molecules at the active site of ammonia monooxygenase (AMO) is responsible for transformations observed in the presence of NAS and pure culture *N. europaea* [11, 13]. Recent work by our research team confirmed that AMO is indeed capable of acting on EE2 producing two stable metabolites that were generated by hydroxylation (ammonia-limited conditions) and epoxidation (ammonia rich) reactions [45]. These reactions are similar to those observed during experiments with cytochrome P450 extracts obtained from liver microsomes [34, 46]. Despite strong evidence for nitrifier involvement in EE2 biotransformation, others propose that EE2 biotransformation in NAS is completely mediated by heterotrophic activity and that claims of nitrifier involvement are erroneous [47]. Nitro-EE2 was also detected in experiments performed with axenically cultured *N. europaea* [45, 47] and was attributed to abiotic interactions under nitrite rich conditions that are not typical of WWTPs. These nitration reactions are not unexpected since electrophilic substitutions onto the aromatic ring are predicted by frontier electron density (FED) distribution modeling [11].

Hydroxylation of EE2 can be performed by both AOBs and heterotrophic bacteria. Ring cleavage via ortho or meta pathways to form catabolic metabolites that are shuttled to central pathways is hypothesized to be dictated by heterotrophic organisms. It is unknown whether EE2 degradation in AS proceeds via ring A or B cleavage. Experiments performed with *Sphingobacterium sp.* JCR5 isolates, at high concentrations of EE2 (30 mg/L), suggest that EE2 is first oxidized to estrone (E1) and subsequently undergoes ring B cleavage [43]. Yi et al.

suggest ring A cleavage after formation of catechol-EE2 [11]. Upon formation of catechol-EE2 , it is possible that degradation can proceed via cleavage between C-4 and C-5 subunits by protocatechuate-3,4-intradiol dioxygenase homologues. Further reactions can result in the formation of pyruvic acid which can be shuttled to biosynthesis pathways [48, 49].

2.2.4 TMP degradation occurs by heterotrophic activity

Trimethoprim is an antimicrobial drug that is primarily used in combination with the sulfonamide, sulfamethoxazole, for treatment of urinary tract infections in humans [50]. TMP has been detected in sewage as well as receiving water bodies [51, 52]; however, there exist conflicting reports regarding the fate of TMP during activated sludge treatment with some studies reporting low treatment efficiencies in both fullscale and benchscale systems [7, 52] and others reporting over 50% removal at longer SRTs [53, 54]. Researchers have hypothesized that these discrepancies are the result of varying nitrifier activity [53, 55].

Biotransformation of nitrogen heterocyclics like TMP can be catalyzed by oxygenase reactions utilizing NAD(P)H to produce mono/dihydroxylated intermediates, leading to carbon-nitrogen bond cleavage [56, 57]. The inability to detect hydroxylated metabolites in activated sludge may be a consequence of activity by heterotrophic organisms on catechol-TMP. It is also possible that degradation of TMP in a manner similar to that observed during incubations with various cytochrome P450 extracts [58, 59], is limited by *O*-demethylation reactions (

Table 2.4). Limited detection of TMP metabolites could also be due to the presence of glutathione-conjugated TMP metabolites. This conjugation of TMP with glutathione (GSH) is the result of detoxification mechanisms that form GSH-TMP adducts which are inert to further reactions.

Table 2.2 . Description of conditions used to generate various EE2 metabolites in lab-scale batch reactors.

Culture	Transformation products		SRT (day)	HRT (day)	Initial electron donor concentration[1]	Residual substrate concentration	Other conditions
Nitrosomonas europaea batch culture [45]	4-OH-EE2	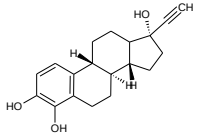	N/A	N/A	NH_3-N: 706 mg/L COD: N/A EE2: 1 mg/L	NH_3-N: 350 - 650 mg/L COD: N/A EE2: Below detection	NO_2^--N: 350 - 650 mg/L NO_3^--N: N/A pH: 6.8 to 7.5
	2-nitro-EE2	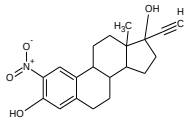					
	4-nitro-EE2	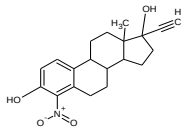					
	M386	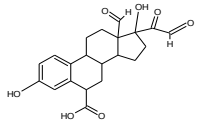					

Microalgae batch reactor [41]	6-OH-EE2 17α-ethinyl-1,4-estradien-10, 17β -diol-3-one	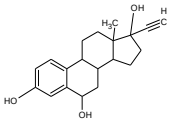 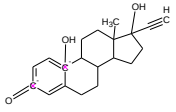	N/A	N/A	NH_3-N: N/A COD: N/A EE2: 0.2 mg EE2/L Degradation experiments performed in batch over 7 days.	NH_3-N: N/A COD: N/A EE2: 0.008 - 0.056 mg/L	NO_2^--N: N/A NO_3^--N: N/A pH: 7.5
Batch tests with NAS from lab-scale SBR [44]	N/A	N/A	N/A	N/A	NH_3-N: 12.3 mg/L COD: 655 mg/L (glucose) EE2: 0.1 mg/L Degradation experiments performed in batch at OLRs: 0.5, 1.6, 4.1 mg COD/mg TSS-day.	NH_3-N: 6-12 mg/L COD: 0 mg/L EE2: 0.04 - 0.06 mg/L	NO_2^--N: N/A NO_3^-N: 0 - 8 mg N/L pH: 7.4
Batch tests with activated sludge from municipal WWTP [37]	N/A	N/A	N/A	N/A	NH_3-N: N/A COD: N/A EE2: 3 - 5 mg/L	NH_3-N: N/A COD: N/A EE2: 3 - 5 mg/L	NO_2^--N: N/A NO_3^--: N/A pH: 7.4
Nitrifying Activated Sludge from Lab-Scale CSTR [40]	Unidentified Hydrophilic By-products	N/A	20	1.8	NH_3-N: 249 mg/g VSS-day COD: N/A EE2: 0.05 mg/L Degradation experiments performed in batch over 6.25 days.	NH3: N/A COD: N/A EE2: <0.001 mg/L	NO_2^--N: N/A NO_3^--N: N/A pH: 7.5

Sphingobacterium sp. JCR5 Batch Cultures [43]	Estrone	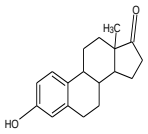	N/A	N/A	NH_3-N: 212 mg/L COD: N/A EE2: 30 mg/L Degradation experiments performed in batch over 10 days.	NH_3-N: N/A COD: N/A EE2: 3.9 mg/L	NO_2^--N: N/A NO_3^--N: N/A pH: 7.5
	2-hydroxy-2,4-diene-1,6-dioic acid	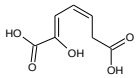					
	2-hydroxy-2,4-dienevaleric acid	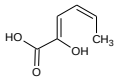					

[1]Initial electron donor concentration applicable to batch systems.
N/A – not applicable

Table 2.3. Description of conditions used to generate various EE2 metabolites in lab-scale continuous flow reactors.

Culture	Transformation products		SRT (day)	HRT (day)	Loading rate(s)[1]	Residual substrate concentration	Other conditions
Nitrosomonas europaea Chemostat [45]	4-OH-EE2	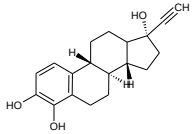	7	7	NH_3-N: 1017 mg/g VSS-day COD: N/A EE2: 1.44 mg/g VSS-day	NH_3-N: 0.2 - 10 mg/L COD: N/A EE2: 200 μg/L	NO_2^--N: 650 - 750 mg/L NO_3^--N:-: N/A pH: 7.5
	2-nitro-EE2	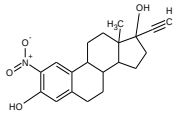					
	4- nitro-EE2	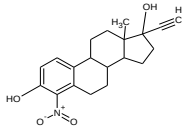					

NAS from Lab-Scale CSTR [11]	2-OH-EE2 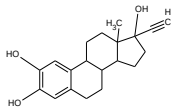 3-sulfo-EE2 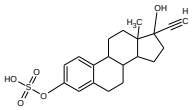 ETDC 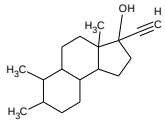		20	2	NH_3-N: 4 - 153 mg/g VSS-day COD: N/A EE2: 0.22 mg/g VSS-day	NH_3-N: 10 - 40 mg/L COD: N/A EE2: 0.18 mg/L	NO_2^--N: < 2 mg/L NO_3^--N: N/A pH 7.5 - 8.5
Activated Sludge from Lab-Scale Membrane Bioreactor [60]	Mono-OH-EE2 m/z 366	N/A N/A	25	0.6	NH_3-N: 0.05 mg/g VSS-day COD: 178 mg/g VSS-day EE2: 0.02 mg/g VSS-day	NH_3-N: N/A COD: 20 - 100 mg/L EE2: 0.02 mg/L	NO_2^--N: N/A NO_3^--N: N/A pH: 7.0
NAS from membrane bioreactor [12]	N/A	N/A	Infinite	4	NH_3-N: 4 - 127 mg/g VSS-day COD: N/A EE2: 0.65 mg/g VSS-day		NO_2^--N: N/A NO_3^--N: 15.7 mg/L pH: 7.4

[1]Loading rates for continuous flow systems.
N/A – Not applicable.

Table 2.4. Description of operating conditions used to generated various TMP metabolites in lab-scale reactors.

Culture	Transformation products		SRT (day)	HRT (day)	Initial electron donor concentration[1]or Loading rate(s)[2]	Residual substrate concentration	Other conditions
Nitrifying Activated Sludge from Municipal WWTP [61]	m/z 322	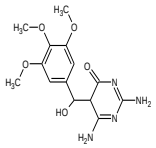	N/A	N/A	NH_3-N: N/A COD: N/A TMP: 0.02 - 20 mg/L Batch tests performed over 5 days	NH_3-N: N/A COD: N/A TMP: 0.004 - 4 mg/L	NO_2^--N: N/A NO_3^--N -: N/A pH: 4.8 to 7.2
	m/z 306	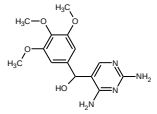					
	m/z 304	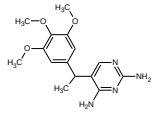					
Activated sludge from Lab-scale Reactor [7]	N/A	N/A	>10	0.25	NH_3-N: N/A COD: N/A TMP: 0.05 mg/g VSS-day	NH_3-N: N/A COD: N/A TMP: 0.03 mg/L	NO_2^--N: N/A NO_3^--N: N/A pH: 7.5 to 8.5

[1]Initial electron donor concentration applicable to batch systems.
[2]Loading rates for continuous flow systems.
N/A – Not applicable.

2.3 Factors that affect the biotransformation of microconstituents

Despite an abundance of literature that documents the fate of microconstituents in AS, no coherent picture exists that describes how operating parameters affect transformation. It is important that we evaluate the various factors that can influence microconstituent degradation with a view to extrapolating our results to process control at WWTPs.

2.3.1 Microconstituent availability can be affected by pH and the presence of colloidal organic matter, exopolymeric substances and soluble microbial products

Sorption can reduce the fraction of microconstituent available for biotransformation reactions. Studies performed to determine partitioning coefficients indicate that CBZ and IOP do not sorb to a significant degree. EE2 sorbs well to biomass and other particulates [8, 16, 17, 62] with studies showing removal ranging from 10-70% [60]. Sorption of TMP has been reported to be minimal (0-3%) although extensive characterization has not been performed [18, 52]. These results indicate that any CBZ, IOP and TMP losses observed in activated sludge systems can primarily be attributed to biotransformation, while EE2 fate is influenced by sorption and biotransformation.

Sorption behavior can be affected by pH, cell surface characteristics, particle size and organic matter composition. Protonation of microconstituents and biomass substituents can impede sorption of microconstituents like steroidal estrogens [63]. Sorption can also be affected by particle size where larger specific surface areas associated with smaller particles allow for a higher degree of sorption [8]. Partitioning to organic matter can also impact microconstituent fate. Since organic matter can exhibit both hydrophilic and hydrophobic properties [64, 65], speciation of microconstituents and organic matter substituent groups can influence potential interactions. In light of these findings, we postulate that microconstituent interactions with colloidal organic matter [66] as well as humic and fulvic acids present in wastewater, affects microconstituent solubility by altering mass transfer of conjugated microconstituent across bacterial membranes and reducing the bioavailability of the microconstituent. These changes can be ultimately manifested through reduced enzymatic affinity for the modified compound resulting in diminished biochemical interaction and transformation.

Results from Holbrook et al. suggest that sorption of estrogens is affected by the mass and composition of organic matter present in the sorbent [66]. Activated sludge floc structure can be affected by exopolymeric substance (EPS) content, which is primarily composed of polysaccharides, proteins and nucleic acids [67-69]. This EPS can comprise up to 15% of mixed liquor and we postulate that sorption of microconstituents by activated sludge is enhanced by the presence of EPS. Consequently, sorption can be the dominant mechanism of microconstituent removal in cultures that have a high EPS content. Enhanced EPS formation has been observed at both high [70, 71] and low growth rates [72] indicating that EPS formation in activated sludge systems is dependent on both the microbial community and reactor configuration employed [71, 73]. In low growth rate systems, it is also important to note that EPS can be hydrolyzed to form biomass-associated products (BAP), which are a subset of the total soluble microbial products (SMP) pool. Therefore, in systems where EPS formation dominates at longer SRTs, interactions between microconstituents and BAPs should also be considered. Microconstituent can also interact with utilization-associated products (UAP), which are the other major component of the SMP pool. UAP predominates in high rate systems where high organic loading rates and low SRT are employed. In these high rate systems, microconstituent interactions with UAPs can occur. It is possible that low rates of microconstituent biotransformation in activated sludge systems are a manifestation of reduced bioavailabity due to sequestration of microconstituents by EPS and SMPs. At present, no research has elucidated whether there is a tradeoff that might occur between sorption and biotransformation in systems where EPS and SMP formation are significant.

2.3.2 Sludge history and growth conditions can affect the fraction of biomass that acts on microconstituents

Degradation of microconstituents by activated sludge (AS) can be performed by a general community capable of degrading a broad range of compounds, specialist communities capable of using these compounds as growth substrates [74, 75], or a combination of both. In the latter strategy, specialist organisms are hypothesized to perform initial reactions that produce metabolites more amenable to further transformation by generalists. The presence and activity of these specialists can be affected by various factors, including sludge origin as well as growth conditions (reactor configuration, feed composition, redox conditions, solids retention time (SRT)) [75].

Wastewater typically contains multiple organic and inorganic substrates that promote continuous selective pressure among different groups of organisms present in activated sludge with a predisposition towards those that have the highest affinity for specific substrates [74]. Since microconstituents are present at trace concentrations in WWTPs, the theoretical fraction of specialist biomass supported by these compounds is small [76]; however, there may be other SOCs in wastewater that can induce enzymes common to aerobic SOC and microconstituent degradation pathways. It is also possible that basal level expression of unspecific enzymes may be sufficient to afford biotransformation of these microconstituents. At present, it is unclear whether microconstituents are transformed accidentally or are intentionally used as a substrate.

Microconstituent biotransformation can also be significantly influenced by the physiological state of cultures used in experiments. Metabolites generated by cells under "feast" conditions can be different than those generated by cells under "famine" conditions [45]. That physiological state has a significant impact on microconstituent degradation has been largely ignored but should not be discounted since it can explain the differences in observed transformation rates/metabolites observed in full-scale versus lab-scale studies and between full-scale systems.

2.3.3 Microconstituent biotransformation may involve co-metabolism, fortuitous metabolism and mixed substrate utilization reactions

To date, the primary mechanisms involved in microconstituent biotransformation have not been elucidated. Processes like co-metabolism, co-oxidation, fortuitous metabolism and mixed substrate utilization have not been discussed in significant detail despite the fact that microconstituent biodegradation probably involves some combination of all these processes. Within this context, it is important that we review the definitions of these processes with a view to how they may apply to microconstituent biodegradation.

Traditionally, co-metabolism, co-oxidation and fortuitous metabolism have been used to define similar concepts with subtle differences. Co-oxidation was defined in the early 1950's as "the oxidation of non-growth hydrocarbons when present in a medium where one or more different hydrocarbons are furnished for growth" [77]. In these co-oxidation experiments, transformation of the non-growth hydrocarbon was performed by actively growing cells using a single primary

hydrocarbon for growth and production of reducing energy. This primary substrate induced the non-specific enzyme that was responsible for the transformation of the non-growth co-substrate. No energy was recovered from oxidation of the non-growth co-substrate.

Fortuitous oxidation was defined by Dalton and coworkers as "the oxidation of a non-growth substrate in the absence of a primary substrate" [78]. Fortuitious metabolism has been subsequently defined as the biotransformation of a compound that is an analog to the natural substrate for the enzyme [79]. The focus is on the role of the enzyme and less on how energy flows due to the metabolism. In Grady's interpretation of this metabolism, fortuitous metabolism occurs due to the non-specificity of the enzyme, does not require the presence of a primary growth substrate, and may or may not generate growth-supporting energy and reducing power [79]. However, for fortuitious metabolism to be sustained, energy must be derived from the reaction somehow (either by the fortuitously metabolized compound or through byproduct metabolism) or from a primary substrate that maintains the cells performing the fortuitous metabolism. Applied to microconstituents, this means that fortuitous metabolism of a microconstituent would occur if its structure is sufficiently similar to naturally occurring enzymatic substrates, that the metabolism may or may not be a first step in mineralization, and that energy and growth may or may not be derived by it. If energy is not derived, the fortuitously metabolizing cells would have to be maintained through some other means in order for the metabolism to be sustained. One can envision this happening in a complex microbial community like activated sludge.

In contrast to fortuitous metabolism, co-metabolism was defined by Stirling and Dalton in 1979, as the "transformation of a non-growth substrate in the obligate presence of a growth supporting substrate" [78]. In the experiments investigating co-metabolism, cells were originally grown in the presence of a single primary growth substrate that induced the non-specific enzyme of interest. These actively growing cells were then removed from the presence of the original primary substrate and supplemented with a non-growth co-substrate and multiple alternative growth substrates (not the original primary growth substrate) [77, 78, 80]. Results from these experiments defined the range of primary substrates that could be used by the cells for growth, maintenance and biotransformation of the non-growth co-substrate. More recent definitions of

co-metabolism also account for the biotransformation of co-substrates by resting cells in the presence or absence of growth substrates [81]. , but benefiting from the presence of enzymes that are induced by a growth substrate, or enzymes that are present in the absence of a growth substrate due to basal activity. This expanded definition of co-metabolism makes the concept of co-oxidation obsolete. Furthermore, the definition of co-metabolism explicitly retains the notion that cells performing the co-metabolic transformation necessarily require the presence of a growth or energy deriving substrate, because energy is required either to transport the co-substrate or for the enzymes transforming it to function [79]. Notably, many of the oxygenase-based enzymes involved with transformation of SOCs [82, 83] and that may be involved with the transformation of microconstituents [6, 11] require reducing power or other forms of energy to function [80, 84]. Furthermore, co-metabolism always results in the accumulation of byproducts because beneficial use of these byproducts would not be co-metabolism but, rather, fortuitous metabolism. Finally, byproducts of co-metabolism may be inert or they may be toxic and, therefore, detrimental to the viability of the cells that created them [85, 86] Overall, for co-metabolism to be sustained, the cells performing the metabolism must be able to grow through some other means.

Microconstituent biodegradation can also be due to mixed substrate utilization. In this process, bacterial communities recover electron equivalents present in SOCs or microconstituents and other metabolizable substrates simultaneously [87]. Sustained growth of competent biomass solely on trace concentrations of microconstituents may not be possible [88]; however utilization of multiple substrates to supplement energy required for cellular growth and maintenance functions can occur [89]. There is substantial literature that confirms the ability of pure/mixed cultures to simultaneously use multiple substrates under continuous flow conditions without observed diauxic lag typical of batch configurations [82, 90, 91]. Under these continous flow conditions, catabolite repression does not occur, allowing the cells to synthesize enzymes required for degradation of multiple substrates without experiencing biphasic growth typically associated with diauxie. The induction of enzymes by co-substrates differentiates mixed substrate utilization from co-metabolism (summarized in **Table 2.5**). That mixed microbial communities can employ combinations of co-metabolism, fortuitious metabolism and mixed substrate utilization helps to explain why activated sludge treatment processes are robust options

for reducing concentrations of various SOCs in multicomponent wastestreams [75, 82, 88, 92, 93].

Table 2.5. Comparison of co-metabolism, fortuitous metabolism and mixed substrate utilization as they apply to SOCs (and might apply to microconstituents).

	Primary Substrate(s)	SOC	Enzyme activity
Co-metabolism	Provides energy required for biotransformation[1] and/or transport of co-substrate, but is not required because co-metabolism can occur under endogenous conditions devoid of primary substrates but containing sufficient reducing power to enable some co-metabolic biotransformations.	Does not yield energy. Byproducts are not further metabolized by co-metabolizing cells.	Enzymes that cause co-metabolism are induced by a primary substrate.
Fortuitous Metabolism	Not required. If present, can provide energy for growth and maintenance of fortuitous metabolizing cells.	Is analog to natural substrate for enzyme that catalyzes biotransformation of SOC. SOC may or may not serve as growth and energy source. Yields byproducts that can either accumulate or subsequently be used for growth and maintenance by fortuitious metabolizing cells.	Can be induced by SOC, which serves as an analog to natural substrates for the enzyme.
Mixed Substrate Utilization	Multiple primary substrates provide energy for growth and maintenance	Yields energy for growth and maintenance	Induced by multiple substrates, including SOCs

[1]Biotransformation is defined as the conversion of parent organic microconstituent to less complex intermediates by microorganisms. If further degradation of these microconstituents and intermediates yields carbon dioxide, this process is referred to as mineralization.

Effective treatment of microconstituents in activated sludge can only be achieved if sufficient levels of enzymes that are capable of acting on the microconstituents are present [82]. These reactions can be catalyzed by multiple organisms/enzymes on parent compounds as well as byproducts. Initial partial transformation of microconstituents can occur via co-metabolic processes. Subsequent mineralization can occur via fortuitous metabolism and mixed substrate utilization. At present, few reports have addressed the relevancy of these concepts as related to microconstituent fate.

If co-metabolism is responsible for all observed microconstituent transformations in prior studies [63, 87], these reactions would be dependent on the availability of non-specific enzymes induced

by biogenic (in)organic compounds. Mineralization would also not be observed since co-metabolism only involves partial transformations of the microconstituent. If the microconstituents are used as an electron donor (fortuitous metabolism or mixed substrate utilization), mineralization and biomass growth can be expected. The dilute nature of these microconstituents allows for all three processes to be feasible options.

2.3.4 Aerobic biotransformation of aromatic microconstituents is governed by oxygenase activity

The aromatic and heterocyclic nature of the CBZ, EE2, IOP and TMP (**Table 2.1**) will dictate how these compounds are degraded under aerobic conditions. Aerobic transformation of aromatic SOCs is driven by the action of unspecific monooxygenase and dioxygenase enzymes (expressed by autotrophic and heterotrophic bacteria found in activated sludge) [94]. These monooxygenases combine a single oxygen atom with inorganic/organic substrates to form a hydroxylated byproduct which can then be subject to dehydrogenation and subsequent unspecific dioxygenation. Unspecific dioxygenases such as toluene dioxygenase produce hydroxylated products with a loss of aromaticity e.g. dihydrodiols. These oxygenations by unspecific mono and dioxygenases require reducing power which is obtained through electron transfer from NAD(P)H. Hydroxylation reactions destabilize the aromatic ring which could then be cleaved through the actions of a different class of dioxygenase enzymes, found in heterotrophs only. Ring cleavage reactions, catalyzed by catechol dioxygenases homologues, e.g catechol 1,2 dioxygenase (C12O) and catechol 2,3 dioxygenase (C23O), do not require reducing equivalents from a co-substrate and produce low molecular weight (MW) metabolites. These metabolites can undergo further reactions to produce pyruvic acid which can be shuttled to the tricarboxylic acid cycle. Reducing energy in the form of NAD(P)H is regenerated from these central metabolic pathways, fueling subsequent oxygenations.

We hypothesize that microconstituent biodegradation under aerobic conditions is limited by the ability of the microbial community to synthesize oxygenases. Initial oxygenation reactions may be co-metabolic in nature while subsequent ring cleavage during fortuitous oxidation or mixed substrate utilization can yield energy that fuels growth and maintenance as well as further biotransformation of the microconstituent. Within NAS, initial oxygenations can be performed by AOBs and heterotrophs while subsequent degradation can only be performed by heterotrophs

since AOBs do not possess the catabolic flexibility to utilize complex organic compounds as electron donors or carbon sources. Cultures that possess enriched ring cleavage dioxygenase activity may have an enhanced ability to biotransform and mineralize microconstituents. Based on this information, we hypothesize that the potential for enhanced microconstituent mineralization increases as the oxygenase activity of the sludge increases.

2.3.5 Reactor configuration and operation can significantly impact microconstituent degradation by affecting sludge diversity

Researchers have suggested that SRT is the single most important parameter influencing microconstituent degradation [87] despite the fact that strong statistical correlations between SRT and microconstituent removal do not exist [28, 95]. This uncertainty needs to be acknowledged in the literature if researchers are to elucidate the impact of other operating conditions on microconstituent fate. It is unwise to alter SRTs of plants under the pretext of achieving optimum treatment of microconstituents since the effect of other factors on microconstituent degradation is largely unknown. In this dissertation, microconstituent fate is hypothesized to be dependent on reactor configuration, organic loading rates, microconstituent loading rates and the presence of residual organic carbon.

Reactor configuration can influence organic and microconstituent loading rates. Although conventional activated sludge (CAS) or completely mixed activated sludge (CMAS) systems are loaded to similar degrees (0.2-0.4 kg BOD_5/kg MLVSS-day) [96, 97], microconstituent behavior can differ. In CAS systems where organic loading can be extremely high near the inlet due to lack of horizontal mixing characteristic of plug flow regimes, we believe that microconstituent degradation will not occur since other substrates are readily available. In CMAS systems where wastewater is uniformly distributed [98], we hypothesize that microconstituent degradation will be more prevalent since homogenous dispersion can allow simultaneous utilization of various organic donors by different microbial communities. Nevertheless, microconstituent degradation by heterotrophs is not expected to occur to a significant degree until nutrient limited conditions dominate i.e. readily biodegradable organic substrate (rbCOD) concentration is less than or equal to the half saturation constant for rbCOD ($K_{S,rbCOD}$).

Continuous selective pressure at longer retention times can allow for the development of a population capable of using recalcitrant compounds as electron donors [28, 63] thereby increasing sludge diversity [99]. Under these conditions, where microconstituents become attractive energy sources to heterotrophic scavengers, nitrification also occurs. As a result, co-metabolic action by AOB on microconstituents susceptible to transformation can occur. For microconstituents that are not biotransformed by AOBs, degradation would be limited to heterotrophic activity. Thus, the ammonia oxidation step of nitrification can only provide a benefit if the microconstituent under consideration is biotransformed by AOBs. Even then, the relative kinetics of AOB and heterotroph mediated microconstituent degradation should be estimated to determine who will potentially dominate the biotransformation reactions. The benefits of combined AOB and heterotrophic activity may explain findings where certain microconstituents are biotransformed in systems configured to run at long SRTs (> 14 days), such as sequential batch reactors (SBRs; 0.04 – 0.1 kg BOD_5/kg MLVSS-day) and extended aeration activated sludge systems (EAAS; 0.04 – 0.1 kg BOD_5/kg MLVSS-day), in both cases where AOBs and heterotrophs are active.

Residual organic carbon is also speculated to influence degradation of microconstituents in biological nutrient removal (BNR) systems. In pre-anoxic BNR systems (e.g MLE, first two tanks in four stage Bardenpho systems), removal of rbCOD is achieved in the anoxic zone prior to nitrification. Microconstituents are postulated to become attractive electron donors when rbCOD levels are sufficiently low to prevent preferential utilization of other metabolizable substrates. Similarly, microconstituent degradation in post-anoxic BNR systems (e.g. oxidation ditches, last two tanks in Bardenpho system) may only be most relevant in the anoxic zones where endogenous respiration dominates. In cases where an external carbon source is added to increase denitrification rates, we hypothesize that preferential degradation of the carbon source (e.g. methanol) will hinder microconstituent degradation. Since data that compares the fate of microconstituents versus rbCOD concentrations are largely absent from the literature, conclusions are premature at this point.

The relative recalcitrance of microconstituents in full-scale and lab-scale studies may also be explained by the presence of SMPs in mixed liquor. Specifically, SMPs can be the primary form

of soluble organic carbon that is present in reactor effluent [100]. Although SMPs are not thought to be readily biodegradable, cells can utilize SMPs as electron donors for growth and maintenance reactions in the absence of other readily biodegradable matter [73]. Previous work has suggested that SMP production can be minimized by operating aerobic reactors at SRTs between 2 and 15 days and at OLRs ranging from 0.3 to 1.2 g COD/g MLSS-day (0.2 – 0.8 g BOD/g MLSS-day) [101], which coincides with conditions that allow for microconstituent biodegradation. At longer SRTs, high molecular weight products (> 1kDa), resulting from polymerization of low MW products (< 1kDa) [101, 102], are the primary form of effluent organic matter (EfOM). These high MW compounds are more amenable to aerobic degradation than the low MW products, which are highly recalcitrant [103]. Lack of removal of microconstituents in some treatment plants operating at long SRTs [28] could be a partial consequence of cells utilizing SMPs as the preferred electron donor. In this scenario, microconstituent removal may be slowed since the SMPs would be preferentially utilized by the cells as a more readily biodegradable substrate. This is particularly important since SMPs are universally present in these systems while microconstituents may not always be present in sewage. Consequently, the fraction of the microbial community adapted to utilizing SMPs would be greater than the fraction adapted to using microconstituents as electron donors. For mixed utilization of both SMPs and microconstituents to occur, both substrates may need to be present at or below their respective half saturation constants ($K_{S,\ SMP}$ and $K_{S,\ microconstituent}$). Further work is needed to investigation whether SMPs can impact microconstituent biotransformation.

If the presence of rbCOD and SMPs influences the extent of treatment of certain microconstituents, there may be threshold values below which simultaneous degradation of rbCOD, SMPs and microconstituents may be expected to occur ($K_{S,rbCOD}$ and $K_{S,SMP}$). These low concentrations could be attained in activated sludge systems that maintain sufficiently high SRTs and are not overloaded with organic matter. We hypothesize that microconstituent degradation in these systems can result from a combination of unspecific co-metabolic reactions by AOBs as well as through fortuitous and mixed substrate utilization by heterotrophs that have been acclimated to nutrient-limited comnditions. To properly describe this action by heterotrophs, estimation of microconstituent biokinetic parameters describing growth on microconstituents utilization is needed. If we can determine maximum specific growth rates for microconstituents

(μ_{max}), we can calculate the theoretical minmum SRT required for removal of individual compounds ($\theta_{C,min}$). This data will provide us with a framework to determine which microconstituents can be removed under specific operating parameters.

2.4 Future work needs to focus on coupling biological nitrogen removal and microconstituent degradation

It is prudent for wastewater engineers to consider the benefits that can be achieved through coupling microconstituent degradation and biological nutrient removal. Longer solids retention times combined with lower organic loading appears to encourage development of microbial consortia capable of degrading recalcitrant compounds. A combination of co-metabolic action by AOBs on some microconstituents and fortuitous metabolism and mixed substrate utilization reactions by heterotrophs can make microconstituent removal a feasible option for activated sludge systems that achieve endogenous conditions. In circumstances where exogenous carbon sources are traditionally utilized to enhance nitrate removal post nitrification, it is worth investigating the feasibility of coupling microconstituent degradation and denitrification. Further work is needed to properly elucidate the effects of varying redox conditions on microconstituent biodegradation.

There is also a need to accurately determine the dominate metabolism employed by microorganisms for degradation of individual microconstituents. For this work, researchers need to focus on developing biokinetic parameters that describe how cells oxidize microconstituents via co-metabolism or use them for growth and maintenance via fortuitous metabolism and mixed substrate utilization. The experimental requirements for determining these parameters are difficult; however, these efforts should be pursued as the results can have a broad impact on how engineers design activated sludge systems for nitrogen and microconstituent degradation. In performing these experiments, we should also try to determine how population dynamics of activated sludge systems can influence biodegradation. To perform these analyses, we can employ molecular techniques to fingerprint the fractions of biomass capable of metabolizing microconstituents. Development of 16S rRNA clone libraries as well as use of terminal restriction length polymorphism (T-RFLP) and automated approaches for ribosomal intergenic spacer analyses (ARISA) can help us determine whether changes in community profiles correlate with changes in microconstituent removal rates [104]. Further work can also focus on using

techniques like stable isotope probing (SIP) and fluorescence in situ hybridization coupled with microautoradiogaphy (FISH-MAR) [105] to link microbial structure and function.

2.5 References

1. Paxeus, N., Removal of Selected Non-steroidal Anti-inflammatory Drugs (NSAIDs), Gemfibrozil, Carbamazepine, β-blockers, Trimethoprim and Triclosan in Conventional Wastewater Treatment Plants in five EU Countries and their Discharge to the Aquatic Environment. *Water Science and Technology* **2004,** *50*, (5), 253-260.
2. Perez, S., Eichhorn, P., Aga, D.S., Evaluating the Biodegradability of Sufamethazine, Sulfamethoxazole, Sulfathiazole, and Trimethoprim at Different Stages of Sewage Treatment. *Environmental Toxicology and Chemistry*, **2005,** *24*, (6), 1361–1367.
3. Perez, S., Eichhorn, P., Celiz, M.D., Aga, D.S., Structural Characterization of Metabolites of the X-ray Contrast Agent Iopromide in Activated Sludge Using Ion Trap Mass Spectrometry. *Analytical Chemistry* **2006,** *78*, 1866-1874.
4. Ternes, T. A., P. Keckel, Mueller, J. , Behaviour and Occurrence of Estrogens in Municipal Sewage Treatment Plants. 1. Investigations in Germany, Canada and Brazil. *Science Total Environment* **1999,** *225*, 91-99.
5. Ternes, T. A., P. Keckel, Mueller, J., Behaviour and Occurrence of Estrogens in Municipal Sewage Treatment Plants. II. Aerobic Batch Experiments With Activated Sludge. *Science Total Environment* **1999,** *225*.
6. Yoshimoto, T., Nagai, F., Fujimoto, J., Watanabe, K., Mizukoshi, H., Makino, T., Kimura, K., Saino, H., Sawada, H., Omura, H., Degradation of Estrogens by *Rhodococcus zopfii* and *Rhodococcus equi* Isolates from Activated Sludge in Wastewater Treatment Plants. *Applied and Environmental Microbiology* **2004,** *70*, (9), 5283-5289.
7. Junker, T., Alexy, R., Knacker, T., Kummerer, K., Biodegradability of 14C-Labeled Antibiotics in a Modified Laboratory Scale Sewage Treatment Plant at Environmentally Relevant Concentrations. *Environmental Science and Technology* **2006,** *40*, 318-324.
8. Yi, T., Harper Jr., W.F.,Holbrook, R.D., Love, N.G., Role of Particle Size and Ammonium Oxidation in Removalof 17α-Ethinyl Estradiol in Bioreactors. *Journal of Environmental Engineering* **2006,** *132*, (11), 1527-1529.
9. Loffler, D., Rombke, J., Meller, M., Ternes, T.A., Environmental Fate of Pharmaceuticals in Water/Sediment Systems. *Environmental Science Technology* **2005,** *39*, 5209-5218.
10. Ternes, T. A., Janex-Habibi, M.L., Knacker, T., Kreuzinger, N., Siegrist, H. *Assessment of Technologies for the Removal of Pharmaceuticals and Personal Care Products in Sewage and Drinking Water Facilities to Improve the Indirect Potable Water Reuse.*; Wiesbaden, Germany, 2006.
11. Yi, T., Harper Jr., W.F., The Link between Nitrification and Biotransformation of 17α-Ethinylestradiol. *Environmental Science Technology* **2007,** *41*, 4311-4316.
12. Gusseme, B. D.; Pycke, B.; Hennebel, T.; Marcoen, A.; Vlaeminck, S. E.; Noppe, H.; Boon, N.; Verstraete, W., Biological Removal of 17α-ethinylestradiol by a Nitrifier Enrichment Culture in a Membrane Bioreactor. *Water Research* **2009,** *43*, 2493-2503.
13. Shi, J., Fujisawa, Saori, Nakai, Satoshi, Hosomi, M., Biodegradation of Natural and Synthetic Estrogens by Nitrifying Activated Sludge and Ammonia Oxidizing Bacterium *Nitrosomonas europaea*. . *Water Research* **2004,** *38*, 2323-2330.

14. Carballa, M., Omil, F., Lema, J.M., Llompart, M., Garcia-Jares, C., Rodriguez, I., Gomes, M., Ternes, T., Behavior of Pharmaceuticals, Cosmetics and Hormones in a Sewage Treatment Plant. *Water Research* **2004,** *38*, 2918-2926.
15. National Institutes of Health, D. o. H. H. S. ChemIDplus Advanced.
16. Ternes, T. A., Herrmann, N., Bonerz, M., Knacker, T., Siegrist H., Joss, A., A Rapid Method to Measure the Solid–Water Distribution Coefficient (K_d) for Pharmaceuticals and Musk Fragrances in Sewage Sludge. *Water Research* **2004,** *38*, 4075-4084.
17. Andersen, H. R., Hansen, M., Kjolholt, J., Stuer-Lauridsen, F., Ternes, T.A., Halling-Sorensen, B., Assessment of the Importance of Sorption for Steroid Estrogens Removal During Activated Sludge Treatment. *Chemosphere* **2005,** *61*, 139-146.
18. Gobel, A., Thomsen, A., McArdell, C.S., Joss, A., Giger, W. , Occurrence and Sorption Behavior of Sulfonamides, Macrolides, and Trimethoprim in Activated Sludge Treatment *Environmental Science and Technology* **2005,** *39*, (11), 3981 -3989.
19. Lertratanangkoon, K., Horning, M.G., Metabolism of Carbamazepine. *Drug Metabolism and Disposition* **1982,** *10*, (1), 1-10.
20. Maggs, J. L., Pirmohamed, M., Kitteringham, N.R., Park, N.K., Characterization of the Metabolites of Carbamazepine in Patient Urine by Liquid Chromatography/Mass Spectrometry. *Drug Metabolism and Disposition* **1997,** *25*, (3), 275-280.
21. Onesios, K. M., Yu, J.T., Bouwer, E.J., Biodegradation and Removal of Pharmaceuticals and Personal Care Products in Treatment Systems: a Review. *Biodegradation* **2009,** *20*, 441-466.
22. Strenn, B., Clara, M., Gans, O., Kreuzinger, N., Carbamazepine, Diclofenac, Ibuprofen and Bezafibrate – Investigations on the Behaviour of Selected Pharmaceuticals During Wastewater Treatment. *Water Science and Technology* **2004,** *50*, (5), 269-276.
23. Kolpin, D. W., Furlong, E.T., Meyer, M.T., Thurman, E.M., Zaugg, S.D., Barber, L.B., Buxton, H.T., Pharmaceuticals, Hormones, and Other Organic Wastewater Contaminants in U.S. Streams, 1999-2000: A National Reconnaissance. *Environmental Science Technology* **2000,** *36*, 1202-1211.
24. Vogna, D., Marotta, R., Andreozzi, R., Napolitano, A., d'Ischia, M., Kinetic and Chemical Assessment of the UV/H_2O_2 Treatment of Antiepileptic Drug Carbamazepine. *Chemosphere* **2004,** *54*, 497-505.
25. Ikehata, K., Naghashkar, N.J., El-Dina, M.G., Degradation of Aqueous Pharmaceuticals by Ozonation and Advanced Oxidation Processes: A Review. *Ozone: Science & Engineering* **2006,** *28*, 353-414.
26. McDowell, D. C., Huber, M.M., Wagner, M., Von Gunten, U., Ternes, T.A., Ozonation of Carbamazepine in Drinking Water: Identification and Kinetic Study of Major Oxidation Products. *Environmental Science and Technology* **2005,** *39*, (20), 8014-8022.
27. Perez, S., Barcelo, D., Fate and Occurrence of X-ray Contrast Media in the Environment. *Analytical and Bioanalytical Chemistry* **2007,** *387*, 1235-1246.
28. Kreuzinger, N., Clara, M., Strenn, B., Kroiss, H., Relevance of the Sludge Retention Time (SRT) as Design Criteria for Wastewater Treatment Plants for the Removal of Endocrine Disruptors and Pharmaceuticals from Wastewater. *Water Science and Technology* **2004,** *50*, (5), 149-156.
29. Hartmann, T. S., Lange, R., Schweinfurth, H., Tschampel, M., Rehmann, I., Investigations into the Environmental Fate and Effects of Iopromide (ultravist),a Widely Used Iodinated X-ray Contrast Medium. *Water Research* **2002,** *36*, 266-274.

30. Fetzner, S., Bacterial Dehalogenation. *Applied Microbiology Biotechnology* **1998,** *50*, 633-657.
31. Haggblom, M. M., Bossert, I.D., *Dehalogenation - Microbial Processes and Environmental Applications*. Kluwer Academic Publishers: Boston, 2003.
32. Hartmann, T. S., Lange, R., Schweinfurth, H., Environmental Risk Assessment for the Widely Used Iodinated X-Ray Contrast Agent Iopromide (Ultravist). *Ecotoxicology and Environmental Safety* **1999,** *42*, 274-281.
33. Drewes, J. E., Sedlak, D., Snyder, S., Dickenson, E. *Development of Indicators and Surrogates from Chemical Contaminant Removal during Wastewater Treatment and Reclamation.*; Water Reuse Foundation: Alexandria VA, 2008.
34. Kent, U. M., Mills, D.E., Rajnarayanan, R.V., Alworth, W.L., Hollenberg, P.F., Effect of 17α-Ethynylestradiol on Activities of Cytochrome P450 2B (P450 2B) Enzymes: Characterization of Inactivation of P450s 2B1 and 2B6 and Identification of Metabolites. *The Journal of Pharmacology and Experimental Therapeutics* **2002,** *300*, (2), 549-558.
35. Tyler, C. R.; Jobling, S.; Sumpter, J. P., Endocrine Disruption in Wildlife: A Critical Review of the Evidence. *Critical Reviews in Toxicology* **1998,** *28*, (4), 319-361.
36. Khanal, S. K., Xie, B., Thompson, M. L., Sung, S., Ong, S.K., Van Leeuwen, J. H., Fate, Transport, and Biodegradation of Natural Estrogens in the Environment and Engineered Systems. *Environmental Science and Technology* **2006,** *40*, (21), 6537-6546.
37. Weber, S., Leuschner, P., Kaempfer, P., Dott, W., Hollender, J., Degradation of Estradiol and Ethinyl Estradiol by Activated Sludge and by a Defined Mixed Culture. . *Applied Microbiology Biotechnology* **2005,** *67*, (1), 106-112.
38. Lavado, R., Thibaut, R., Raldua, D., Martın, R., Porte, C., First Evidence of Endocrine Disruption in Feral Carp from the Ebro River. *Toxicology and Applied Pharmacology* **2004,** *196*, 247-257.
39. Gomes, R. L., Scrimshaw, M.D., Lester, J.N., Determination of Endocine Disrupters in Sewage Treatment and Receiving Waters. *Trends in Analytical Chemistry* **2003,** *22*, (10), 697-707.
40. Vader, J. S., Ginkel, C.G., van Stokman, F.M, Sperling, G.M., Jong, J., de Boer, W., de Graaf, J.S., de Most, M., van der Stokman, P.G.W. , Degradation of Ethinylestradiol by Nitrifying Activated Sludge. . *Chemosphere* **2000,** *41*, (8), 1239-1243.
41. Della Greca, M., Pinto, G., Pistillo, P., Pollio, A., Previtera, L., Temussi, F., Biotransformation of Ethinylestradiol by Microalgae. *Chemosphere* **2008,** *70*, 2047-2053.
42. Lai, K. M., Scrimshaw, M.D., Lester, J.N., Biotransformation and Bioconcentration of Steroid Estrogens by *Chlorella vulgaris. Applied and Environmental Microbiology* **2002,** *68*, (2), 859-864.
43. Haiyan, R., Shulan, J., Ud din Ahmad, N., Dao, W., Chengwu, C., Degradation Characteristics and Metabolic Pathway of 17α-ethynylestradiol by *Sphingobacterium* sp. JCR5. *Chemosphere* **2007,** *66*, (2), 340-346.
44. Ren, Y. X., Nakano, K., Nomura, M., Chiba, N., Nishimura, O., Effects of Bacterial Activity on Estrogen Removal in Nitrifying Activated Sludge. *Water Research* **2007,** *41*, 3089-3096.
45. Skotnicka Pitak, J., Khunjar, W.O., Aga, D.S., Love, N.G., Characterization of Metabolites Formed During the Biotransformation of 17α-Ethinylestradiol by *Nitrosomonas europaea* in Batch and Continuous Flow Bioreactors. *Environmental Science and Technology* **2009,** *43*, (10), 3549–3555.

46. Lee, A. J., Kosh, J.W., Conney, A.H., Zhu, B.T., Characterization of the NADPH-Dependent Metabolism of 17β-Estradiol to Multiple Metabolites by Human Liver Microsomes and Selectively Expressed Human Cytochrome P450 3A4 and 3A5. *The Journal of Pharmacology and Experimental Therapeutics* **2001,** *298*, (2), 420-432.
47. Gaulke, L. S., Strand, S.E., Kalhorn, T.F., Stensel, H.D., 17α-ethinylestradiol Transformation via Abiotic Nitration in the Presence of Ammonia Oxidizing Bacteria. *Environmental Science and Technology* **2008,** *42*, (20), 7622-7627.
48. Coombe, R. G., Tsong, Y.Y., Hamilton, P.B., Sih, C.J., Mechanisms of Steroid Oxidation by Microorganisms, X - Oxidative Cleavage of Estrone. *The Journal of Biological Chemistry* **1966,** *241*, (7), 1587-1595.
49. Gibson, D. T., Wang, K.C., Sih, C.J., Whitlock Jr., H., Mechanisms of steroid oxidation by microorganisms. IX - On the mechanism of Ring A cleavage in the degradation of 9,10 seco steroids by microorganisms. *The Journal of Biological Chemistry* **1966,** *241*, (3), 551 - 559.
50. Nolan, T., Lubitz, L., Oberklaid, F., Single Dose Trimethoprim for Urinary Tract Infection. *Archives of Disease in Childhood* **1989,** *64*, 581-586.
51. Lindberg, R., Jarnheimer, P.A., Olsen, B., Johansson, M., Tysklind, M., Determination of Antibiotic Substances in Hospital Sewage Water using Solid Phase Extraction and Liquid Chromatography/Mass Spectrometry and Group Analogue Internal Standards. *Chemosphere* **2004,** *57*, 1479-1488.
52. Lindberg, R. H., Olofsson, U., Rendahl, P., Johansson, M.I., Tysklind, M., Anderrson, B.A., Behavior of Fluoroquinolones and Trimethoprim During Mechanical, Chemical, and Active Sludge Treatment of Sewage Water and Digestion of Sludge. *Environmental Science and Technology* **2006,** *40*, (3), 1042-1048.
53. Batt, A. L., Kim, S., Aga, D. S, Enhanced Biodegradation of Iopromide and Trimethoprim in Nitrifying Activated Sludge. *Environmental Science and Technology* **2006,** *40*, 7367-7373.
54. Gobel, A., McArdell, C.S., Joss, A., Siegrist, H., Giger, W., Fate of Sulfonamides, Macrolides, and Trimethoprim in Different Wastewater Treatment Technologies. *Science of the Total Environment* **2007,** *372*, 361-371.
55. Lim, M. H., Snyder, S.A., Sedlak, D.L., Use of Biodegradable Dissolved Organic Carbon (BDOC) to Assess the Potential for Tansformation of Wastewater-derived Contaminants in Surface Waters. *Water Research* **2008,** *42*, 2943-2952.
56. Vickers, S., Polsky, S.L., The Biotransformation of Nitrogen Containing Xenobiotics to Lactams. *Current Drug Metabolism* **2000,** *1*, 357-389.
57. Xu, P., Yu, B., Li Li, F., Cai, X.F., Ma, C.Q., Microbial degradation of sulfur, nitrogen and oxygen heterocycles *Trends in Microbiology* **2006,** *14*, (9), 398-405.
58. Damsten, M. C., de Vlieger, J.S.B., Niessen, W.M.A., Irth, H., Vermeulen, N.P.E., Commandeur, J.N.M., Trimethoprim: Novel Reactive Intermediates and Bioactivation Pathways by Cytochrome P450s. *Chemical Research in Toxicology* **2008,** *21*, (11), 2181-2187.
59. Van, T., Klooster, G. A., Kolker, H. J., Woutersen-Van Nijnanten, F. M., Noordhoek, J., Van Miert, A., Determination of Trimethoprim and its Oxidative Metabolites in Cell Culture Media and Microsomal Incubation Mixtures by High-Performance Liquid Chromatography. *Journal of Chromatography* **1992,** *579*, 355-360.

60. Cirja, M., Zuehlke, S., Ivashechkin, P., Hollender, J., Schaeffer, A., Corvini, P. F. X., Behavior of Two Differently Radiolabelled 17α-ethinylestradiols Continuously Applied to a Laboratory-scale Membrane Bioreactor with Adapted Industrial Activated Sludge. . *Water Research* **2007,** *41*, (19), 4403-4412.
61. Eichhorn, P., Ferguson, P.L., Perez, S., Aga, D.S., Application of Ion Trap-MS with H/D Exchange and QqTOF-MS in the Identification of Microbial Degradates of Trimethoprim in Nitrifying Activated Sludge. *Analytical Chemistry* **2005,** *77*, 4176-4184.
62. Ren, Y. X., Nakano, K., Nomura, M., Chiba, N., Nishimura, O., A Thermodynamic Analysis on Adsorption of Estrogens in Activated Sludge Process. . *Water Research* **2007,** *41*, 2341-2348.
63. Cirja, M., Ivashechkin, P., Schaffer, A., Corvini, P.F.X., Factors Affecting the Removal of Organic Micropollutants from Wastewater in Conventional Treatment Plants (CTP) and Membrane Bioreactors (MBR). *Reviews in Environmental Science and Biotechnology* **2007**.
64. Chiou, C. T., *Partion and Adsorption of Organic Contaminants in Environmental Systems*. John Wiley and Sons: New Jersey, 2002; p 257.
65. Schwarzenbach, R. P., Gschwend, P.M., Imboden, D.M., *Environmental Organic Chemistry*. 2nd Edition ed.; Wiley Interscience: Hoboken, N.J, 2003.
66. Holbrook, R. D., Love, N.G., Novak, J.T., Sorption of 17β-Estradiol and 17α-Ethinylestradiol by Colloidal Organic Carbon Derived from Biological Wastewater Treatment Systems. *Environmental Science and Technology* **2004,** *38*, 3322-3329.
67. Adav, S. S., Lee, D.J., Tay, J.H., Extracellular Polymeric Substances and Structural Stability of Aerobic Granule. *Water Research* **2008,** *42*, 1644-1650.
68. Frolund, B., Palmgrend, R., Keiding, K., Nielsen, P.K., Extraction of Extracellular Polymers from Activated Sludge using a Cation Exchange Resin. *Water Research* **1996,** *30*, (8), 1749-1758.
69. Tsuneda, S., Park, Hayashi, H., Jung, J., Hirata, A., Enhancement of Nitrifying Biofilm Formation using Selected EPS Produced by Heterotrophic Bacteria. *Water Science and Technology* **2001,** *43*, (6), 197-204.
70. Merlo, R. P., Trussel, R.S., Hermanowicz, S.W., Jenkins, D., Effects of Sludge Properties on the Thickening and Dewatering of Waste Activated Sludge. *Water Environment Research* **2007,** *79*, 2412- 2419.
71. Merlo, R. P., Trussel, R.S., Hermanowicz, S.W., Jenkins, D., A Comparison of the Physical, Chemical, and Biological Properties of Sludges from a Complete-Mix Activated Sludge Reactor and a Submerged Membrane Bioreactor. *Water Environment Research* **2007,** *79*, (3), 320-328.
72. Evans, E., Brown, M.R.W., Gilbert , P., Iron Chelator, Exopolysaccharide and Protease Production in *Staphylococcus epidermidis*: A Comparative Study of the Effects of Specific Growth Rate in Biofilm and Planktonic Culture. *Microbiology* **1994,** *140*, (153-157.).
73. Laspidou, C. S., Rittman, B.E., A Unified Theory for Extracellular Polymeric Substances, Soluble Microbial Products, and Active and Inert Biomass. *Water Research* **2002,** *36*, (11), 2711-2720.
74. Grady Jr., C. P. L., Smet, B.F., Barbeau, D.S., Variability in Kinetic Parameter Estimates: A Review of Possible Causes and a Proposed Terminology. *Water Research* **1996,** *30*, (3), 742-748.

75. Grady Jr., C. P. L., Factors Influencing Biodegradation of Synthetic Organic Chemicals in Natural and Engineered Aquatic Environments. *Pure and Applied Chemistry* **1998,** *70*, (7), 1363-1373.
76. Magbanua Jr., B. S., Poole, L.J., Grady Jr., C.P.L, Estimation of the Competent Biomass Concentration for the Degradation of Synthetic Organic Compounds in an Activated Sludge Culture receiving a Multicomponent Feed. *Water Science and Technology* **1998,** *38*, (8-9), 55-62.
77. Foster, J. W., *Bacterial Oxidation of Hydrocarbons.* Academic Press Inc.: New York, 1962.
78. Stirling, D. I., Dalton, H., The Fortuitous Oxidation and Cometabolism of Various Carbon Compounds by Whole-Cell Suspensions of *Methylococcus capsulatus* (BATH). *FEMS Microbiology Letters* **1979,** *5*, 315-318.
79. Grady Jr., C. P. L., Biodegradation: Its Measurement and Microbiological Basis. *Biotechnology and Bioengineering* **1985,** *27*, 660-674.
80. Arp, D. J., Yeager, C.M., Hyman, M.R, Molecular and Cellular Fundamentals of Aerobic Cometabolism of Trichloroethylene. *Biodegradation* **2001,** *12*, 81-103.
81. Criddle, C. S., The Kinetics of Cometabolism. *Biotechnology and Bioengineering* **1993,** *41*, 1048-1056.
82. Rudolph, J. M., Grady Jr., C.P.L, Catabolic Enzyme Levels in Bacteria Grown on Binary and Ternary Substrate Mixtures in Continuous Cultures. *Biotechnology and Bioengineering* **2002,** *79*, (2), 188-199.
83. Cinar, O., Deniz, T., Grady Jr., C.P.L., Effects of Oxygen on Anoxic Biodegradation of Benzoate during Continuous Culture. *Water Environment Research* **2003,** *75*, (5), 434-443.
84. Chang, H. L., Alvarez Cohen, L., Model for the Cometabolic Biodegradation of Chlorinated Organics. *Environmental Science and Technology* **1995,** *29*, 2357-2367.
85. Alvarez-Cohen, L., McCarty, P.L., Effects of toxicity, aeration, and reductant supply on trichloroethylene transformation by a mixed methanotrophic culture. *Applied and Environmental Microbiology* **1991,** *57*, (1), 228-235.
86. Chang, W. K., Criddle, C.S., Experimental Evaluation of a Model for Cometabolism: Prediction of Simultaneous Degradation of Trichloroethylene and Methane by a Methanotrophic Mixed Culture. *Biotechnology and Bioengineering* **1997,** *56*, (5), 492-501.
87. Joss, A., Zabczynski, Z., Gobel, A., Hoffmann, B., Loffler, D., McArdell, C.S., Ternes, T.A., Thomsen, A., Siegrist H., Biological Degradation of Pharmaceuticals in Municipal Wastewater Treatment: Proposing a Classification Scheme. *Water Research* **2006,** *40*, 1686-1696.
88. Schmidt, S. K., Alexander, M., Effects of Dissolved Organic Carbon and Second Substrates on the Biodegradation of Organic Compounds at Low Concentrations. *Applied and Environmental Microbiology* **1985,** *49*, (4), 822-827.
89. Kovarova-Kovar, K., Egli, T., Growth Kinetics of Suspended Microbial Cells: From Single-Substrate-Controlled Growth to Mixed-Substrate Kinetics. *Microbiology and Molecular Biology Reviews* **1998,** *62*, (3), 646-666.
90. Lendenmann, U., Snozzi, M., Egli, T., Kinetics of the Simultaneous Utilization of Sugar Mixtures by Escherichia coli in Continuous Culture. *Applied and Environmental Microbiology* **1996,** *62*, (5), 1493-1499.

91. Harder, W., Dijkhuizen, L., Strategies of Mixed Substrate Utilization in Microorganisms. *Philosophical Transactions of the Royal Society Biological Sciences* **1982,** *297*, 459-480.
92. Grady Jr., C. P. L., Daigger, G. T., The Dynamics of Microbial Growth on Soluble Substrates - A Unifying Theory. *Water Research* **1982,** *16*, 365-382.
93. Andrews, J. F., A Mathematical Model for the Continuous Culture of Microorganisms Utilizing Inhibitory Substrates. *Biotechnology and Bioengineering* **1968,** *10*, 707-723.
94. Ellis, L. B. M., Roe, D., Wackett, L.P. , The University of Minnesota Biocatalysis/Biodegradation Database: The First Decade. *Nucleic Acids Research* **2006,** *34*, D517-D521.
95. Koh, Y. K. K., Chiu, T.Y., Boobis, A., Cartmell, E., Scrimshaw, M.D., Lester, J.N., Treatment and Removal Strategies for Estrogens from Wastewater. *Environmental Technology* **2008,** *29*, 245-267.
96. Inc., M. a. E., *Wastewater Engineering: Treatment and Reuse.* 4th ed.; McGraw Hill: New York, 2003.
97. Rittmann, B. E., and P. L. McCarty., *Environmental Biotechnology: Principles and Applications*. McGraw-Hill: Boston, MA, 2001.
98. Grady Jr., C. P. L., Daigger, G.T., and Lim, H.C., *Biological Wastewater Treatment,*. Second ed.; Marcel Dekker, Inc.: New York, NY., 1999.
99. Akarsubasi, A. T., Eyice, O., Miskin, I., Head, I.M., Curtis, T.P., Effect of Sludge Age on the Bacterial Diversity of Bench Scale Sequencing Batch Reactors. *Environmental Science and Technology* **2009,** *43*, (8), 2950-2956.
100. Ni, B.-J., Fang, F., Rittman, B.E., Yu, H-Q., Modeling Microbial Products in Activated Sludge under Feast-Famine Conditions. *Environmental Science and Technology* **2009,** *43*, (7), 2489-2497.
101. Barker, D. J., Stuckey, D.C., A Review of Soluble Microbial Products (SMP) in Wastewater Treatment Systems. *Water Research* **1999,** *33*, (14), 3063-3082.
102. Pribyl, M., Tucek, F., Wilderer, P.A., Wanner, J., Amount and Nature of Soluble Refractory Organics Produced by Activated Sludge Microorganisms in Sequencing Batch and Continuous Flow Reactors. *Water Science and Technology* **1997,** *35*, (1), 27-34.
103. Barker, D. J., Mannucchi, G.A., Salvi, S.L., Stuckey, D.C., Characterisation of the Soluble Residual Chemical Oxygen Demand (COD) in Anaerobic Wastewater Treatment Effluents. *Water Research* **1999,** *33*, (11), 2499-2510.
104. Fisher, M. M., Triplett, E.W., Automated Approach for Ribosomal Intergenic Spacer Analysis of Microbial Diversity and Its Application to Freshwater Bacterial Communities. *Applied and Environmental Microbiology* **1999,** *65*, (10), 4630-4636.
105. Wagner, M., Nielsen, P.H., Loy, A., Nielsen, J.L., Daim, H., Linking Microbial Community Structure with Function: Fluorescence in situ Hybridization-Microautoradiography and Isotope Arrays. *Current Opinion in Microbiology* **2006,** *17*, 83-91.

CHAPTER 3 – MATERIALS AND METHODS

Christine Klein, Jolanta Skotnicka-Pitak, Dawn Celiz, Seungyun Baik, Susie Mackintosh, Diana Aga contributed to material in this chapter as outlined in the attribution section of this dissertation.

3.1 Materials

Radiolabeled iopromide (^{14}C- IOP) and carbamazepine (^{14}C-CBZ) were obtained from American Radiolabeled Chemicals (St. Louis, MO) and Sigma Chemical Co. (St. Louis, MO, USA), respectively. Non-labeled IOP was purchased from US Pharmacopeia (Rockville, MD) and non-labeled CBZ was purchased from from Sigma Chemical Co. (St. Louis, MO, USA). Deuterium (d4)-labeled 17α-ethinylestradiol-2,4,16,16-d_4 (EE2-d4) was purchased from C/D/N Isotopes, Inc. (Pointe-Claire, Quebec, Canada) and C-14 labeled EE2 (^{14}C-EE2) was a gift from Schering AG, Germany. Non-labeled EE2 was purchased from Sigma Chemical Co. (St. Louis, MO, USA). Dueterium (d9)-labeled trimethoprim (TMP) was purchased from Toronto Research Chemicals Inc, (North York, Ontario, Canada). Non-labeled TMP was obtained from MP Biomedicals (Solon, OH, USA). The purity of all organic microconstituents exceeded 99%.

Acetonitrile, sodium bicarbonate, methanol, and ammonium acetate were obtained from J.T. Baker (Phillipsburg, NJ, USA) and Thermo Fisher Scientific Inc. (Pittsburg, PA). Acetone, formic acid, and toluene were purchased from EM Science (Gibbstown, NJ. USA). Dansyl chloride was purchased from MP Biomedicals (Solon, OH, USA). Catalase (from *Aspergillus niger*) was purchased from Sigma Chemical Co. (St. Louis, MO, USA). All other chemicals used in this study were reagent grade and purchased from Fisher/Thermo Scientific (Pittsburgh, PA).

Stock solutions of non-radiolabeled CBZ (10 g CBZ/L) and non-radiolabeled EE2 (20 g EE2/L) were prepared in acetone. Non-radiolabeled IOP (20 mg/L) and TMP (400 mg/L) were prepared in Nanopure™ water. Various concentrations of radiolabeled CBZ, IOP and EE2 solutions were prepared in acetone.

3.2 Bioreactor Culturing

3.2.1 *Nitrosomonas europaea* culture maintenance

The ammonia oxidizing bacterium (AOB) *Nitrosomonas europaea* (ATCC 19718) was cultured using batch reactors (2 to 5 L) and chemostat reactors (2 L; solids residence time = 7 days) using autotrophic media containing (mg/L): $MgSO_4 \cdot 7H_2O$ (200), $CaCl_2 \cdot 2H_2O$ (20), K_2HPO_4 (87), KH_2PO_4 (405), $Na_2MoO_4 \cdot 2H_2O$ (0.01), $MnSO_4 \cdot H_2O$ (0.017), $CoCl_2 \cdot 7H_20$ (.0004), $CuCl_2 \cdot 2H_2O$ (0.17), $ZnSO_4 \cdot 7H_2O$ (0.01), chelated iron (1), and $(NH_4)_2SO_4$ (3,330). Sterile aeration was provided via stirring for batch reactors or air pumps outfitted with 0.22 μm HEPA® filters for chemostats. pH was controlled by manual (batch; pH 7.5 ± 0.5) addition or automated (chemostat; pH 7.5 ± 0.01) addition of $NaHCO_3$ (50 g/L). Undiluted aliquots (100 μL) from all reactors were periodically plated on Luria Bertani (LB) solid microbiological media and incubated at room temperature for 7 days to determine if heterotrophic contamination was present. Preliminary batch experiments performed to investigate the transformations of all four model microconstituents revealed that phenol red, initially used as a pH indicator in the media, resulted in ionization suppression during liquid chromatography/mass spectrometry (LC-MS) analyses (**Appendix II: Figure II-1**). Therefore, all subsequent experiments were performed using media devoid of phenol red.

3.2.2 Enriched heterotrophic culture chemostat maintenance (designated Ox^- and Ox^+)

Nitrifying mixed liquors from the Blacksburg-VPI Sanitation Authority WWTP (BVPISA) and Peppers Ferry Regional Wastewater Treatment Facility (PFRWWTF) were used to seed a heterotrophic enrichment culture that was acclimated to toluene and benzoate (Ox^+), and a heterotrophic enrichment culture that was grown on acetate and no known aromatic organics (Ox^-). Each enrichment culture was maintained in a well mixed chemostat reactor configured to achieve a solids retention time of 7 days. The Ox^+ reactor was fed an organic feed mixture of toluene (333 mg COD/L), sodium benzoate (333 mg COD/L), and acetic acid (333 mg COD/L). The Ox- reactor was fed 1,000 mg/L acetic acid as COD. Both reactors also received a mineral salts media (MSM) comprised of (mg/L): NH_3-N/L (100), $CaCl_2 \cdot 2H_2O$ (5.3), $FeCl_3 \cdot 6H_2O$ (3), $CoCl_2 \cdot 6H_2O$ (0.3), $ZnCl_2$ (0.31), $CuCl_2 \cdot 2H_2O$ (0.09), H_3BO_3 (0.03), $MgSO_4 \cdot 7H_2O$ (30), $MnSO_4 \cdot 7H_2O$ (0.85), $Na_2MoO_4 \cdot 2H_2O$ (0.12), KH_2PO_4 (54), mg/L K_2HPO_4 (136) and allythiourea (ATU; 10), an inhibitor of AOBs. Dissolved oxygen was provided to the Ox^+ reactor by blending

H_2O_2 (9%) and catalase (16 U/mL; 7 times the stoichiometric requirement) in a drip tube upstream of the reactor to form dissolved O_2 without degassing volatile feed constituents [1]. Oxygen uptake rate measurements indicated that the biomass activity was not inhibited by the addition of chemically-produced O_2 (**Appendix II: Table II.1**). Overall, this aeration method was sufficient for our purposes and an adequate level of dissolved oxygen was maintained in the reactor (DO_{avg} = 4 to 5 mg/L). The Ox^- culture was aerated using air pumps to maintain a dissolved oxygen concentration of 7 to 8 mg/L O_2. Experiments were performed once the mixed liquor suspended solids (MLVSS) of the reactors had stabilized around 200 mg/L and achieved 85 to 95% chemical oxygen demand removal efficiency ($Y_{obs,Ox+}$ = 0.32, $Y_{obs,Ox-}$ = 0.30).

3.2.3 *Pseudomonas aeruginosa* and *Pseudomonas putida* PaW164 culture maintenance

Pseudomonas putida (PaW164) [2] and a strain of *Pseudomonas aeruginosa* capable of degrading methyl ethyl ketoxime [3], were used as positive controls for catechol and toluene dioxygenase assays (Sections **3.10.2** and **3.10.3**) respectively. The strains were reconstituted from frozen stock on LB agar plates and grown at 37°C. Cells from single colonies were transferred and grown in a mineral salt medium denoted PAM9 and comprised of: (mg/L), NaH_2PO_4 (3,000), $NaHPO_4$ (6,000), NH_4Cl (1,000), NaCl (500), $MgSO_4.7H_2O$ (246), $CaCl_2$ (14.7), KH_2PO_4 (17.4), $FeSO_4.7H_2O$ (2.5), $ZnCl_2$ (0.25), $MnSO_4.H_2O$ (0.185), $CuSO_4$ (0.030), $NaMoO_4.2H_2O$ (0.006), $CoCl_2.6H_2O$ (0.001), H_3BO_3 (0.03), and glacial acetic acid (929). pH was adjusted to 7.0 using concentrated HCl. The bacterial cultures were grown at 37°C and stirred at approximately 600 rpm to achieve aeration until mid-exponential phase (optical density of approximately 1.0 at 600 nm). Protein assays were used as an indicator of biomass concentration.

3.3 Sorption Experiments

3.3.1 Sorption experiments with CBZ, EE2, IOP and TMP

Biomass samples were concentrated by centrifugation (10,000×g) and resuspended in MSM. ^{14}C-CBZ (1 μg/L), ^{14}C-IOP (1 μg/L), ^{14}C-EE2 (10 μg/L) and non-radiolabeled TMP (1 mg/L) were added to sacrificial vials containing various biomass concentrations as follows: for NAS, Ox^- and Ox^+ cultures, 100, 500, 1,000, 4,000, and 8,000 mg/L; for AOB, 10, 80, 200, 400, and 800 mg/L. Each vial was supplemented with 650 mg/L sodium azide (NaN_3), which was previously

determined to completely inhibit oxygen uptake (**Appendix II: Table II.2**). Samples were taken at 30 minutes, 24 hour and 7 days after adding the compounds. Each sample was centrifuged at 12,000×g for 30 minutes, after which the supernatant was immediately subjected to liquid scintillation counting (for radiolabeled CBZ, IOP and EE2) or stored for HPLC-UV analyses (TMP) using protocols outlined in **section 3.12.1**. The fraction of compound sorbed to biomass was calculated as the difference between initial and final readings. Abiotic controls were also performed for all experiments and showed that other fates were insignificant (**Appendix I: Tables I.1 to I.19**). All experiments were performed in triplicate at pH 7.5 and at 23^0C.

3.3.2 EPS Extraction and sorption experiment with EE2 and TMP

EPS extractions were performed in the presence of a cation exchange resin (CER, DOWEX 50 × 8, 20-50) as described previously [4]. Briefly, biomass samples suspended in MSM were combined with the CER (70 g DOWEX/g VSS) and mixed at 0.322×g for 12 hours at 4^0C. The CER was removed by centrifugation for 1 min at 13,000×g. The remaining solution contained both biomass and extracted EPS; these fractions were separated by centrifuging at 13,000×g for 15 minutes at 4^0C and retaining the biomass (bottom fraction) and extracted EPS (liquid fraction) separately. Harvested EPS was stored at -20^0C until further analyses could be performed. The solids remaining after EPS extraction were aliquot for additional sorption experiments (^{14}C-EE2 and TMP) using the procedure outlined above (24 hour equilibrium condition only). Control experiments were performed with the CER and showed that residual CER did not affect sorption (**Appendix I: Tables I.17 to I.19**). The membrane integrity of the cells prior to and after EPS extraction was examined via LIVE/DEAD ® *Bac*Light™ Bacterial Viability Kit (Molecular Probes, Invitrogen Corporation, Carlsbad, CA) using the manufacturer's protocol. Slides were analyzed by acquiring ten images per condition using an epi-fluorescence microscope (Axioskop 2, Carl Zeiss, Oberkochen, Germany) controlled by Axiovision® software (Carl Zeiss, Oberkochen, Germany). The LIVE cell numbers and DEAD cell numbers in each image were quantified using ImageJ® (Scion Corp, Frederick, MD). The LIVE fraction (% LIVE) was calculated as the number of LIVE cells divided by the total number of cells stained.

3.3.3 Biomass and EPS Characterization

Biomass, EPS and CER-extracted biomass were characterized by various methods. Total and volatile suspended solids (TSS and VSS) were performed in duplicate using protocols described in **section 3.13.1** [5]. Particle size distribution (PSD) was measured in triplicate using a Horiba LA-700 laser scattering particle size distribution analyzer (HORIBA, Lda., Kyoto, Japan). Zeta potential measurements of cell suspensions were obtained in triplicate using a Malvern Zetasizer Nano ZS (Malvern Instruments Ltd, Worcestershire, UK). Biomass hydrophobicity was measured in duplicate by the microbial adhesion to hydrocarbon (MATH) test [6]. Biomass samples were resuspended in MSM to an initial optical density (OD_{600I}) of 0.5 ± 0.05. Resuspended cells (4 mL) were then mixed vigorously with 0.8 mL of *n*-hexadecane by vortexing for 3 minutes. The mixture was allowed to settle for 15 minutes after which the final aqueous phase OD (OD_{600F}) was measured spectrophotometrically. Microbial adhesion to *n*-hexadecane (the hydrophobic phase) was calculated as a percentage:

$$\%\ \text{Adhesion} = 100\% \times \left[1 - \frac{OD_{600I}}{OD_{500F}}\right] \qquad (3\text{-}1)$$

EPS carbohydrate content was determined by the Dubois method [7]. Total biomass and EPS protein concentrations were measured using the micro-bicinchoninic acid (BCA) method modified with an alkaline digestion step as described in **section 3.13.1**.

3.3.4 Isotherm Development for Sorption Experiments

Data were analyzed using MS Excel® and SigmaPlot 11.0 (SPSS Inc.) by fitting to the Freundlich [8], linear [9] and Langmuir [10] isotherm equations. Linear (TMP only) and non-linear Freundlich (EE2 only) isotherms were determined to provide the best fit to the data and were used as appropriate. Biomass-water distribution coefficients were determined from Freundlich parameters using equation 3-2:

$$K_D = \frac{K_F C_W^{\,n}}{C_W} \qquad (3\text{-}2)$$

Where:

K_D = biomass-water distribution coefficient ($L/kg_{biomass,TSS}$),

K_F = Freundlich coefficient describing sorption to biomass ($\mu g_{pharmaceutical}/kg_{biomass,\ TSS}$)($\mu g_{pharmaceutical}/L)^{-n}$ where biomass is presented on a TSS basis,

n = dimensionless Freundlich constant describing non-linearity,

C_W = aqueous concentration of pharmaceutical at equilibrium ($\mu g_{pharmaceutical}/L$).

The organic matter sorption coefficients were calculated by dividing biomass-water coefficients by the organic matter content of each culture:

$$K_{OM} = \frac{K_D}{f_{OM}} \quad (3\text{-}3)$$

where:

K_{OM} = pharmaceutical sorbed per unit of organic carbon ($L/kg_{biomass,VSS}$),

f_{OM} = VSS/TSS ratio.

Assuming equilibrium conditions and steady state reactor performance, the fraction of sorbed microconstituent was estimated using biomass-water distribution coefficients and mixed liquor concentrations measured in Ox^- and Ox^+ chemostats achieving steady state removal of microconstituents [11]:

$$f_{IS}(\%) = \frac{VSS \times K_{OM}}{1 + (VSS \times K_{OM})} \times 100\% \quad (3\text{-}4)$$

where f_{IS} is the fraction of total microconstituent sorbed onto the organic fraction of biomass (%).

3.4 Batch experiments to investigate the transformation of CBZ, IOP, EE2 and TMP in the presence of AOBs

Batch AOB cultures (2 L) were supplemented with CBZ (1 mg/L ^{12}C-CBZ), EE2 (1 mg/L ^{12}C-EE2 and 10 μg/L ^{14}C-EE2), IOP (1 mg/L ^{12}C-IOP and 10 μg/L ^{14}C-IOP) or TMP (1 mg/L ^{12}C-TMP) and incubated over a single growth curve as confirmed by control reactors (9 days for CBZ or 28 days for EE2, IOP and TMP). Cultures supplemented with EE2, IOP and TMP experiments were inoculated with less biomass (~6 x 10^5 cells) than CBZ experiments (~2 x 10^6 cells) in an effort to minimize heterotrophic contamination. This resulted in the longer incubation period required for EE2, IOP and TMP experiments. For experiments with radiolabeled

substrates, reactors were outfitted with two 1 N NaOH traps in series to capture volatilized radiolabeled carbon dioxide. Samples from these caustic traps were analyzed for radioactivity using protocols discussed **in section 3.13.5**. CBZ, EE2 and TMP samples obtained from these AOB batch experiments were centrifuged at 13,000×g and the aqueous phase was lyophilized at -80^{0}C and shipped to SUNY Buffalo for LC/MS analysis. IOP samples from AOB experiments were loaded onto OASIS® HLB cartridges (500 mg) at a rate of 2 mL/min and shipped to SUNY Buffalo for LC-radiochromatograph/MS analysis. These cartridges were preconditioned with 6 mL of ACN followed by 12 mL of Nanopure water. Negative control experiments (no microconstituent) and abiotic experiments (with microconstituent, but no bacteria) were also performed. All biological fate experiments (except AOB CBZ experiments) were performed in duplicate.

3.5 Batch experiments to investigate the transformation of CBZ, EE2 and TMP in the presence of heterotrophic cultures

Ox^- and Ox^+ batch cultures were supplemented with 100 mg/L primary substrate (acetate for Ox^-; 33 mg acetate-COD/L, 33 mg benzoate-COD/L, and 33 mg toluene-COD/L for Ox^+) and 1 mg/L non-radiolabeled CBZ, EE2 or TMP, and incubated for 7 days. Grab samples (250 mL) at specific timepoints were collected and processed for subsequent analysis. Each aliquot was centrifuged at 12,000×g for 30 min at 4^{0}C to remove suspended solids and frozen at -80^{0}C. Samples from Ox^- and Ox^+ batch tests were subsequently analyzed via HPLC-UV protocols outlined in **section 3.12.1**. All biological fate experiments were performed in duplicate.

3.6 Chemostat experiments to investigate the transformation of EE2 and TMP under nutrient-limited conditions

3.6.1 EE2 and TMP transformation with Ox^- and Ox^+ chemostats

Feed stocks for continuous flow Ox^- and Ox^+ cultures were supplemented to a final concentration of 1 mg unlabeled EE2/L and 10 μg ^{14}EE2/L, or 1 mg TMP/L. Duplicate chemostat cultures were maintained for at least 21 days during which grab samples (100 to 200 mL, depending upon experimental need) were obtained and centrifuged at 10,000×g for 30 min at room temperature to remove suspended solids, then stored at -80^{0}C. EE2 samples were lyophilized at -80^{0}C while TMP samples were loaded onto OASIS® HLB cartridges (5 mg) that were preconditioned with 4

mL of ACN followed by 8 mL of Nanopure water. Two NaOH traps were connected in series to the ^{14}EE2-fed chemostat to sequester $^{14}CO_2$ from the headspace. Oxygenase assays (toluene dioxygenase and catechol dioxygenase) were performed before radiolabeled substrates were introduced, as described in **section 3.10**.

3.6.2 EE2, TMP and byproduct transformation by AOB-Ox^- and AOB-Ox^+ chemostats in series

Duplicate Ox^- and Ox^+ chemostats were fed effluent from AOB chemostats to determine the subsequent fate of metabolites generated from these reactors. Experiments were performed over 21 days during which grab samples (100 mL) were collected. These grab samples were centrifuged at 10,000×g for 30 min at room temperature and then stored at -80^{0}C. Subsequently, these samples were combined (400 mL) to ensure that sufficient radioactivity was present for radiochromatographic analysis (as described in section **3.12.5**). NaOH traps were used to monitor the degree to which radiolabeled substrates and metabolites were mineralized.

3.6.3 Transient organic loading experiments with Ox^- chemostats

Ox^- reactors, supplemented with 1 mg/L EE2 or TMP, were operated to achieve steady state removal of readily biodegradable substrate (rbCOD) and microconstituents (at least 3 SRTs). Once steady state was achieved, a step input of 100 mg acetate-COD/L was introduced to the chemostats and effluent samples were monitored for soluble COD and microconstituent concentrations. Extant biotransformation kinetic measurements were also performed on each culture at different stages of recovery (Pre-spike, 2 hr, and 7 days after the spike). Extra- and intra-cellular NADH concentrations were also monitored. Experiments were performed in duplicate.

3.7 Kinetic experiments

3.7.1 Whole cell EE2 and TMP biotransformation rates in chemostats

Chemostat cultured cells (AOB, Ox^-, Ox^+) were harvested, washed and resuspended into MSM that was supplemented with chloramphenicol (100 mg/L) to inhibit new protein synthesis [12]. EE2 (200 µg/L) or TMP (200 µg/L) and NH_3 (15 mg N/L for AOB experiments) were added and well mixed to start the kinetic assay. Aliquots were collected ever y 30 minutes and monitored

for nitrite, total protein, and microconstituent (EE2 or TMP) concentrations. Aliquots for nitrite analysis were filtered through a 0.45 μm nylon filter while aliquots for protein or microconstituent concentration were centrifuged for 10 min. at 10,000×g and immediately frozen at -80^{0}C. Defined mixtures of AOB (5 or 6% protein content) and Ox^- (94% protein content) and Ox^+ (95% protein content) cultures were also prepared for batch EE2 kinetic experiments. Abiotic (EE2 or TMP in sterile MSM) and sorption (EE2 or TMP with NaN_3 inactivated biomass) controls were also performed.

To determine the effect of nitrite and soluble microbial products (SMPs) on EE2 degradation rates, chloramphenicol treated cells were supplemented with various concentrations of nitrite (10, 200, 600 mg NO_2^--N/L) or extracted SMPs and 200 μg/L EE2. EE2 degradation and total protein content were monitored as described in section **3.12.1** and **3.13.1** respectively. All experiments were performed in duplicate and results were tested for statistical difference from the unspiked control using the two-tailed students's t-test ($\alpha = 0.025$).

3.7.2 Estimation of pseudo-first order rate constant (k_{EE2} and k_{TMP})

Biodegradation of microconstituents (**equation 3-5**) and growth of biomass (**equation 3-6)** under batch conditions can be described using substrate consumption or Monod kinetics (ignoring biomass decay):

$$\frac{dS_{EE2\ or\ TMP}}{dt} = -q_{max,H,EE2\ or\ TMP}\left[\frac{S_{EE2\ or\ TMP}}{K_{S,EE2\ or\ TMP} + S_{EE2\ or\ TMP}}\right]X_H \qquad (3\text{-}5)$$

$$\frac{dX_H}{dt} = \mu_{H,EE2\ or\ TMP}\left[\frac{S_{EE2\ or\ TMP}}{K_{S,EE2\ TMP} + S_{EE2\ or\ TMP}}\right]X_H \qquad (3\text{-}6)$$

where

$q_{max,H,EE2\ or\ TMP}$ = maximum specific utilization rate (mg EE2 or TMP as COD/mg biomass as COD-day),

$\mu_{EE2,H,EE2\ or\ TMP}$ = maximum specific growth rate (1/day),

$S_{EE2\ or\ TMP}$ = microconstituent concentration (mg EE2 or TMP as COD/L),

X_H = biomass concentration (mg biomass as COD/L),

$K_{S,EE2\ or\ TMP}$ = half saturation constant (mg EE2 or TMP as COD/L).

Under extant condition when S_0/X_0 ratios are below 20 [13], it is not necessary to solve **equation 3-6** since growth can be ignored [14]. Additionally, it was assumed that both microconstituents were present at concentrations below the half saturation constant, i.e. S_{EE2} and $S_{TMP} << K_{S,EE2}$ and $K_{S,TMP}$ respectively). This allowed simplification of **equation 3.5** to:

$$\frac{dS_{EE2\ or\ TMP}}{dt} = -\left[k_{EE2\ or\ TMP}\right]\left[S_{EE2\ or\ TMP}\right]\left[X_H\right] \qquad (3\text{-}7)$$

where

$$k_{EE2\ or\ TMP} = \left[\frac{q_{max,H,EE2\ or\ TMP}}{K_{S,EE2\ or\ TMP}}\right] \qquad (3\text{-}8)$$

$k_{,EE2\ or\ TMP}$ is the pseudo-first order rate constant (L/mg biomass as COD-day). Pseudo-first order transformation rate constants were estimated from extant batch test data in Matlab® by combining non-linear regression techniques and fourth order Runge Kutta approximations to solve equation 3-7 (**Appendix II: Section II-4.a**).

3.8 Short term co-metabolism experiments

Ox^- and Ox^+ chemostat cultures were centrifuged at 13,000×g for 30 min at room temperature to remove residual organics, and resuspended in MSM. To initiate the assays, duplicate batch reactor vessels (40 mL in scintillation vials) were supplemented with ^{14}C-EE2 only (200 μg/L) or ^{14}C-EE2 (200 μg/L) plus NADH (5 mM). Sorption controls consisted of cell suspensions supplemented with sodium azide (650 mg/L), previously shown to inhibit oxygen uptake rates (**Appendix II: Table II.2**), and ^{14}C-EE2 (200 μg/L). Negative controls consisted of MSM, EE2 and sodium azide at concentrations mentioned previously. Each vial was equipped with a 1N NaOH trap and was aerated using sterile humidified air. Samples, taken at 12 hr intervals over the course of a 48 hour incubation, were centrifuged at 10,000×g for 30 min at room temperature

and the aqueous fraction was subject to immediate liquid scintillation counts (LS) as described in **section 3.13.5**. Solid fractions were digested with 1N NaOH at 105^0C for 15 mins and then subject to LS counting protocols and protein determination as described in **sections 3.13.5** and **3.13.1** respectively. Samples from caustic traps were also counted using similar procedures. Intracellular and extracellular NADH concentrations were also determined as detailed in **section 3.13.4**.

3.9 Long term co-metabolism experiments

Various concentrations of acetate (5.4, 2.7, 1.4, mg as COD/L) and EE2 or TMP (5.4, 2.7, 1.4 mg as COD/L) were added in triplicate to untreated 96 well polypropylene plates (Fisher/Thermo Scientific (Pittsburgh, PA) and evaporated to dryness. Cell suspensions, containing diluted Ox^- or Ox^+ cells were prepared as described for the short term experiments and added to each well. Plates were incubated in a humidified chamber at room temperature for 14 days during which turbidity (600 nm) measurements were quantified using a Biotek uQuant microplate spectrophotometer (Vermont, USA). Controls (water, solvent, negative, abiotic) were also run in triplicate. Changes in OD_{600} were compared to control wells to determine whether growth occurred. Direct comparison of slopes describing exponential growth phases in wells supplemented with EE2 versus wells supplemented with acetate only were performed in MS Excel® using the two-tailed student's *t*-test ($\alpha = 0.025$, n = 9). To confirm the relevance of using the parametric *t*-test, normality was checked using the Kolmogorov-Smirnov test in SigmaPlot 11 (SPSS, 2008).

3.10 Enzyme kinetic bioassays

3.10.1 Whole cell ammonia monooxygenase assay

Ammonia monooxygenase (AMO) activity was measured indirectly by a specific whole cell nitrite generation rates (NGR) assay as described previously [15] with modifications as follows. Cells from continuous flow AOB reactors were immediately supplemented with 100 mg/L chloramphenicol to minimize new protein synthesis [16], centrifuged at 13,000×g for 10 min at room temperature and resuspended into autotrophic media minus ammonia and amended with chloramphenicol. The reaction was initiated by adding 15 mg NH_3-N/L, and samples were collected every 30 minutes over a period of 3 hours at room temperature. Samples were analyzed

for nitrite concentrations according to the method given in section 3.13.2. Plots of nitrite versus time were generated, and the slope of the line that gave the lowest residual square error was determined and called the nitrite generation rate (NGR, mg N/L-min). Specific NGR (sNGR, mg N/mg protein-day) values were calculated by dividing NGRs by the protein concentration of the assay mixture. Experiments confirmed that minimal cell growth occurred over the 3 hour incubation period (data not shown). All AMO assays were performed in duplicate.

3.10.2 Toluene dioxygenase assay

Toluene dioxygenase (Tod) activity was measured by monitoring the conversion of indole to indigo by whole cell suspensions as described previously [17]. Briefly, cells from Ox^- and Ox^+ reactors were centrifuged at 12,000×g for 10 min at room temperature and resuspended in 1 X phosphate buffered saline solution (PBS; NaCl 7.6 g/L, NaH_2PO_4 0.38 g/L; Na_2HPO_4 0.97 g/L, pH 7.5). This procedure was repeated three (3) times to ensure complete removal of electron donor. The assay was performed at 37^0C for 60 min and was initiated by the addition of indole (100 μM). Cell associated indigo was extracted by resuspending cells in dimethyl-formamide (DMF) and centrifuging at 12,000×g for 5 min. The rate of indigo production was determined by measuring the optical density of the supernatant at 610 nm over time and converting to a molar basis using the extinction coefficient for indigo (ε = 15900 L/mol-cm) [18]. Specific rates of indigo production were obtained by normalizing rates using the protein concentration of the cell mixture. Experiments confirmed that minimal cell growth occurred over the 1 hour incubation period (data not shown). All Tod assays were performed in duplicate.

3.10.3 Catechol 1,2-dioxygenase (C12O) and catechol 2,3-dioxygenase (C23O) assays

Intradiol and extradiol catechol dioxygenase activities were measured as described previously [19, 20]. Briefly, cells from Ox^- and Ox^+ reactors were prepared as per the Tod assay described above. The cell suspension was then subjected to six rounds of sonication (30 sec bursts at 30% output with 30 sec rest period on ice) using a Branson Sonifier 250 (Branson Ultrasonics Corp., Danbury, CT). Cell free extracts (CFE) were then obtained by centrifuging the lysed cell mixture at 12,000×g for 60 min at 4^0C. Catechol 1,2 dioxygenase (C12O) activity was determined by adding catechol (4 mM) to the CFE and monitoring the rate of cis,cis muconate formation at

OD_{260nm} over a 5 min period at room temperature. The conversion of 1 μmol of catechol to cis, cis muconate results in a change of absorbance of 5.6 units at 260 nm [21]. Catechol 2,3 dioxygenase (C23O) activity was determined by measuring the rate of 2-hydoxy-cis,cis muconic semialdehyde formation at OD_{375nm}. The conversion of 1 μmol of catechol to 2-hydoxy-cis,cis muconic semialdehyde results in a change of absorbance of 14.7 units at 375 nm [21]. Specific C12O and C23O activities were determined by normalizing to CFE protein content. All C12O and C23O assays were performed in duplicate.

3.11 Inhibition assays

Oxygen uptake (sOURs) and NGRs were used to determine the degree of inhibition exerted by various concentrations of microconstituents on heterotrophic and AOB cultures.

3.11.1 Specific oxygen uptake rate assay for heterotrophic inhibition

Forty mL of cells from heterotrophic chemostats were harvested, aerated and supplemented with various concentrations of EE2 or TMP (0.01, 1, 10 mg/L) and acetate (0, 50 mg as COD/L). Oxygen uptake rates (OURs) were determined in duplicate using Orion model 97-08 oxygen electrodes (Orion Research, Inc., Beverly, MA) connected to an Accumet dual channel pH/Ion meter (model AR25) such that DO readings were recorded every 6 seconds using an automated data acquisition system (Labview 6.0). The OUR is the slope of the line representing the least residual square error fit to the dissolved oxygen concentration versus time. Endogenous and solvent controls were also performed. sOUR values were determined by dividing OUR values by the protein content of samples obtained at the end of each test. To determine the effect of nitrite on heterotrophic respiration, sOURs were obtained for heterotrophic cultures that were supplemented with various concentrations of nitrite (10, 200, 600 mg NO_2^--N/L). Percent inhibition was calculated as the difference between rates in the absence (control) and presence of EE2 or TMP divided by the control rate (x 100%):

$$\text{Percent Inhibition (\%) sOUR} = \frac{\text{sOUR}_{\text{control}} - \text{sOUR}_{\text{EE2 or TMP}}}{\text{sOUR}_{\text{control}}} \times 100\% \qquad (3\text{-}9)$$

All experiments were performed in duplicate or quadruplicate and results from cultures supplemented with EE2, TMP or nitrite were tested for statistical difference against control cultures (no microconstituent or nitrite additions) using the two-tailed student's t-test ($\alpha = 0.025$) using MS Excel®.

3.11.2 Specific nitrite generation rate assay for AOB inhibition

For NGRs, 500 mL of AOB cells at mid exponential phase were harvested, washed in $MgPO_4$ buffer (100 mM KH_2PO_4, 1 mM $MgCl_2$, pH 8.0) at 13,000 x g for 30 min and resuspended in 300 mL of autotrophic media devoid of ammonia. This cell mixture was aerated and then supplemented with various concentrations of EE2 or TMP (0.01, 1, 10 mg/L) and 28 mg NH_3-N/L. Nitrite generation was monitored every 30 minutes over a period of 3 hours, and the least squared error of the best fit line of a plot of nitrite concentration versus time was used to determine NGR. sNGR values were determined by dividing NGR values by the protein concentration of samples collected at the end of each test. Percent inhibition as determined by sNGR was calculated in a similar manner to that described for sOURs (**Section 3.11.1**):

$$\text{Percent Inhibition (\%) sNGR} = \frac{\text{sNGR}_{\text{control}} - \text{sNGR}_{\text{EE2 or TMP}}}{\text{sNGR}_{\text{control}}} \times 100\% \qquad (3\text{-}10)$$

All experiments were performed in duplicate or quadruplicate and results from cultures supplemented with EE2 or TMP were tested for statistical difference against control cultures (no microconstituent additions) using the two-tailed student's t-test ($\alpha = 0.025$) using MS Excel®.

3.12 Spectrometric and spectroscopic chemical analyses

All analyses described in sections **3.12.2** to **3.12.6** were performed by researchers at SUNY Buffalo as outlined in the attribution section of this dissertation. All other analyses were performed at Virginia Tech.

3.12.1 High performance liquid chromatography and UV-VIS diode array (LC-UV)

CBZ, EE2 and TMP were analyzed with a Hewlett Packard 1090 HPLC equipped with UV–VIS diode array detector. Separation was achieved using a Thermo Scientific Betabasic C_{18} column

(100 x 2.1 mm i.d., 3.0 µm particle size) with a Thermo Scientific Betabasic C_{18} guard column (10 x 2.1 mm i.d., 3 µm particle size). The mobile phases are described in **Table 3.1** and were delivered at a constant flow rate of 0.2 mL/min. Quantification was performed by constructing external standard curves (10 mg CBZ/L to 0.1 mg CBZ/L; 2 mg EE2/L to 200 ng EE2/L; 2 mg TMP/L to 0.01 mg TMP/L) with use of internal standards (**Table 3.1**). Recovery of spiked additions exceeded 85% for all microconstituents tested.

Benzoate was also measured in duplicate using the Hewlett Packard 1090 HPLC. Separation was achieved using an Alltech Econosphere C_{18} column (250 x 4.6 mm i.d., 5.0 µm particle size) with a Thermo Scientific Betabasic C_{18} guard column (10 x 2.1 mm i.d., 3 µm particle size) and a mobile phase (pH 4.2) comprised of acetonitrile (10%) and ammonium acetate (3.8 mM; 90%) delivered at a constant flow rate of 1 mL/min. The total runtime of the HPLC analysis was 20 min with detection at 225 nm. Quantification was performed through use of an external standard curve (1 mg benzoate/L to 500 mg benzoate/L). Samples were filtered through 0.45 µm nylon filters and stored at -20^0C for up to 1 month prior to analyses.

Table 3.1. Conditions used for HPLC-UV detection of microconstituents.

Compound	Internal Standard	Mobile Phase	Runtime (min)	UV Detection Wavelength (nm)	% Recoveries
CBZ	10,11-dihydrocarbamazepine; 1 mg/L	Methanol (75%) /NANOpure™ water (25%)	15	254, 281	90-105
EE2	17β-estradiol; 0.1 mg/L	Acetonitrile (35%)/NANOpure™ water (65%)	15	254, 281	95-102
TMP	Allythiourea; 10 mg/L	Methanol (11%) / 20 mM NaH_2PO_4 (89%)	45	231, 254	85-104

3.12.2 EE2 analysis by liquid chromatography/mass spectrometry (LC/MS)

Lyophilized samples from AOB, Ox^- and Ox^+ experiments (**Sections 3.4 and 3.6**) were reconstituted in 10 mL of Nanopure™ water, supplemented with deuterated internal standards (EE2-d_4) and analyzed using a single quadrupole Agilent 1100 MSD LC/MS system. Separation was achieved using a Thermo Scientific Betabasic C_{18} column (100 x 2.1 mm i.d., 3.5 μm particle size) with a Thermo Scientific Betabasic C_{18} guard column (10 x 2.1 mm i.d., 3 μm particle size), using gradient elution starting with 40% acetonitrile (ACN) and 60% H_2O with 50 mM ammonium acetate, to 100% ACN over a 16 minute gradient. Mass spectrometry was performed in negative mode using selective ion monitoring (SIM) of EE2, the internal standard, and the known metabolites E1 and E3. Full scan monitoring of m/z ratios from 200 – 500 was also performed on each sample. As scans in positive mode did not yield any useful data, all subsequent analyses were performed in negative ESI mode. To enhance the signal of EE2 in LC/MS, EE2 was derivatized with dansyl chloride to produce a derivative (**Figure 3-1**) that has higher ionization efficiency in LC/MS, thereby improving the detection limit for EE2.

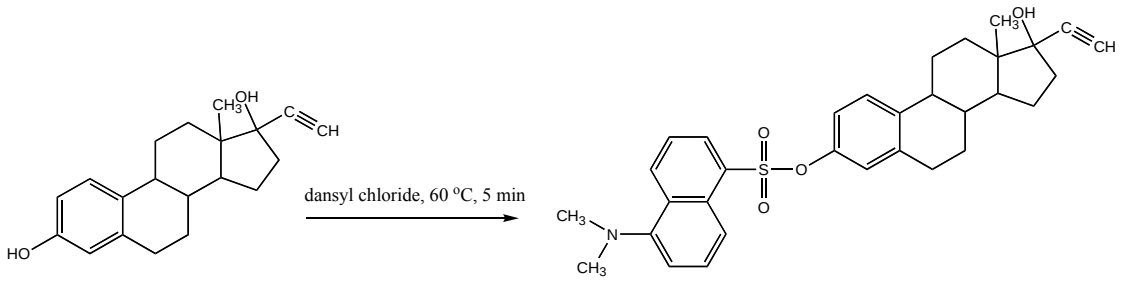

Figure 3-1. Derivitization of EE2 (left) with dansyl chloride to produce conjugate (right). Adapted from [22].

3.12.3 TMP analysis by liquid chromatography/mass spectrometry (LC/MS)

Oasis® HLB SPE cartridges that had been loaded with samples at Virginia Tech were sent to the University of Buffalo. Once there, they were eluted twice with 4 mL of acetonitrile into a glass tube, evaporated under nitrogen and then diluted to a final sample volume of 1 mL. The samples were analyzed by LC/MS/MS using a LCQ Advantage™ ion trap mass spectrometer with an electrospray ionization (ESI) source in positive ion mode (Thermo Finnigan, San Jose, CA, USA). Separation was achieved using a Thermo Scientific Betabasic C18 column, (100 X 2.1mm i.d, 3µm particle size), equipped with a Thermo Scientific guard cartridge (10 X 2.1mm i.d., 3µm particle size), using gradient elution starting with 5% ACN and 95% water with 0.3% formic acid, which was to 70% ACN over 11 minutes and then held for10 minutes. The flow rate was set at 250 µL/min, the injection volume was 10 µL, and the column oven temperature was held at 30°C. The total run time was 22 minutes including post-run protocols.

3.12.4 Identification of EE2 metabolites using liquid chromatography with ion-trap mass spectrometry (LC-ITMS)

In order to obtain more information on the chemical structure of unknown metabolites, reconstituted samples were further analyzed by LC-ITMS using an LCQ Advantage™ liquid chromatograph / ion trap mass spectrometer system equipped with an electrospray ionization (ESI) source (Thermo Finnigan). The chromatographic conditions were the same as described in section 3.12.2. Negative ESI was used for all analytes, either in SIM or selected reaction monitoring (SRM) to minimize the matrix effects from the samples and to increase sensitivity. The parent ion (m/z of unknown metabolite, as identified using single quad LC/MS) was

fragmented into its daughter ions, which in turn were fragmented to produce MS^3 spectra for structural characterization.

3.12.5 Liquid radiochromatography and mass spectrometry (LrC/MS) analysis

For samples with ^{14}C IOP and EE2, analysis was performed using the Agilent 1100 HPLC equipped with an on-line radiochromatographic detector (IN/US Systems, Inc., Tampa, FL), which uses a flow through cell with a volume of 0.5 mL and a 3:1 scintillation fluid:eluent ratio (Ecoscint, National Diagnostics, Atlanta, GA). Separation was achieved using a C8 column (Agilent ZORBAX C8 5µm, 4.6 x 250mm) using a gradient elution starting at 30/70 (v:v) ACN:H_2O with 50 mM ammonium acetate, with solvent composition changed to 100% ACN over a 30-min run using a constant flow rate of 3.5 mL/min. Once retention times of the peaks were established, an aliquot of the sample was re-injected into the LC column and fractionated to isolate each of the radioactive peaks. The isolated peaks were then analyzed by LC/MS.

3.12.6 Nuclear Magnetic Resonance (NMR) Analysis of Pharmaceutical Metabolite

EE2 and metabolites identified through mass spectrometry were eluted from OASIS® HLB cartridges (500 mg) using acetone and subsequently evaporated to dryness. Samples were reconstituted in H_2O/Acetonitrile (ACN) (90%/10%) and initially fractionated via HPLC (Waters Delta 600, MA, USA). Separation was achieved with a reversed phase C-18 column (Agilent ZORBAX C8 5µm, 4.6 x 250mm) using a gradient elution starting with acetonitrile and 50 mM ammonium acetate (25%/75%) to 85% ACN over a 45 minute period at a constant flow rate of 3.5 mL/min. Fractions were collected every 1 min and further analyzed using a single quadrupole Agilent 1100 MSD LC/MS system (Agilent Technologies, CA, USA) to verify presence and purity of the M386 metabolite. Separation was performed with a reversed phase C-18 column (BetaBasic-18 3µm, 100 x 2.1mm) and gradient elution starting with 40% acetonitrile and 60% 50 mM ammonium acetate, changing to 100% ACN over a 10 minute interval. Mass spectrometry was performed in negative mode using SIM for EE2, and metabolites. Full scan monitoring of m/z ratios from 200 – 500 was also performed. Fractions containing metabolites were evaporated to dryness, reconstituted in CD_3OD and transferred to NMR tubes. ^1H NMR data was performed with Inova-500 MHz NMR Spectrometer (Varian, CA, USA).

3.12.7 Ion chromatography

Acetate was measured in duplicate using a DX-120 ion chromatograph equipped with an AG4A-HC guard column (4 mm), IonPac AS4A-SC (4 x 250 mm) column and an IonPac AS14 (4 x 250 mm) column arranged in series (Dionex Corporation, Sunnyvale, CA). The eluent consisted of 5 mM sodium borate and was delivered at a flow rate of 1.0 mL/minute. Concentrations were determined using an external standard calibration curve with a linear range from 2 to 200 mg/L acetate. Samples were passed through 0.45 μm nylon filters and stored at -20^{0}C for up to 1 month prior to analyses.

3.12.8 Gas chromatography

Toluene was analyzed with a Hewlett Packard 5890 gas chromatograph (GC) equipped with a 30 m poly(alkylene glycerol) 0.25 mm i.d. capillary column , with a film thickness of 0.25 μm (Supelco Inc., Bellefonte, PA), and a 5 m guard column using procedures outlined previously [1]. Briefly, a split injection was used at a ratio of 1:30. The injection port temperature was 250^{0}C, and the FID temperature was 260^{0}C. Helium was used as a carrier gas at a column head pressure of 15 psi and a column flow rate of 1.46 mL/min. The initial column temperature was 70^{0}C for 10 minutes then the temperature was increased at a rate of 10^{0}C/min up to a final temperature of 120^{0}C. Toluene in mixed liquid suspended solids samples collected from the reactors was determined by directly extracting with hexanes for 2 hours on a rotary mixer at an extraction ratio of 7 parts sample to 1 part hexanes in a 16 ml vial containing a teflon-lined cap. After extraction, the liquid and solvent mixture was separated by centrifugation (1900 ×g) and the extract was transferred into a 2 ml GC autosampler vial and stored at 4 °C until analyzed.

3.13 Wet chemistry analytical methods

3.13.1 Solids analyses, cell counts and total protein determination

Total and volatile suspended solids (TSS and VSS) were performed as described previously [5]. Briefly, 0.1 L of heterotrophic culture was filtered through pre-weighed 1.2 μm glass fiber filters (W_0 in grams) that were prepared by rinsing with NANOpure™ water and baking at 550^{0}C for 20 minutes. Filters loaded with samples were incubated at 105^{0}C for 1 hour, weighed (W_1 in grams), baked at 550^{0}C for 20 minutes and then weighed again (W_3 in grams). TSS and VSS

were computed as explained in Standard Methods [5]. All mass measurements were made using a Mettler H10 balance with sensitivity to 0.0001 grams. TSS and VSS were only performed on reactors not receiving radiolabeled substrates.

Cell counts for *N. europaea, P. aeruginosa, P. putida* were performed using a Helber bacteria single round cell counting chamber manufactured by Weber Scientific International (Middlesex, UK). Briefly, 10 μL of cells were placed onto the chamber and viewed in phase contrast mode using a using an epi-fluorescence microscope (Axioskop 2, Carl Zeiss, Oberkochen, Germany) controlled by Axiovision® software (Carl Zeiss, Oberkochen, Germany). Cells within ten randomly chosen grids were counted and averaged. Total cells counted were calculated as follow:

$$\text{Cell counts}\left(\frac{\text{cells}}{\text{mL}}\right)=\frac{(\text{X})\left(1000\frac{\text{mm}^3}{\text{mL}}\right)}{(\text{S}^2)(\text{D})} \qquad (3\text{-}13)$$

Where X = average number of cells counted in 10 wells (cells)

S = dimension of counting square (0.05 mm)

D = depth between coverslip and counting chamber (0.02 mm)

Total protein content was measured using the micro-bicinchoninic acid (BCA) method modified with an alkaline digestion step [23]. Briefly, cells were resuspended to a final concentration of 1 M NaOH and incubated at 105^0C for 15 min prior to addition of microBCA reagents. All standards were prepared in 1N NaOH and supplemented with chloramphenicol or sodium azide as necessary per experimental conditions. Total protein content was used to monitor biomass concentrations in reactors receiving radiolabeled substrates.

3.13.2 Nitrogen species analyses

Samples for nitrogen analyses were filtered through 0.45 μm filters and frozen (nitrite and nitrate) or acidified with 5N H_2SO_4 to pH 2 and stored at 4^0C for up to 1 month. Nitrite and ammonia concentrations were analyzed colorimetrically in duplicate using the Griess reagent and

phenate methods, respectively [5]. Nitrate was determined via ultraviolet spectrophotometric detection at 229 nm [24]. To account for nitrite interference, samples were acidified with concentrated H_2SO_4 and total oxidized nitrogen was measured. Nitrate concentrations were determined by subtracting nitrite concentrations obtained from Greiss assays from the total oxidized nitrogen concentration. Controls were performed using spiked additions to determine the percent recovery of standards in the matrix of the samples; recoveries always exceeded 85%.

3.13.3 Soluble chemical oxygen demand analyses

Soluble chemical oxygen demand was measured via the closed reflux method as described previously [5] with minor modifications. Briefly, samples were filtered through 0.45 μm filters and acidified with 5N H_2SO_4 to pH 2 and stored at 4^0C for up to 1 month. Upon addition of reagents (17 mM $K_2Cr_2O_7$, 5.6 mM $HgSO_4$, 32 mM $AgSO_4$), samples were digested at 150^0C for 2 hours and then cooled to room temperature. At this point, samples were analyzed via spectrophotometry at 600 nm. External standard curves were constructed using potassium hydrogen phthalate (0 – 500 mg as COD/L) and sample concentrations were determined by direct comparison to this standard curve. Spiked additions were also performed during each digestion and used to determine the percent recovery, which always exceeded 90%.

3.13.4 Nicotinamide adenine dinucleotide extraction and analyses

The reduced form of nicotinamide adenine dinucleotide (NADH) was determined using protocols outlined by Wos et al. [25] with minor modifications. Briefly, extracellular NADH content was measured in centrifuged supernatant by obtaining absorbance readings at 370 nm using a Biotek uQuant microplate spectrophotometer (Vermont, USA) and comparing to an external standard curve (1 mM to 350 mM). Solid fractions were resuspended in Tris buffer (0.02 M) and heated at 80^0C for 30 min. Intracellular NADH measurements (OD_{370nm}) of the aqueous fraction were obtained after centrifugation of the lysis mixture at 10,000 x g for 15 min. Controls were performed using spiked addition to determine recovery within the sample matix, and recoveries greater than 98% were obtained.

3.13.5 Liquid scintillation counting

Liquid scintillation counts for radiolabeled experiments were performed on an LS1800 Beckman Coulter system (maximum counting time of 5 minutes) by adding 0.1 mL of sample and 5 mL of Scintiverse^{TM} BD scintillation cocktail (Fisher Scientific, USA). Quench was accounted for by using external quench standards and sample to channel ratio. This protocol was adopted after extensive testing of alternative sample to cocktail ratios (**Appendix III: Figure III-1** and **Tables III.1** to **III.3**).

3.13.6 Recombinant Yeast Estrogen Screen (YES) Assay

Estrogenic activity of fractionated and unfractionated reactor effluent was determined using protocols described previously with minor modifications [26-28]. Briefly, a recombinant S*accharomyces cerevisiae* culture containing an expression plasmid carrying the *lac*-Z reporter gene (obtained from Dr. Sumpter of Brunel University (Middlesex, UK)) was incubated in the presence of estrogenic compounds and chlorophenol-red-β–D-galactopyranoside. Upon expression of the *lac*-Z gene, β-galactosidase is secreted into the medium causing a color change (yellow to red) that is proportional to the concentration of estrogenic substance.

Standards (17-β estradiol; E2) and samples were added in triplicate to untreated 96 well polypropylene plates (Fisher/Thermo Scientific (Pittsburgh, PA)) and evaporated to dryness. Cell suspensions containing CPRG and *S. cerevesiae* cells sampled from exponential growth phase (100 μL at OD 1.0 per 50 mL YES medium) were added to each well. Plates were incubated at 32^0C for 48 hours after which turbidity (620 nm) and color change (575 nm) were quantified using a Biotek uQuant microplate spectrophotometer (Vermont, USA). Absorbance was corrected for turbidity interference using equation 3-14 [26], and E2 standard curves were plotted for each plate:

Corrected ABS =

$$\text{ABS 575 nm}_{(\text{sample})} - [(\text{ABS 620 nm}_{(\text{sample})} - \text{ABS 620 nm}_{(\text{blank})})] \qquad (3\text{-}14)$$

The estrogenic activity of samples (quantified as E2 equivalence) was determined by direct comparison of corrected sample absorbances to the linear portion of 17β-estradiol standard

curves. Negative controls were run on each plate and consisted of absolute ethanol and sterilized NANOpure™ water while abiotic controls consisted of YES medium minus *S. cerevesiae* cells.

3.14 References

1. Ma, G., Love, N.G., BTX Biodegradation in Activated Sludge under multiple Redox Conditions. *Journal of Environmental Engineering* **2001,** *127*, (6), 509-516.
2. Love, N. G., Grady Jr., C.P.L, Impact of Growth in Benzoate and m-Toluate Liquid Media on Culturability of *Pseudomonas putida* on Benzoate and m-Toluate Plates. *Applied and Environmental Microbiology* **1995,** *61*, (8), 3142-3144.
3. Love, N. G., Rust, M.E., Terlesky, K.C. , Enrichment and Characterization of an Anaerobic Methyl Ethyl Ketoxime Degrading Culture from an Anoxic/Anaerobic/Aerobic Activated Sludge Sequencing Batch Reactor *Water Science and Technology* **1998,** *37*, 95-98.
4. Frolund, B., Palmgrend, R., Keiding, K., Nielsen, P.K., Extraction of Extracellular Polymers from Activated Sludge using a Cation Exchange Resin. *Water Research* **1996,** *30*, (8), 1749-1758.
5. American Public Health Association, A. W. W. A., Water Pollution Control Federation, (APHA/AWWA/WPCF). *Standard Methods for the Examination of Water and Wastewater*. . 18th ed.; Washington D.C., 1992.
6. Dorobantu, L. S., Yeung, A.K.C., Foght, J.M., Gray, M.R, Stabilization of Oil-Water Emulsions by Hydrophobic Bacteria. *Applied and Environmental Microbiology* **2004,** *70*, (10), 6333-6336.
7. Dubois, M., Gilles, K.A., Hamilton, J.K., Rebers, P.A., Smith, F., Colorimetric Method for Determination of Sugars and Related Substances. *Analytical Chemistry* **1956,** *28*, (3), 350-356.
8. Freundlich, H., The Elements of Colloidal Chemistry. **1924**, 58-61.
9. Eddy, M. a., *Wastewater Engineering: Treatment and Reuse*. 4th Edition ed.; McGraw-Hill New, 2003.
10. Langmuir, I., The Constitution and Fundamental Properties of Solids and Liquids. Part I. Solids. . *Journal of American Chemical Society* **1916,** *38*, 2221-2295.
11. Schwarzenbach, R. P., Gschwend, P.M., Imboden, D.M., *Environmental Organic Chemistry*. 2nd Edition ed.; Wiley Interscience: Hoboken, N.J, 2003.
12. Sokol W., M. C. L. C., Metabolic Responses of Microorganisms Growing on Inhibitory Substrates in Nonsteady State Culture. *Journal of Chemical Technology Biotechnology* **1992,** *54*, 223-229.
13. Ellis, T. G., Barbeau, D.S., Smets, B.F. Grady Jr., C.P.L., Respirometric Technique for Determination of Extant Kinetic Parameters Describing Biodegradation. *Water Environment Research* **1996,** *68*, (5), 917-926.
14. Grady Jr., C. P. L., Smet, B.F., Barbeau, D.S., Variability in Kinetic Parameter Estimates: A Review of Possible Causes and a Proposed Terminology. *Water Research* **1996,** *30*, (3), 742-748.
15. Keener, W. K., Arp, D.J., Kinetic Studies of Ammonia Monooxygenase Inhibition in *Nitrosomonas europaea* by Hydrocarbons and Halogenated Hydrocarbons in an Optimized Whole-Cell Assay. *Applied and Environmental Microbiology* **1993,** *59*, (8), 2501-2510.

16. Sokol, W., Oxidation of an Inhibitory Substrate by Washed Celts (Oxidation of Phenol by *Pseudornonas putida*). *Biotechnology and Bioengineering* **1986,** *30,* 921-927.
17. Woo, H., Sanseverino, J., Cox, C.D., Robinson, K.G., Sayler, G.S., The Measurement of Toluene Dioxygenase Activity in Biofilm Culture of *Pseudomonas putida* F1. *Journal of Microbiological Methods* **2000,** *40,* 181-191.
18. O'Connor, K. E., Dobson, A.D.W., Hartman, S., Indigo Formation by Microorganisms Expressing Styrene Monooxygenase Activity. *Applied and Environmental Microbiology* **1997,** *63,* (11), 4287-4291.
19. Klecka, G. M., Gibson, D.T., Inhibition of Catechol 2,3-Dioxygenase from *Pseudomonas putida* by 3-Chlorocatechol. *Applied and Environmental Microbiology* **1981,** *41,* (5), 1159-1165.
20. Strachen, P. D., Freer, A.A., Fewson, C.A., Purification and Characterization of Catechol 1,2-dioxygenase from *Rhodococcus rhodochrous* NCIMB 13259 and Cloning and Sequencing of its *catA* Gene. *Biochemical Journal* **1998,** *333,* 741-747.
21. Hegeman, G. D., Synthesis of the Enzymes of the Mandelate Pathway by *Pseudomonas putida* - I. Synthesis of Enzymes by the Wild Type. *Journal of Bacteriology* **1966,** *91,* (3), 1140-1154.
22. Skotnicka Pitak, J., Khunjar, W.O., Aga, D.S., Love, N.G., Characterization of Metabolites Formed During the Biotransformation of 17α-Ethinylestradiol by *Nitrosomonas europaea* in Batch and Continuous Flow Bioreactors. *Environmental Science and Technology* **2009,** *43,* (10), 3549–3555.
23. Lowry, O. H., Rosebrough, N.J., Farr, A.L., Randall, R.J., Protein Measurement with the Folin Phenol Reagent. *The Journal of Biological Chemistry* **1951,** *193,* (1), 265-275.
24. Kelly II, R. T., Love, N.G., Ultraviolet Spectrophotometric Determination of Nitrate: Detecting Nitrification Rates and Inhibition. *Water Environment Research* **2007,** *79,* (7), 808-812.
25. Wos, M., Pollard, P., Sensitive and Meaningful Measures of Bacterial Metabolic Activity using NADH fluorescence. *Water Research* **2006,** *40,* (10), 2084-2092.
26. Desbrow, C., Routledge, E.J., Brighty, G.C., Sumpter, J.P., Waldock, M., Identification of Estrogenic Chemicals in STW Effluent. 1. Chemical Fractionation and in Vitro Biological Screening. *Environmental Science and Technology* **1998,** *32,* (11), 1549-1558.
27. Fernandez, M. P., Ikonomou, M.G., Buchanan, I., An Assessment of Estrogenic Organic Contaminants in Canadian wastewaters. *Science of the Total Environment* **2007,** *373,* 250-269.
28. Holbook, R. D., Novak, J.T., Grizzard, T.J., Love, N.G., Estrogen Receptor Agonist Fate during Wastewater and Biosolids Treatment Processes: A Mass Balance Analysis. *Environmental Science Technology* **2002,** *36,* 4533-4539.

CHAPTER 4 - RESULTS AND DISCUSSION

Jolanta Skotnicka-Pitak, Dawn Celiz, Seungyun Baik, Susie Mackintosh and Diana Aga contributed to material in this chapter as outlined in the attribution section of this dissertation.

4.1 Partitioning Behavior of CBZ, EE2, IOP and TMP in the presence of Ammonia Oxidizing and Heterotrophic Cultures

Sorption to particles and biomass is an important mechanism that can contribute to the removal of microconstituents during wastewater treatment [1, 2]. Although a number of published studies have described the fate of microconstituents in natural and engineered environments [3-5], a comprehensive framework that describes how these compounds sorb to activated sludge biomass is lacking. Sorption can be affected by pH, cell surface characteristics, particle size and organic matter composition; however, the role that exopolymeric substances (EPS), an important ingredient in floc formation, plays in microconstituent sorption is not well understood. Sorption of microconstituents to ammonia oxidizing and heterotrophic cultures that produced variable quantities of EPS was investigated. Experiments with AOBs were performed with radiolabeled (^{14}C) carbamazepine (CBZ), 17α-ethinylestradiol (EE2), iopromide (IOP) while experiments with heterotrophs were performed with radiolabeled CBZ, EE2, IOP and non-radiolabeled trimethoprim (TMP). The relative importance of EPS in enabling sorption of microconstituents was addressed by evaluating sorption in the presence and absence of divalent cation-linked EPS. Results from these experiments were also used to inform subsequent biotransformation experiments performed with each microconstituent.

4.1.1 Sorption of CBZ, IOP and EE2 to AOBs was not significant.

Results from experiments with AOB biomass indicate that sorption of CBZ, IOP and EE2 was not significant at the 95% confidence interval (**Figure 4-1** and **Appendix I: Tables I.1, I.6, I.11** and **I.17**). This lack of sorption to AOBs is postulated to be related to the low EPS content of the culture. In full-scale suspended growth treatment systems, AOBs co-exist with flocculant, EPS-generating heterotrophic bacteria. Increased EPS production by the heterotrophs could enhance sorption of microconstituents; however, sorption is not expected to be a significant loss

mechanism for CBZ, IOP and EE2 during laboratory studies that use AOB cultures grown in a manner that does not promote floc formation. Based on these results, it is logical to postulate that TMP will not sorb significantly to AOBs. These results suggest that all the microconstitutents studied here will primarily partition into the aqueous phase during AOB batch and chemostat experiments (**Section 4.2**).

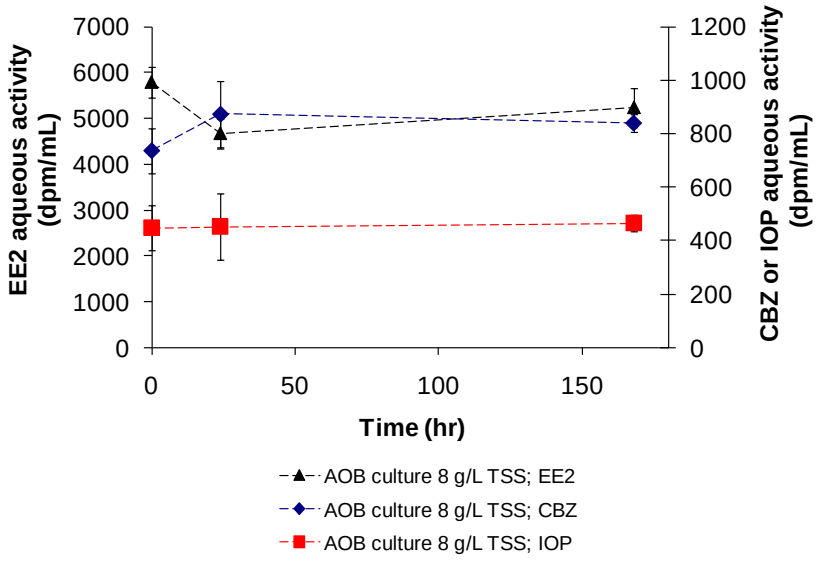

Figure 4-1. Measured ^{14}C aqueous activity in AOB batch isotherm assays. These results are representative of the activity profiles observed at all biomass concentrations. Full data sets are presented in Appendix I: Tables I.1, I.6, I.11 and I.17.

4.1.2 Sorption of CBZ and IOP to Ox^- and Ox^+ biomass was not significant.

Neither CBZ nor IOP sorbed to Ox^- or Ox^+ biomass (**Figure 4-2 and Appendix I: Tables I.2** to **I.5, I.11** to **I.15**). Therefore, CBZ and IOP losses that are observed during batch and chemostat experiments with heterotrophic cultures can be attributed to biotransformation phenomena only. The lack of CBZ and IOP sorption to biomass is consistent with results observed in studies performed with activated sludge from full-scale treatment facilities [5, 6]. However, it should be noted that other sorption coefficients reported in the literature were derived from experiments performed over a concentration range spanning six orders of magnitude (0.01 µg/L to 10,000 µg/L) [2]. Although these coefficients indicate that sorption is low, the approach used assumes that sorption is consistent across a broad concentration range. This is not a reasonable assumption since sorption at high concentrations can bias partitioning that is observed at lower concentrations [7]. In the current study, CBZ and IOP sorption to biomass were statistically

insignificant (**Figure 4-2**) over a concentration range of 0.1 to 1 μg/L. Although the range of concentrations over which these sorption experiments were conducted are larger than what is typically observed in the environment, these results indicate that partition coefficients should only be applied over a narrow concentration range within which the results will be applied.

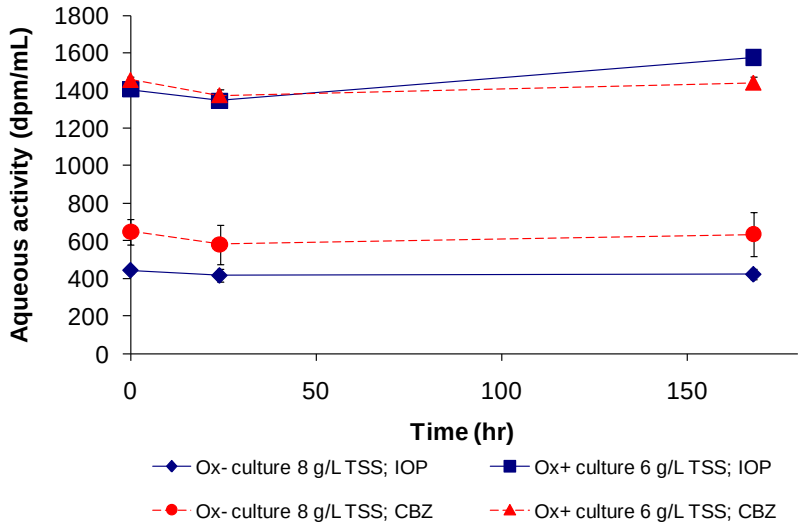

Figure 4-2. Measured ^{14}C aqueous activity in Ox^- and Ox^+ batch isotherm assays. These results are representative of the activity profiles observed at all biomass concentrations. Full data sets are presented in Appendix I: Tables I.2 to I.5, I.11 to I.15.

4.1.3 Sorption of EE2 to Ox^-, Ox^+ and NAS biomass was significant and varied with EPS content.

EE2 sorbed to all heterotrophic cultures (Ox^-, Ox^+, NAS; **Table 4.1**). The zeta potential of the biomass cultures did not correlate well with $K_{OM,EE2}$ (R^2 = 0.258), indicating that surface charge had little effect on EE2 sorption in these experiments. Moderately strong correlations between % adhesion and $K_{OM,EE2}$ (R^2 = 0.823), median particle size and $K_{OM,EE2}$ (R^2= 0.838), organic matter content (R^2 = 0.973) and $K_{OM,EE2}$, and EPS content and $K_{OM,EE2}$ (R^2 = 0.613) were observed, suggesting that these physical characteristics of biomass could influence sorption of EE2 (**Table 4.1** and **Table 4.4.**). These results are consistent with the conclusions drawn by Yi et al. (2006) who asserted that particle size and % adhesion can influence sorption of EE2 to biomass [8]. Results from the current study also provide evidence that other factors like organic matter content and EPS content can impact EE2 sorption. That organic matter affects sorption of non-ionic compounds like EE2 is well known [9]; however, prior confirmation of a link between EE2 sorption and EPS content is absent in the literature.

Results from additional experiments confirmed that cation-linked EPS affects sorption of EE2 (**Table 4.1**). Sorption coefficients describing EE2 partitioning (K_{OM}) to each culture were reduced by approximately 50% (506 ± 91 $L/kg_{biomass,VSS}$) after EPS extraction. Correlations between % adhesion and $K_{OM,EE2}$ (R^2 = 0.586), median particle size and $K_{OM,EE2}$ (R^2 = 0.558), organic matter content and $K_{OM,EE2}$ (R^2 = 0.794) and zeta potential and $K_{OM,EE2}$ (R^2 = 0.001) weakened as compared to pre-EPS extraction relationships (**Table 4.1** and **Table 4.2**). Interestingly, sorption to Ox^-, Ox^+ and NAS biomass devoid of cation-linked EPS was moderately uniform (**Table 4.1**), suggesting that it is possible to describe sorption to biomass and EPS as separate events. Further investigation of this observation is presented in **Section 4.1.5**.

Collectively, these results imply that EPS influences sorption of EE2 to biomass. This phenomenon may be a manifestation of reversible physi-sorption. Recent work by Yi et al. has suggested that EE2 sorption to biomass is largely driven by physi-sorption [10], which means that diffusion will limit EE2 partitioning into and out of the EPS matrix, resulting in sorption hysteresis. Sorption to EPS may also be affected to a lesser extent by non-reversible chemi-sorption processes [10, 11] involving multiple interactions between highly functionalized groups on EE2 and protein or polysaccharide components of biomass or colloidal organic matter [10, 11]. Although confirmation of chemi-sorption is not provided in this study, it should not be discounted entirely.

Correlations between EPS protein content and $K_{OM,EE2}$ (R^2 = 0.588) and EPS polysaccharide content and $K_{OM,EE2}$ (R^2 = 0.176) indicate that EE2 sorption was influenced to a greater degree by EPS protein than polysaccharide content (**Table 4.4**). This result contrasts with results from a previous study that examined EE2 sorption to the protein and polysaccharide content of colloidal organic matter (COM) [12]. In that study, EE2 sorption had a stronger correlation with the colloidal polysaccharide concentration than with the colloidal protein concentration. Although the precise reason for this divergence in results was not investigated, it is postulated that the difference in protein and polysaccharide content of COM versus EPS may influence sorption. EPS also contains lipids, which can affect EE2 sorption, but the exocellular lipid content of the EPS in this study was not characterized and further conclusions are premature. Since EPS comprises mixtures of various proteins, polysaccharides, nucleic acids and lipids [13, 14], further

work needs to address the multiple interactions that can occur between EE2 and EPS constituents.

Description of sorption using single parameter linear free energy relationships (sp-LFERs) based on octanol water coefficients, have been used to predict estrogen sorption with limited success [1]. These sp-LFERs have a narrow applicability since they do not account for the multiple interactions that can influence sorption of microconstituents to biomass. Results from the current work confirm that sorption of microconstituents like EE2 is complex. Attempts have been made to develop poly-parameter LFERs (pp-LFERs) that seek to quantify the impact of factors like London dispersive forces (induced dipole-induced dipole interactions), cavity formation between solute and solvents and hydrogen-bond basicity (electron donor characteristics of solute and solvent) on microconstituent sorption [9, 15]. In this study, attempts to describe EE2 sorption to biomass using pp-LFERs yielded coefficients that were greater than experimentally determined sorption coefficients (**Appendix I: Table I.23**). This result suggests that that existing six parameter LFERs are still not sufficient to describe sorption of EE2 to organic matter.

4.1.4 Sorption of TMP to Ox^-, Ox^+ and NAS biomass was significant.

TMP sorbed significantly onto biomass after 24 hours of incubation (**Table 4.3)**. Linear regression of this data yielded solid-water distribution coefficients ($K_{D,TMP}$) that were higher than values previously reported for secondary sludge samples [16, 17].. The elevated degree of sorption observed in this study could be an artifact of the experimental protocols used. TMP sorption experiments were performed at 1 mg TMP/L, which is three orders of magnitude higher than concentrations used in prior sorption experiments [16, 17]. Linear regression of data collected at high concentrations can overestimate sorption that occurs at lower concentrations. Another reason for the difference in results between the prior studies and current investigation is that the test conditions used in this study (inactivated biomass in batch assays at 23^0C for 24 hr period) were more appropriate than mass flow data to describe TMP sorption [16]. The approach employed by Gobel et al. (2005) compared daily aqueous phase concentrations with weekly solid phase concentrations [16]. This is not suitable since solid phase concentrations can be affected by diurnal and seasonal variations of TMP. In light of this, it is possible that TMP coefficients reported in the literature represent incomplete partitioning.

In the current study, correlations between % adhesion and $K_{OM,TMP}$ (R^2 = 0.426), median particle size and $K_{OM,TMP}$ (R^2 = 0.446), organic matter content and $K_{OM,TMP}$ (R^2 = 0.017) were weak. The relationships between EPS content (R^2 = 0.678), zeta potential (R^2 = 0.945) and $K_{OM,TMP}$ were stronger. This implies that that TMP sorption may be governed by ionic interactions with the cell surface and charged EPS constituents. Sorption of TMP decreased after EPS extraction and was best described using the non-linear Freundlich isotherm (**Table 4.3**). Correlations between median particle size and $K_{OM,TMP}$ (R^2 = 0.889), % adhesion and $K_{OM,TMP}$ (R^2 = 0.906), organic matter content and $K_{OM,TMP}$ (R^2 = 0.993) were stronger after EPS extraction.

Strong relationships between EPS protein content and $K_{OM,TMP}$ (R^2 = 0.701) and EPS polysaccharide content and $K_{OM,TMP}$ (R^2 = 0.556) indicated that TMP sorption is affected by interactions with both protein and polysaccharide components (**Table 4.4**). The sorption behavior of TMP can be partially explained by its chemical properties. TMP is hydrophilic and was partially protonated at the pH used in this study (**Table 2.1**). No other correlations between TMP sorption and protein or polysaccharide content were found in the literature. TMP sorption to biomass is postulated to be primarily influenced by ionic and hydrogen bond interactions with EPS constituents.

Table 4.1. Sorption results for EE2 prior to and after EPS extraction.

Culture	Pre-EPS Extraction					Post-EPS Extraction				
	Log K_F	n	Log K_D	Log K_{OM}	f_{IS}	Log K_F	n	Log K_D	Log K_{OM}	f_{IS}
Ox^- culture	2.61	1.11	2.75 ± 0.03	2.91 ± 0.03	7.8 ± 0.3	2.30	1.07	2.36 ± 0.01	2.43 ± 0.01	3.4 ± 0.1
Ox^+ culture	2.30	1.63	2.85 ± 0.13	2.95 ± 0.13	9.8 ± 2.5	2.45	0.87	2.34 ± 0.02	2.45 ± 0.02	3.2 ± 0.1
NAS	2.78	1.02	2.80 ± 0.01	2.89 ± 0.01	8.6 ± 0.1	2.08	1.42	2.43 ± 0.06	2.53 ± 0.06	3.9 ± 0.5

The values reported were calculated from data obtained from triplicate experiments and are reported as $\bar{x} \pm s_x$ where s_x is the standard deviation. Individual data sets available in Appendix I: Tables I.6 to I.10.

Table 4.2. Physical properties of cultures prior to and after EPS extraction.

Culture	Pre-EPS Extraction				Post-EPS Extraction			
	f_{OM}	Median Particle size diameter (μm)	% Adhesion	Zeta Potential (mV)	f_{OM}	Median Particle size diameter (μm)	% Adhesion	Zeta Potential (mV)
Ox^- culture	69 ± 2	120 ± 1	71.6 ± 5.3	-30.9 ± 7.8	85 ± 1	65 ± 1	63.7 ± 1.4	-15.1 ± 1.6
Ox^+ culture	80 ± 5	215 ± 7	13.4 ± 2.5	-34.7 ± 0.9	77 ± 16	86 ± 14	44.4 ± 25.9	-29.7 ± 3.3
NAS	80 ± 2	96 ± 7	84.6 ± 1.7	-20.3 ± 5.2	78 ± 5	45 ± 3	84.0 ± 5.1	-25.3 ± 2.9

The values reported were calculated from data obtained from triplicate experiments with EE2 and TMP and are reported as $\bar{x} \pm s_x$ where s_x is the standard deviation. Individual data sets are available in Appendix I: Tables I.20 and I.21.

Table 4.3. Sorption results for TMP prior to and after EPS extraction.

Culture	Pre-EPS Extraction			Post-EPS Extraction				
	Log K_D	Log K_{OM}	f_{IS}	Log K_F	n	Log K_D	Log K_{OM}	f_{IS}
Ox^- culture	3.68	3.76	41	0.51	1.75	2.83 ± 0.15	2.84 ± 0.15	9.4 ± 2.7
Ox^+ culture	3.67	3.75	41	-1.82	2.41	2.63 ± 0.19	2.68 ± 0.19	6.4 ± 2.4
NAS	4.19	4.32	70	1.75	1.62	3.33 ± 0.38	3.45 ± 0.38	26.7 ± 14.5

The values reported were calculated from data obtained from triplicate experiments and are reported as $\bar{x} \pm s_x$ where s_x is the standard deviation. Individual data sets available in Appendix I: Tables I.16 and I.19.

Table 4.4. Composition of extracted EPS from cultures used in sorption experiments.

Culture	EPS Protein Content (mg protein[1]/g VSS)	EPS Polysaccharide Content (mg glucose/g VSS)
Ox^- culture	210 ± 6	3 ± 1
Ox^+ culture	275 ± 8	5 ± 1
NAS	159 ± 5	6 ± 1

[1]–measured as bovine serum albumin

The values reported were calculated from data obtained from triplicates and are reported as $\bar{x} \pm s_x$ where s_x is the standard deviation.

4.1.5 Use of a dual mode sorption isotherm to describe sorption of EE2 biomass and EPS was not beneficial.

Sorption of EE2 to biomass and cation-linked EPS was postulated to be separate events. To evaluate this hypothesis, a dual mode sorption isotherm [18] was proposed where the Freundlich component described sorption to biomass only and the linear component described sorption to cation-linked EPS only;

$$C_S^D = K_F^D C_W{}^n + K_D^D C_W \qquad (4\text{-}1)$$

where

C_S^D = mass of microconstituent sorbed per unit biomass at equilibrium ($\mu g_{microconstituent}/kg_{biomass,TSS}$),

K_F^D = Freundlich coefficient describing sorption to biomass devoid of EPS ($\mu g_{microconstituent}/kg_{biomass,\ TSS})(\mu g_{microconstituent}/L)^{-n}$.

n = dimensionless Freundlich constant describing non-linearity,

K_D^D = biomass-water distribution coefficient describing sorption to EPS only ($L/kg_{biomass,TSS}$),

C_W = aqueous concentration of microconstituent at equilibrium (μg/L).

No statistical benefit was observed when using the dual mode isotherm as compared to a single Freundlich isotherm to describe EE2 partitioning to Ox^-, Ox^+ and NAS cultures (**Table 4.5 and Appendix I: Figure I-1**). Since the data set used to calculate Freundlich parameters that describe sorption to biomass only (**Table 4.5**) was small (n = 3), further work is needed to define more robust parameters. One should also note that iron and/or aluminum-linked EPS was still bound to the biomass samples used in these experiments since CER extraction only targets divalent (Ca^{2+} and Mg^{2+}) bound EPS. To elucidate the impact of the different EPS fractions on

microconstituent sorption, sorption experiments with biomass that have undergone sequential EPS extraction protocols that target different EPS fractions are recommended.

Table 4.5. Freundlich and dual mode sorption parameters describing partitioning of EE2 to biomass with EPS.

Freundlich Fit only			
	Ox^-	**Ox^+**	**NAS**
log K_F	2.63	2.30	2.78
n	1.113	1.631	1.022
R^2	0.904	0.953	0.928
Dual mode Fit			
log K_F	2.31		
n	1.120		
Log K_D	2.43	2.65	2.43
R^2	0.903	0.848	0.903

4.1.6 Sorption is not expected to play an important role in the fate of CBZ or IOP in biotransformation experiments while sorption of EE2 and TMP is expected to be significant.

Within the context of the current investigation, these results indicate that neither CBZ nor IOP would sorb to AOBs or heterotrophs. Any losses of these microconstituents during biotransformation tests could be attributed to AOB or heterotrophic activity. EE2 and TMP were expected to sorb most significantly to heterotrophs but not AOBs. Consequently, both abiotic and sorption controls were included into all biotransformation experiments to account for sorption of EE2 and TMP. Mass balances of radiolabeled substrates were also performed to confirm partitioning when appropriate.

4.2 Elucidating the Role of Ammonia Oxidizing Bacteria versus Heterotrophic Bacteria during the Biotransformation of Microconstituents.

Very little is known about the mechanisms driving biodegradation of microconstituents in activated sludge systems. Although numerous studies have reported overall removal rates between 10 and 90% for various microconstituents during wastewater treatment (10-90%) [16, 17, 19-27], we do not understand the interactions that occur between microbial communities present in activated sludge when exposed to microconstituents. Some insight regarding the role of nitrifiers has been gained from previous work that showed partial EE2 transformation in the presence of pure cultures of ammonia oxidizing bacteria (AOBs)[28, 29] and nitrifying activated sludge (NAS) [30, 31]. While this work suggests a role for AOBs in the transformation of EE2, it does not address the potential contribution of other microorganisms present in NAS. In a similar manner, work done with pure cultures of various heterotrophs considered EE2 degradation as exclusive to heterotrophs [32, 33]. Little emphasis has been placed on developing our knowledge of the interaction between these two functionally important subgroups of NAS. Results in this section summarize efforts made to understand how microconstituent fate is affected by AOB and heterotrophic activity. In performing these biotransformation experiments, inhibition of AOB and heterotrophic bacteria when exposed to elevated concentrations of microconstituents were also evaluated.

4.2.1 Inhibition of AOBs by EE2 and TMP was not observed at concentrations up to 1 mg/L.

Since EE2 and TMP are present at trace concentrations in domestic and hospital wastewaters (0.2 to 114 ng EE2/L [34, 35]; 878 – 7600 ng TMP/L [17, 36]), it was important to determine whether AOB inhibition would occur at the elevated EE2 and TMP concentrations used in subsequent biotransformation experiments (1 mg EE2 or TMP/L). Inhibition of AOBs by EE2 or TMP was not observed at concentrations up to 1 mg/L of EE2 or TMP (**Table 4.6;** For EE2 exponential phase cells $p > 0.15$, For EE2 chemostat cells $p > 0.24$, For TMP exponential phase cells $p > 0.15$, For EE2 chemostat cells $p > 0.24$). Control experiments with acetone (co-solvent for EE2 stock solutions; **Section 3.1**) were also performed. Results indicate that acetone-mediated inhibition was not significant (For EE2 exponential phase cells $p > 0.18$, For EE2 chemostat cells $p > 0.09$). Collectively, these results indicate that AOB activity will not be inhibited during subsequent batch and chemostat experiments.

Table 4.6. Specific nitrite generation rates for AOB cultures in presence of EE2 or TMP.

Concentration (mg/L)	sNGR (mg N/mg protein.day)			
	EE2		TMP	
	Exponential Phase cells	Chemostat cells	Exponential Phase cells	Chemostat cells
0	1140 ± 370	630 ± 140	2380 ± 980	980 ± 150
0.01	930 ± 290	490 ± 60	1930 ± 0.00	670 ± 40
10	1250 ± 120	570 ± 60	1560 ± 490	880 ± 210
1000	1060 ± 70	470 ± 10	1450 ± 690	780 ± 100
Acetone Control	1.22 ± 0.32		N/A	

N/A – TMP stock solution was prepared in Nanopure™ water.

Rates were calculated from duplicate reactor vessels and are reported as $\bar{x} \pm RMD$ where RMD is the relative mean difference.

4.2.2 Inhibition of Ox^- and Ox^+ cultures by EE2 and TMP was not observed.

Short term biokinetic assays with heterotrophic cultures indicated that significant inhibition of respiration would not be achieved at concentrations up to 10 mg EE2 or TMP/L (**Table 4.7** and **Table 4.8;** For Ox^- cells exposed to EE2 only $p > 0.273$, For Ox^+ cells exposed to EE2 only $p > 0.176$, For Ox^- cells exposed to TMP only $p > 0.075$, For Ox^+ cells exposed to TMP only $p > 0.406$, For Ox^- cells exposed to EE2 and acetate $p > 0.052$, For Ox^+ cells exposed to EE2 and acetate $p > 0.068$, For Ox^- cells exposed to TMP and acetate $p > 0.384$, For Ox^+ cells exposed to TMP and acetate $p > 0.366$). Results were consistent in assays performed in the presence (mimicking batch conditions; **Table 4.7**) or absence (mimicking chemostat; **Table 4.8**) of acetate, which represented an exogenous electron donor other than EE2 or TMP. These results clearly show that neither microconstituent would inhibit bacterial respiration at the levels used in the experiments discussed here.

Table 4.7. Specific oxygen uptake rates for heterotrophic cultures in the presence of EE2 or TMP, and acetate.

Concentration (mg EE2 or TMP/L)	sOUR (mg O_2/g protein.day)			
	EE2[a]		TMP[b]	
	Ox^- culture	Ox^+ culture	Ox^- culture	Ox^+ culture
0	192 ± 76	472 ± 37	297 ± 0.046	262 ± 0.113
0.01	568 ± 30	2536 ± 242	1752 ± 0.204	1635 ± 0.210
1	633 ± 94	2381 ± 439	1863 ± 0.170	2254 ± 0.188
10	613 ± 40	2577 ± 94	1859 ± 0.092	1936 ± 0.204
Acetate (50 mg COD/L)	518 ± 97	2186 ± 93	1795 ± 0.150	1689 ± 0.034
Acetone	648 ± 76	2540 ± 194	N/A	

N/A – TMP stock solution was prepared in Nanopure™ water.

[a]Rates were calculated from triplicate or quadruplicate reactor vessels and are reported as $\bar{x} \pm s_x$ where s_x is the standard deviation.

[b]Rates were calculated from duplicate reactor vessels and are reported as $\bar{x} \pm RMD$ where RMD is the relative mean difference.

Table 4.8. Specific oxygen uptake rates for heterotrophic cultures in presence of EE2 or TMP only.

Concentration (mg EE2 or TMP/L)	sOUR (mg O_2/g protein.day)			
	EE2		TMP	
	Ox^- culture	Ox^+ culture	Ox^- culture	Ox^+ culture
0	283 ± 61	274 ± 34	68 ± 9	84 ± 28
0.01	309 ± 123	440 ± 31	96 ± 16	68 ± 14
1	348 ± 161	443 ± 112	98 ± 11	99 ± 28
10	265 ± 88	472 ± 45	79 ± 19	71 ± 16
Acetone (46 mg/L)	300 ± 68	503 ± 47	N/A	

N/A – TMP stock solution was prepared in Nanopure™ water.

Rates were calculated from triplicate or quadruplicate reactor vessels and are reported as $\bar{x} \pm s_x$ where s_x is the standard deviation.

4.2.3 CBZ, IOP and TMP were not transformed by AOB batch cultures.

Biotransformation of CBZ, IOP and TMP by batch AOB cultures actively growing on ammonia did not occur (**Figure 4-3)**. The stability observed with CBZ is consistent with previous work by others [25, 37]; however, other researchers have seen enhanced degradation of IOP and TMP by nitrifying activated sludge (NAS) and hypothesized that it was due primarily to AOB activity [23]. Differences in microconstituent biotransformation observed in current experiments versus those performed by Batt et al. (2006) may be partially explained by substrate affinity and oxygen limitations [23].

Prior work has established that AMO possesses two substrate binding sites [38]. One site binds to ammonia and small organics (C_1 or C_2 hydrocarbons) while the other can bind to large

organics (>C_2 compounds). Oxidation of substrates at both sites requires oxygen and can occur simultaneously provided sufficient oxygen is available. In cases where oxygen is the limiting reactant, the site with the higher affinity for substrate will dominate oxygen consumption [38]. The half saturation constant for ammonia affinity ranges from 0.5 to 2.15 mg NH_3-N/L [29, 39, 40]. For efficient microconstituent biotransformation to occur under oxygen tension, the affinity constant for individual compounds would need to be equal to or less than the affinity constant for ammonia. Since biotransformation of CBZ, IOP and TMP was not observed, it is possible that the affinity constant for these microconstituents is higher than that for ammonia. Consequently, oxygen consumption by AOBs would be driven by ammonia oxidation only. Unfortunately, microconstituent affinity constants were not determined in this study and are not reported in the literature so it is impossible to substantiate these claims; however, it should be noted that in the current study, ammonia was always present in excess during batch incubations (100-150 mg NH_3-N/L) whereas oxygen concentrations decreased as cell density increased (data not shown). During late exponential and stationary growth phase, oxygen concentrations could have become limiting (K_O = 0.5 mg O_2/L for AOBs [41]); however, accurate dissolved oxygen measurements were not possible due to the design of the experiment. In experiments performed by Batt et al. (2006), ammonia was also in excess (10 – 50 mg NH_3-N/L) however the oxygen concentrations were not reported [23]. If oxygen was not limiting, simultaneous oxidation of ammonia and microconstituents as observed by Batt et al. could occur [23]. In cases where ammonia is limiting, microconstituent biotransformation is hypothesized to occur more readily provided sufficient enzymes are present.

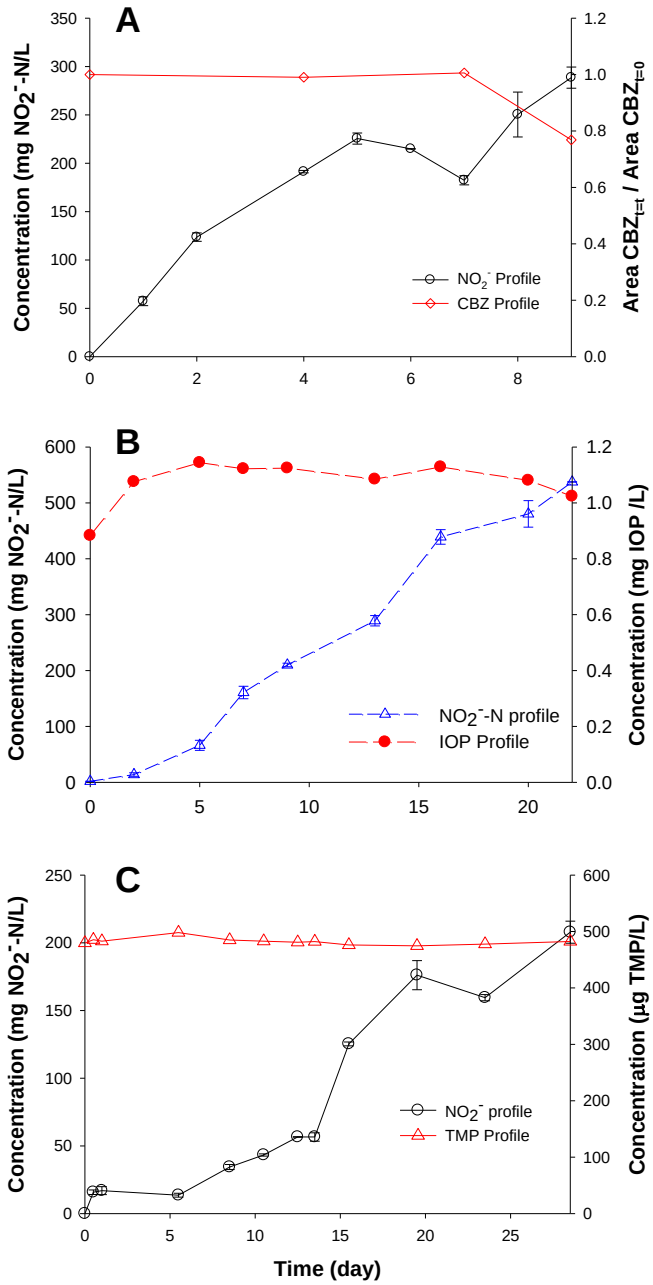

Figure 4-3. Microconstituent concentration profile for AOB batch experiments. A: AOB culture supplemented with 1 mg CBZ/L, B: AOB culture supplemented with 1 mg IOP/L, C: AOB culture supplemented with 0.5 mg TMP/L. These results are representative of microconstituent profiles observed in duplicate reactors.

4.2.4 CBZ and TMP were not transformed by Ox^- and Ox^+ batch cultures.

Further experiments were performed to determine the fate of microconstituents during batch incubations with heterotrophic cultures. Due to time and resource constraints, it was not possible to test all four microconstituents. IOP was not tested in subsequent experiments since existing

data suggest that risks associated with IOP output to the environment are low (Hartmann 2002). Neither CBZ nor TMP were biotransformed by batch Ox^- and Ox^+ cultures (**Figure 4-4 A-D**). Results from other studies were mixed. Bernhard et al. (2006) found that CBZ was not biotransformed in the presence of heterotrophic bacteria [25] whereas Batt et al. (2006) and Lim et al. (2008) indicated that TMP was biotransformed when exposed to heterotrophic cultures [23, 42]. The recalcitrance of CBZ and TMP in current batch cultures could be explained by diauxic growth, which occurs when growth substrates are metabolized sequentially, with the most energetically favorable substrate being used first. If diauxie were a factor during this experiment, acetate, benzoate or toluene would be used first because they were the growth substrate(s) to which each culture was acclimated. Upon depletion of the primary substrate(s), CBZ and TMP degradation would occur after a sufficient acclimation period. It is possible that the 7 day incubation employed in this study was too short to allow use of CBZ or TMP as growth substrates. These results also indicate that CBZ and TMP degradation by heterotrophs under batch conditions is not solely dependent upon enriched non-specific oxygenase activity.

4.2.5 Biotransformation of EE2 was observed in Ox^+ but not Ox^- batch cultures.

EE2 was not degraded to a significant degree by heterotrophic cells possessing minimal oxygenase activity (Ox^- ; $p > 0.034$) over a period of 7 days (**Figure 4-4 E**). In contrast, rapid biotransformation of EE2 by cells enriched for oxygenase activity (Ox^+; **Figure 4-4 F**) was observed. These observations in Ox^- reactors can be explained by the phenomenon of diauxic growth as previously discussed in **section 4.2.4**. The slight decrease in EE2 concentration, observed upon depletion of acetate (**Figure 4-4 E**), suggests that the 7 day incubation period was insufficient to capture substantial EE2 biotransformation. These results indicate that EE2 is only degraded by Ox^- cells in the absence of an alternative readily biodegradable substrate.

To explain concomitant degradation of EE2 and primary substrates in Ox^+ batch reactors, it is possible that some combination of mixed substrate utilization, fortuitous metabolism or co-metabolism occurred. Mixed substrate utilization by heterotrophic organisms has been documented under batch conditions by Kovarova-Kovar et al. (1998) [43]; however, the high concentrations of substrates used in our study (100 mg sCOD/L and 1 mg EE2/L) contrasts with the nutrient limited conditions used in their experiments. Therefore, mixed substrate utilization is

unlikely. Co-metabolism can explain EE2 removal observed in Ox^+ batch cultures in this study (**Figure 4-4 F**). It is also possible that fortuitous metabolism of EE2 could have taken place. Since biomass production and b-product formation due to EE2 degradation only was not measured in the current experiment, it is difficult to elucidate whether co-metabolism or fortuitous metabolism by Ox^+ cells governed EE2 degradation; however, it should be noted that EE2 was removed in the experiment with high oxygenase activity (Ox^+ versus Ox^-). This finding suggests that the induced oxygenase activity may have contributed to the enhanced degradation observed despite the presence of residual readily biodegradable matter. Both fortuitous metabolism and co-metabolism are feasible explanations for these observations.

Collectively, our findings indicate that EE2 biotransformation by heterotrophs under batch conditions is dependent on the presence of alternative substrates as well as oxygenase enzyme activity. Interestingly, EE2 concentrations did not drop below 0.2 mg EE2/L in Ox^+ batch incubations which indicates that biodegradation was limited by an unmeasured factor. In light of these batch study results, further experiments were performed with EE2 and TMP to investigate factors that might affect heterotrophic biotransformation of microconstituents under nutrient limited conditions. CBZ was not included in further experiments since biotransformation does not appear to be a significant mechanism of removal for this compound [6].

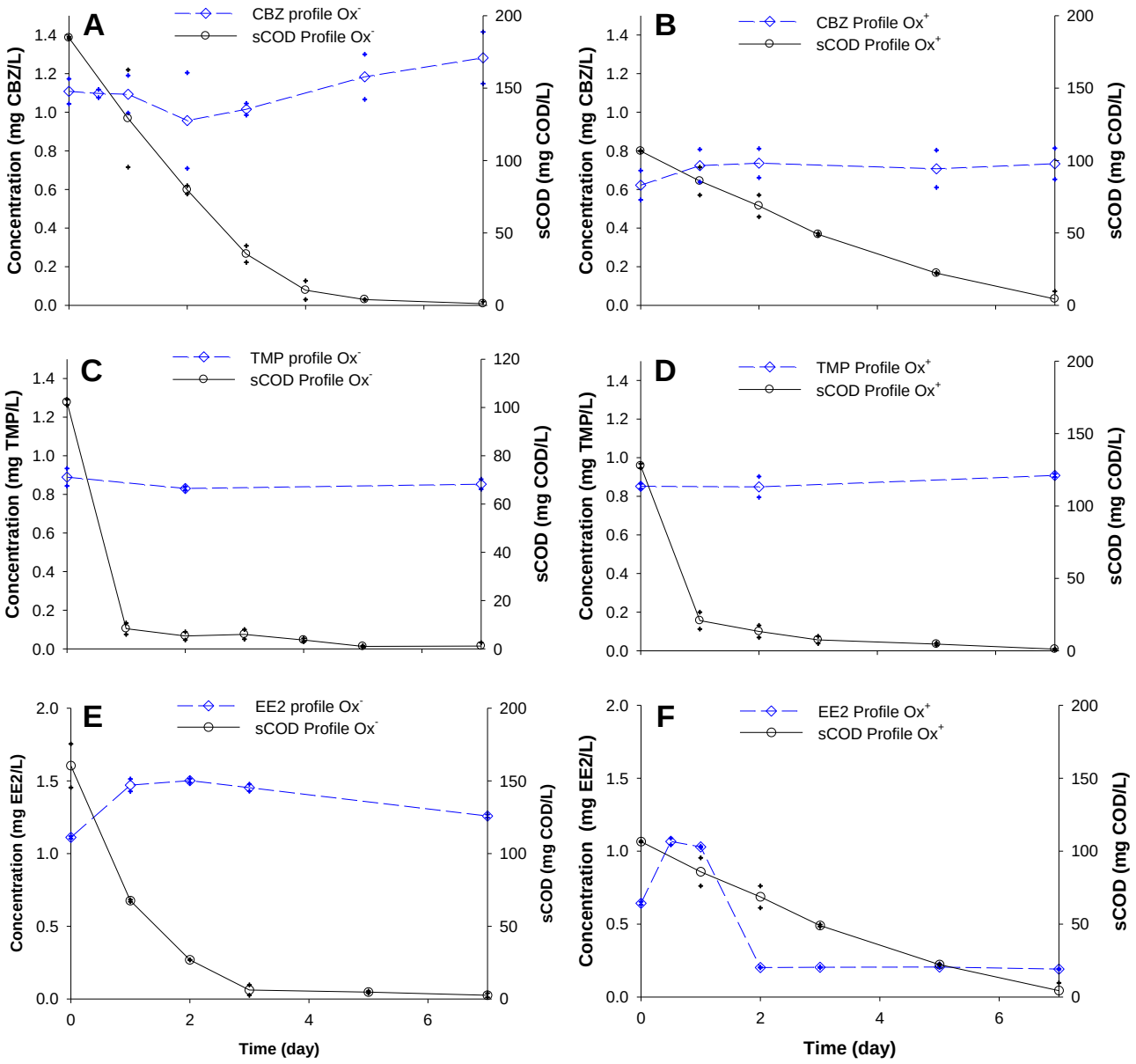

Figure 4-4. CBZ, TMP and EE2 transformation profiles from non-radiolabeled batch experiments with heterotrophic biomass. A: Ox^- culture fed 1 mg/L CBZ, B: Ox^+ culture fed 1 mg CBZ/L, C: Ox^- culture fed 1 mg/L TMP, D: Ox^+ culture fed 1 mg/L TMP, E: Ox^- culture fed 1 mg/L EE2, F: Ox^+ culture fed 1 mg/L EE2. The results shown are average values of duplicate reactor vessels.

4.2.6 Chemostat-grown AOB, Ox^- and Ox^+ cultures biotransformed EE2.

Chemostat experiments with AOB [29], Ox^- and Ox^+ cultures were performed to determine the fate of EE2 under physiological conditions approximating those that are found in activated sludge systems. No mineralization was observed in AOB chemostats; however, four

transformation products were detected. Detailed characterization of three of these products (4-hydroxy-EE2, 4-nitro-EE2 and 2-nitro-EE2) is reported elsewhere [29, 44]. Further characterization of the fourth metabolite (M375) was not performed due to low sample mass.

EE2 was mineralized to similar extents by both Ox^- (60-65%) and Ox^+ (55-58%) cultures despite the latter reactor having significantly higher oxygenase enzyme activities (**Figure 4-5 and Table 4.9**). Three (3) stable transformation products were observed in Ox^- and Ox^+ chemostat cultures fed EE2 ($[M-H]^-$ *m/z* 295; **Figure 4-5 A and B).** The mass to charge ratio of two metabolites, measured via negative mode ESI LC/MS ($[M-H]^-$), corresponded to *m/z* 375 (M376) and 311 (4-OH-EE2; **Figure 4-5)** while the other metabolite (U1 in **Figure 4-5)** has not been extensively characterized further due to limited sample mass, a consequence of radiolabeled protocols. Interestingly, 4-OH-EE2 appears in AOB [29] and Ox^- reactors but not Ox^+ reactors. This presence of 4-OH-EE2 in the Ox- culture is surprising since unspecific oxygenase activity in this culture was low (**Table 4.9**); however, it should be noted that the toluene dioxygenase assay used in our study was developed to measure indigo formation (λ_{max} = 605 nm) [45, 46] catalyzed by toluene/naphthalene mono/dioxygenases and their respective homologues. Indole oxidation by other monooxygenases can result in the formation of alternative products, e.g. isoindigo or 7-hydroxyindole [47, 48] that do not absorb to a high degree at the wavelength (610 nm) used in this study. Consequently, this assay is not sufficient to capture all mono/dioxygenase activity in Ox^- cultures. Lack of detection of 4-OH-EE2 in Ox^+ cultures does not preclude its existence. It is possible that 4-OH-EE2 was further transformed/mineralized by Ox^+ cultures since catechol dioxygenase enzyme activities were high (**Table 4.9**). These findings are significant since catechol estrogens like 4-OH-EE2 are noted to be less estrogenic than EE2 [29] but have been implicated as liver tumor promoters and weak hepatocarcinogens in rat, mice and hamster models [49, 50].

To determine whether EE2 degradation under steady state conditions was limited by catechol oxygenase activity, the following mass balance was considered:

$$(Q)(C_0)=(Q)(C)+(k)(X)(V) \qquad (4\text{-}2)$$

where

Q = Flowrate (0.288 L/day),

V = Volume of reactor (2 L),

C_0 = Influent EE2 concentration (1 mg EE2/L = 2.71 mg COD/L assuming complete degradation to carbon dioxide and water),

C = Effluent EE2 concentration (assumed to be 0 mg COD/L for conservative estimate),

k = Catechol oxygenase activity (μm catechol/mg protein-day; **Table 4.9**)

X = Biomass concentration (199 mg protein/L; **Section 3.2.2**).

If the rate of EE2 supplied to the system ($(Q)(C_0)$) is greater than the theoretical rate of oxygenation that can be performed by available catechol dioxygenases ($(k)(X)(V)$), ring cleavage reactions will limit EE2 biodegradation. In this study, EE2 was supplied to the reactors at a constant rate of 0.78 mg EE2 as COD/day. Theoretical rates of oxygen utilization were calculated by assuming catechol oxygenases performed oxidation of catechol to cis,cis muconate (C12O) or 2-hydoxy-cis,cis muconic semialdehyde (C23O) only (**Appendix II: Tables II.3 to II.14**). From these calculations, the rate of oxygen utilization by the C12O (Ox^- = 0.55 mg O_2/day, Ox^+ = 1.33 mg O_2/day) and C23O (Ox^- = 32.1 mg O_2/day, Ox^+ = 30.8 mg O_2/day) enzymes exceeded the theoretical rate of oxygen demand associated with complete EE2 degradation to carbon dioxide to a large degree (**Appendix II: Tables II.3 to II.8**). Therefore, ring cleavage was not rate limiting and basal level expression of heterotrophic catechol dioxygenases, as observed in Ox^- chemostats, was sufficient to afford a high degree of transformation under chemostat conditions at the long retention times used in the current study. These findings help to explain the lack of difference in mineralization of EE2 observed in Ox^- and Ox^+ chemostats.

Concomitant losses of primary substrates and EE2 in heterotrophic chemostat may be due to mixed substrate utilization, co-metabolism or fortuitous metabolism. Since growth of biomass due to strictly EE2 metabolism was not measured in this experiment, conclusions regarding the dominant metabolism are presumptive; however, the low concentration of residual organic matter (10-20 mg sCOD/L; **Appendix II: Figure II-2**) and EE2 (0.2 to 1 mg/L) is postulated to provide conditions that allow for mixed substrate utilization of EE2 and other electron donors.

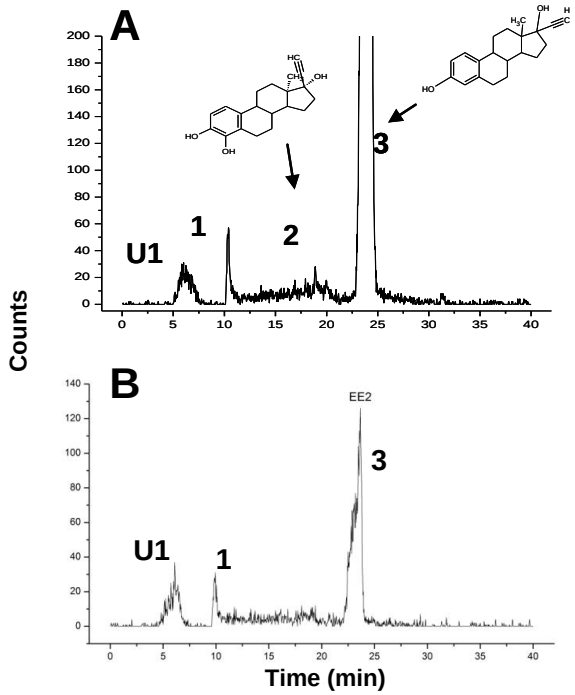

Fraction	Identity	Ret. Time	$[M-H]^-$	% Contribution to ^{14}C activity added
1	N/A	9.5	375	0.8 ± 0.3
2	4-hydroxy-EE2	20	311	0.6 ± 0.3
3	EE2	24	295	18.5 ± 7.6
U1	N/A	6	Unknown	0.8 ± 0.3
$^{14}CO2$	-	N/A	N/A	54.8 ± 14.6
Solids	-	N/A	N/A	9.8 ± 3.2
Avg ^{14}C Mass balance				85.2 ± 26.2

Fraction	Identity	Ret. Time	$[M-H]^-$	% Contribution to ^{14}C activity added
1	N/A	9.5	375	9.9 ± 0.5
3	EE2	24	295	35.3 ± 1.8
U1	N/A	6	Unknown	4.5 ± 0.2
$^{14}CO2$	-	N/A	N/A	22.4 ± 23.9
Solids	-	N/A	N/A	16.1 ± 3.4
Avg ^{14}C Mass balance				88.2 ± 22.1

Figure 4-5. Selected radiochromatograms of EE2 and metabolites generated during chemostat experiments. A: Chemostat Ox^- cells fed 1 mg/L ^{12}C-EE2 and 10 μg/L ^{14}C-EE2, B: Chemostat Ox^+ cells fed 1 mg/L ^{12}C-EE2 and 10 μg/L ^{14}C-EE2. For complete ^{14}C mass balance on reactors, see Appendix II: Table II-15. Detailed calculations describing percent contribution of transformation products to the overall ^{14}C input to the system are summarized in Appendix II: Table II.16.

Table 4.9. Summary of oxygenase activity in Ox^- and Ox^+ chemostat cultures.

	Ox^- culture[1]	Ox^+ culture[2]	Ox^- culture[3]	Ox^+ culture[4]
Catechol 1,2 dioxygenase (Ortho) activity (μM catechol consumed/g protein-hr)	1.48 ± 1.06 1.59 ± 0.23	93.7 ± 17.2 86.3 ± 95.7	2.63 ± 0.43 2.50 ± 1.18	54.4 ± 54.5 90.4 ± 91.5
Catechol 2,3 dioxygenase (Meta) activity (μM catechol consumed/g protein-hr)	5.77 ± 2.93 3.18 ± 2.64	136 ± 53.6 73.3 ± 5.58	0.10 ± 0.11 0.09 ± 0.08	4.42 ± 3.47 24.5 ± 2.08
Toluene Dioxygenase activity (μmol indigo/g protein-hr)	Below detection	0.09 ± 0.05	Below detection	N/D

[1] Ox^- culture fed 1000 mg acetate as COD/L.
[2] Ox^+ culture fed 333 mg acetate as COD/L, 333 mg benzoate as COD/L and 333 mg toluene as COD/L.
[3] Ox^- culture fed AOB reactor effluent supplemented with 1000 mg acetate as COD/L.
[4] Ox^+ culture fed AOB reactor effluent supplemented with 333 mg acetate as COD/L, 333 mg benzoate as COD/L and 333 mg toluene as COD/L.
[a,b] Results from April 2007 and June 2007 replicates.
[c,d] Results from June 2008 and September 2008 replicates.
[e,f] Results from July 2008 and November 2008 replicates.
[g,h] Results from November 2008 and December 2008 replicates.
N/D – Not determined.
Rates were calculated from duplicate reactor vessels and are reported as $\bar{x} \pm RMD$ where RMD is the relative mean difference.

4.2.7 Heterotrophs can further degrade EE2 associated transformation products generated from AOB chemostats.

Kinetic experiments performed in this study (summarized in **section 4.2.10)** indicate that AOBs can biotransform EE2 faster than heterotrophs; however, since AOBs do not possess the enzymatic machinery to mineralize complex organic compounds [51], the ultimate fate of EE2 and its transformation products in activated sludge was hypothesized to dependent on heterotrophic activity. Previous work has confirmed that AOBs do not mineralize EE2 under batch or chemostat conditions [29]; however, transformation products that are formed can be subject to sorption and/or further biotransformation reactions by heterotrophs. Results from the current study confirm that heterotrophic cultures can further degrade metabolites generated by AOB cultures (**Figure 4-6**). Mineralization of radiolabeled content was also observed in duplicate Ox^- (25-37%) and Ox^+ (30-33%) reactors fed effluent from AOB chemostats that were initially fed radiolabeled EE2. In these experiments, oxygenase activity did not limit EE2 mineralization (**Figure 4-6 B and C**). This result is not unexpected based on the oxygenase activity requirements discussed in **section 4.2.6**.

Radiochromatograms for Ox^- and Ox^+ cultures fed effluent from AOB reactors show similar metabolite profiles, suggesting a conserved biotransformation pathway regardless of oxygenase activity enrichment status. One exception to this relates to metabolite U1, which appears in Ox^+ cultures but not Ox^- cultures. Fractionation and further analysis of U1 indicated that this peak comprised low molecular weight polar compounds. Further characterization was not possible due to limited sample mass. It is postulated that U1 represents a collection of anapleurotic metabolites resulting from central metabolism pathways. That U1 was not detected in Ox^- cultures is surprising and cannot be explained at this point.

Metabolite M376 was present in AOB, Ox^- and Ox^+ chemostats. Its presence in AOB reactors was not the result of dioxygenase mediated aromatic ring cleavage reactions since the AOB strain utilized in this study does not possess comparable homologues [51]. Detection of M376 fractions at 254 nm further indicates that this metabolite possesses aromaticity (data not shown). It is therefore postulated that M376 is formed from several mechanisms including methylhydroxylase activity [52, 53] on 4-OH-EE2, monooxygenation of nitro-EE2 to form an epoxide which can be further converted to catechol-EE2 [54, 55] or abiotic photodegradation.

Although bioreactors were covered to prevent light penetration, samples were exposed to ambient light during preparation for lyophilization. Nevertheless, the mechanism dictating M376 formation cannot be confirmed at present.

Reduced mineralization of EE2 by heterotrophs after treatment by AOB cultures may be partially explained by accumulation of nitrite in heterotrophic reactors. Since the feed to these reactors was rich with nitrite (700-800 mg NO_2^--N/L) and the pH was maintained at 7.5, reactive nitrogen species such as NO^+ and NO could have affected bacterial activity [56]. Exposure to nitrite and nitrogenous radicals can result in inhibition of cytochrome oxidases, negatively affecting aerobic respiration [57, 58]. Experiments performed to determine whether nitrite inhibited Ox^- and Ox^+ aerobic respiration suggested that 600 mg NO_2^--N/L was required to significantly inhibit Ox^- respiration ($p = 0.002$); however, Ox^+ respiration was not inhibited at concentrations up to 600 mg NO_2^--N/L ($p > 0.025$; **Table 4.10**). Further experiments that investigated whether high nitrite concentrations slowed the rate of EE2 transformation were also performed and the results are discussed in **section 4.2.10**.

Table 4.10. Specific oxygen uptake rates for Ox^- and Ox^+ cultures exposed to various concentrations of nitrite.

Concentration (mg NO_2^--N/L)	sOUR (mg O_2/g protein.day)	
	Ox^- culture	Ox^+ culture
0	527 ± 67	335 ± 42
10	506 ± 74	278 ± 27
200	375 ± 92	274 ± 98
600	359 ± 36	281 ± 85

Rates were calculated from triplicate or quadruplicate reactor vessels and are reported as $\bar{x} \pm s_x$ where s_x is the standard deviation.

Further transformation and mineralization of EE2 and its metabolites may also be limited by nitroaromatic recalcitrance to biotransformation [54] [59, 60]. It is hypothesized that the slower reaction kinetics involving 4-nitro-EE2 and 2-nitro-EE2 degradation may be manifest through decreased mineralization of radiolabeled content as observed in heterotrophic cultures (**Figure 4-6 B and C**). Since no biotransformation kinetic experiments with isolated nitro-EE2 metabolites were performed in this study, it is difficult to ascertain whether nitro-EE2 recalcitrance may have affected overall EE2 removal. Recent work by Gaulke et al. has suggested that 2-nitro-EE2 is biotransformed up to four times as slowly as EE2 [61]. Although

these researchers did not differentiate the effects that nitro substituents at different locations (C2 versus C4 location) may have on the overall rate of biotransformation observed, it is not illogical to assume that nitro-EE2 recalcitrance partially decreased the extent of mineralization observed in this study. If all the nitro-EE2 formed in the chemostats from this study were mineralized, the radiolabeled carbon dioxide fraction would rise by 11%. This would theoretically increase the mineralization observed in Ox^- and Ox^+ chemostats to 36% and 41% respectively. These theoretical values are still lower than those observed for chemostats with low nitrite concentrations (**Figure 4-5**). Thus, there may be other unforeseen factors that cause a decrease in mineralization in chemostats receiving effluent from AOB reactors. It should be noted that the high nitrite concentrations found in our reactors are an artifact of AOB culturing protocols and do not exist in conventional wastewater treatment plants. Therefore, formation of nitrated estrogens is not expected to be significant in the treatment plants accomplishing complete nitrification. Consequently, EE2 removal in activated sludge systems with low nitrite concentrations should not be affected by nitrite inhibition or nitro-EE2 recalcitrance.

Collectively, our findings confirm that heterotrophic organisms can degrade EE2 and metabolites formed by AOBs. Heterotrophs that are present in activated sludge possess an intrinsic ability to rehabilitate waters contaminated with these compounds. This is significant since catechol and nitrated estrogens possess carcinogenic and mutagenic properties [50]. Thus, our work clearly indicates that heterotrophic activity is crucial to ensuring production of wastewater effluents that have low concentrations of parent and transformation products, and that nitrifiers alone are not sufficient to reach those low concentrations. However, our results also show that nitrifiers can play a critical role in partnering with heterotrophic bacteria to enable this biotransformation.

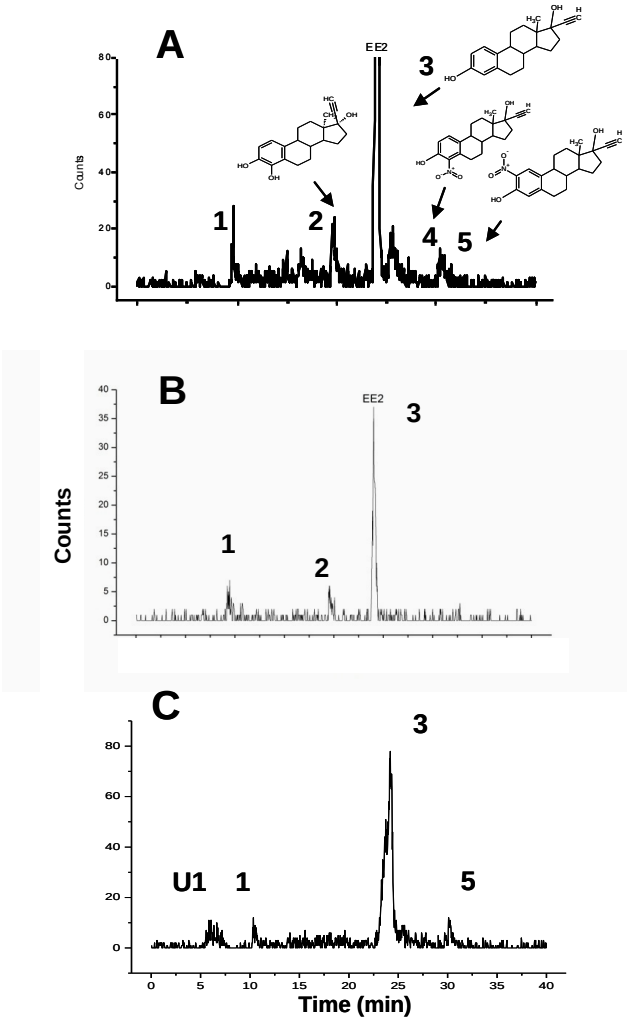

Fraction	Identity	Ret. Time	$[M-H]^-$	% Contribution to ^{14}C activity added
1	N/A	9.5	375	3.6 ± 0.6
2	4-hydroxy-EE2	20	311	5.5 ± 0.9
3	EE2	24	295	70.1 ± 12
4	4-nitro-EE2	26	340	7.3 ± 1.2
5	2-nitro-EE2	31	340	4.5 ± 0.8
$^{14}CO2$	-	N/A	N/A	0
Solids	-	N/A	N/A	0
Avg ^{14}C Mass balance				91.0 ± 15.6

Fraction	Identity	Ret. Time	$[M-H]^-$	% Contribution to ^{14}C activity added
1	N/A	9.5	375	7.2 ± 0.3
2	4-hydroxy-EE2	20	Unknown	6.7 ± 0.3
3	EE2	24	295	37.4 ± 1.7
$^{14}CO2$	-	N/A	N/A	13.0 ± 13.2
Solids	-	N/A	N/A	15.5 ± 4.7
Avg ^{14}C Mass balance				79.8 ± 15.1

Fraction	Identity	Ret. Time	$[M-H]^-$	% Contribution to ^{14}C activity added
1	N/A	9.5	375	3.8 ± 1.9
3	EE2	24	295	48.7 ± 24.3
5	2-nitro-EE2	31	340	5.8 ± 2.9
U1	N/A	6	Unknown	5.8 ± 2.9
$^{14}CO2$	-	N/A	N/A	26.2 ± 7.4
Solids	-	N/A	N/A	14.3 ± 5.7
Avg ^{14}C Mass balance				104.5 ± 37.3

Figure 4-6. Selected radiochromatograms of EE2 and metabolites generated during chemostat experiments. A: Chemostat cultured AOB fed 1 mg/L ^{12}C-EE2 and 10 μg/L ^{14}C-EE2 [29], B: Chemostat Ox^- culture fed effluent from AOB reactor, C: Chemostat Ox^+ culture fed effluent from AOB reactor. Results are representative of analyses performed on duplicate reactors. For complete ^{14}C mass balance on reactors, see Appendix II: Table II.15. Detailed calculations describing percent contribution of transformation products to the overall ^{14}C input to the system are summarized in Appendix II: Table II.16.

4.2.8 TMP was not biotransformed in AOB chemostats but was transformed by Ox^- and Ox^+ chemostat cultures.

TMP was not biotransformed by chemostat cultured AOBs; however, TMP was biotransformed by Ox^- (49%) and Ox^+ (27%) chemostat cultures (**Figure 4-7**), forming 2 metabolites (**Figure 4-8**). These metabolites, detected via positive mode ESI LC/MS ($[M-H]^+$), correspond to *m/*z 221 (M220) and 183 (M182). Both metabolites appeared in Ox^- and Ox^+ reactors, suggesting that TMP degradation by heterotrophs proceeds via a similar pathway. These metabolites also appear to be resistant to further degradation under the conditions tested in this study. Quantification of both metabolites formed in this study was not possible because purified standards could not be obtained.

TMP biotransformation was not enhanced by enriched oxygenase activity present in Ox^+ chemostats. This result is expected since the basal level oxygenase activity present in both Ox^- and Ox^+ cultures is theoretically sufficient to achieve complete oxidation of TMP to carbon dioxide (**Appendix II: Tables II.9 to II.14**). These findings validate thoughts that TMP losses in activated sludge systems are primarily due to heterotrophic activity as compared to AOB activity as explained by Batt et al. (2006) [23]. Since heterotrophs may be the key microbial consortia responsible for TMP degradation, future investigations are needed to determine whether TMP removal is governed by co-metabolism, fortuitous metabolism or mixed substrate utilization processes.

4.2.9 TMP was biotransformed by Ox^- and Ox^+ chemostat cultures fed effluent from AOB reactors.

TMP biotransformation was also observed in heterotrophic chemostats fed effluent from AOB reactors initially fed TMP. In these heterotrophic reactors, the theoretical distribution profiles assuming well mixed reactor hydraulics and no TMP reactions greatly over-predicted the measured TMP concentration in the system (**Figure 4-9**). This suggests that TMP was removed from the heterotrophic reactors through processes like sorption and biotransformation. It is unclear whether nitrite accumulation influenced TMP biodegradation since this study was only carried out for 21 days. If high nitrite concentrations do affect aerobic respiration, decreased biotransformation of TMP would be expected in a manner similar to the reduced EE2 mineralization observed.

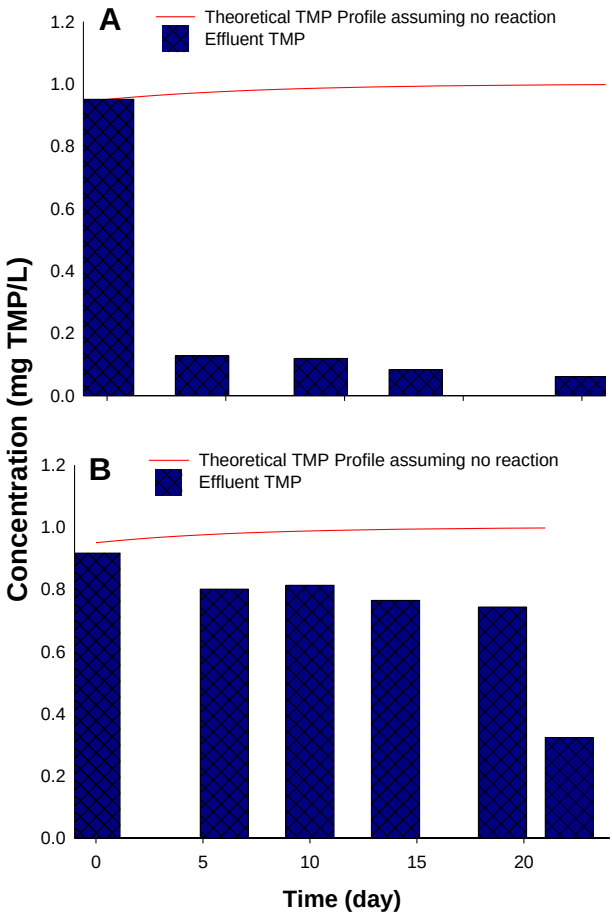

Figure 4-7. TMP profile for heterotrophic chemostat reactors. A: Ox^- reactor fed 1000 mg sCOD/L and 1 mg TMP/L, B: Ox^+ reactor fed 1000 mg sCOD/L and 1 mg TMP/L. Results are representative of profiles observed in duplicate reactors.

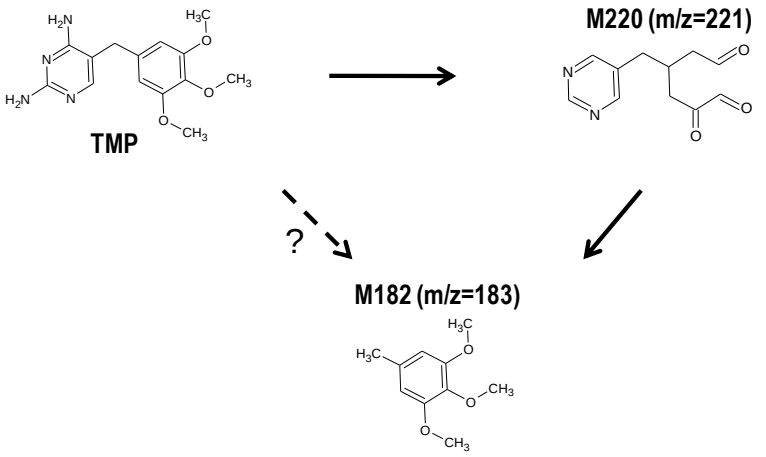

Figure 4-8. Transformation products of TMP generated in heterotrophic reactors. M220: 2-oxo-4-(pyrimidin-5-methyl)hexanedial, M182: 1,2,3-trimethoxy-5-methylbenzene

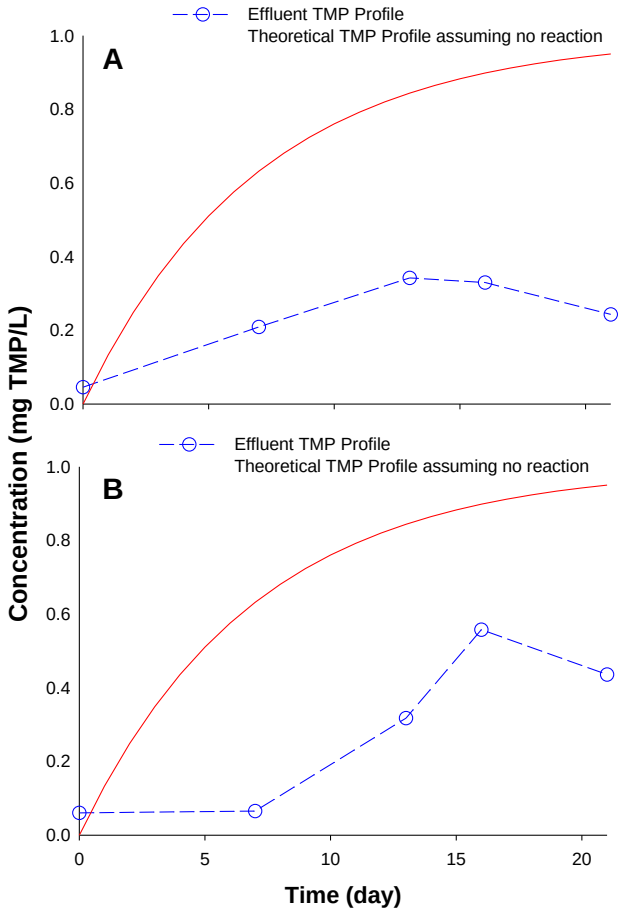

Figure 4-9. TMP profile for heterotrophic chemostat reactors fed effluent from AOB reactor. A: Ox^- reactor fed effluent from AOB reactor, B: Ox^+ reactor fed effluent from AOB reactor. Results are representative of profiles observed in duplicate reactors.

4.2.10 Kinetics suggests that initial biotransformation of EE2 is governed by AOBs while TMP is transformed by heterotrophs only.

It is hypothesized that EE2 biotransformation in NAS occurs via reactions with both AOBs and heterotrophs. To further evaluate the contribution of AOBs versus heterotrophs during EE2 biotransformation, extant kinetic assays were performed with aliquots of chemostat grown AOB, Ox^- and Ox^+ cultures. The rate of EE2 biotransformation by each culture alone and in combination as mixtures of AOB/Ox^- and AOB/Ox^+ cells was evaluated. The results are presented in **Table 4.11** and suggest that pure AOBs transform EE2 approximately 5 times faster than Ox^- or Ox^+ cultures. The experiments with AOB/Ox^- and AOB/Ox^+ mixtures confirmed that AOBs can increase the rate of EE2 biotransformation (**Table 4.11**). The considerable increase in biotransformation rate observed with defined mixtures cannot be explained using simple linear extrapolation of AOB and heterotrophic activities. This increase in activity due to the presence of AOBs is assumed to be the result of high levels of ammonia monooxygenase activity (AMO) [31] whereas transformation by the heterotrophs may result from diauxie and mixed substrate utilization processes.

The faster reaction rate observed for AOBs versus heterotrophs is postulated to be due to the fact that EE2 biotransformation by AOBs involves a single monohydroxylation reaction. EE2 biotransformation by heterotrophs is expected to involve multiple reactions with various enzymes resulting in ring cleavage and mineralization (**Sections 4.2.6** and **4.2.7**). These numerous interactions can be manifest through a slower biotransformation rate. The slower EE2 biotransformation rate observed with heterotrophic cultures can also be consequence of synergistic reactions that are catalyzed by multiple microorganisms. Since EE2 is present at low concentrations in WWTPs, biotransformation reactions cannot yield sufficient energy to select for a populous specialist community. EE2 biodegradation by heterotrophs would need to be coupled to removal of other metabolizable substrates. Since chemostat cells were washed in our experiments to remove electron donors and no external organic substrates other than EE2 (and NH_3 for AOB mixture experiments) were supplemented into extant assays, it is possible that a lack of a suitable co-substrate to help fuel mixed substrate utilization reactions slowed EE2 biodegradation by heterotrophs.

In contrast to EE2 experiments, TMP was not biotransformed by AOBs; however TMP was biotransformed by Ox^- and Ox^+ cells (**Table 4.11**). These results confirm our hypothesis that heterotrophs are primarily responsible for TMP degradation as observed in activated sludge. These results also indicate that basal levels of oxygenase activity do not limit TMP biotransformation. In fact, Ox^- cultures transformed TMP faster than Ox^+ cells; the reason for this difference is unclear.

Table 4.11: Extant kinetic characterization of EE2 and TMP biotransformation by defined mixtures of AOB, Ox^- and Ox^+ cultures.

Culture Details	k_{EE2} (L/g biomass as COD-day)	k_{TMP} (L/g biomass as COD-day)	sNGR (mg N/g biomass as COD-day)
AOB	15.0 ± 0.10	-	143 ± 0.08
100% Ox^-	3.11 ± 0.64	1.20 ± 0.13	-
5% AOB; 95 % Ox^{-a}	15.8 ± 0.03	-	14 ± 0.28
Theoretical 5% AOB; 95% Ox^-	3.7	-	-
100% Ox^+	3.06 ± 0.14	0.58 ± 0.09	N/A
6% AOB; 94 % Ox^{+a}	20.4 ± 0.03	-	28 ± 0.16
Theoretical 6% AOB; 94% Ox^+	3.8	-	-

[a]Mixtures are reported on mass basis.

Rates were calculated from duplicate reactor vessels and are reported as $\bar{x} \pm RMD$ where RMD is the relative mean difference.

Extant kinetic texts performed with Ox^- cultures supplemented with various nitrite concentrations (10, 200, 600 mg NO_2^- -N/L) indicated that EE2 transformation slowed in the presence of nitrite concentrations in excess of 10 mg NO_2^- -N/L (**Table 4.12**). Taken together with results from respirometric assays (**Table 4.10**), nitrite accumulation in heterotrophic reactors can explain reduced EE2 biodegradation observed in heterotrophic chemostats fed effluent from AOB reactors (**Section 4.2.7**).

Table 4.12. Extant kinetic characterization of EE2 transformation by Ox^- culture in the presence of elevated nitrite concentrations.

Culture Details	k_{EE2} (L/g biomass as COD-day)
600 mg NO_2^--N/L	1.01 ± 0.00
200 mg NO_2^--N/L	1.43 ± 0.63
10 mg NO_2^--N/L	2.18 ± 0.41
0 mg NO_2^--N/L	3.11 ± 0.61

Rates were calculated from duplicate reactor vessels and are reported as $\bar{x} \pm RMD$ where RMD is the relative mean difference.

Results from chemostat experiments and extant bioassays suggest that the ultimate fate of both EE2 and TMP in activated sludge is rate limited by heterotrophic activity. Even though AOBs transform EE2 to hydroxylated intermediates, it is the heterotrophic community that will subsequently mineralize residual EE2 and transformation products that are formed. Similarly, TMP loss in activated sludge appears to be primarily due to heterotrophic biotransformation.

4.2.11 EE2 biotransformation in nitrifying activated sludge is proposed to proceed via Ring A cleavage.

There exists no coherent framework that describes how EE2 degradation proceeds during activated sludge treatment even though overall EE2 removal rates are widely reported. Using metabolite data generated from this study and from the existing literature, EE2 degradation is proposed to proceed via ring A cleavage (**Figure 4-10**). Initial modification of EE2 can involve hydroxylation of ring A at the C-2, C-4 or C-10 location to produce an unstable hydroxy-EE2 metabolite (In this study, 4-hydroxy-EE2 (4-OH-EE2)). This initial reaction is catalyzed by AOBs and heterotrophic bacteria that contain enzymes with similar activity as cytochrome P450 monooxygenases [62, 63]. Subsequent ring A cleavage by heterotrophs can then occur via ortho or meta pathways to form catabolic metabolites (ETP 1 – 3) that may be shuttled to central pathways. In this study, ring A cleavage is hypothesized to occur via oxidative cleavage of 4-OH-EE2 between C-4 and C-5 subunits by protocatechuate-3,4- intradiol dioxygenase homologues.

Upon ring cleavage, transformation products can be subject to hydration and decarboxylation reactions (**Figure 4-10**), resulting in the formation of pyruvic acid which may then be shuttled to the tricarboxylic acid cycle [64, 65]. Detection of metabolites without ring A remains elusive and suggests that they have short half lives. Nevertheless, the presence of radiolabeled CO_2 in heterotrophic chemostat cultures confirms that mineralization is possible and when combined with past research that examined the degradation of steroids [64-66], provides evidence that the proposed pathway is plausible.

EE2 can also undergo modification of the acetylenic moiety. Epoxidation of the ethinyl substituent by AOBs under ammonia rich conditions will lead to the formation of M386 [29]. Conversion of EE2 to estrone (E1) by heterotrophs has also been reported [32] but this reaction is yet to be confirmed elsewhere in the literature. Hydroxylation at the C-9 position and subsequent cleavage of non-aromatic ring B are possible [66, 67]; however C-17 epoxidation/oxidation and C-9 hydroxylation are not expected to play a major role in initial EE2 reactions that may occur in activated sludge.

4.2.12 Biotransformation of TMP is hypothesized to be limited by demethylation reactions.

Although little information is available regarding TMP fate during activated sludge treatment, TMP degradation is postulated to proceed via *O*-demethylation and oxygenation reactions that produce mono/di-hydroxylated intermediates (3-OH-TMP, 4-OH-TMP, 3,4-OH-TMP and 5-OH-TMP respectively). These reactions are hypothesized to be performed by heterotrophic organisms and rely on a supply of energy cofactors like NAD(P)H [68]. Aromatic ring cleavage and carbon-nitrogen bond cleavage can occur but only after hydroxylation [69, 70]. Metabolites formed after ring cleavage are postulated to undergo hydration and decarboxylation before entering the tricarboxylic acid cycle (**Figure 4-11**). It is also possible that TMP can undergo conjugation with glutathione (GSH) to produce GSH-TMP adducts (TMP G). These adducts are largely inert to further transformation and will accumulate in the environment. To properly account for TMP fate in activated sludge systems, it is imperative that future surveys account for these conjugated metabolites.

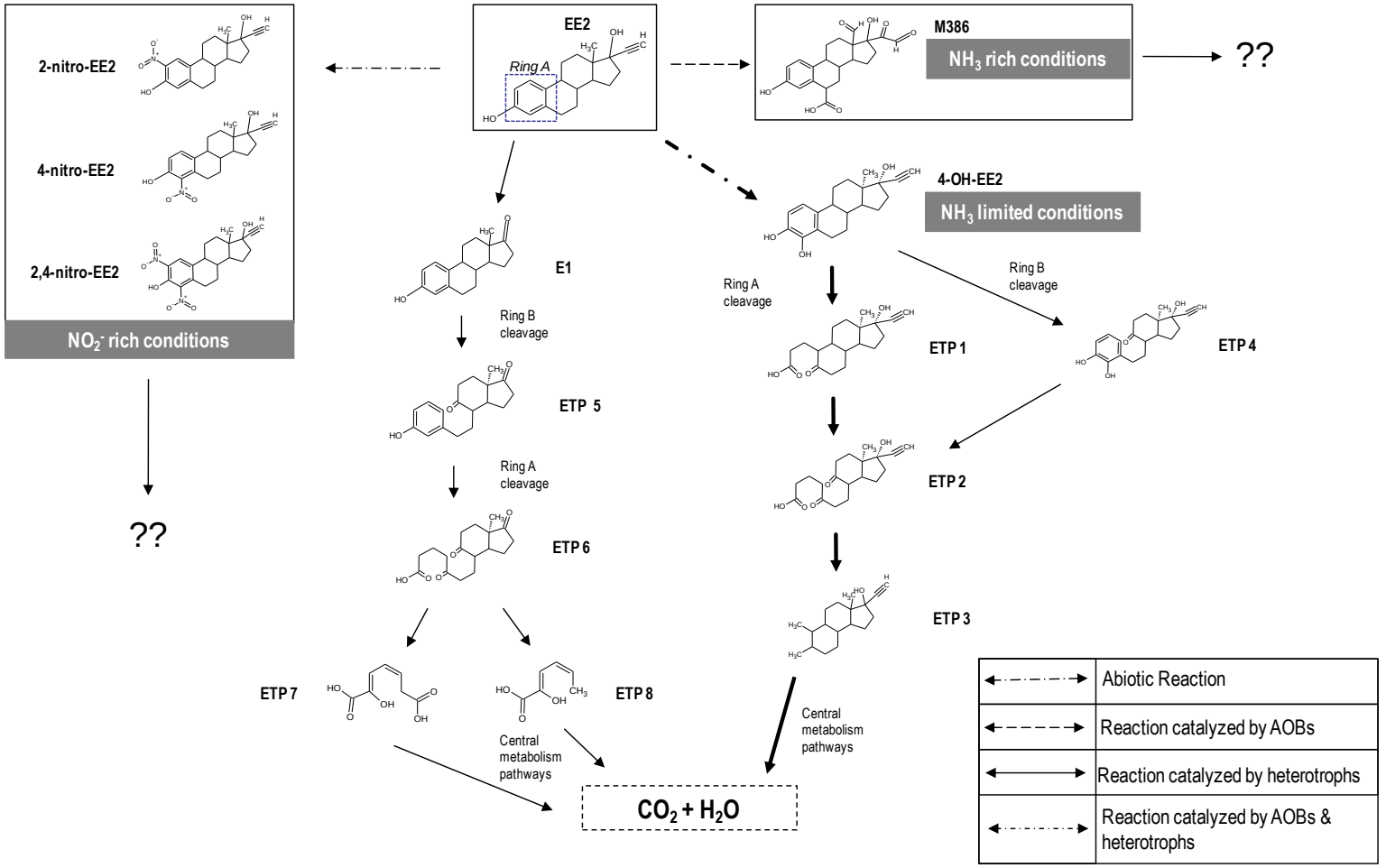

Figure 4-10. Proposed reaction cascade for EE2 during treatment with activated sludge. EE2: 17 α-ethinylestradiol ($[M-H]^-$ = 295), E1: estrone ($[M-H]^-$ = 269), 4-OH-EE2: 4-hydroxy-ethinylestradiol ($[M-H]^-$ = 311), ETP 1: $[M-H]^-$ = 317, ETP 2: $[M-H]^-$ = 333, ETP 3: 3-ethynyl-3a,6,7-trimethyl-2,3,3a,4,5,5a,8,9,9a,9b-decahydro-1H-cyclopenta[a]naphthalen-3-ol ($[M-H]^-$ = 259) [31], ETP 4: $[M-H]^-$ = 317, ETP 5: 3-hydroxy-9, 10-secoandrosta- 1,3,5(10)-triene-9,17-dione ($[M-H]^-$ = 285) [66], ETP 6: $[M-H]^-$ = 307, ETP 7: 2-hydroxy-2,4-diene-1,6-dioic acid $[M-H]^-$ = 171 [32], ETP 8: 2-hydroxy-2,4-dienevaleric acid $[M-H]^-$ = 127 [32], ETPs 1-6 may not be detected due to short half lives.

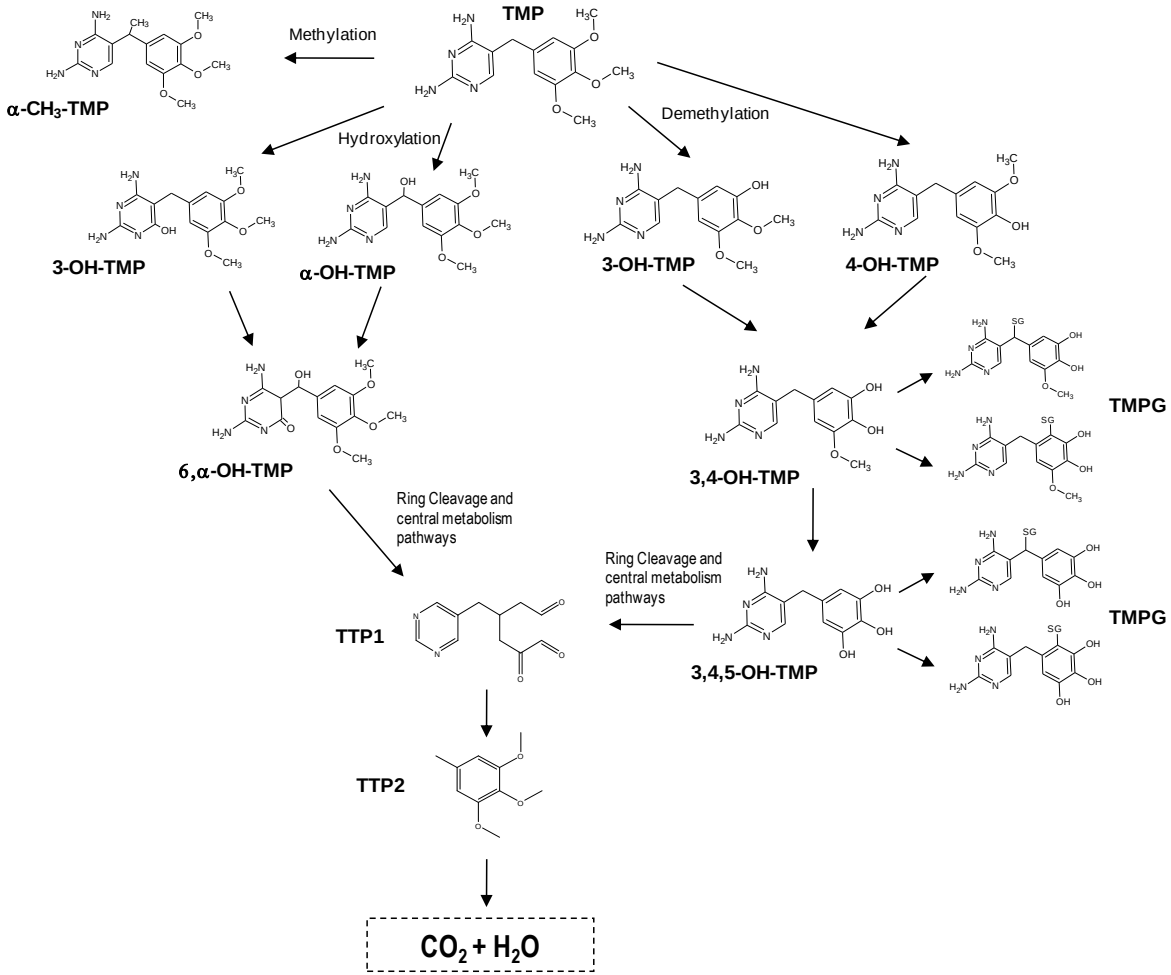

Figure 4-11. Proposed reaction cascade for TMP during activated sludge treatment. TMP: Trimethoprim, α-OH-TMP: Cα-hydroxytrimethoprim, α-CH_3-TMP: Cα–methyl-hydroxytrimethoprim, 3-OH-TMP: 3-hydroxytrimethoprim, 4-OH-TMP: 4-hydroxytrimthoprim, 3,4-OH-TMP: 3,4-hydroxytrimethoprim, 3,4,5-OH-TMP: 3,4,5-hydroxytrimethoprim, 6,α-OH-TMP: 6,Cα-hydroxytrimthoprim, TMPG: Trimethoprim-glutathione adducts, TTP1:$[M-H]^-$ = 221, TTP2: $[M-H]^-$ = 183.

4.3 The Role of Readily Biodegradable Substrates and Physiology in the Biotransformation of EE2 and TMP during Activated Sludge Treatment.

Microconstituent fate during activated sludge treatment can be influenced by AOBs, heterotrophs or a combination of both communities. Work done in this study indicates that EE2 biotransformation is linked to AOB and heterotrophic activity whereas TMP appears to be primarily biotransformed by heterotrophs only (**Section 4.2**). While this shows that microbial ecology can influence microconstituent biodegradation, it is unclear how factors like SRT, sludge history, organic loading and presence/absence of readily biodegradable substrates can impact degradation in activated sludge systems. Recent findings have indicated that statistical correlations between SRT and microconstituent removal are weak [71-73]. Thus, there are other factors that need to be considered. Few studies have addressed the influence of these factors on the fate of microconstituents under physiological conditions approaching those experienced in WWTPs [26, 74] (Cirja 2007; Ren 2007). Results in this section provide an insight into the influence that organic and microconstituent loading and residual organic matter can have on heterotrophic degradation of microconstituents. A simple kinetic model that describes microconstituent degradation using sorption coefficients (**Section 4.1**) and pseudo-first order biotransformation rates (**Section 4.2**) is also presented and results from this empirical model are compared to data.

4.3.1 Organic and microconstituent loading impacts microconstituent degradation.

EE2 and TMP were introduced over the course of a 5 week period to Ox^- reactors operated at an SRT of 7 days and loaded at 685 mg COD/g VSS-day and 0.685 mg EE2 or TMP/g VSS-day. Steady state removal of EE2 (~0.6 mg EE2/g VSS-day; 80% removal efficiency) was achieved within 2-3 SRTs of start of operation and was maintained throughout the experiment, except during perturbation events, confirming findings from our previous experiments (**Section 4.2**). Similar removal rates for EE2 are reported in the literature, although the mechanisms of removal are different from those observed in this study. In one activated sludge reactor that was operated at a SRT ranging from 20 – 25 days and loaded at 178 mg COD/g VSS-day and 0.02 mg EE2/g VSS-day [26], 80% EE2 removal was observed (70% sorption, 15% liquid effluent, 1% $^{14}CO_2$, 14% unaccounted). In another study where an enriched nitrifier culture was operated at an SRT of 20 days and loaded at 181 mg N/g VSS-day and 0.39 mg EE2/g VSS-day (no exogenous COD added), 66% EE2 removal was observed. No mineralization was reported and removal rates

ranged from 7.8 to 29.1 mg EE2/g VSS-day [31]. While the percent removal reported by Cirja et al. (2007) [26] was similar to that observed in the present study, mass balances around Ox^- and Ox^+ reactors indicated an alternative fate for EE2 (12-15% sorption, 28-30% liquid effluent, 55-65% $^{14}CO_2$) (**Section 4.2**). The higher degree of mineralization in our study could be an artifact of the high EE2 loading rate. It is possible these conditions selected for the development of a heterotrophic community acclimated to using EE2 as an electron donor through mixed substrate utilization reactions. Although, removal rates from the nitrifier reactor reported by Yi et al. (2007) [31] greatly exceeded rates observed in Ox^- and Ox^+ heterotrophic chemostats, these results should not be unexpected since work in **Section 4.2.10** has shown that AOBs convert EE2 five times faster than heterotrophs in the absence of nitrifiers (**Section 4.2.10 and Table 4.11**).

Steady state removal of TMP (~0.4 mg TMP/g VSS-day; 57% removal efficiency) was also achieved in Ox^- reactors within 2-3 SRTs of start of operation. Although biomass associated TMP could not be measured, sorption experiments showed that up to 40% of the input TMP can be removed via sorption to Ox^- biomass (**Section 4.1.4, Table 4.3**). If it is assumed that biotransformation of aqueous phase TMP makes up the difference, then 17% biotransformation occurred in the Ox^- reactors. Another study that looked at TMP fate in an extended aeration full-scale treatment plant operated at an SRT of 17 days and loaded at 37 mg BOD/g VSS-day and 0.002 mg TMP/g VSS-day [17] found that greater than 95% removal of TMP was consistently achieved; those researchers did not explicitly measure sorption of TMP to the biomass so the degree of biotransformation cannot be determined. In another study that investigated the fate of radiolabeled TMP in a lab-scale activated sludge reactor operated at an SRT of 10 days and loaded at 0.05 mg TMP/g VSS-day (no data on influent organic loading), no removal was observed [75]. Therefore TMP biotransformation has not been confirmed with activated sludge studies that assess fate through mass balances. Furthermore, there does not appear to be a clear correlation between TMP removal and SRT.

Results from chemostat bioreactors confirm that EE2 and TMP can be transformed by heterotrophic communities. Experimental results indicate that EE2 removal is enhanced by AOB activity while TMP is not transformed by AOBs (**Section 4.2.10**). Since removal of both microconstituents by heterotrophs is influenced by factors like the presence of AOBs and

organic/microconstituent loading rates, further studies were performed to study the impact of these factors on the fate of EE2 and TMP.

4.3.2 The presence of exogenous rbCOD negatively affects EE2 and TMP removal by chemostat Ox^- cultures.

To elucidate the impact of readily biodegradable organic matter on EE2 degradation, acetate was spiked into duplicate Ox^- chemostats achieving steady state removal of EE2 (~0.6 mg EE2/g VSS-day). EE2 concentrations increased by 0.028 mg/L and then decreased to pre-perturbation levels (~0.15 mg/L) after supplementation of 100 mg acetate-COD/L (**Figure 4-12**). Intracellular NADH concentrations also increased after supplementation. EE2 accumulated to 88% of the theoretical value that would be achieved if the rbCOD spike was assumed to completely inhibit EE2 degradation (**Figure 4-12 C**). Although this increase was not statistically different when compared to results obtained during steady state operation ($p = 0.75$), visual inspection confirmed that rbCOD load perturbations affected steady state EE2 removal. A rapid upregulation of enzymatic machinery to degrade the abundant rbCOD source is postulated to have resulted in the higher EE2 effluent concentrations from Ox^- reactors; however, it is clear that EE2 degradation still occurred in the presence of the readily biodegradable substrate.

TMP also accumulated in duplicate Ox^- reactors supplemented with a readily biodegradable organic substrate (100 mg acetate-COD/L) (**Figure 4-12**). This increase was not statistically different when compared to results obtained during steady state operation ($p = 0.23$); however, the buildup accounted for 75% of the theoretical value that would be expected if the rbCOD spike completely inhibited TMP degradation. In contrast to results from EE2 experiments though, intracellular NADH concentrations remained fairly constant. These results suggest that TMP degradation by heterotrophs was not as acutely affected by the rbCOD transient loads used in this study as was EE2 degradation. It is hypothesized that the Ox^- cultures were able to rapidly adapt to the increased organic load without affecting TMP removal.

Interestingly, EE2 and TMP biotransformation rates did not correspond well with accumulation observed in the chemostats (**Table 4.13**). The EE2 biotransformation rate slowed and did not recover to pre-spike levels after 2 days. In contrast, TMP rates recovered to pre-spike levels after 2 days. In the absence of rate data from parallel control reactors not subjected to acetate

supplementation, it is difficult to conclude that the biotransformation rates were affected by the rbCOD spike. Nevertheless, it is possible that physiological adaptation to nutrient rich conditions imposed by the acetate spike could result in a tradeoff where enzymes previously degrading EE2 or TMP are diverted to metabolize rbCOD. The accumulation of both EE2 and TMP in the chemostats may be a manifestation of that physiological response. Significantly though, EE2 and TMP degradation proceeded, albeit to slower extents, in the presence of rbCOD.

These results clearly indicate that readily biodegradable substrates can slow biodegradation of EE2 and TMP. They also explain why microconstituent degradation is not observed in systems with high organic loading and residual readily biodegradable matter. Although not tested in this current work, it is postulated that the intensity and frequency of organic load perturbations can lengthen the acclimation period required by biomass to allow simultaneous degradation of microconstituents and readily biodegradable organic matter.

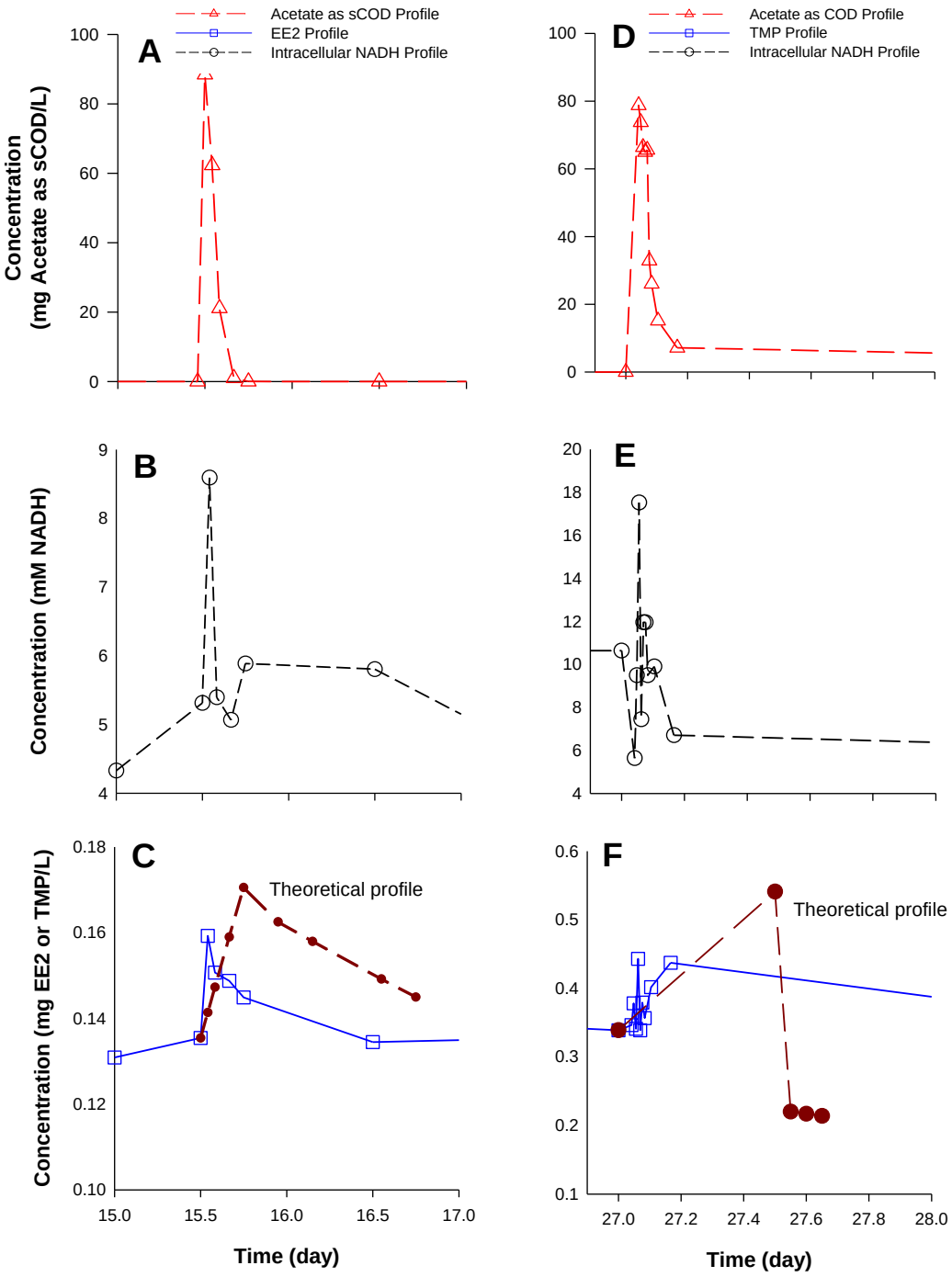

Figure 4-12. Impact of rbCOD supplementation on Acetate, EE2, TMP and Intracellular NADH concentrations in Ox^- chemostats. A – C: Ox^- reactor fed 1 mg EE2/L, D - F: Ox^- reactor fed 1 mg TMP/L. Figures summarize results obtained immediately after supplementation of 100 mg acetate-COD/L. Results are representative of duplicate reactors. See Appendix II: Figures II-5 and II-6 for complete profiles.

Table 4.13. Extant kinetic characterization of EE2 and TMP utilization by Ox^- cultures at various timepoints after rbCOD supplementation.

	k_{EE2} (L/g biomass as COD-day)	k_{TMP} (L/g biomass as COD-day)
Ox^- Pre-Spike	6.15 ± 0.24	1.82 ± 0.58
Ox^- Post Spike (2 hour)	3.48 ± 0.02	0.78 ± 0.25
Ox^- Post Spike (2 day)	1.22 ± 0.29	3.48 ± 1.57
Ox^- Post Spike (7 day)	2.89 ± 0.21	2.67 ± 0.81

Rates were calculated from duplicate reactor vessels and are reported as $\bar{x} \pm RMD$ where RMD is the relative mean difference.

4.3.3 The presence of exopolymeric substances (EPS) and soluble microbial products had a negligible effect on EE2 degradation rates.

Readily biodegradable matter is largely absent in effluents of treatment plants operating at longer SRTs (1.5 – 10 days). In these plants, effluent organic matter (EfOM) is primarily comprised of mixtures containing EPS, soluble microbial products (SMPs) and refractory compounds of anthropogenic origin (e.g. microconstituents). It has been noted that heterotrophic organisms can utilize EPS and SMPs as electron donors [76, 77]. At present it is unclear whether these substrates can slow microconstituent degradation in a manner similar to that observed with readily biodegradable matter (**Section 4.3.2**). Experiments were performed to determine whether the presence of EPS and SMPs can impact EE2 biodegradation by heterotrophs.

Results from extant kinetic assays, in which extracted EPS and SMPs were supplemented into reaction mixtures, suggest that EfOM has limited impact on pseudo-first order rate constants used to describe EE2 degradation (**Table 4.14**). Since extracted EPS/SMPs was not supplemented directly into chemostats, it is premature to conclude that EPS/SMPs can alter the EE2 concentration profiles; however, these results provide partial evidence that EE2 biotransformation rates may not be slowed by these cell-associated substrates. Further studies on the impact of EfOM on microconstituent degradation are needed.

Table 4.14. Extant kinetic characterization of EE2 utilization by Ox^- cultures supplemented with extracted EPS.

Culture Details	k_{EE2} (L/g biomass as COD-day)
Ox^- cells; supplemented with extracted Ox^+ EPS/SMPs[1]	6.06 ± 0.33
Ox^- cells; supplemented with extracted Ox^- EPS/SMPs[2]	3.47 ± 0.05
Ox^- cells; no EPS supplementation	3.11 ± 0.64

[1]Ox+ EPS/SMP extract contained 206 mg BSA-protein/L and 388 mg glucose-COD/L
[2]Ox- EPS/SMP extract contained 506 mg BSA-protein/L and 484 mg glucose-COD/L

4.3.4 EE2 mineralization by heterotrophic cultures can occur in the absence of other organic substrates.

Results from short term experiments confirm that EE2 can be used as an electron donor by Ox^- and Ox^+ cell suspensions (**Figure 4-13**). A mass balance on radiolabeled content indicated that 10% of the activity applied to the system was detected in the solids fractions (minus sorption) and 7% was measured as $^{14}CO_2$. Exogenous NADH supplementation (5 mM) to batch cultures did not increase mineralization (For Ox^- reactors $p = 0.415$; For Ox^+ reactors $p = 0.432$). These results suggest that EE2 degradation is not limited by NADH availability. Interestingly, intracellular NADH concentrations did not vary over the course of these experiments suggesting that it is not an appropriate proxy to predict or monitor EE2 biodegradation (**Appendix II: Figure II-7**). Based on results from chemostat studies in **Section 4.2**, it should be expected that other anapleurotic metabolites are generated from EE2 metabolism. These metabolites were not isolated in the present experiment but may account for a portion of the increased radiolabeled content in the solids fraction observed for both Ox^- and Ox^+ cultures.

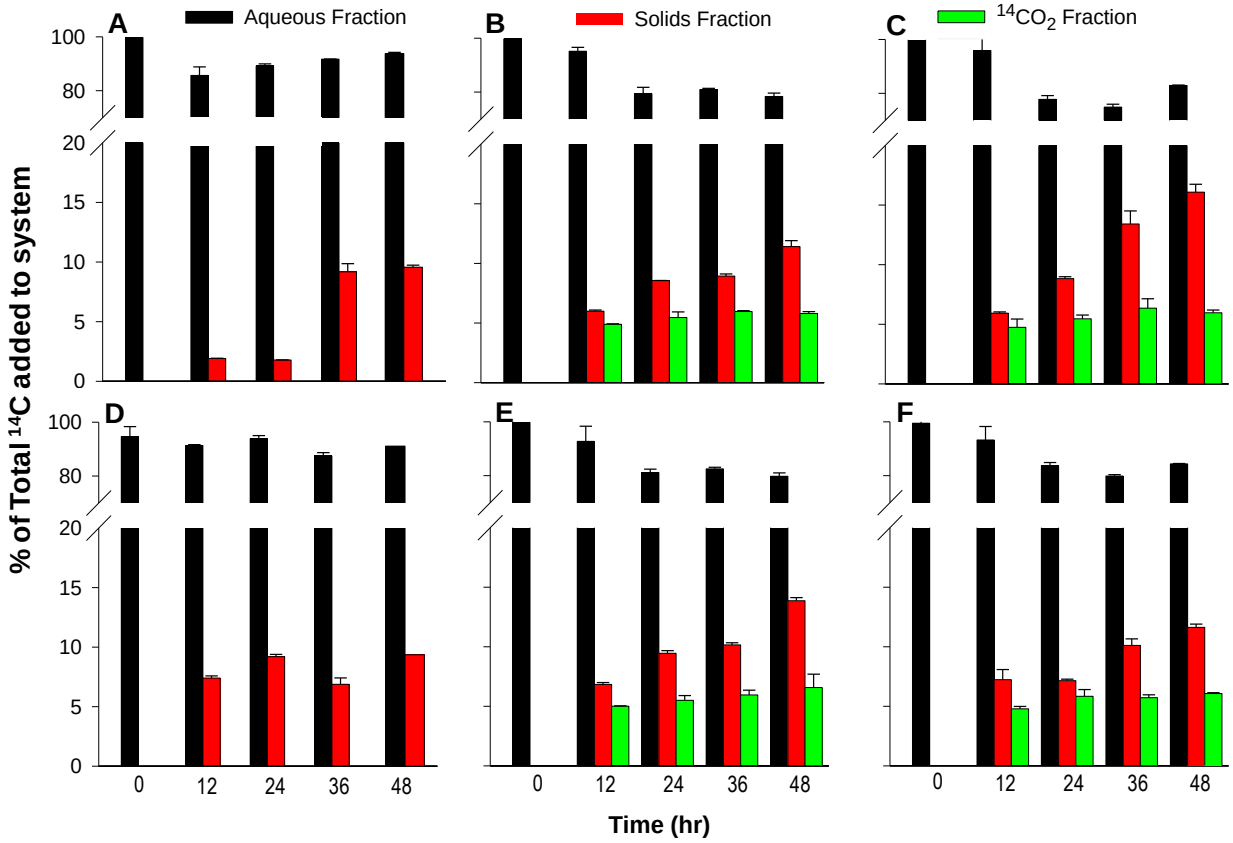

Figure 4-13. Results from short-term incubations of Ox^- and Ox^+ cultures with EE2. A: Ox^- sorption control, B: Ox^- supplemented with 200 μg/L ^{14}C-EE2, C: Ox^- supplemented with 200 μg/L ^{14}C-EE2 and 5 mM NADH, D: Ox^+ sorption control, E: Ox^+ supplemented with 200 μg/L ^{14}C-EE2, F: Ox^+ supplemented with 200 μg/L ^{14}C-EE2 and 5 mM NADH. Results are calculated from 3 replicates.

4.3.5 Cell growth occured on low concentrations of EE2 whereas negligible growth occurred on TMP.

Quantifiable cell growth was observed in long term heterotrophic batch cultures incubated with various EE2 concentrations (5.4, 2.7, 1.4 mg EE2 as COD/L) (**Figure 4-14**) but not in cultures incubated with TMP (**Appendix II: Figure II-8**). These results complement findings from short term experiments (**Section 4.3.4**) and strengthen the hypothesis that heterotrophic cultures have the ability to utilize EE2 as an electron donor in the absence of alternative substrates. Lack of cell growth on TMP is hypothesized to be due to a combination of inhibition and slow transformation kinetics. Although inhibition of Ox^- and Ox^+ cells by TMP was not observed in prior experiments (**Section 4.2.2**), the higher loading of TMP on a per cell basis in these long term experiments (0.17 mg TMP/mg VSS for the current experiment versus 0.04 mg TMP/mg

VSS for sOUR experiments) could have resulted in inhibition. Transformation rates for TMP are also a fraction of the rates (~1/3) measured for EE2 degradation by heterotrophic cultures (**Section 4.2.10**). Both factors could have contributed to the lack of growth observed in TMP experiments.

The rate of exponential phase growth did not vary with EE2 or acetate concentrations used in this study (**Figure 4-14 and Table 4.15;** For EE2 experiments $p > 0.057$; For acetate experiments $p > 0.033$). This can be explained by the fact that both substrates were provided in excess of their half saturation constant values. Correspondingly, growth would not be substrate limited and could have approached the maximum specific growth rate associated with each compound (μ_{max}). That growth rates on acetate and EE2 did not differ at the 95% confidence interval is surprising ($p > 0.114$); however, these results imply that the maximum specific growth rate for cells utilizing EE2 is similar to the maximum specific growth rate for cells using acetate under the conditions tested. Taken together with results from **Section 4.2**, it is clear that heterotrophs can significantly influence the ultimate fate of EE2 during activated sludge treatment. Further experiments should seek to quantify the Monod kinetic parameters associated with heterotrophic EE2 metabolism. This would allow direct comparison of EE2 utilization and biomass growth parameters ($\mu_{max,EE2}$, $K_{S,EE2,}$ $Y_{H,EE2}$) to parameters that exist for readily and slowly biodegradation organic matter.

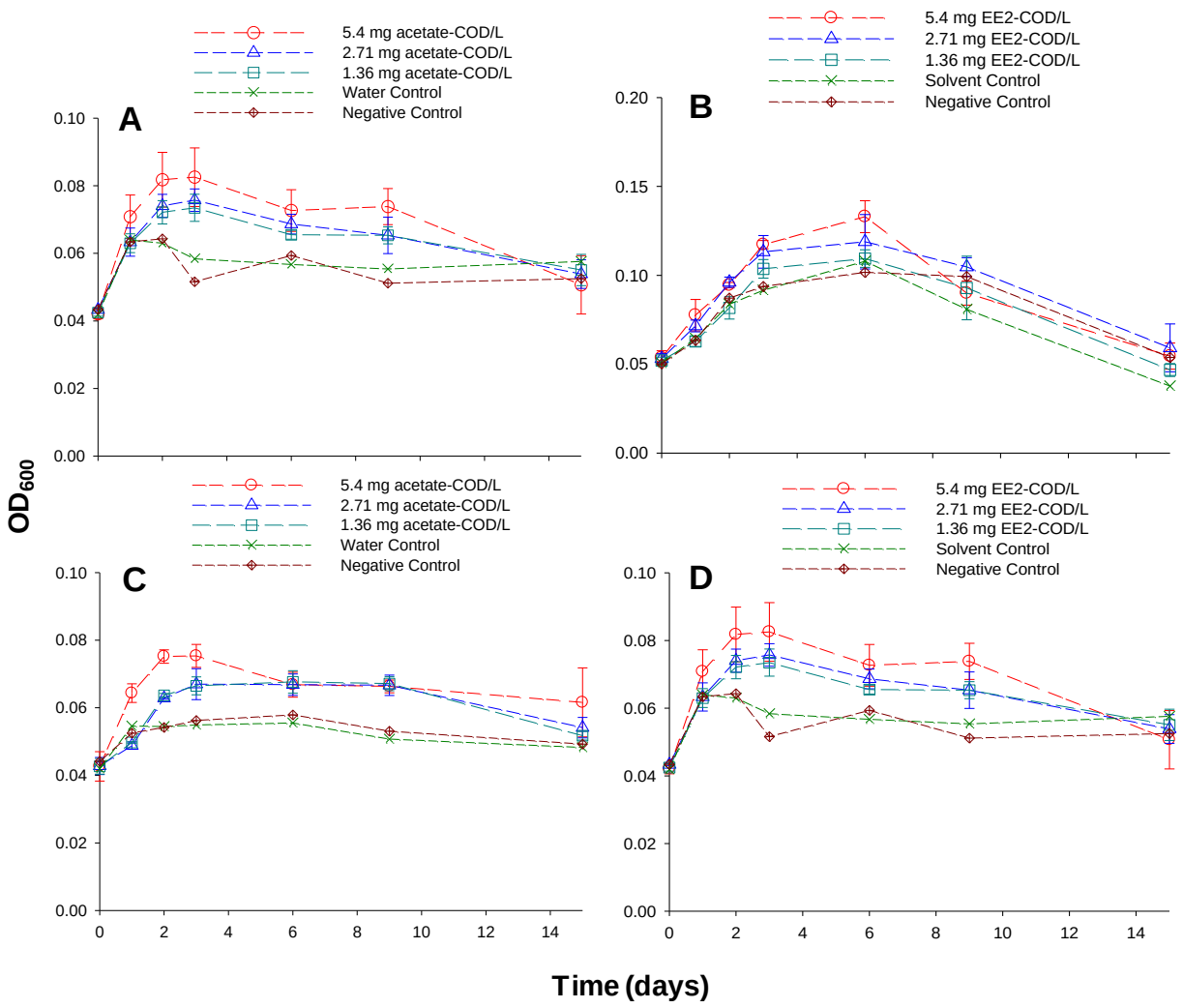

Figure 4-14. Growth profile of Ox^- and Ox^+ cells incubated with various concentrations of acetate and EE2. A: Ox^- cells incubated with acetate only, B: Ox^- cells incubated with EE2 only, C: Ox^+ cells incubated with acetate only, D: Ox^+ cells incubated with EE2 only. Results are calculated from 9 replicates.

Table 4.15. Growth rates for heterotrophic cultures in the presence of acetate and EE2.

Substrate Addition	Slope (1/day)[a]					
	Ox^- cells			Ox^+ cells		
	5.46 mg COD/L	2.71 mg COD/L	1.36 mg COD/L	5.46 mg COD/L	2.71 mg COD/L	1.36 mg COD/L
Acetate addition	0.273 ± 0.039	0.293 ± 0.033	0.272 ± 0.025	0.193 ± 0.049	0.193 ± 0.028	0.181 ± 0.032
EE2 addition	0.256 ± 0.024	0.256 ± 0.026	0.232 ± 0.017	0.141 ± 0.028	0.145 ± 0.055	0.147 ± 0.049
Negative Control	0.098 ± 0.021					

[a]Slopes were determined from 9 replicate wells.

4.3.6 Development of a conceptual model that describes microconstituent degradation.

Conceptual models that describe microconstituent degradation should utilize aspects of existing frameworks that have been used to predict removal of synthetic organic carbon (SOCs) from wastewater [78-83]. These existing models account for the oxidation of non-growth substrates in the presence or absence of growth substrates [78, 79] and are dependent on a variety of factors including facilitated transport into and out of cells, enzyme availability for cooxidation or mixed substrate utilization and reducing energy availability. A simple model that describes microconstituent degradation by heterotrophs was developed. This model was used to determine whether sorption coefficients (**Section 4.1**) and biotransformation rates (**Section 4.2**) determined in this study can appropriately describe microconstituent removal in bioreactors.

In this model, two main phenomena can be assumed to describe transport processes: facilitated diffusion and active transport. As EE2 and TMP both possess biologically active structures, it is possible that biopolymer type transport systems or ABC transport systems allow transfer of these xenobiotics into cells. Although included in the conceptual model, transport processes were not included in model simulations since data that describe these processes are unavailable. Primary substrate degradation, oxygen consumption and biomass growth were modeled according to traditional approach describing biomass decay and loss of viability using Monod kinetics [83]. Microconstituent degradation was modeled using pseudo-first order kinetics. Although heterotrophs can utilize EE2 and possibly TMP as electron donors (**Section 4.3.4**), estimates of maximum specific growth rate and half saturation constants associated with EE2 and TMP metabolism were not performed in this study. Correspondingly, it is inappropriate to utilize biokinetic parameters from the literature that were estimated under completely different physiological conditions [43, 84] since microbial physiology has been shown to significantly affect microconstituent biodegradation by heterotrophs (**Section 4.2**). Degradation of microconstituent transformation products was also not included in this model since little information is currently available regarding this process.

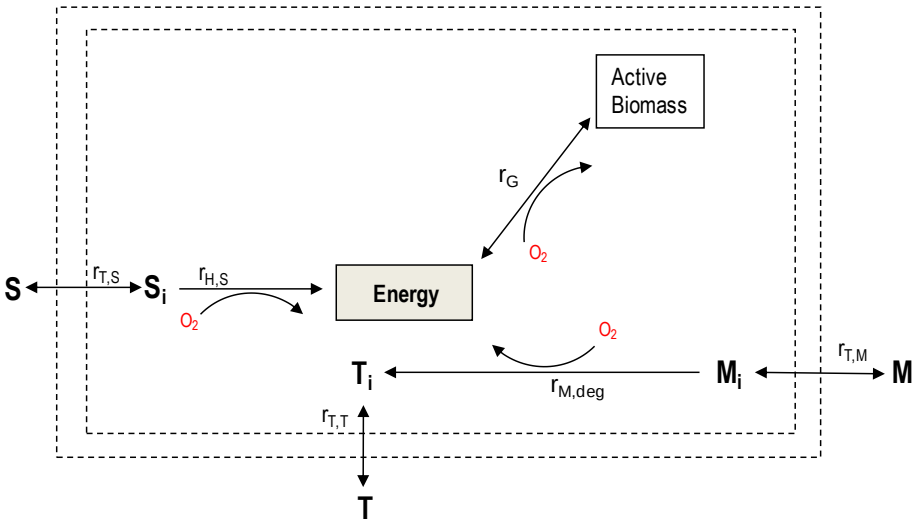

Figure 4-15. Conceptual model describing degradation of microconstituents by heterotrophic bacteria. S: readily biodegradable COD (rbCOD), M: microconstituent, Q: microconstituent transformation product.

Table 4.16. Non-steady state rate expressions and flow model used to describe microconstituent biodegradation in heterotrophic chemostats.

Equation	Process/Model	Process Expression
4-3	Rate of soluble substrate utilization; $r_{H,S}$	$r_{H,S} = -\frac{\mu_{H,S}}{Y_{H,S}}\left[\frac{S_i}{K_{S,i}+S_i}\right]\left[\frac{O_i}{K_{O,i}+O_i}\right]X_{H,i}$
4-4	Rate of microconstituent degradation; $r_{M,deg}$	$r_{M,\mathrm{deg}} = -k_M M X_{H,i}$
4-5	Rate of Biomass Growth: r_G	$r_G = \mu_{H,S}\left[\frac{S_i}{K_{S,i}+S_i}\right]\left[\frac{O_i}{K_{O,i}+O_i}\right]X_{H,i} - (b_{L,H})(1-f_i)\left[\frac{O_i}{K_{O,i}+O_i}\right]X_{H,i}$
4-6	Rate of oxygen utilization; r_O	$r_O = k_L a(O_O - O_i) - \left(\frac{1-Y_H}{Y_H}\right)\mu_{H,S}\left[\frac{S_i}{K_{S,i}+S_i}\right]\left[\frac{O_i}{K_{O,i}+O_i}\right]X_{H,i} - \left[(b_{L,H})(1-f_i)\right]\left[\frac{O_i}{K_{O,i}+O_i}\right]X_{H,i}$
4-7	Microconstituent sorption $k_{M,sorp}$	$k_{M,sorp} = -k_{D,M} M X_{H,i}$
4-8	Flow Model[a]	$\frac{dC}{dt}V = QC_0 - QC - Qk_{sorp} \pm rV$

[a] The "C" notation is used as a generic term to represent substituent concentration.

Table 4.17. Values used in the model describing microconstituent removal.

Coefficient	Definition	Value	Units	Reference
$Y_{H,S}$	Heterotrophic yield for growth on substrate S	0.30	g biomass-COD/g substrate S as COD	This study (**Section 3.2.2**)
f_i	Fraction of active biomass contributing to biomass debris	0.20	g biomass-COD/g biomass as COD	(Grady Jr. 1999)
b_H	Heterotrophic biomass decay rate	0.24	1/day	
$\mu_{maxH,S}$	Maximum specific growth rate on substrate S	6.25	1/day	(Hiatt 2008)
$K_{S,S}$	Half saturation constant for substrate S	20.0	mg substrate S as COD/L	
K_O	Half saturation constant for dissolved oxygen	0.10	mg O_2/L	
k_{EE2}	Pseudo-first order rate constant for EE2	3.11 ± 0.64	L/g biomass as COD-day	This study **Table 4.1**, **Table 4.3** and **Table 4.11**
$k_{D,EE2}$	Solid-water distribution coefficient for EE2	0.47	L/g biomass as COD	
k_{TMP}	Pseudo-first order rate constant for TMP	1.20 ± 0.13	L/g biomass as COD-day	
$k_{D,TMP}$	Solid-water distribution coefficient for TMP	4.80	L/g biomass as COD	
Q	Flowrate	0.29	L/day	This study
V	Volume of reactor	2	L	
S_{in}	Influent acetate concentration	1000	mg acetate as COD/L	
E_{in}	Influent EE2 concentration	2.71	mg EE2 as COD/L	
O_{in}	Influent oxygen concentration	8.0	mg O_2/L	
K_{La}	Oxygen transfer rate	140	1/day	(Laspidou 2002)

4.3.7 EE2 and TMP removal from heterotrophic chemostats are sensitive to pseudo-first order rate constants.

Simulations were performed to evaluate EE2 and TMP fate in heterotrophic chemostats by substituting rate expressions (equations 4-3 to 4-6 in **Table 4.16**) into the flow model described by equation 4-8 in **Table 4.16**. Equations were solved simultaneously using fourth order Runge-Kutta methods in Matlab® over a 48 day interval. Initial conditions for simulations were defined as follows:

a) For EE2, S_0 = 1000 mg COD/L (readily biodegradable substrate; **Figure 4-15**), M_0 = 2.71 mg EE2 as COD/L (microconstituent; **Figure 4-15**), X_0 = 262 mg biomass as COD/L; O_0 = 8 mg O_2/L.
b) For TMP, S_0 = 1000 mg COD/L, M_0 = 1.54 mg TMP as COD/L, X_0 = 262 mg biomass as COD/L; O_0 = 8 mg O_2/L.

Predicted EE2 concentrations using pseudo-first order rate constants from **Table 4.17** were higher than the experimentally determined values (**Figure 4-16**). Manual manipulation of the pseudo-first order rate constant (k_{EE2} = 6.22 L/mg biomass as COD-day) yielded model values that approached experimental data (**Appendix II: Tables II.23 to II.26**). Although this increase doubled the rate constant, it should be noted that the rate used (k_{EE2} = 6.22 L/mg biomass as COD-day) was within the range of values estimated for k_{EE2} from multiple experiments in this study (**Table 4.10 and Table 4.13**). These results indicate that selection of the pseudo-first order rate constant describing EE2 biodegradation is important when modeling EE2 fate. Sorption was not a significant mechanism of removal of EE2 due to the low biomass concentration in bioreactors (**Section 4.1**). As mixed liquor concentrations increase, sorption is expected to become more relevant [26]. Simulations performed assuming a zero order model for EE2 degradation did not predict EE2 removal well even when zero order rate constants were increased to the maximum values estimated in this study (**Appendix II: Table II.30**). These results confirm that EE2 removal is more accurately modeled using pseudo-first order assumptions. Further, accurate estimation of pseudo-first order transformation rates is essential to describing EE2 removal.

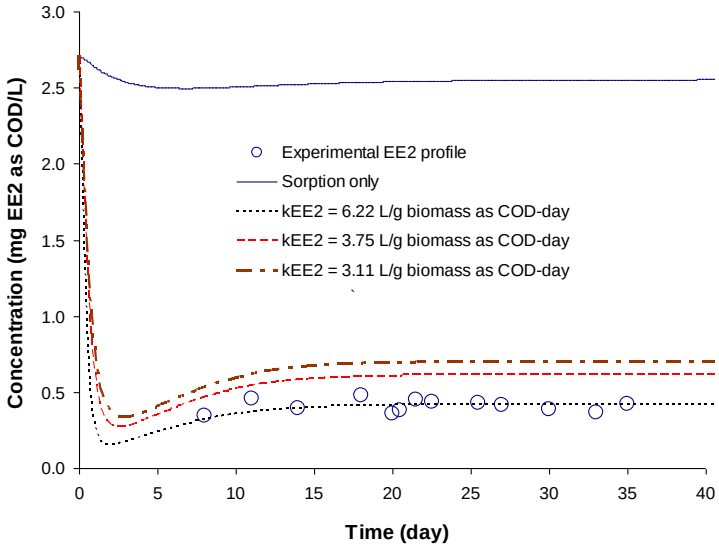

Figure 4-16. Comparison of experimental data and model results describing EE2 removal from Ox^- chemostat. Sorption only trendline ignores biodegradation. All other simulations include sorption and biodegradation. Data are provided in Appendix II: Tables II.23 to II.26.

TMP fate was also modeled reasonably well assuming pseudo-first order biotransformation (**Figure 4-17**). Removal was under-estimated when pseudo-first order rate constants from **Table 4.17** were used; however, the model matched experimental data when the rate constant was doubled (k_{TMP} was set to 2.4 L/g biomass as COD-day). This rate is within the range of values determined for TMP degradation reported in this study (**Table 4.10 and Table 4.13**). Similar to results from EE2 simulations, sorption of TMP was not a significant mechanism of removal. Simulations performed assuming a zero order model for TMP degradation significantly under-estimated TMP removal even when zero order rate constants were increased to the maximum values estimated in this study (**Appendix II: Tables II.28 to II.31**).

Results from this simple model indicate that microconstituent fate prediction is highly dependent on the reaction rate constant used to model biodegradation. These reaction rates are influenced by microbial ecology (**Section 4.2**), physiology and the presence of residual biodegradable matter (**Section 4.3**). Thus, future efforts that are made to model microconstituent fate should account for the kinetic variation that occurs.

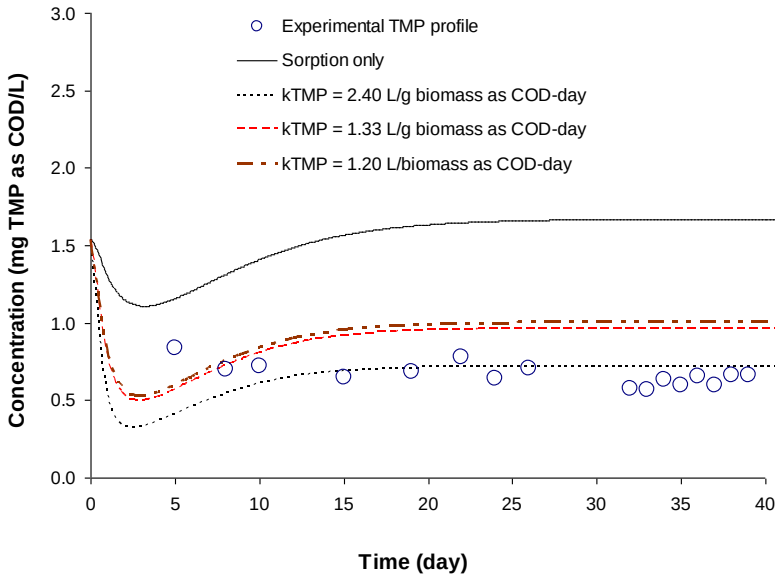

Figure 4-17. Comparison of experimental data and model results describing TMP removal from Ox^- chemostat. Sorption only trendline ignores biodegradation. All other simulations include sorption and biodegradation. Data are provided in Appendix II: Tables II.27 to II.29.

4.3.8 EE2 and TMP fate after supplementation of readily biodegradable substrate was not accurately described using the existing model.

Simulations were also performed to evaluate EE2 and TMP fate in Ox^- chemostats after a pulse input of acetate was applied to the system (**Section 4.3.2**). Rate expressions (equations 4-3 to 4-6 in **Table 4.16**) were substituted into the flow model described by equation 4-8 in **Table 4.16** and these systems were solved simultaneously using fourth order Runge-Kutta methods in Matlab® over a 5 day interval. Conditions for simulations were defined as follows:

a) For EE2, S_0 = 100 mg COD/L, M_0 = 0.452 mg EE2 as COD/L, X_0 = 262 mg biomass as COD/L; O_0 = 8 mg O_2/L.
b) For TMP, S_0 = 100 mg COD/L, M_0 = 0.657 mg TMP as COD/L, X_0 = 262 mg biomass as COD/L; O_0 = 8 mg O_2/L.

Initial concentrations of EE2 and TMP corresponded with the maximum values observed in the experimental profiles after acetate supplementation (**Figure 4-12**).

Predicted EE2 concentrations under-estimated EE2 removal in the chemostat; however, the model values paralleled the trend observed for experimental values over the first 24 hours after acetate supplementation (Figure 4-18). Model and experimental values diverged after this period

(Appendix II: Figure II-9 and Table II.32). This deviation could be a manifestation of the fact that EE2 pseudo-first order rates constants varied as the cells adapted to the feast conditions imposed by the acetate spike. As EE2 degradation is postulated to be slowed during periods where cells metabolize more readily biodegradable substrates, it may be appropriate to use the Andrews equation to describe the inhibitory effect that other substrates may have on EE2 biodegradation by heterotrophs. It is also important to ensure that biokinetic parameters describing EE2 degradation are obtained under conditions where microbial physiology approximates that observed in the bioreactors.

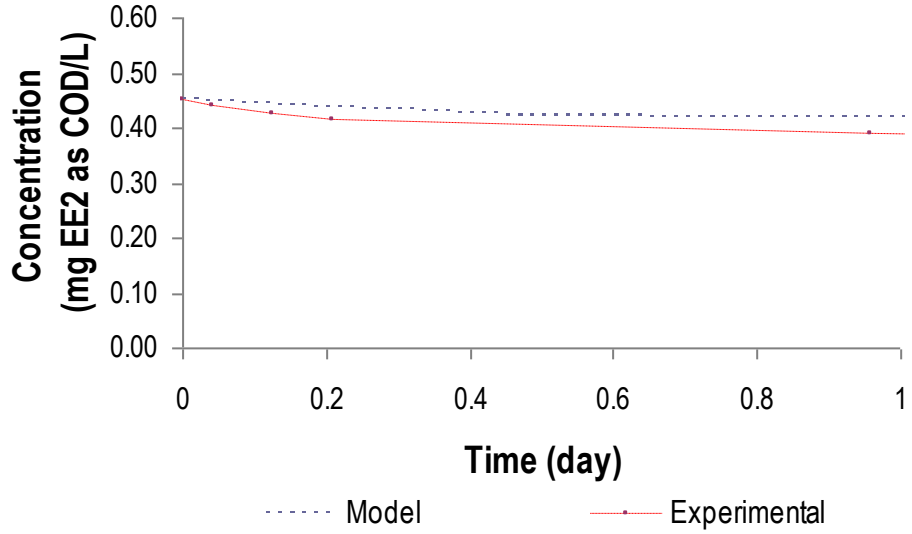

Figure 4-18. Comparison of experimental data and model results describing EE2 removal from Ox^- chemostat after acetate supplementation. Complete profiles are provided in Appendix II: Figure II-9 and Table II.32.

Predicted TMP concentrations did not match experimental data (Figure 4-19 and Appendix II: Figure II-10 and Table II.33). This large variation is postulated to be due in part to the differences in TMP removal rate constants that may be encountered in the presence of an alternative substrate. If TMP removal in NAS is driven by heterotrophs as postulated in this work, removal in the presence of another substrate would need to account for the fact that multiples substrates can affect the growth rate and consequently substrate utilization.

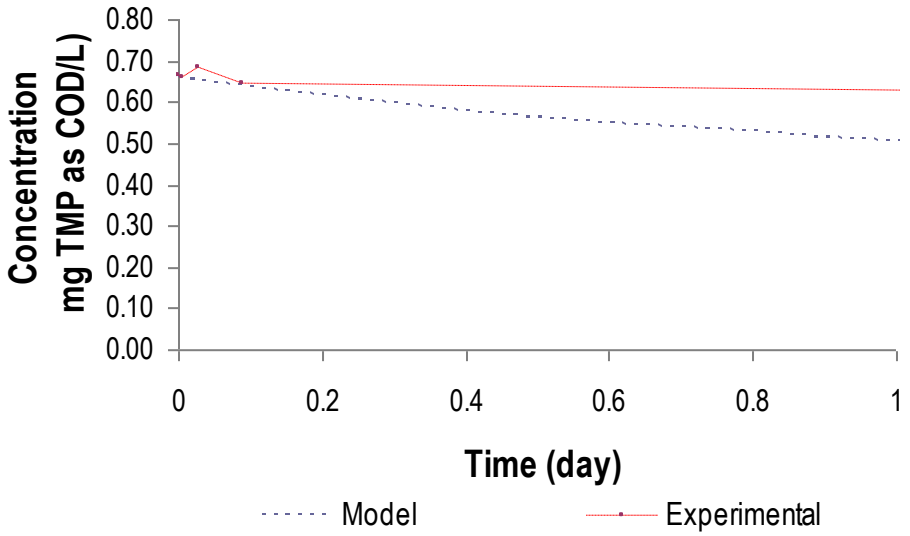

Figure 4-19. Comparison of experimental data and model results describing TMP removal from Ox^- chemostat after acetate supplementation. Complete profiles are provided in Appendix II: Figure II-10 and Table II.33.

Results from this study suggest that the specific substrate removal rate for EE2 and TMP can vary as the system experiences transient loads of readily biodegradable substrates. There are numerous approaches that researchers can employ to account for the effects that may be encountered. Inhibition of microconstituent removal by rbCOD can be modeled using Andrews kinetics [85]. Researchers can also account for the effects that microbial physiology and substrate concentration can have on substrate removal rates by employing the dynamic Powell expression [86]. Combination of these two techniques will lead to the development of a rate expression that accounts for changes in physiology and substrate concentration as well as due to the inhibitory effects that other substrates may have on biodegradation. This model can then be extended to account for the effects that other limiting substrates (electron donors) can have on microconstituent removal using the multiple Monod approach [83].

4.4 References

1. Andersen, H. R., Hansen, M., Kjolholt, J., Stuer-Lauridsen, F., Ternes, T.A., Halling-Sorensen, B., Assessment of the Importance of Sorption for Steroid Estrogens Removal During Activated Sludge Treatment. *Chemosphere* **2005,** *61*, 139-146.
2. Ternes, T. A., Herrmann, N., Bonerz, M., Knacker, T., Siegrist H., Joss, A., A Rapid Method to Measure the Solid–Water Distribution Coefficient (K_d) for Pharmaceuticals and Musk Fragrances in Sewage Sludge. *Water Research* **2004,** *38*, 4075-4084.
3. Khanal, S. K., Xie, B., Thompson, M. L., Sung, S., Ong, S.K., Van Leeuwen, J. H., Fate, Transport, and Biodegradation of Natural Estrogens in the Environment and Engineered Systems. *Environmental Science and Technology* **2006,** *40*, (21), 6537-6546.
4. Lindberg, R. H., Olofsson, U., Rendahl, P., Johansson, M.I., Tysklind, M., Anderrson, B.A., Behavior of Fluoroquinolones and Trimethoprim During Mechanical, Chemical, and Active Sludge Treatment of Sewage Water and Digestion of Sludge. *Environmental Science and Technology* **2006,** *40*, (3), 1042-1048.
5. Williams, C. F., Adamsen, F.J., Sorption–Desorption of Carbamazepine from Irrigated Soils. *Journal of Environmental Quality* **2006,** *35*, 1779-1783.
6. Loffler, D., Rombke, J., Meller, M., Ternes, T.A., Environmental Fate of Pharmaceuticals in Water/Sediment Systems. *Environmental Science Technology* **2005,** *39*, 5209-5218.
7. Chiou, C. T., *Partion and Adsorption of Organic Contaminants in Environmental Systems.* John Wiley and Sons: New Jersey, 2002; p 257.
8. Yi, T., Harper Jr., W.F.,Holbrook, R.D., Love, N.G., Role of Particle Size and Ammonium Oxidation in Removalof 17α-Ethinyl Estradiol in Bioreactors. *Journal of Environmental Engineering* **2006,** *132*, (11), 1527-1529.
9. Poole, S. K., Poole, C.F., Chromatographic Models for the Sorption of Neutral Organic Compounds by Soil from Water and Air. *Journal of Chromatography A* **1999,** *845*, 381-400.
10. Xu, K., Harper Jr., W.F., Zhao, D., 17α-Ethinylestradiol sorption to activated sludge biomass: Thermodynamic properties and reaction mechanisms. *Water Research* **2008,** *42*, 3146-3152.
11. Ren, Y. X., Nakano, K., Nomura, M., Chiba, N., Nishimura, O., A Thermodynamic Analysis on Adsorption of Estrogens in Activated Sludge Process. . *Water Research* **2007,** *41*, 2341-2348.
12. Holbrook, R. D., Love, N.G., Novak, J.T., Sorption of 17β-Estradiol and 17α-Ethinylestradiol by Colloidal Organic Carbon Derived from Biological Wastewater Treatment Systems. *Environmental Science and Technology* **2004,** *38*, 3322-3329.
13. Flemming, H. C., Wingender, J., Relevance of Microbial Extracellular Polymeric Substances (EPSs) – Part I: Structural and Ecological Aspects. *Water Science and Technology* **2001,** *43*, (6), 1-8.
14. Frolund, B., Palmgrend, R., Keiding, K., Nielsen, P.K., Extraction of Extracellular Polymers from Activated Sludge using a Cation Exchange Resin. *Water Research* **1996,** *30*, (8), 1749-1758.
15. Nguyen, T. H., Goss, K.U., Ball, W.P., Polyparameter Linear Free Energy Relationships for Estimating the Equilibrium Partition of Organic Compounds between Water and the Natural Organic Matter in Soils and Sediments. *Environmental Science and Technology* **2005,** *39*, (4), 913-924.

16. Gobel, A., Thomsen, A., McArdell, C.S., Joss, A., Giger, W. , Occurrence and Sorption Behavior of Sulfonamides, Macrolides, and Trimethoprim in Activated Sludge Treatment *Environmental Science and Technology* **2005,** *39*, (11), 3981 -3989.
17. Batt, A. L., Kim, S., Aga, D.S. , Comparison of the Occurrence of Antibiotics in Four Full-scale Wastewater Treatment Plants with Varying Designs and Operations. *Chemosphere* **2007,** *68*, (3), 428-435.
18. Schwarzenbach, R. P., Gschwend, P.M., Imboden, D.M., *Environmental Organic Chemistry*. 2nd Edition ed.; Wiley Interscience: Hoboken, N.J, 2003.
19. Ternes, T. A., P. Keckel, Mueller, J. , Behaviour and Occurrence of Estrogens in Municipal Sewage Treatment Plants. 1. Investigations in Germany, Canada and Brazil. *Science Total Environment* **1999,** *225*, 91-99.
20. Ternes, T. A., P. Keckel, Mueller, J., Behaviour and Occurrence of Estrogens in Municipal Sewage Treatment Plants. II. Aerobic Batch Experiments With Activated Sludge. *Science Total Environment* **1999,** *225*.
21. Carballa, M., Omil, F., Lema, J.M., Llompart, M., Garcia-Jares, C., Rodriguez, I., Gomes, M., Ternes, T., Behavior of Pharmaceuticals, Cosmetics and Hormones in a Sewage Treatment Plant. *Water Research* **2004,** *38*, 2918-2926.
22. de Mes, T., Zeeman, G., Lettinga, G., Occurrence and Fate of Estrone, 17β-estradiol and 17α-ethynylestradiol in STPs for Domestic Wastewater. *Reviews in Environmental Science and Bio/Technology* **2005,** *4*, 275-311.
23. Batt, A. L., Kim, S., Aga, D. S, Enhanced Biodegradation of Iopromide and Trimethoprim in Nitrifying Activated Sludge. *Environmental Science and Technology* **2006,** *40*, 7367-7373.
24. Perez, S., Eichhorn, P., Aga, D.S., Evaluating the Biodegradability of Sufamethazine, Sulfamethoxazole, Sulfathiazole, and Trimethoprim at Different Stages of Sewage Treatment. *Environmental Toxicology and Chemistry*, **2005,** *24*, (6), 1361–1367.
25. Bernhard, M., Muller, J., Knepper, T. P. , Biodegradation of Persistent Polar Pollutants in Wastewater: Comparison of an Optimized Lab-scale Membrane Bioreactor and Activated Sludge Treatment. *Water Research* **2006,** *40*, 3419-3428.
26. Cirja, M., Zuehlke, S., Ivashechkin, P., Hollender, J., Schaeffer, A., Corvini, P. F. X., Behavior of Two Differently Radiolabelled 17α-ethinylestradiols Continuously Applied to a Laboratory-scale Membrane Bioreactor with Adapted Industrial Activated Sludge. . *Water Research* **2007,** *41*, (19), 4403-4412.
27. Dytzak, M. A., Londry, K.L., Oleszkiewicz, J.A., Biotransformation of Estrogens in Nitrifying Activated Sludge Under Aerobic and Alternating Anoxic/Aerobic Conditions. *Water Environment Research* **2008,** *80*, (1), 47-52.
28. Shi, J., Fujisawa, Saori, Nakai, Satoshi, Hosomi, M., Biodegradation of Natural and Synthetic Estrogens by Nitrifying Activated Sludge and Ammonia Oxidizing Bacterium *Nitrosomonas europaea*. . *Water Research* **2004,** *38*, 2323-2330.
29. Skotnicka Pitak, J., Khunjar, W.O., Aga, D.S., Love, N.G., Characterization of Metabolites Formed During the Biotransformation of 17α-Ethinylestradiol by *Nitrosomonas europaea* in Batch and Continuous Flow Bioreactors. *Environmental Science and Technology* **2009,** *43*, (10), 3549–3555.
30. Vader, J. S., Ginkel, C.G., van Stokman, F.M, Sperling, G.M., Jong, J., de Boer, W., de Graaf, J.S., de Most, M., van der Stokman, P.G.W. , Degradation of Ethinylestradiol by Nitrifying Activated Sludge. . *Chemosphere* **2000,** *41*, (8), 1239-1243.

31. Yi, T., Harper Jr., W.F., The Link between Nitrification and Biotransformation of 17α-Ethinylestradiol. *Environmental Science Technology* **2007,** *41*, 4311-4316.
32. Haiyan, R., Shulan, J., Ud din Ahmad, N., Dao, W., Chengwu, C., Degradation Characteristics and Metabolic Pathway of 17α-ethynylestradiol by *Sphingobacterium* sp. JCR5. *Chemosphere* **2007,** *66*, (2), 340-346.
33. Yoshimoto, T., Nagai, F., Fujimoto, J., Watanabe, K., Mizukoshi, H., Makino, T., Kimura, K., Saino, H., Sawada, H., Omura, H., Degradation of Estrogens by *Rhodococcus zopfii* and *Rhodococcus equi* Isolates from Activated Sludge in Wastewater Treatment Plants. *Applied and Environmental Microbiology* **2004,** *70*, (9), 5283-5289.
34. Drewes, J. E., Sedlak, D., Snyder, S., Dickenson, E. *Development of Indicators and Surrogates from Chemical Contaminant Removal during Wastewater Treatment and Reclamation.*; Water Reuse Foundation: Alexandria VA, 2008.
35. Pauwels, B., Noppe, H., De Brabander, H., Verstraete, W., Comparison of Steroid Hormone Concentrations in Domestic and Hospital Wastewater Treatment Plants. *Journal of Environmental Engineering* **2008,** *134*, (11), 933-936.
36. Lindberg, R., Jarnheimer, P.A., Olsen, B., Johansson, M., Tysklind, M., Determination of Antibiotic Substances in Hospital Sewage Water using Solid Phase Extraction and Liquid Chromatography/Mass Spectrometry and Group Analogue Internal Standards. *Chemosphere* **2004,** *57*, 1479-1488.
37. Strenn, B., Clara, M., Gans, O., Kreuzinger, N., Carbamazepine, Diclofenac, Ibuprofen and Bezafibrate – Investigations on the Behaviour of Selected Pharmaceuticals During Wastewater Treatment. *Water Science and Technology* **2004,** *50*, (5), 269-276.
38. Keener, W. K., Arp, D.J., Kinetic Studies of Ammonia Monooxygenase Inhibition in *Nitrosomonas europaea* by Hydrocarbons and Halogenated Hydrocarbons in an Optimized Whole-Cell Assay. *Applied and Environmental Microbiology* **1993,** *59*, (8), 2501-2510.
39. Suzuki, I., Kwok,S.C., Cell-free Ammonia Oxidation by *Nitrosomonas europaea* Extracts: Effects of Polyamines, Mg21 and Albumin. . *Biochemical and Biophysical Research Communications* **1970,** *39*, 950–955.
40. Suzuki, I., S.-C. Kwok, U. Dular, Tsang, D. C. Y. , Cell-free Ammonia Oxidizing System of *Nitrosomonas europaea*: General Conditions and Properties. *Canadian Journal of Biochemistry* **1981,** *59*, (477–483.).
41. Rittmann, B. E., and P. L. McCarty., *Environmental Biotechnology: Principles and Applications*. McGraw-Hill: Boston, MA, 2001.
42. Lim, M. H., Snyder, S.A., Sedlak, D.L., Use of Biodegradable Dissolved Organic Carbon (BDOC) to Assess the Potential for Tansformation of Wastewater-derived Contaminants in Surface Waters. *Water Research* **2008,** *42*, 2943-2952.
43. Kovarova-Kovar, K., Egli, T., Growth Kinetics of Suspended Microbial Cells: From Single-Substrate-Controlled Growth to Mixed-Substrate Kinetics. *Microbiology and Molecular Biology Reviews* **1998,** *62*, (3), 646-666.
44. Skotnicka Pitak, J., Garcia, E.M., Pitak, M., Aga, D.S., Identification of the Transformation Products of 17α-ethinylestradiol and 17β-estradiol by Mass Spectrometry and Other Instrumental Techniques. *Trends in Analytical Chemistry* **2008,** *27*, (11), 1036-1052.
45. Jenkins, R. O., Dalton, H., The Use of Indole as a Spectrophotometric Assay Substrate for Toluene Dioxygenase. *FEMS Microbiology Letters* **1985,** *30*, 227-231.

46. O'Connor, K. E., Hartman, S., Indigo Formation by Aromatic Hydrocarbon-degrading Bacteria. *Biotechnology Letters* **1998,** *20*, (3), 219-233.
47. McClay, K., Boss, C., Keresztes, I.. Steffan, R.J., Mutations of Toluene-4-Monooxygenase That Alter Regiospecificity of Indole Oxidation and Lead to Production of Novel Indigoid Pigments. *Applied and Environmental Microbiology* **2005,** *71*, (9), 5476-5481.
48. Sadler, P. W., Absorption Spectra of Indigoid Dyes. *Journal of Organic Chemistry* **1955,** *21*, (3), 316-318.
49. Seacat, A. M., Kuppusamy, P., Zweier, J.L., Yager, J.D., ESR Identification of Free Radicals Formed from the Oxidation of Catechol Estrogens by Cu^{2+}. *Archives of Biochemistry and Biophysics* **1997,** *347*, (1), 45-52.
50. Yager, J. D., Liehr, J.G., Molecular Mechanisms of Estrogen Carcinogenesis. *Annual Review of Pharmacology and Toxicology* **1996,** *36*, 203-232.
51. Chain, P., Lamerdin, J. Larimer, F., Regala, W. Lao, V., Land, M., Hauser, L., Hooper, A.B., Klotz, M.G., Norton, J.M., Sayavedra-Soto, L.A., Arciero, D. M., Hommes, N.G., Whittaker, M.R., Arp, D.J., Complete Genome Sequence of the Ammonia-Oxidizing Bacterium and Obligate Chemolithoautotroph *Nitrosomonas europaea. Journal of Bacteriology* **2003,** *185*, (9), 2759-2773.
52. Chang, S. W., Hyman, Michael R., Williamson, Kenneth J. , Cooxidation of Naphthalene and Other Polycyclic Aromatic Hydrocarbons by the Nitrifying Bacterium, *Nitrosomonas europaea. . Biodegradation* **2002,** *13*, 373-381.
53. Keener, W. K., Arp, D.J., Transformations of Aromatic Compounds by Nitrosomonas europaea. *Applied and Environmental Microbiology* **1994,** *60*, (6), 1914-1920.
54. Marvin-Sikkema, F. D., de Bont, J.A.M., Degradation of Nitroaromatic Compounds by Microorganisms. *Applied Microbiology Biotechnology* **1994,** *42*, 499-507.
55. Hofstetter, T. B., Spain, J.C., Nishino, S.F.,Bolotin,J., Schwarzenbach, R.P., Identifying Competing Aerobic Nitrobenzene Biodegradation Pathways by Compound-Specific Isotope Analysis. *Environmental Science and Technology* **2008,** *42*, 4764–4770.
56. Zumft, W. G., The Biological Role of Nitric Oxde in Bcteria. *Archives of Microbiology* **1993,** *160*, (4), 253-264.
57. Yang, T., Nitrite Inhibition of a Bacterial Oxidase. *Annals of the New York Academy of Sciences* **1984,** *435*, 232-234.
58. Rowe, J. J., Yarbrough, J.M., Rake, J.B., Eagon, R.G., Nitrite Inhibition of Aerobic Bacteria. *Current Microbiology* **1979,** *2*, (1), 51-54.
59. Soojhawon, I., Lokhande, P.D., Kodam, K.M., Gawai, K.R., Biotransformation of Nitroaromatics and Their Effects on Mixed Function Oxidase System. *Enzyme and Microbial Technology* **2005,** *37*, 527-533.
60. Symons, Z. C., Bruce, N.C., Bacterial Pathways for Degradation of Nitroaromatics. *Natural Product Reports* **2006,** *23*, 845-850.
61. Gaulke, L. S., Strand, S.E., Kalhorn, T.F., Stensel, H.D., Estrogen Biodegradation Kinetics and Estrogenic Activity Reduction for Two Biological Wastewater Treatment Methods. *Environmental Science and Technology* **2009,** *43*, (18), 7111-7116.
62. Kent, U. M., Mills, D.E., Rajnarayanan, R.V., Alworth, W.L., Hollenberg, P.F., Effect of 17α-Ethynylestradiol on Activities of Cytochrome P450 2B (P450 2B) Enzymes: Characterization of Inactivation of P450s 2B1 and 2B6 and Identification of Metabolites. *The Journal of Pharmacology and Experimental Therapeutics* **2002,** *300*, (2), 549-558.

63. Lee, A. J., Kosh, J.W., Conney, A.H., Zhu, B.T., Characterization of the NADPH-Dependent Metabolism of 17β-Estradiol to Multiple Metabolites by Human Liver Microsomes and Selectively Expressed Human Cytochrome P450 3A4 and 3A5. *The Journal of Pharmacology and Experimental Therapeutics* **2001,** *298*, (2), 420-432.
64. Coombe, R. G., Tsong, Y.Y., Hamilton, P.B., Sih, C.J., Mechanisms of Steroid Oxidation by Microorganisms, X - Oxidative Cleavage of Estrone. *The Journal of Biological Chemistry* **1966,** *241*, (7), 1587-1595.
65. Gibson, D. T., Wang, K.C., Sih, C.J., Whitlock Jr., H., Mechanisms of steroid oxidation by microorganisms. IX - On the mechanism of Ring A cleavage in the degradation of 9,10 seco steroids by microorganisms. *The Journal of Biological Chemistry* **1966,** *241*, (3), 551 - 559.
66. Sih, C. J., Lee, S.S.,Tsong, Y.Y., Wang, K.C., Mechanisms of Steroid Oxidation by Microorganisms, VIII. - 3,4-dihydroxy-9,10-secoandrosta-1,3,5(10)-triene-9,17-dione, an Intermediate in the Microbiological Degradation of ring A of androst-4-ene-3,17-dione. *The Journal of Biological Chemistry* **1966,** *241*, (3), 540-550.
67. Wang, K. C., Sih, C.J., Mechanisms of Steroid Oxidation by Microorganisms. IV - Seco Intermediates. *Biochemistry* **1963,** *2*, (6), 1238-1243.
68. Lai, K. M., Scrimshaw, M.D., Lester, J.N., Biotransformation and Bioconcentration of Steroid Estrogens by *Chlorella vulgaris. Applied and Environmental Microbiology* **2002,** *68*, (2), 859-864.
69. Vickers, S., Polsky, S.L., The Biotransformation of Nitrogen Containing Xenobiotics to Lactams. *Current Drug Metabolism* **2000,** *1*, 357-389.
70. Xu, P., Yu, B., Li Li, F., Cai, X.F., Ma, C.Q., Microbial degradation of sulfur, nitrogen and oxygen heterocycles *Trends in Microbiology* **2006,** *14*, (9), 398-405.
71. Johnson, A. C., Aerni, H.-R., Gerritsen, A., Gibert, M., Giger, W., Hylland, K., Jurgens, M., Nakari, T., Pickering, A., Suter, M.J.-F., Comparing Steroid Estrogen, and Nonylphenol Content across a Range of European Sewage Plants with Different Treatment and Management Practices. *Water Research* **2005,** *39*, 47-58.
72. Koh, Y. K. K., Chiu, T.Y., Boobis, A., Cartmell, E., Scrimshaw, M.D., Lester, J.N., Treatment and Removal Strategies for Estrogens from Wastewater. *Environmental Technology* **2008,** *29*, 245-267.
73. Kreuzinger, N., Clara, M., Strenn, B., Kroiss, H., Relevance of the Sludge Retention Time (SRT) as Design Criteria for Wastewater Treatment Plants for the Removal of Endocrine Disruptors and Pharmaceuticals from Wastewater. *Water Science and Technology* **2004,** *50*, (5), 149-156.
74. Ren, Y. X., Nakano, K., Nomura, M., Chiba, N., Nishimura, O., Effects of Bacterial Activity on Estrogen Removal in Nitrifying Activated Sludge. *Water Research* **2007,** *41*, 3089-3096.
75. Junker, T., Alexy, R., Knacker, T., Kummerer, K., Biodegradability of 14C-Labeled Antibiotics in a Modified Laboratory Scale Sewage Treatment Plant at Environmentally Relevant Concentrations. *Environmental Science and Technology* **2006,** *40*, 318-324.
76. Laspidou, C. S., Rittman, B.E., A Unified Theory for Extracellular Polymeric Substances, Soluble Microbial Products, and Active and Inert Biomass. *Water Research* **2002,** *36*, (11), 2711-2720.

77. Laspidou, C. S., Rittman, B.E., Non-steady State Modeling of Extracellular Polymeric Substances, Soluble Microbial Products, and Active and Inert Biomass. *Water Research* **2002,** *36*, (8), 1983-1992.
78. Chang, H. L., Alvarez Cohen, L., Model for the Cometabolic Biodegradation of Chlorinated Organics. *Environmental Science and Technology* **1995,** *29*, 2357-2367.
79. Chang, S. W. Cometabolic Biodegradation of Polycyclic Aromatic Hydrocarbons (PAHs) and Aromatic Ether by Phenol and Ammonia-oxidizing Bacteria. Oregon State University, Corvallis, Oregon., 1997.
80. Criddle, C. S., The Kinetics of Cometabolism. *Biotechnology and Bioengineering* **1993,** *41*, 1048-1056.
81. Ely, R. L., Hyman, M.R., Arp, D.J., Guenther, R.B., Williamson, K.J., A Cometabolic Kinetics Model Incorporating Enzyme Inhibition, Inactivation, and Recovery: II. Trichloroethylene Degradation Experiments. *Biotechnology and Bioengineering* **1995,** *46*, 232-245.
82. Ely, R. L., Williamson, K.J., Guenther, R.B., Hyman, M.R., Arp, D.J., A Cometabolic Kinetics Model Incorporating Enzyme Inhibition, Inactivation, and Recovery: 1. Model Development, Analysis, and Testing. *Biotechnology and Bioengineering* **1995,** *46*, 218-231.
83. Grady Jr., C. P. L., Daigger, G.T., and Lim, H.C., *Biological Wastewater Treatment*,. Second ed.; Marcel Dekker, Inc.: New York, NY., 1999.
84. Grady Jr., C. P. L., Smet, B.F., Barbeau, D.S., Variability in Kinetic Parameter Estimates: A Review of Possible Causes and a Proposed Terminology. *Water Research* **1996,** *30*, (3), 742-748.
85. Andrews, J. F., A Mathematical Model for the Continuous Culture of Microorganisms Utilizing Inhibitory Substrates. *Biotechnology and Bioengineering* **1968,** *10*, 707-723.
86. Powell, E. O., *The Growth Rate of Microorganisms as a Function of Substrate Concentration.* HMSO: London, 1967; p 34-56.

CHAPTER 5 - CONCLUSIONS

5.1 Carbamazepine fate

CBZ does not sorb to biomass (**Sections 4.1.1 and 4.1.2**). It is also highly resistant to biodegradation by AOBs or heterotrophs under conditions experienced at WWTPs (**Sections 4.2.3 and 4.2.4**). Elimination of this compound may be achieved through application of AOPs like ozonation or hydrogen peroxide/UV treatment. It is important to consider that AOPs do not result in complete mineralization of CBZ. Treatment of CBZ metabolites from AOP processes that are amenable to biodegradation may be achieved using biofilters.

5.2 Iopromide fate

IOP also does not sorb to biomass (**Sections 4.1.1 and 4.1.2**); however it appears to be amenable to biotransformation by activated sludge [1]. In this study, IOP was not biotransformed by batch cultures of AOBs (**Section 4.2.3**). These results are interpreted to mean that IOP biotransformation in NAS may be due to heterotrophs.

5.3 17α-ethinylestradiol fate

EE2 sorption to biomass is affected by the EPS content and organic matter composition of mixed liquor (**Sections 4.1.3**). Protein content of EPS and mixed liquor affects EE2 sorption more strongly than polysaccharide content. These protein-EE2 interactions may explain findings that suggest chemisorption influences EE2 partitioning [2]. Although EE2 sorption to biomass devoid of cation-linked EPS was homogenous, no benefit was derived when using the proposed dual mode sorption isotherm.

EE2 was biotransformed but not mineralized by AOB batch and chemostat cultures (**Section 4.2.6**). Interestingly, the primary metabolites formed were unique to each reactor configuration; epoxidation of the acetylenic moiety occurred under batch conditions whereas hydroxylation of the phenol moiety occurred under nutrient limited conditions. It was evident that physiological state influenced EE2 biotransformation by AOBs. Nitrated-EE2 metabolite formation was an

artifact of high nitrite concentrations in reactors and is not expected to be relevant under conditions typical of WWTPs.

EE2 was also biotransformed and eventually mineralized (55-65%) by heterotrophs. Oxygenase enzyme activity was not limiting in Ox^- reactors, and explains the lack of difference of mineralization. Three stable metabolites were formed in these experiments, M376, 4-OH-EE2 and U1. Heterotrophs were also capable of degrading metabolites generated in AOB reactors, although overall mineralization decreased (25-37%). Inhibition of heterotrophic respiration by high nitrite concentrations was observed; however, it was not clear whether this contributed to the lower degree of mineralization. It was also hypothesized that nitro-EE2 recalcitrance to degradation may have also affected mineralization (**Sections 4.2.6 and 4.2.7**).

Initial transformation of EE2 was dominated by AOBs; however subsequent degradation was driven by heterotrophs (**Section 4.2.10**). This transformation was enhanced in cultures comprised of mixtures of AOBs and heterotrophs. This result cannot be explained with the current data but suggests a mutually beneficial relationship between AOBs and heterotrophs.

EE2 fate in bioreactors was affected by organic and microconstituent loading rates (**Section 4.3.1**). Pulse inputs of readily biodegradable substrates negatively affected EE2 effluent concentrations briefly (**Section 4.3.2**). In the absence of readily biodegradable substrate, EE2 mineralization correlated with biomass growth (**Section 4.3.4**). Finally, model simulations suggested that EE2 fate in heterotrophic reactors was most sensitive to pseudo-first order reaction rate coefficient. Model results indicated that sorption would not significantly affect effluent EE2 concentrations (**Sections 4.3.6 and 4.3.7**)

5.4 Trimethoprim fate

TMP sorption to biomass was also influenced by the EPS content and organic matter composition of mixed liquor. Protein and polysaccharide content of EPS correlated well with TMP sorption. In the absence of cation-linked EPS, TMP sorption was highly variable. This suggested that sorption was partially driven by interactions between protein and polysaccharides constituents of EPS and TMP (**Section 4.1.4**).

TMP was not biotransformed by AOB batch and chemostat cultures. These results suggest that TMP transformation as observed in prior studies [1] can be attributed solely to heterotrophic activity. TMP was transformed by heterotrophic cultures to similar degrees. Biotransformation rates were also similar. This confirms our findings that oxygenase activity had little effect on TMP degradation since basal level expression was sufficient to achieve complete mineralization of TMP. Two stable metabolites were formed in these experiments, M220 and M182 (**Sections 4.2.8** and **4.2.9**).

TMP degradation was affected by organic and microconstituent loading rates. TMP removal was also negatively affected by pulse inputs of readily biodegradable substrates slowed but not as significantly as observed in EE2 experiments (**Section 4.3.2**). These results indicate that TMP degradation could be affected by the intensity of transient rbCOD loads. Model simulations confirmed that TMP effluent concentrations is affected by the pseudo-first order reaction rate coefficient and partitioning coefficients (**Sections 4.3.6** and **4.3.7**).

5.5 References

1. Batt, A. L., Kim, S., Aga, D. S, Enhanced Biodegradation of Iopromide and Trimethoprim in Nitrifying Activated Sludge. *Environmental Science and Technology* **2006,** *40*, 7367-7373.
2. Xu, K., Harper Jr., W.F., Zhao, D., 17α-Ethinylestradiol sorption to activated sludge biomass: Thermodynamic properties and reaction mechanisms. *Water Research* **2008,** *42*, 3146-3152.

CHAPTER 6 – ENGINEERING SIGNIFICANCE

Effective treatment of microconstituents during wastewater treatment is currently elusive. Sorption, biotransformation and advanced oxidation processes have been touted as options for removal of various microconstituents. For engineers to design treatments that exploit these processes, we need to understand mechanisms that drive removal. This study was performed to elucidate factors affecting biotransformation by microorganisms found in NAS.

6.1 Implications from sorption experiments.

In this study, it was noted that CBZ and IOP remained unsorbed during activated sludge treatment. Conversely, EE2 and TMP sorbed to biomass. This sorption was affected by EPS. It was hypothesized that this behavior was the result of interactions between highly functionalized groups allowing for preferential dissolution of microconstituents into organic matter as compared to water. That EPS plays a role in sequestration of microconstituents is important since EPS content can be variable under high and low growth conditions [1]. It is not illogical to assume that EE2 and TMP bioavailability can be affected by sorption to EPS produced under these conditions. Correlations between sorption and protein content of cation-linked EPS could also be exploited. If one can determine how compounds are sorbed to different fractions of EPS, it should be possible to utilize EPS generating biomass as a selective sorbent for specific microconstituents.

Subsequent treatment of this microconstituent rich biomass can involve advanced oxidations processes (e.g. ozonation) which would convert the complex compounds into byproducts that are more amenable to biological treatment. Anaerobic digestion processes coupled with aerobic bioreactors designed for polishing nutrient and microconstituent degradation could also be applied. In these long SRT anaerobic systems, hydrolysis of EPS can result in desorption of the partitioned microconstituents, making them available for biotransformation in the aerobic polishing reactor. Further work is needed to elucidate whether sorption of microconstituents is

driven by chemical reactions or is limited by diffusion. In the latter case, microconstituents associated with the solid phase could still be available for biotransformation. In this case, EPS could be considered as a concentrating medium from which organisms can tap into the sequestered microconstituent. Fixed film systems would be most suitable for application of this strategy.

6.2 Implication from biotransformation experiments.

Literature that describes the fate of microconstituents during NAS treatment is, at times, conflicting. Some authors predict that microconstituent transformation is governed by AOBs and that heterotrophs have little impact on the transformation [2-5]. Other researchers claim that heterotrophs are responsible for removal observed in NAS, particularly as related to EE2 [5-7]. None of these studies evaluated if heterotrophs and AOBs interacted in a way that enhanced or enabled biotransformation of these compounds. This study directly addressed the relative roles of these two groups of bacteria, and it shows that microconstituent fate during biological treatment is affected by both.

CBZ was found to be resistant to biotransformation by AOBs and heterotrophs regardless of the reactor configuration used. AOP treatment is recommended for this compound [8]. Metabolites formed during AOP treatment of CBZ could then be further degraded in bioreactors employed to polish water quality. The efficacy of this sequential treatment scheme has not been evaluated at present. Findings from the current study also indicate that IOP transformation in NAS may be due to heterotrophs and not AOBs. IOP degradation is hypothesized to be limited by lack of oxidative de-iodination. For effective IOP treatment, alternating anaerobic and aerobic reactors can provide conditions conducive to reductive de-iodination [9]. Upon loss of the iodine atoms, further degradation should be possible under aerobic conditions.

AOBs transform EE2 more rapidly than heterotrophic organisms under physiological conditions typically of activated sludge treatment. Heterotrophs can mineralize EE2 independent of AOB activity. These heterotrophic cultures can also further degrade EE2 and some EE2-associated metabolites generated from AOB reactors. Thus, it is clear that EE2 degradation by NAS cannot

be explained by focusing on one functional group. For mineralization of EE2, the contribution of heterotrophs must be acknowledged. Conversely, results from the present study indicate that TMP biotransformation in NAS can be attributed solely to heterotrophic activity. This heterotrophic activity on EE2 and TMP is dependent on physiological state, organic and microconstituent loading rates and the presence of readily biodegradable substrates.

Results from this study clearly indicate that aerobic biological treatment of microconstituents is possible. There is promise in using enriched NAS to rehabilitate wastewaters contaminated with EE2 and TMP. To accomplish this degradation in existing systems, it is recommended that reactors be operated in a manner that encourages endogenous conditions. Under these circumstances, microconstituents can undergo co-metabolic transformation by AOBs, or be metabolized by heterotrophs as an alternative electron donor.

Small polishing bioreactors can also exploit AOB hydroxylation of EE2 to catechol-EE2. Subsequent mineralization of EE2 and catechol-EE2 can be accomplished by heterotrophs. Again, nutrient limited conditions in these bioreactors can also encourage TMP degradation by heterotrophs. For optimum operation, these reactors should be fed sufficient ammonia to prevent AOB inactivity ($> K_{S,NH3}$). Organic loading should be kept to a minimum and microconstituent loading should be maximized to maintain selective pressure on specialist communities. If nitritation is achieved in these reactors, care must be taken to determine whether abiotic nitration reactions with microconstituents occurs. Nitroaromatic microconstituents can be more recalcitrant to biotransformation processes and may possess increased eco-toxicity as compared to the parent compound. Design of these reactors can be aided through use of the pseudo-first order rate constants reported in this study; however, care must be applied such that that bioreactor design accounts for variable rates of microconstituent degradation. This is an important requirement since the basic model presented in this work indicates that microconstituent removal is very sensitive to biodegradation rate. Ideally though, reactor design should be based on Monod biokinetic expressions that describing microconstituent biodegradation by AOBs and heterotrophs. Further work is needed to bridge this gap in the literature.

Treatment of these wastes also results in decreased estrogenicity [10] and lower antibiotic concentrations in treatment plant effluents. This is particularly important as researchers seek to minimize endocrine disruption of aquatic life and eliminate conditions that select for antibiotic resistance. Findings from this work are particularly encouraging for systems treating wastes with relatively high concentrations of microconstituents, e.g. hospital wastewater, source separated waste-streams, and pre-concentrated wastes. Lack of inhibition confirms that activated sludge reactors are robust options for treatment of these wastes. Within the larger context of sustainable wastewater treatment, anaerobic processes are becoming favorable options for organic carbon removal due to their lower energy costs as compared to aerobic systems. Results from this study suggest that aerobic treatment technologies should be considered as potent options for removal of microconstituents that will be present in effluents of anaerobic treatment process.

6.3 References

1. Merlo, R. P., Trussel, R.S., Hermanowicz, S.W., Jenkins, D., Effects of Sludge Properties on the Thickening and Dewatering of Waste Activated Sludge. *Water Environment Research* **2007,** *79*, 2412- 2419.
2. Batt, A. L., Kim, S., Aga, D. S, Enhanced Biodegradation of Iopromide and Trimethoprim in Nitrifying Activated Sludge. *Environmental Science and Technology* **2006,** *40*, 7367-7373.
3. Ren, Y. X., Nakano, K., Nomura, M., Chiba, N., Nishimura, O., Effects of Bacterial Activity on Estrogen Removal in Nitrifying Activated Sludge. *Water Research* **2007,** *41*, 3089-3096.
4. Shi, J., Fujisawa, Saori, Nakai, Satoshi, Hosomi, M., Biodegradation of Natural and Synthetic Estrogens by Nitrifying Activated Sludge and Ammonia Oxidizing Bacterium *Nitrosomonas europaea*. . *Water Research* **2004,** *38*, 2323-2330.
5. Yi, T., Harper Jr., W.F., The Link between Nitrification and Biotransformation of 17α-Ethinylestradiol. *Environmental Science Technology* **2007,** *41*, 4311-4316.
6. Gaulke, L. S., Strand, S.E., Kalhorn, T.F., Stensel, H.D., 17α-ethinylestradiol Transformation via Abiotic Nitration in the Presence of Ammonia Oxidizing Bacteria. *Environmental Science and Technology* **2008,** *42*, (20), 7622-7627.
7. Gaulke, L. S., Strand, S.E., Kalhorn, T.F., Stensel, H.D., Estrogen Biodegradation Kinetics and Estrogenic Activity Reduction for Two Biological Wastewater Treatment Methods. *Environmental Science and Technology* **2009,** *43*, (18), 7111-7116.
8. McDowell, D. C., Huber, M.M., Wagner, M., Von Gunten, U., Ternes, T.A., Ozonation of Carbamazepine in Drinking Water: Identification and Kinetic Study of Major Oxidation Products. *Environmental Science and Technology* **2005,** *39*, (20), 8014-8022.
9. Haggblom, M. M., Bossert, I.D., *Dehalogenation - Microbial Processes and Environmental Applications*. Kluwer Academic Publishers: Boston, 2003.

10. Skotnicka Pitak, J., Khunjar, W.O., Aga, D.S., Love, N.G., Characterization of Metabolites Formed During the Biotransformation of 17α-Ethinylestradiol by *Nitrosomonas europaea* in Batch and Continuous Flow Bioreactors. *Environmental Science and Technology* **2009,** *43*, (10), 3549–3555.

APPENDIX I

Data in Appendix I was derived from sorption experiments performed with biomass prior to and after EPS extraction.

I-1 Results from sorption experiments

All data was obtained according to methods outlined in **Section 3.3**. Processed data is discussed in **Section 4.1**).

Table I.1. Results from sorption experiments with AOB cultures and ^{14}C-CBZ. Data relevant to Figure 4-1.

Replicate	Solids (mg TSS/L)	CBZ (dpm/mL)		
		t_0 (0 day)	t_1 (1 day)	t_2 (7 day)
1	800	607	794	846
		610	716	839
		679	850	887
2	800	817	1147	833
		802	801	875
		836	772	812
3	800	713	854	769
		749	949	857
		811	982	844
1	400	748	1062	832
		734	802	883
		680	778	853
2	400	844	870	723
		804	2099	874
		788	859	836
3	400	825	834	819
		830	1101	949
		852	815	948
1	200	816	941	803
		867	959	934
		880	962	920
2	200	793	802	779
		902	882	795
		856	927	894
3	200	835	788	897
		829	792	884
		934	903	921
1	80	795	837	730
		942	893	781
		912	842	847
2	80	788	759	801
		827	737	893
		820	811	839
3	80	838	734	831
		893	827	871
		933	763	891
1	10	863	847	799
		861	889	784
		885	831	900

2	10	725 713 755	794 794 778	807 793 840
3	10	930 957 994	754 868 761	877 937 882
1	Negative Control	823 871 867	822 740 810	933 913 905
2	Negative Control	824 828 900	788 825 784	720 688 911
3	Negative Control	820 840 830	854 792 898	878 753 846

Table I.2. Results from sorption experiments with Ox^- culture and ^{14}C-CBZ. Data relevant to Figure 4-2.

Replicate	Solids (mg TSS/L)	CBZ (dpm/mL)		
		t_0 (0 day)	t_1 (1 day)	t_2 (7 day)
1	5000	541 570 577	458 434 491	591 541 581
2	5000	663 695 694	705 675 718	649 572 653
3	5000	689 709 706	568 603 582	618 593 930
1	2500	733 815 776	622 651 632	613 805 653
2	2500	687 716 788	622 651 632	714 764 701
3	2500	745 822 765	688 718 723	771 761 772
1	1000	762 757 752	682 726 715	788 819 729
2	1000	747 757 814	667 695 680	651 773 740
3	1000	813 812 775	761 744 713	713 746 751
1	500	734 752 779	669 670 739	685 678 725
2	500	699 766 712	756 717 671	750 805 749

3	500	741 718 789	589 605 642	716 801 844
1	100	786 828 834	719 734 737	721 793 789
2	100	793 786 817	745 780 704	735 691 672
3	100	719 760 802	667 630 723	740 744 718

Table I.3. Results from sorption experiments with Ox^+ cultures and ^{14}C-CBZ. Data relevant to Figure 4-2.

Replicate	Solids (mg TSS/L)	CBZ (dpm/mL)		
		t_0 (0 day)	t_1 (1 day)	t_2 (7 day)
1	5000	536 514 568	626 659 749	615 744 657
2	5000	628 692 725	739 704 687	719 706 727
3	5000	590 626 660	762 766 719	611 544 663
1	2500	755 737 772	700 782 814	751 765 780
2	2500	712 668 685	512 581 560	688 729 823
3	2500	729 732 716	387 505 405	609 613 670
1	1000	711 792 693	661 693 738	663 645 619
2	1000	755 724 744	649 0 728	749 789 756
3	1000	714 760 663	708 729 703	649 708 810
1	500	768 778 802	734 768 812	822 837 779
2	500	747 805 794	769 768 769	809 822 743

3	500	628 663 721	678 701 673	707 748 741
1	100	729 720 768	795 0 853	736 666 726
2	100	697 719 790	741 779 956	772 730 709
3	100	689 807 740	754 709 727	620 627 643
1	Negative Control	823 871 867	822 740 810	933 913 905
2	Negative Control	824 828 900	788 825 784	720 688 911
3	Negative Control	820 840 830	854 792 898	878 753 846

Table I.4. Results from sorption experiments with MBR NAS culture (from Auburn University) and ^{14}C-CBZ. Data relevant to Section 4.1.2.

Replicate	Solids	CBZ (dpm/mL)		
		t_0 (0 day)	t_1 (24 hr)	t_2 (7 day)
1	2500	616	705	794
		590	764	798
		655	825	786
2	2500	709	629	755
		725	668	761
		836	636	768
3	2500	731	701	747
		841	678	757
		764	699	844
1	1000	754	689	813
		849	833	766
		801	795	836
2	1000	747	717	836
		790	740	863
		780	725	807
3	1000	767	690	799
		799	759	769
		846	752	817
1	500	772	787	706
		795	782	767
		698	747	712
2	500	1294	758	747
		886	759	817
		852	762	774
3	500	759	783	777
		767	786	778
		707	831	833
1	100	716	761	768
		736	0	758
		798	779	795
2	100	692	738	766
		711	753	759
		833	767	751
3	100	626	741	740
		701	736	772
		763	724	794
1	Negative Control	775	775	775
		763	763	763
		798	798	798
2	Negative Control	722	722	722
		786	786	786
		738	738	738
3	Negative Control	806	806	806
		776	776	776

		792	792	792

Table I.5. Results from sorption experiments with PFWWTF NAS culture and ^{14}C-CBZ. Data relevant to Section 4.1.2.

Replicate	Solids (mg TSS/L)	CBZ (dpm/mL)		
		t_0 (0 day)	t_1 (1 day)	t_2 (7 day)
1	5000	536 514 568	626 659 749	615 744 657
2	5000	628 692 725	739 704 687	719 706 727
3	5000	590 626 660	762 766 719	611 544 663
1	2500	755 737 772	700 782 814	751 765 780
2	2500	712 668 685	512 581 560	688 729 823
3	2500	729 732 716	387 505 405	609 613 670
1	1000	711 792 693	661 693 738	663 645 619
2	1000	755 724 744	649 0 728	749 789 756
3	1000	714 760 663	708 729 703	649 708 810
1	500	768 778 802	734 768 812	822 837 779
2	500	747 805 794	769 768 769	809 822 743

3	500	628 663 721	678 701 673	707 748 741
1	100	729 720 768	795 0 853	736 666 726
2	100	697 719 790	741 779 956	772 730 709
3	100	689 807 740	754 709 727	620 627 643
1	Negative Control	823 871 867	822 740 810	933 913 905
2	Negative Control	824 828 900	788 825 784	720 688 911
3	Negative Control	820 840 830	854 792 898	878 753 846

Table I.6. Results from sorption experiments with AOB culture and ^{14}C-EE2. Data relevant to Figure 4-1.

Replicate	Solids (mg TSS/L)	EE2 (dpm/mL)		
		t_0 (0 day)	t_1 (1 day)	t_2 (7 day)
1	800	6157 6367 6191	4021 4290 4472	4845 4464 4822
2	800	5392 5537 5465	4979 4826 5147	5087 5282 5595
3	800	5541 5737 5692	4844 4683 4749	5692 5717 5610
1	400	6419 6462 6468	5334 5617 5311	5571 5813 5598
2	400	5238 5067 5179	4996 5346 6210	5750 6258 5970
3	400	6112 5880 6092	5383 4821 5530	5294 5632 5405
1	200	6026 6035 6221	5961 6244 6392	5458 6392 5735
2	200	6633 6327 6932	4867 5266 5757	5973 6640 6480
3	200	5912 6324 5877	5147 5655 5342	5858 6023 6000
1	80	6409 6489 6324	5083 5149 5349	5737 6471 6456
2	80	6503 6589 6808	6369 6427 6241	5785 5719 5828

3	80	5628 7600 5600	5672 5451 5490	6886 6366 6359
1	10	6573 6837 6803	5929 5449 6593	6799 6590 7229
2	10	6321 6670 6531	5778 5848 5959	6255 6651 6521
3	10	6732 6845 6621	5489 5466 5431	5686 5965 6065
1	Negative Control	7758 7751 7492	6330 7273 6559	6756 6932 6698
2	Negative Control	6922 6907 7203	6725 6811 6890	6753 6502 6780
3	Negative Control	6925 7017 6999	6954 8805 7190	6996 7250 7165

Table I.7. Results from sorption experiments with Ox^- culture and ^{14}C-EE2. Data relevant to Table 4.1.

Replicate	Solids (mg TSS/L)	EE2 (dpm/mL)		
		t_0 (0 day)	t_1 (1 day)	t_2 (7 day)
1	5000	1925 1921 1965	1251 1349 1316	1282 1438 1396
2	5000	1985 2118 1882	1453 1484 1574	1452 1483 1507
3	5000	1946 1995 2098	1516 1469 1527	1384 1376 1342
1	2500	2635 2800 2709	2198 2212 2129	1932 1903 2087
2	2500	2539 2606 2733	1801 1950 2074	2270 2475 2179
3	2500		1789 1939 1924	2079 2141 2137
1	1000	3954 3014 0	6102 6249 6360	2995 3104 3183
2	1000	4461 4265 4382	2993 3058 3036	3640 3198 3255
3	1000	3959 4094 4162	3213 3270 3254	2916 2921 2946
1	500	4750 5036 4848	4218 4262 4361	3987 0 4123
2	500	5541 5785 5806	3864 3973 3928	3340 3683 4209

3	500	5218 6011 5502	4043 4194 4161	3589 3716 3814
1	100	6225 6570 6551	4890 4897 4929	4432 4786 4653
2	100	6078 6416 6203	5173 5401 5316	4924 5023 4984
3	100	6083 6380 8447	4927 4860 5091	4991 5332 5257
1	Negative Control	6287 6463 6360	5308 5358 5228	5185 5285 5314
2	Negative Control	5870 6016 6088	5441 5434 5448	4333 4879 5058
3	Negative Control	6200 6402 6295	5292 5482 5510	6007 6833 7124

Table I.8. Results from sorption experiments with Ox^+ and ^{14}C-EE2. Data relevant to Table 4.1.

Replicate	Solids (mg TSS/L)	EE2 (dpm/mL)		
		t_0 (0 day)	t_1 (1 day)	t_2 (7 day)
1	5000	1800 1886 1830	1285 1464 1380	1169 1168 1278
2	5000	1833 1888 1812	1320 1435 1414	1286 1393 1393
3	5000	1845 1910 1994	1337 1429 1330	1276 1224 1340
1	2500	2596 2760 2798	2119 2162 2161	1962 2065 2069
2	2500	2890 2756 2962	2219 2291 2294	2473 2633 2696
3	2500	2894 3058 3034	2345 2585 2443	2079 2172 2081
1	1000	3581 3700 3795	3064 3250 3143	3343 3425 3468
2	1000	3921 3873 3798	3586 3613 3626	3079 3151 3152
3	1000	3881 3986 3811	3136 3139 3281	3217 0 3317
1	500	3519 4022 3895	3629 3741 3876	3806 3983 3838
2	500	4358 4459 4467	4311 4192 4208	4037 4159 4228

3	500	3687 3885 3869	3642 3710 3847	3937 4140 4013
1	100	5582 5721 5803	4519 4318 4330	5206 5429 5399
2	100	5513 5616 5968	4435 4807 4638	4876 5178 4936
3	100	5309 5645 5616	5052 5433 5368	4942 4951 5127
1	Negative Control	6287 6463 6360	5308 5358 5228	5185 5285 5314
2	Negative Control	5870 6016 6088	5441 5434 5448	4333 4879 5058
3	Negative Control	6200 6402 6295	5292 5482 5510	6007 6833 7124

Table I.9. Results from sorption experiments with MBR NAS (from Auburn University) and ^{14}C-EE2. Data relevant to Table 4.1.

Replicate	Solids (mg TSS/L)	EE2 (dpm/mL)		
		t_0 (0 day)	t_1 (1 day)	t_2 (7 day)
1	2500	976 1158 1067	1055 1361 1242	978 1011 1138
2	2500	1421 1552 1521	1081 1103 1024	970 1047 1004
3	2500	1638 1707 1682	1057 1125 1172	1103 1211 1297
1	1000	1818 1983 1759	1567 1752 1581	1511 1300 1444
2	1000	1994 2302 1894	1267 1301 1389	1296 1632 1571
3	1000	2094 2176 1487	1626 1487 1728	1376 1549 1517
1	500	2114 2092 1928	1701 1682 1656	1771 1814 1854
2	500	2019 2252 2215	1490 1684 1471	1967 1895 2126
3	500	2309 2305 2310	2198 2193 2206	1761 1860 1781
1	100	2532 2556 2672	2161 2167 2268	1823 2099 2004
2	100	2420 2551 2452	2067 2284 2190	2040 1846 1799

3	100	2623 2476 2539	2465 2167 2400	1905 1943 2021
1	Negative Control	3071 3118 3020	3071 3118 3020	3071 3118 3020
2	Negative Control	3095 3083 3217	3095 3083 3217	3095 3083 3217
3	Negative Control	3067 2973 3052	3067 2973 3052	3067 2973 3052

Table I.10. Results from sorption experiments with PFWWTF NAS and ^{14}C-EE2. Data relevant to Table 4.1.

Replicate	Solids (mg TSS/L)	EE2 (dpm/mL)		
		t_0 (0 day)	t_1 (1 day)	t_2 (7 day)
1	5000	512 498 550	616 659 705	714 754 701
2	5000	616 689 762	690 797 825	722 718 723
3	5000	630 635 635	760 774 820	730 810 697
1	2500	1082 1088 1107	1267 1263 1185	1010 1134 1122
2	2500	1088 1112 1276	1143 1225 1313	1071 1100 1134
3	2500	1281 1274 1392	1179 1189 1208	1211 1242 1112
1	1000	1909 2074 2244	1735 1789 1916	1765 1794 1727
2	1000	1997 2051 1971	1798 1937 1923	1642 1555 1625
3	1000	1929 2004 1989	1765 1879 2020	1646 1826 1749
1	500	2434 2607 2643	2349 2269 2343	2202 2391 2300
2	500	2368 2438 2383	2364 2626 2530	2090 2403 2124

3	500	2112 2279 2159	2537 2575 2618	2091 2172 2199
1	100	2915 2939 2988	2687 2890 2890	2488 2601 2708
2	100	2620 2552 2726	2738 2817 2920	2353 2483 2528
3	100	2765 3007 3072	2837 2940 2884	2349 2353 2579
1	Negative Control	3071 3118 3020	3071 3118 3020	3071 3118 3020
2	Negative Control	3095 3083 3217	3095 3083 3217	3095 3083 3217
3	Negative Control	3067 2973 3052	3067 2973 3052	3067 2973 3052

Table I.11. Results from sorption experiments with AOB culture and ^{14}C-IOP. Data relevant to Figure 4-1.

Replicate	Solids (mg TSS/L)	IOP (dpm/mL)		
		t_0 (0 day)	t_1 (1 day)	t_2 (7 day)
1	800	411 401 432	457 421 439	535 477 480
2	800	473 423 477	455 434 470	504 434 451
3	800	457 480 465	436 481 469	425 455 425
1	400	406 432 434	431 472 491	461 412 443
2	400	397 424 444	446 457 516	464 446 490
3	400	496 475 436	411 442 400	535 449 494
1	200	450 474 462	452 423 436	496 483 442
2	200	435 428 486	472 402 407	521 418 474
3	200	471 414 411	430 430 509	423 493 471
1	80	453 445 452	472 482 510	529 481 480
2	80	411 453 425	508 468 468	447 470 517

3	80	429 448 480	475 464 476	466 478 465
1	10	462 433 508	452 444 459	N/A
2	10	417 523 401	478 483 449	N/A
1	Negative Control	490 436 448	441 448 436	531 471 500
2	Negative Control	448 452 471	504 479 464	445 449 499
3	Negative Control	420 491 476	456 477 425	477 514 468

Table I.12. Results from sorption experiments with Ox^- culture and ^{14}C- IOP. Data relevant to Figure 4-2.

Replicate	Solids (mg TSS/L)	IOP (dpm/mL)		
		t_0 (0 day)	t_1 (1 day)	t_2 (7 day)
1	5000	454 454 423	391 466 420	385 469 425
2	5000	480 445 434	469 383 382	392 457 433
3	5000	455 417 452	402 449 403	447 392 422
1	2500	503 492 514	450 462 536	431 497 484
2	2500	431 473 472	404 341 389	397 372 349
3	2500	406 487 464	422 411 457	465 465 450
1	1000	457 440 441	429 480 461	419 468 419
2	1000	413 463 448	431 519 460	417 381 423
3	1000	498 448 461	425 473 397	455 450 428
1	500	497 467 458	468 421 416	567 433 433
2	500	474 427 453	447 406 431	389 417 410

3	500	453 438 435	450 410 428	471 462 483
1	100	481 477 446	468 500 394	435 440 460 0
2	100	444 425 459	458 453 423	495 459 447
3	100	441 473 449	466 458	484 481

Table I.13. Results from sorption experiments with Ox^+ culture and ^{14}C-IOP. Data relevant to Figure 4-2.

Replicate	Solids (mg TSS/L)	IOP (dpm/mL)		
		t_0 (0 day)	t_1 (1 day)	t_2 (7 day)
1	5000	1340 1472 1384	1239 1376 1394	1362 1349 1568
2	5000	1275 1443 1448	1343 1374 1398	1527 1422 1360
3	5000	1341 1448 1492	1317 1377 1295	1337 1442 2813
1	2500	1269 1327 1462	1340 1323	4169 2011 1442
2	2500	1358 1658 1445	1330 1326 1326	1324 1367 1282
3	2500	1639 1355 1346	1264 1345 1380	2139 1387 1367
1	1000	1362 1461 1424	1318 1392 1355	1392 1391 1479
2	1000	1335 1444 1415	1391 1310 1403	1375 1388 1393
3	1000	1327 1396 1388	1327 1399 1348	1393 1401 1331
1	500	1443 1747 1428	1319 1463 1397	1326 1448 1390
2	500	1335 1544 1886	1337 1436 1383	1378 1411 1272

3	500	1303 2261 1664	1275 1300 1413	1354 1370 1407
1	100	1438 1413 1405	1445 1376 1305	1304 1385 1312
2	100	1362 1399 1408	1314 1383 1416	1355 1350 1274
3	100	1340 1424 1326	1378 1449 1367	1220 1221 1387
1	Negative Control	1298 1633 1321	2298 1398 1452	1362 1448 1394
2	Negative Control	1516 1353 1371	1370 1542 1323	1395 1322 1412
3	Negative Control	1557 1424	1354 2466 1447	1392 1482 1438

Table I.14. Results from sorption experiments with MBR NAS (from Auburn University) and ^{14}C-IOP. Data relevant to Section 4.1.2.

Replicate	Solids (mg TSS/L)	IOP (dpm/mL)		
		t_0 (0 day)	t_1 (1 day)	t_2 (7 day)
1	2500	250 332 389	344 379 365	331 355 387
2	2500	265 305 303	313 371 370	384 369 330
3	2500	358 471 314	350 343 390	354 358 367
1	1000	293 305 431	365 383 343	386 357 396
2	1000	339 327 399	343 358 367	354 394 373
3	1000	389 356 347	347 397 373	372 369 353
1	500	296 293 329	344 293 332	356 377 431
2	500	332 364 379	358 374 356	336 384 335
3	500	308 308 348	344 427 354	331 330 332
1	100	261 312 303	371 365 312	356 358 358
2	100	359 327 363	338 364 327	361 335 389

3	100	286 326 348	334 358 378	327 366 373
1	Negative Control	327 322 353	327 322 353	327 322 353
2	Negative Control	331 394 365	331 394 365	331 394 365
3	Negative Control	338 349 317	338 349 317	338 349 317

Table I.15. Results from sorption experiments with PFWWTF NAS and ^{14}C- IOP. Data relevant to Section 4.1.2.

Replicate	Solids (mg TSS/L)	IOP (dpm/mL)		
		t_0 (0 day)	t_1 (1 day)	t_2 (7 day)
1	5000	379 427 472	420 483 414	636 385 534
2	5000	445 436 450	397 374 512	421 425 434
3	5000	452 419 424	404 416 416	378 402 494
1	2500	411 421 461	438 433 453	450 422 392
2	2500	392 443 410	459 413 461	403 382 386
3	2500	394 411 382	414 389 433	429 423 456
1	1000	369 476 406	393 413 410	435 612 422
2	1000	471 365 399	440 448 460	442 422 411
3	1000	472 408 375	389 431 433	398 432 454
1	500	420 416	420 513 425	455 392 444
2	500	414 444 353	446 469 389	397 379 425

3	500	420 468 436	453 568 429	372 428 408
1	100	432 442 449	452 437 406	284 330 334
2	100	413 440 436 0	435 456 411	440 435 449
3	100	496 403 461	464 407 0	520 521 563
1	Negative Control	490 436 448	441 448 436	
2	Negative Control	448 452 471	504 479 464	
3	Negative Control	420 491 476	456 477 425	

Table I.16. Results from sorption experiments with Ox^-, Ox^+ and PFWWTF NAS and TMP. Data relevant to Table 4.3.

Culture	Solids (mg TSS/L)	Concentration (mg TMP/L)					
		t_0 (0 day)		t_1 (1 day)		t_2 (7 day)	
		Avg	Stdev	Avg	Stdev	Avg	Stdev
Ox^-	5.0	1.68	0.02	1.39	0.02	1.28	0.03
	2.5	1.56	0.02	1.54	0.05	1.31	0.09
	1.0	1.52	0.01	1.53	0.02	1.36	0.06
	0.5	1.69	0.05	1.49	0.02		
	0.1	1.69	0.07	1.48	0.04	1.51	0.01
Ox^+	5.0	1.68	0.05	1.39	0.02	1.26	0.05
	2.5	1.59	0.04	1.41	0.01	1.27	0.03
	1.0	1.64	0.01	1.49	0.00	1.39	0.02
	0.5			1.44	0.06	1.39	0.02
	0.1	1.60	0.08			1.50	0.00
NAS	5.0	N/A		0.11	0.10	N/A	
	2.5			0.31	0.08		
	1.0			0.66	0.09		
	0.5			0.90	0.15		
	0.1			1.20	0.33		

Table I.17. Results from sorption experiments with AOB culture devoid of EPS and ^{14}C-EE2. Data relevant to Section 4.1.1.

Replicate	Solids (mg TSS/L)	EE2 (dpm/mL)
		t_2 (1 day)
		AOB
1	800	2940 3128 3446
2	800	3409 3348 3467
3	800	3605 3520 3422
1	400	3466 3640 3641
2	400	3174 3407 3520
3	400	3624 3506 3485
1	200	3569 3718 3631
2	200	3433 3533 3546
3	200	3320 3405 3542
1	80	3671 3675 3912
2	80	3571 3716 3671

3	80	3832 3963 3506
1	10	3677 3779 3997
2	10	3653 3580 3696
3	10	3784 3833 3886
1	Negative Control	3737 3934 3910
2	Negative Control	3653 3737 3927
3	Negative Control	3858 3697 3798

Table I.18. Results from sorption experiments with Ox^-, Ox^+ and NAS cultures devoid of EPS and ^{14}C-EE2. Data relevant to Table 4.1.

Solids (mg TSS/L)	EE2 (dpm/mL)			
	t_2 (1 day)			
	Ox^-	Ox^+	NAS	CER control
5000	1802	1432	1334	3872
	1857	1354	1444	3939
	1937	1428	1328	3987
5000	1721	1546	1611	3712
	1952	1652	1611	3694
	1838	1813	1690	3767
5000	1777	1556	1690	3895
	1885	1614	1736	3983
	2044	1708	1730	3821
2500	2240	2386	1873	3588
	2336	1627	2035	3600
	2319	2441	2130	3682
2500	2053	2328	2156	3711
	2124	2241	2274	3646
	2187	2302	2096	3709
2500	2268	2388	2309	3657
	2337	2266	2346	3790
	2226	2349	2501	3752
1000	2569		2966	3776
	2900		3104	3842
	2846		3150	3715
1000	2860	3073	2876	3905
	2963	2984	2896	3953
	3037	2923	2915	3990
1000	2815		2688	3582
	2837		3025	3500
	3057		2913	3578
500	3139	3390	2909	3827
	3285	3355	3111	3829
	3238		3065	4019
500	3455	3190	3048	3977
	3407		3238	3905
	3477	3600	3179	3962

500	3445 3511 3535	3294 3384 3410	3033 3236 3351	3699 3667 3743
100	3593 3657 3792	3865 4063 3813	3267 3369 3482	3892 3900 3913
100	3668 3673 3801	3998 3970 4035	3117 3071 3174	3776 3749 3740
100		3888 3936 3663	3394 3459 3681	3783 3680 3847
Negative Control	3737 3934 3910			
Negative Control	3653 3737 3927			
Negative Control	3858 3697 3798			

Table I.19. Results from sorption experiments with Ox^-, Ox^+ and PFWWTF NAS cultures devoid of EPS and TMP. Data relevant to Table 4.3.

Culture	Solids (mg TSS/L)	TMP (mg TMP/L)	
		t_1 (1 day)	
		Avg	Stdev
Ox^-	5.0	0.69	0.01
	2.5	0.83	0.00
	1.0	1.37	0.09
	0.5	1.67	0.10
	0.1	1.91	0.06
Ox^+	5.0	0.90	0.06
	2.5	1.25	0.41
	1.0	1.49	0.09
	0.5	1.67	0.06
	0.1	2.00	0.03
NAS	5.0	0.05	0.02
	2.5	0.32	0.02
	1.0	0.60	0.26
	0.5	1.24	0.01
	0.1	1.42	0.08

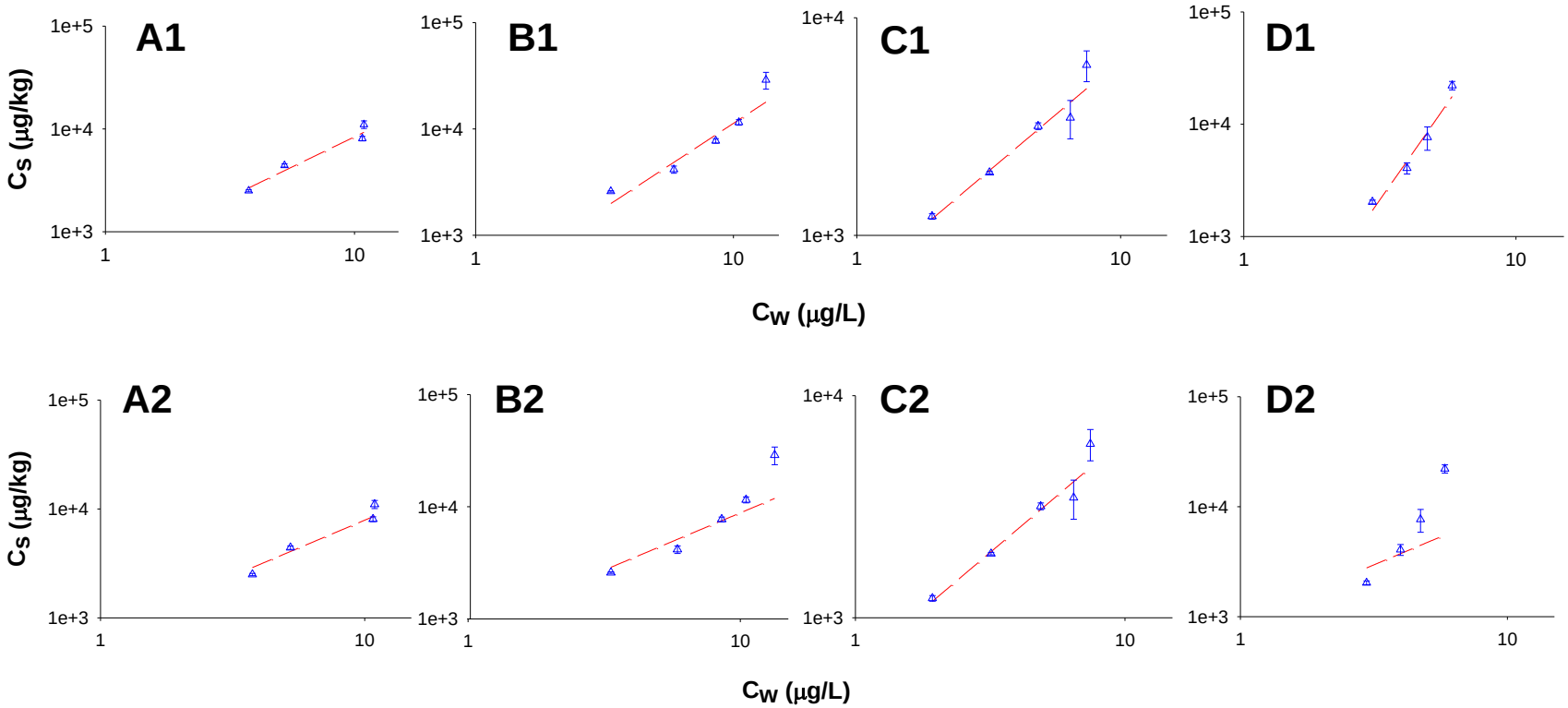

Figure I-1. Comparison of sorption isotherms obtained for biomass with EPS. A1: Ox^- Pre-EPS data with Freundlich fit, A2: Ox^- Pre-EPS data with Dual mode fit, B1: Ox^+ Pre-EPS data with Freundlich fit, B2: Ox^+ Pre-EPS data with Dual mode fit, C1: NAS Ox^- Pre-EPS data with Freundlich fit, C2: NAS Pre-EPS data with Dual mode fit, D1: MBR NAS Pre-EPS data with Freundlich fit, D2: MBR NAS Pre-EPS data with Dual mode fit. Data relevant to Section 4.1.5.

I-2 Results from biomass characterizations

Table I.20. Summary of biomass characteristics from sorption experiments with EE2 before and after EPS extraction. Data relevant to Table 4.2.

Culture	Pre-EPS Extraction				Post-EPS Extraction			
	f_{om}	Median Particle size diameter (μm)	% Adhesion	Zeta Potential (mV)	f_{om}	Median Particle size diameter (μm)	% Adhesion	Zeta Potential (mV)
AOB	80 ± 1	14 ± 5	6.0 ± 0.1	N/D	76 ± 16	N/D	N/D	N/D
Ox^- culture	72 ± 1	89 ± 1	70 ± 10	-35 ± 10	70 ± 3	74 ± 12	60 ± 2	N/D
Ox^+ culture	80 ± 1	198 ± 10	15 ± 5	-30 ± 2	79 ± 2	72 ± 6	25 ± 10	N/D
NAS	80 ± 1	108 ± 10	75 ± 10	-30 ± 10	80 ± 1	30 ± 10	75 ± 6	N/D

The values reported were calculated from data obtained from triplicates and are reported as $\bar{x} \pm s_x$ where s_x is the standard deviation.

Table I.21. Summary of biomass characteristics from sorption experiments with TMP before and after EPS extraction. Data relevant to Table 4.2.

Culture	Pre-EPS Extraction				Post-EPS Extraction			
	f_{om}	Median Particle size diameter (μm)	% Adhesion	Zeta Potential (mV)	f_{om}	Median Particle size diameter (μm)	% Adhesion	Zeta Potential (mV)
AOB	80 ± 3	8 ± 10	3.8 ± 1	N/D	58 ± 2	N/D	N/D	N/D
Ox^- culture	66 ± 1	151 ± 5	73 ± 10.6	-26.8 ± 2	100 ± 2	56 ± 1	67 ± 2	-15.1 ± 1.6
Ox^+ culture	80 ± 5	232 ± 10	12 ± 1	-39 ± 1	75 ± 2	100 ± 22	64 ± 22	-29.7 ± 3.3
NAS	80 ± 2	84 ± 5	94.2 ± 5	-11 ± 2	76 ± 1	60 ± 12	93 ± 4	-25.3 ± 2.9

The values reported were calculated from data obtained from triplicates and are reported as $\bar{x} \pm s_x$ where s_x is the standard deviation.

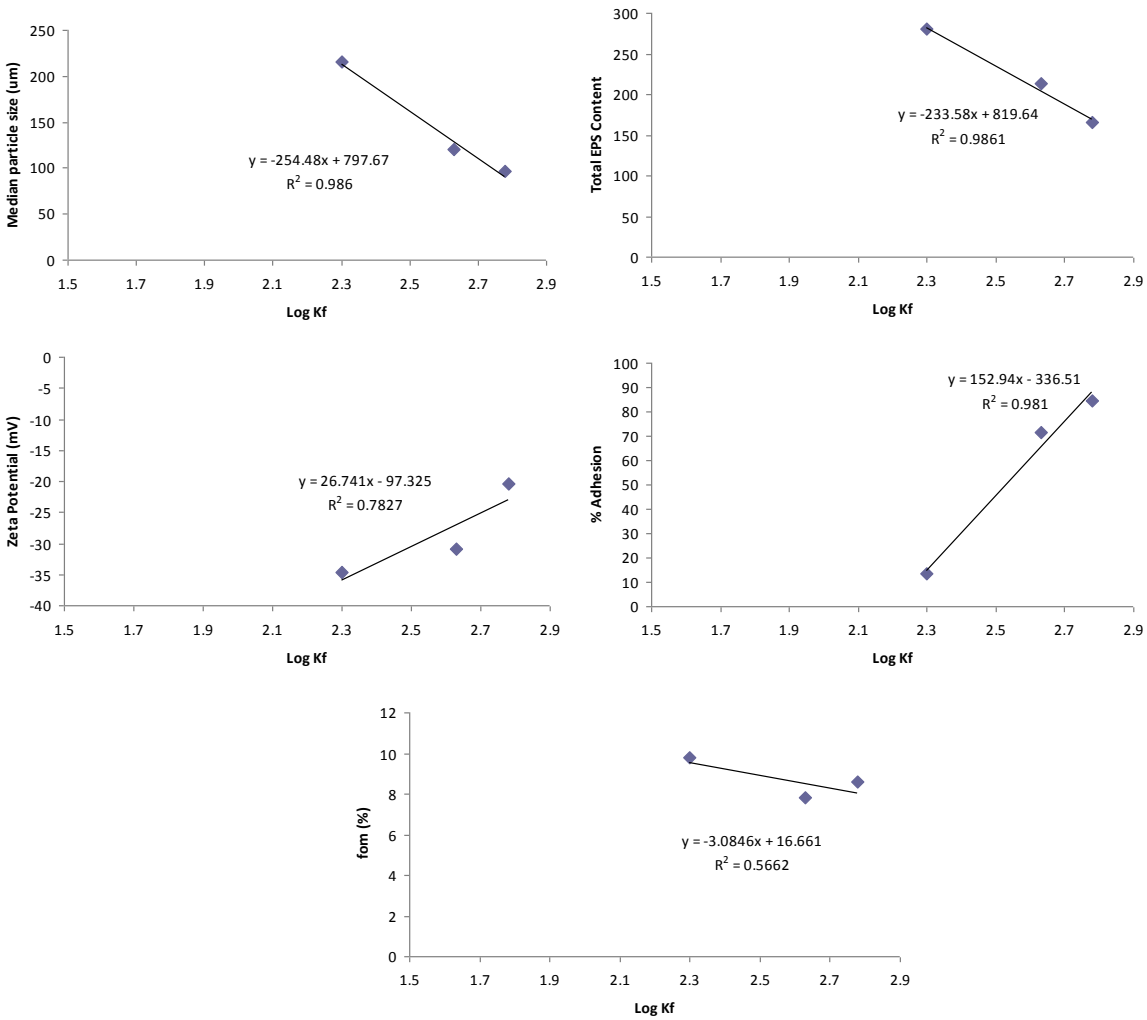

Figure I-2. Correlations between particle size distribution, EPS content, zeta potential, % adhesion, organic matter content (f_{OM}) and log K_F for biomass pre-EPS extraction. Data was specific to EE2 experiments and is most relevant to Tables 4.1 and **4.2.**

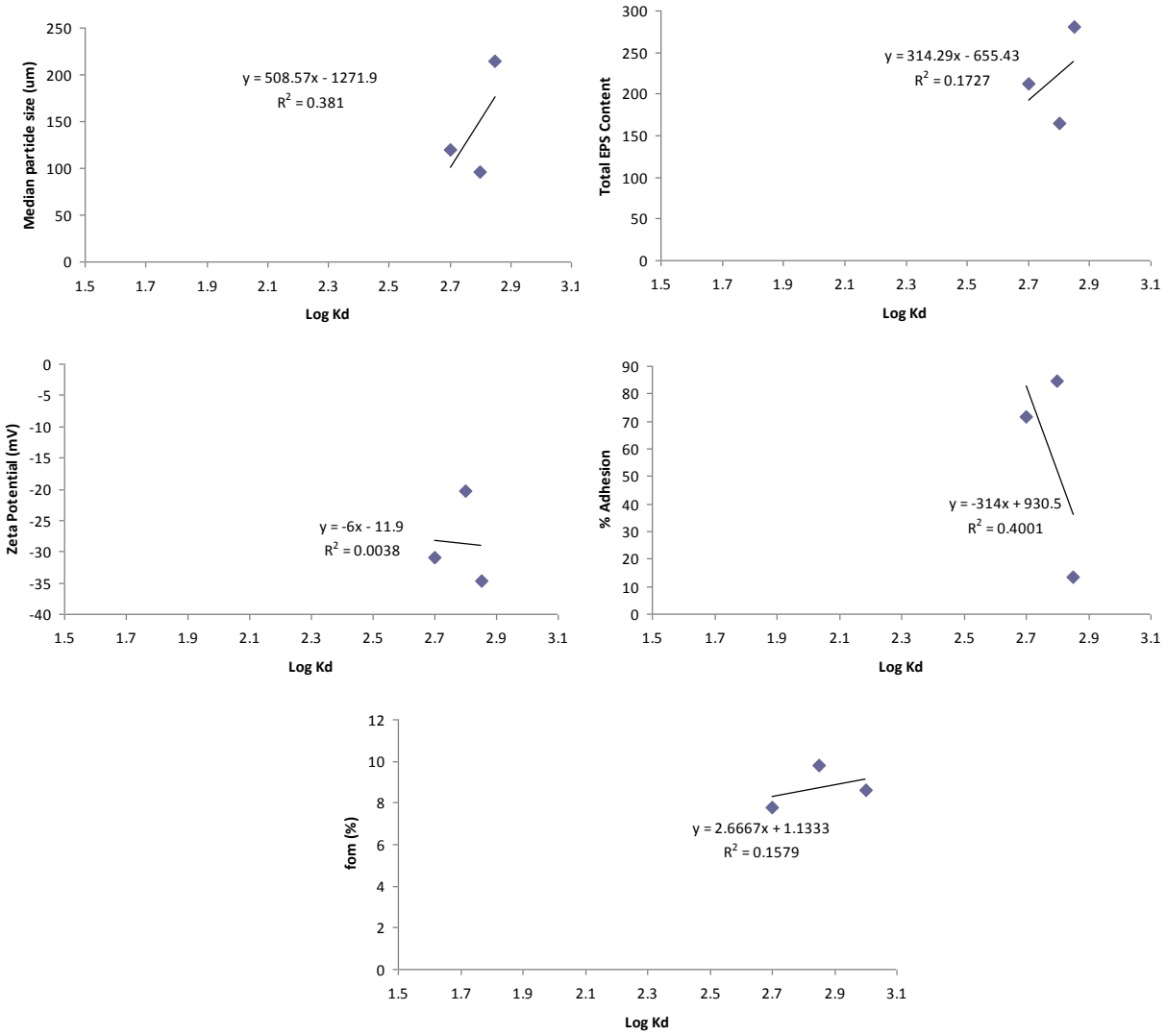

Figure I-3. Correlations between particle size distribution, EPS content, zeta potential, % adhesion, organic matter content (f_{OM}) and log K_D for biomass pre-EPS extraction. Data was specific to EE2 experiments and is most relevant to Tables 4.1 and **4.2.**

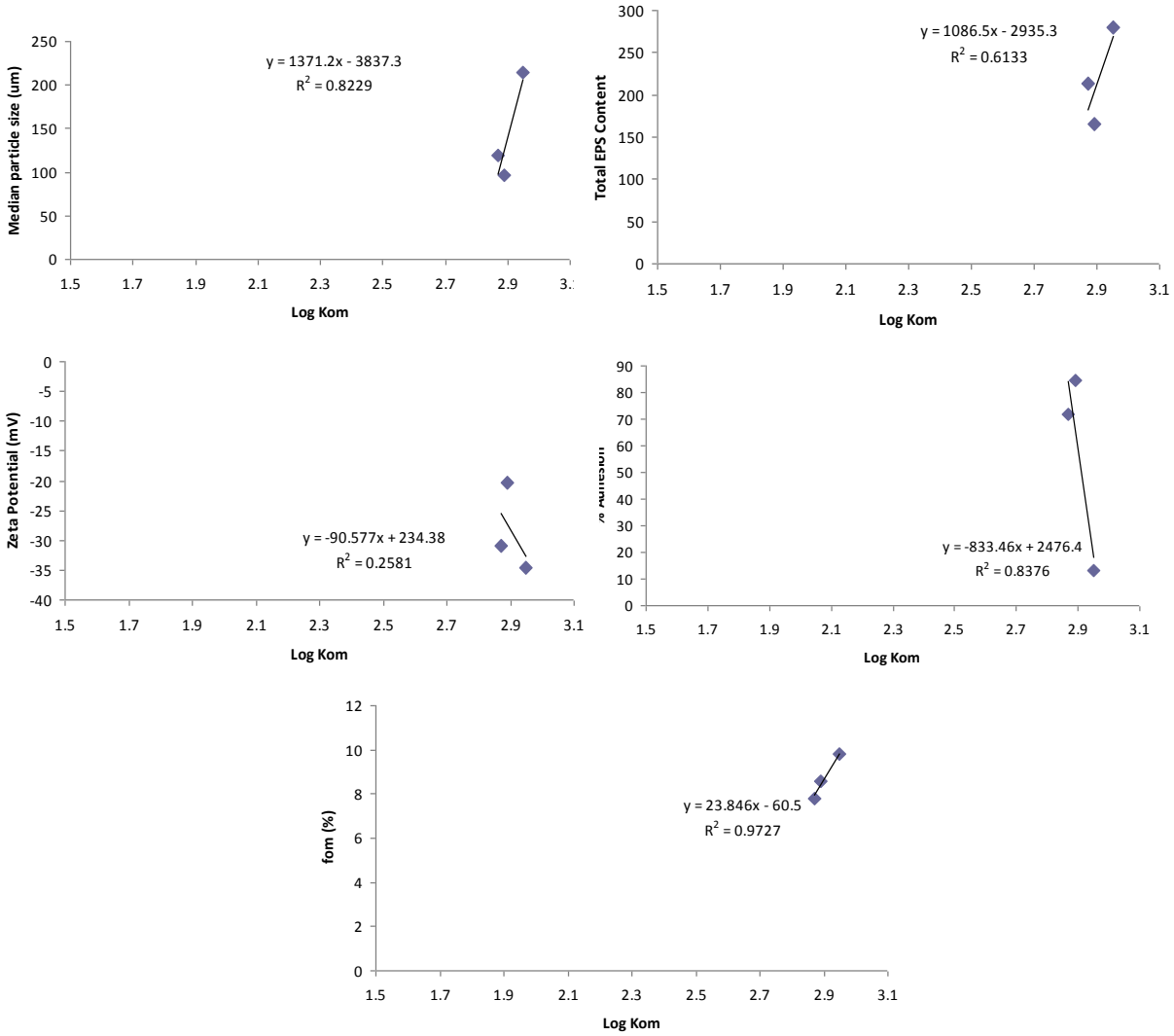

Figure I-4. Correlations between particle size distribution, EPS content, zeta potential, % adhesion, organic matter content (f_{OM}) and log K_{OM} for biomass pre-EPS extraction. Data was specific to EE2 experiments and is most relevant to Tables 4.1 and **4.2.**

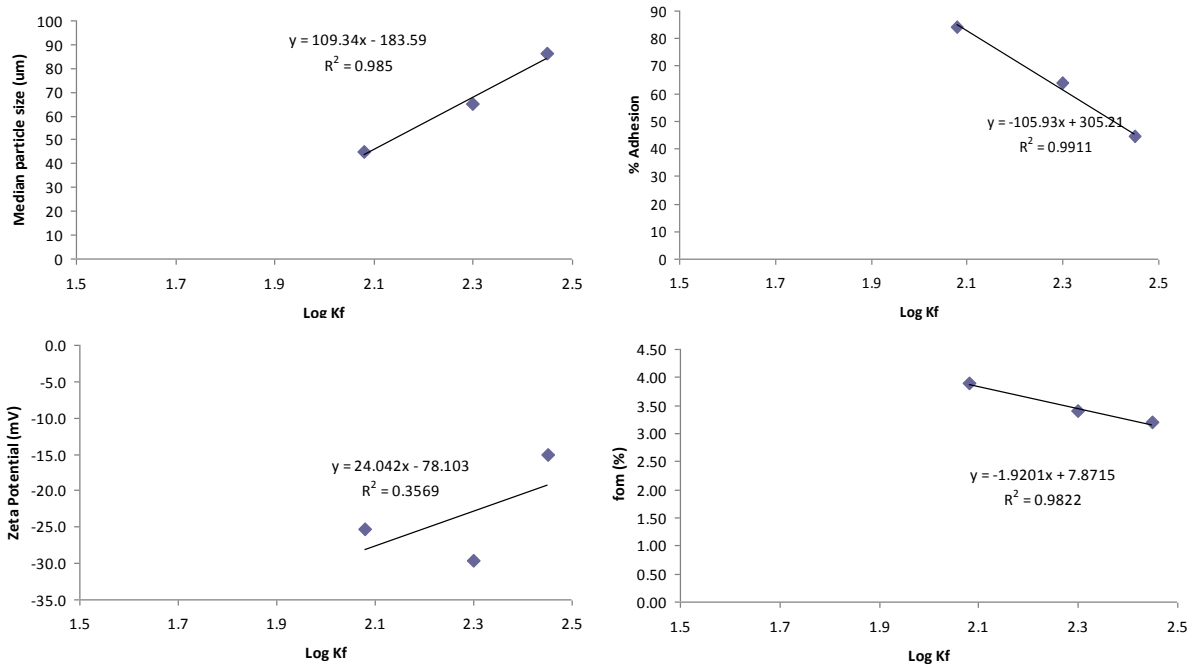

Figure I-5. Correlations between particle size distribution, EPS content, zeta potential, % adhesion, organic matter content (f_{OM}) and log K_F for biomass after EPS extraction. Data was specific to EE2 experiments and is most relevant to Tables 4.1 and **4.2.**

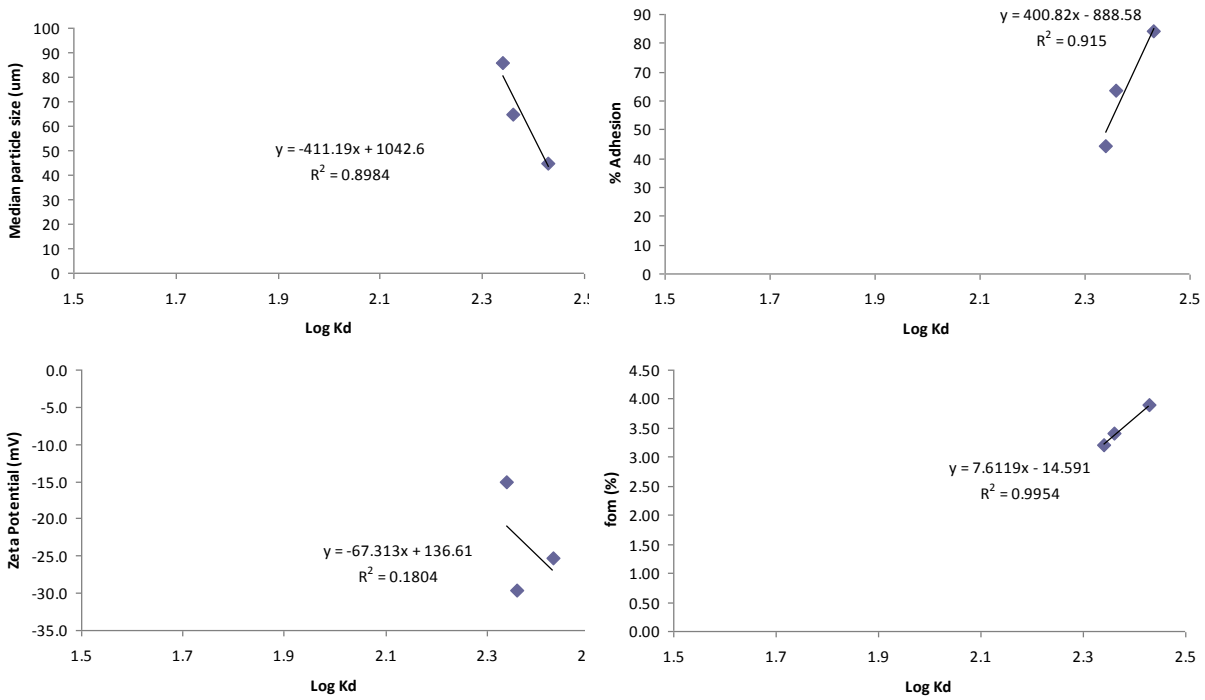

Figure I-6. Correlations between particle size distribution, EPS content, zeta potential, % adhesion, organic matter content (f_{OM}) and log K_D for biomass after EPS extraction. Data was specific to EE2 experiments and is most relevant to Tables 4.1 and **4.2.**

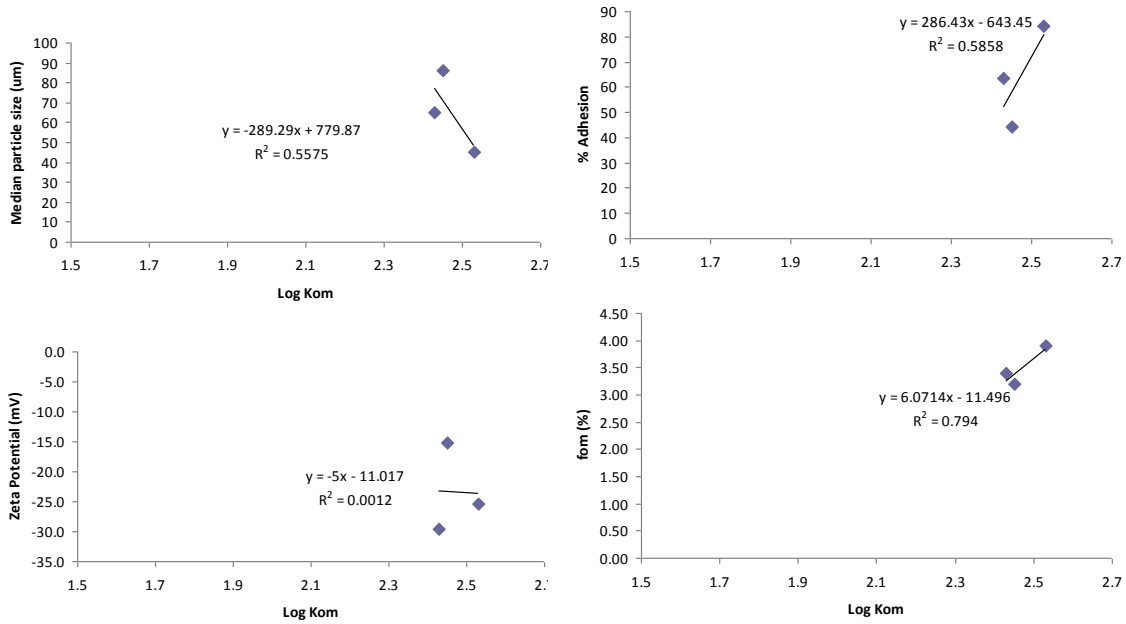

Figure I-7. Correlations between particle size distribution, EPS content, zeta potential, % adhesion, organic matter content (f_{OM}) and log K_{OM} for biomass after EPS extraction. Data was specific to EE2 experiments and is most relevant to Tables 4.1 and **4.2.**

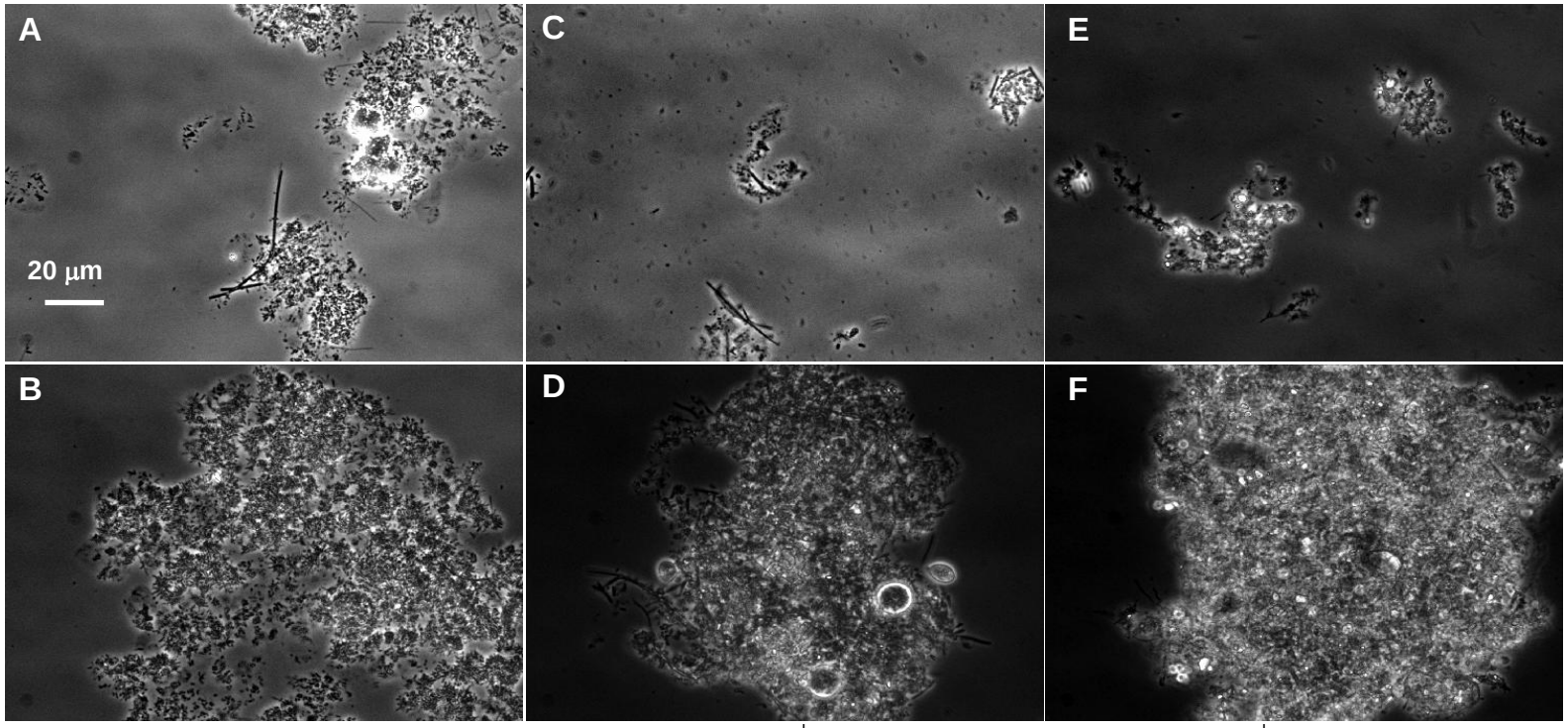

Figure I-8. Phase contrast micrographs of cultures. A: Ox^+ cells post-EPS extraction, B: Ox^+ cells pre-EPS extraction, C: Ox^- cells post-EPS extraction, D: Ox^- cells pre-EPS extraction, E: PFRWWTP NAS post-EPS extraction, F: PFRWWTP NAS pre-EPS extraction. Data is most relevant to Tables 4.2.

I-3 Prediction of K_{OM} and K_{OC} values using existing linear free energy relationships (LFERs)

Organic matter partition coefficients for microconstituents were predicted using several empirical single parameter LFERs (sp-LFER),

$$\log K_{OM} = 0.904 \log(D_{OW}) - 0.779 \quad \text{[I-1, [1]]}$$

$$\log K_{OC} = 1.030 \log(D_{OW}) - 0.610 \quad \text{[I-2, [2]]}$$

where

$$D_{OW} = \alpha_{ia} \times K_{OW}, \quad \text{[I-3]}$$

$$\alpha_{ia} = \frac{1}{1+10^{pH-pK_a}} \quad \text{[I-4]}$$

D_{OW} – distribution coefficient for EE2, α_{ia} = fraction of compound in non-dissociated form.

Efforts have also been made to establish poly-parameter linear free energy relationships (pp-LFER) that predict the multimedia fate of PPCPs [3-7]. These models attempt to characterize compound partitioning by describing intermolecular interactions and are highly sensitive to solute descriptors and system constants,

$$\log K_{OC} = c + eE + sS + aA + bB + vV \quad \text{[I-5]}$$

where,
A- overall hydrogen-bond acidity, B- overall hydrogen-bond basicity, E- excess molar refraction ($cm^3/10$), S- dipolarity/polarizability, V- cavity term ($cm^3/mol/100$).

Solute parameters were obtained from literature or calculated using medicinal chemistry databases while system constants were obtained from literature describing partitioning to sediment/soil systems. These pp-LFERs were then used to estimate the partition coefficient of each microconstituent.

Table I.22. Solute parameters and system constants for CBZ, IOP and EE2. Data was obtained from [3-6, 8].

Solute parameter	EE2 [3]	CBZ [6]	IOP [8]
A	0.97	0.42	1.65
B	1.16	1.11	3.36
E	2.12	2.15	4.33
S	2.50	1.79	4.87
V	2.39	1.81	3.82
System constants	**[5]**	**[4]**	
a	-0.39	0.28	
b	-1.51	-1.85	
e	0.95	1.08	
s	-0.39	-0.83	
v	1.76	2.55	
c	0.55	0.12	

I-3-a Existing sp-LFERs and pp-LFERs overestimate the impact of partitioning of CBZ and IOP onto activated sludge.

Use of sp-LFERs to predict sorption coefficients for organic pollutants has been attempted previously [1, 5, 9]. Coefficients calculated for CBZ and IOP were seen to inaccurately describe the role of sorption for these microconstituents (**Table I.23**). Such inaccuracy may be related to the fact that the sp-LFERs (**Eq. I-1 and I-2**) were developed for a combination of primarily weakly polar compounds and polar compounds that have widely varying sorption characteristics in organic matter. Ideally, prediction of sorption for these microconstituents would utilize class specific sp-LFERs but in the absence of such relationships, models that include a large dataset of structurally unrelated compounds may be applied with caution. Within this context it can be clearly seen that use of such relationships towards describing the intermolecular interactions between CBZ and IOP and organic matter is inadequate.

Polyparameter LFERs have been developed to help overcomes the issues associated with sp-LFERs by seeking to describe specific intermolecular interaction parameters between sorbate and sorbent [3, 7, 9]. Use of such relationships to predict sorption coefficients for CBZ and IOP yielded values that seemingly overestimate partitioning observed in current and previous studies (**Table I.23**). Again, this lack of correlation may be related to inadequacy of the system constants/phase descriptors currently available in the literature (**Table I.23**) to describe sorbate/sorbent interactions particularly as related to organic matter and microconstituents. Values utilized for calculations in this study were generated from soil/sediment systems examining both apolar and weakly polar compounds [4, 5]. As both CBZ and IOP are polar organic microconstituents (carboxamides), existing system constants/phase descriptors associated with the pp-LFERs may be inadequate to completely depict the various interactions involved during partitioning of these two PPCPs onto organic matter. It is anticipated that as more data becomes available regarding the partitioning of microconstituents onto organic matter, improved system parameters/phase descriptors that describe H-donor/acceptor behaviors will be defined.

I-3-b Single parameter LFERs predict sorption of EE2 onto activated sludge reasonably well while pp-LFERs overestimate partitioning of EE2.

Use of sp-LFERs to describe sorption of EE2 was particularly successfully when using models derived from datasets describing sorption of weakly polar and polar compounds (**Table I.23**) [1, 2] since those chemicals more closely mimic the interactions that may occur between EE2 and organic matter. While the pp-LFERs overestimated sorption observed in our experiments, they allowed determination of the relative impact of the different components of sorption of EE2 (data not shown). Neither hydrogen-bond acidity (A) nor the equation constant term (c) contributed significantly to theoretical EE2 sorption. On the other hand, hydrogen-bond basicity (B), excess molar refraction (E), dipolarity/polarizability (S) and the cavity term (V) all contributed significantly to overall sorption. Primarily though, the partition coefficient for EE2 was most affected by cavity formation. This result falls in line with previous results [4]. As with CBZ and IOP, it is anticipated that improved system constants may yield more accurate LFERs resulting in better prediction of EE2 partitioning. There is also the possibility that existing six parameter LFERs is still not sufficiently describe sorption in organic matter.

Table I.23. Predicted values of sorption coefficients for CBZ, IOP and EE2 using sp-LFERs and pp-LFERs.

Compound	Predicted Values (sp-LFER)		Predicted Values (pp-LFER)	
	Log K_{om} [1]	Log K_{oc} [2]	Log K_{oc} [3]	Log K_{oc} [4]
CBZ	1.44	1.91	3.24	3.64
IOP	-2.89	-3.01	3.77	4.75
EE2	2.54	3.17	3.67	4.55

[1]Calculated from equation I-1
[2] Calculated from equation I-2
[3]Calculated from equation I-5 using solute parameters from Zukowska et al. [3].
[4]Calculated from equation I-5 using solute parameters from Nguyen et al. [4]

I-4 References

1. Chiou, C. T., *Partion and Adsorption of Organic Contaminants in Environmental Systems.* John Wiley and Sons: New Jersey, 2002; p 257.
2. Seth, R., Mackay, D., Muncke, J., Estimating the Organic Carbon Partition Coefficient and its Variability for Hydrophobic Chemicals. *Environmental Science and Technology* **1999,** *33,* 2390-2394.
3. Zukowska, B., Breivik, K., Wania, F., Evaluating the Environmental Fate of Pharmaceuticals using a Level III Model Based on Poly-parameter Linear Free Energy Relationships. *Science of the Total Environment* **2006,** *359,* 177-187.
4. Nguyen, T. H., Goss, K.U., Ball, W.P., Polyparameter Linear Free Energy Relationships for Estimating the Equilibrium Partition of Organic Compounds between Water and the Natural Organic Matter in Soils and Sediments. *Environmental Science and Technology* **2005,** *39,* (4), 913-924.
5. Poole, S. K., Poole, C.F., Chromatographic Models for the Sorption of Neutral Organic Compounds by Soil from Water and Air. *Journal of Chromatography A* **1999,** *845*, 381-400.

6. Tulp, H. C., Goss, K.U., Schwarzenbach, R.P., Fenner, K., Experimental Determination of LSER Parameters for a Set of 76 Diverse Pesticides and Pharmaceuticals. *Environmental Science and Technology* **2008,** *42*, 2034-2040.
7. Abraham, M. H., Scales of Solute Hydrogen-Bonding - Their Construction and Application to Physicochemical and Biochemical Processes. *Chemical Society Reviews* **1993,** *22*, 73-83.
8. Inc., P. A. ADME toolbox.
9. Schwarzenbach, R. P., Gschwend, P.M., Imboden, D.M., *Environmental Organic Chemistry*. 2nd Edition ed.; Wiley Interscience: Hoboken, N.J, 2003.

APPENDIX II

Data from appendix II are relevant to results and discussions in **Sections 4.1, 4.2** and **4.3.**

II-1 Results from biotransformation experiments showing ion suppression.

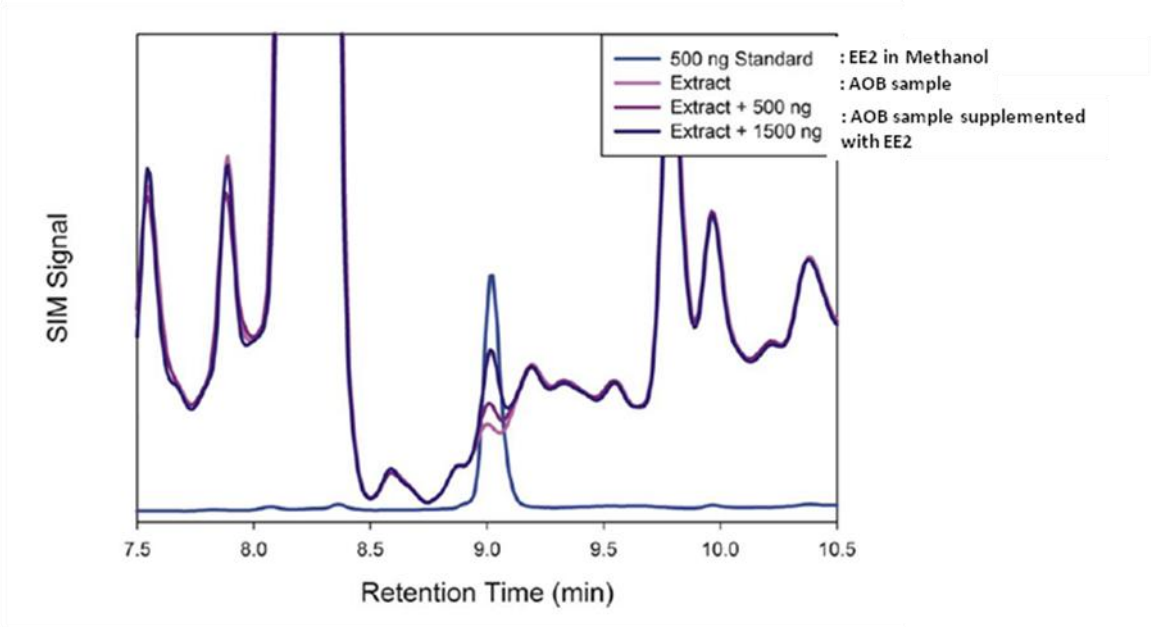

Figure II-1. Mass spectra of EE2 showing ion suppression due to presence of phenol red. Adapted from [1]. Relevant to Section 3.2.1.

II-2 Results from inhibition experiments with hydrogen peroxide and sodium azide.

Table II.1. Results from aeration experiment with catalase and H_2O_2. Data relevant to Section 3.2.2 and all subsequent experiments employing oxygenation strategy.

Condition	sOUR (mg/g VSS-day)	
	Avg	RMD
Endogenous respiration	0.15	0.00
Aeration via Aquarium pump	0.56	0.07
Aeration via Catalase & H2O2	0.43	0.07
Aeration via Aquarium pump supplemented with 70 mg/L NEM	0.06	0.01

N-ethylmaleimide (NEM) was used as a positive control.
Experiment was performed with Ox^- biomass.
Rates were calculated from duplicate reactor vessels and are reported as $\bar{x} \pm RMD$ where RMD is the relative mean difference.

Table II.2. Results from sodium azide inhibition experiment. Data relevant to Sections 3.3.1 and 3.8 and subsequent sorption control experiments.

Condition	sOUR (mg/g VSS-day)	
	Avg	**RMD**
Endogenous respiration	1731	315
1000 mg COD/L only	8110	870
30 min. exposure		
1000 mg COD/L and 2.5 mM azide	2976	330
1000 mg COD/L and 5 mM azide	2796	32
1000 mg COD/L and 10 mM azide	485	109
24 hr. exposure		
1000 mg COD/L and 2.5 mM azide	3353	4532
1000 mg COD/L and 5 mM azide	573	130
1000 mg COD/L and 10 mM azide	58	27
7 day exposure		
1000 mg COD/L and 2.5 mM azide	1767	88
1000 mg COD/L and 5 mM azide	453	97
1000 mg COD/L and 10 mM azide	bdl	bdl

bdl- below detection limit

Experiment was performed with Ox^- biomass.

Rates were calculated from duplicate reactor vessels and are reported as $\bar{x} \pm RMD$ where RMD is the relative mean difference.

II-3 Results from oxygenase analyses.

Data is most relevant to **Sections 4.2.6 to 4.2.9**.

Table II.3. Comparison of EE2 mass loading and C12O activity for Ox^- cultures. Data relevant to Sections 4.2.6, 4.2.7 and Table 4.9.

Concentration (mg EE2 as COD/L)	2.71	<-- This assumes complete oxidation of EE2 to CO_2						
Flowrate (L/day)	0.29							
Mass applied/day (mg EE2 as COD/day)	0.78							
For C120 reaction								
	Catechol		Oxygen		Cis, cis muconate			
	$C_6H_6O_2$	+	O_2	-->	$C_6H_4O_4^{2-}$	+	H_2O	
Stoichiometry of reaction	1		1.5		1		1	
MW (g/mol)	110.1		32		140.1		18	
MW (mg/umol)	0.1101							
Theoretical COD (g O_2/g catechol)	0.44							
C23O Activity for Ox^- cells	1.54E-03	umol catechol/mg protein-hr						
	1.69E-04	mg catechol/mg protein-hr						
	7.37E-05	mg O_2/mg protein-hr						
Assuming zero order reaction	0.03	mg O_2/hr				210	mg VSS/L	
kX	0.70	mg O_2/day				298.2	mg COD/L	
						198.8	mg protein/L	
Mass of EE2 applied to system/day	0.78	mg EE2 as COD/day						
Oxygenase activity	0.70	mg O_2/day						
Based on analyses, Ox^- C120 activity is lower than that required for complete oxidation of EE2.								

Table II.4. Comparison of EE2 mass loading and C12O activity for Ox^+ cultures. Data relevant to Sections 4.2.6, 4.2.7 and Table 4.9.

Concentration (mg EE2 as COD/L)	2.71	<-- This assumes complete oxidation of EE2 to CO_2						
Flowrate (L/day)	0.29							
Mass applied/day (mg EE2 as COD/day)	0.78							
For C120 reaction								
	Catechol		Oxygen		Cis, cis muconate			
	$C_6H_6O_2$	+	O_2	-->	$C_6H_4O_4^{2-}$	+	H_2O	
Stoichiometry of reaction	1		1.5		1		1	
MW (g/mol)	110.1		32		140.1		18	
MW (mg/umol)	0.1101							
Theoretical COD (g O_2/g catechol)	0.44							
C23O Activity for Ox^- cells	0.0900	umol catechol/mg protein-hr						
	0.0099	mg catechol/mg protein-hr						
	0.0043	mg O_2/mg protein-hr						
	1.718							
Assuming zero order reaction		mg O_2/hr			210	mg VSS/L		
kX	41.22	mg O_2/day			298.2	mg COD/L		
					198.8	mg protein/L		
Mass of EE2 applied to system/day	0.78	mg EE2 as COD/day						
Oxygenase activity	41.22	mg O_2/day						
Based on analyses, Ox^+ C120 activity is higher than that required for complete oxidation of EE2								

Table II.5. Comparison of EE2 mass loading and C23O activity for Ox^- cultures. Data relevant to Sections 4.2.6, 4.2.7 and Table 4.9.

Concentration (mg EE2 as COD/L)	2.71	<-- This assumes complete oxidation of EE2 to CO_2					
Flowrate (L/day)	0.29						
Mass applied/day (mg EE2 as COD/day)	0.78						
For C230 reaction							
	Catechol		Oxygen		2-Hydroxy-*cis,cis*-muconate semialdehyde		
	$C_6H_6O_2$	+	O_2	-->	$C_6H_5O_4$	+	H_2O
Stoichiometry of reaction	1		1.25		1		0.5
MW (g/mol)	110.1		32		141.1		18
MW (mg/umol)	0.1101						
Theoretical COD (g O_2/g catechol)	0.36						
C23O Activity for Ox^- cells	4.48E-03	umol catechol/mg protein-hr					
	4.93E-04	mg catechol/mg protein-hr					
	1.79E-04	mg O_2/mg protein-hr					
Assuming zero order reaction	0.07	mg O_2/hr			210	mg VSS/L	
kX	1.71	mg O_2/day			298.2	mg COD/L	
					198.8	mg protein/L	
Mass of EE2 applied to system/day	0.78	mg EE2 as COD/day					
Oxygenase activity	1.71	mg O_2/day					
Based on analyses, Ox^- C230 activity is higher than that required for complete oxidation of EE2							

Table II.6. Comparison of EE2 mass loading and C23O activity for Ox^+ cultures. Data relevant to Sections 4.2.6, 4.2.7 and Table 4.9.

Concentration (mg EE2 as COD/L)	2.71	<-- This assumes complete oxidation of EE2 to CO_2						
Flowrate (L/day)	0.29							
Mass applied/day (mg EE2 as COD/day)	0.78							
For C230 reaction								
	Catechol		Oxygen		2-Hydroxy-*cis*,*cis*-muconate semialdehyde			
	$C_6H_6O_2$	+	O_2	-->	$C_6H_5O_4$	+	H_2O	
Stoichiometry of reaction	1		1.25		1		0.5	
MW (g/mol)	110.1		32		141.1		18	
MW (mg/umol)	0.1101							
Theoretical COD (g O_2/g catechol)	0.36							
C23O Activity for Ox^- cells	0.10	umol catechol/mg protein-hr						
	1.15E-02	mg catechol/mg protein-hr						
	4.19E-03	mg O_2/mg protein-hr						
Assuming zero order reaction	1.66	mg O_2/hr			210	mg VSS/L		
kX	39.94	mg O_2/day			298.2	mg COD/L		
					198.8	mg protein/L		
Mass of EE2 applied to system/day	0.78	mg EE2 as COD/day						
Oxygenase activity	39.94	mg O_2/day						
Based on analyses, Ox^+ C230 activity is higher than that required for complete oxidation of EE2								

Table II.7. Comparison of EE2 mass loading and Tod activity for Ox^+ cultures. Data relevant to Sections 4.2.6, 4.2.7 and Table 4.9.

Concentration (mg EE2 as COD/L)	2.71	<-- This assumes complete oxidation of EE2 to CO_2					
Flowrate (L/day)	0.29						
Mass applied/day (mg EE2 as COD/day)	0.78						
Indole oxidation to indigo							
	Indole		Oxygen		Indigo		
	C_8H_7N	+	O_2	-->	$C_{16}H_{10}N_2O_2$	+	H_2O
Stoichiometry of reaction	2		2		1		2
MW (g/mol)	117.15		32		262.27		18
MW (mg/umol)	0.117				0.262		
Theoretical COD (g O_2/g indigo)	0.55				0.24		
Indigo activity	9.00E-05	umol indigo/mg protein-hr			Biomass concentration		
	1.05E-05	mg indigo/mg protein-hr			210	mg VSS/L	
					298.2	mg COD/L	
Convert to indole oxidized	2.11E-05	mg indole oxidized/mg protein-hr			198.8	mg protein/L	
	1.15E-05	mg O_2/mg protein-hr					
	2.29E-03	mg O_2/hr					
	5.50E-02	mg O_2/day					
Mass of EE2 applied to system/day	0.78	mg EE2 as COD/day					
Oxygenase activity	0.05	mg O_2/day					
Based on analyses, Ox^+ Tod activity is lower than that required for complete oxidation of EE2							

Table II.8. Comparison of EE2 mass loading and AMO activity for AOB cultures. Data relevant to Section 4.2.7.

Concentration (mg EE2 as COD/L)	2.71	<-- This assumes complete oxidation of EE2 to CO_2											
Flowrate (L/day)	0.29												
Mass applied/day (mg EE2 as COD/day)	0.78												
NH3 oxidation to nitrite (assuming no loss of electrons back to AMO)													
	NH_3	+	O_2	+	H^+	-->	NH_2OH	+	H_2O	-->	NO_2^-	+	H^+
Stoichiometry of reaction	1		1		2		1		1		1		5
MW (g/mol)	17		32		1		33		18		46		1
MW (mg/umol)	0.017												
Theoretical COD (g O_2/g NH_3)	1.88												
Theoretical COD (g O_2/g NH_3-N)	2.29												
sNGR	142	mg NO_2^--N/g biomass as COD-day			Biomass concentration								
					90	mg VSS/L							
Convert to NH_3 oxidized	142	mg NH_3-N/g biomass as COD-day			127.8	mg COD/L							
	325	mg O_2/g COD-day			85.2	mg protein/L							
	41	mg O_2/hr											
Mass of EE2 applied to system/day	0.78	mg EE2 as COD/day											
Oxygenase activity	41	mg O_2/day											
Based on analyses, AMO activity is high than that required for complete oxidation of EE2													

Table II.9. Comparison of TMP mass loading and C12O activity for Ox^- cultures. Data relevant to Sections 4.2.8, 4.2.9 and Table 4.9.

Concentration (mg TMP as COD/L)	1.54	<-- This assumes complete oxidation of TMP to CO_2						
Flowrate (L/day)	0.29							
Mass applied/day (mg TMP as COD/day)	0.44							
For C120 reaction								
	Catechol		Oxygen		Cis, cis muconate			
	$C_6H_6O_2$	+	O_2	-->	$C_6H_4O_4^{2-}$	+	H_2O	
Stoichiometry of reaction	1		1.5		1		1	
MW (g/mol)	110.1		32		140.1		18	
MW (mg/umol)	0.1101							
Theoretical COD (g O2/g catechol)	0.44							
C23O Activity for Ox^- cells	1.54E-03	umol catechol/mg protein-hr						
	1.69E-04	mg catechol/mg protein-hr						
	7.37E-05	mg O_2/mg protein-hr						
Assuming zero order reaction	0.03	mg O_2/hr				210	mg VSS/L	
kX	0.70	mg O_2/day				298.2	mg COD/L	
						198.8	mg protein/L	
Mass of TMP applied to system/day	0.44	mg TMP as COD/day						
Oxygenase activity	0.70	mg O_2/day						
Based on analyses, Ox^- C120 activity is higher than that required for complete oxidation of TMP								

Table II.10. Comparison of TMP mass loading and C12O activity for Ox^+ cultures. Data relevant to Sections 4.2.8, 4.2.9 and Table 4.9.

Concentration (mg TMP as COD/L)	1.54	<-- This assumes complete oxidation of TMP to CO_2							
Flowrate (L/day)	0.29								
Mass applied/day (mg TMP as COD/day)	0.44								
For C120 reaction									
	Catechol		Oxygen		Cis, cis muconate				
	$C_6H_6O_2$	+	O_2	-->	$C_6H_4O_4^{2-}$	+	H_2O		
Stoichiometry of reaction	1		1.5		1		1		
MW (g/mol)	110.1		32		140.1		18		
MW (mg/umol)	0.1101								
Theoretical COD (g O_2/g catechol)	0.44								
C23O Activity for Ox^- cells	0.0900	umol catechol/mg protein-hr							
	0.0099	mg catechol/mg protein-hr							
	0.0432	mg O2/mg protein-hr							
Assuming zero order reaction	1.718	mg O_2/hr					210	mg VSS/L	
kX	41.22	mg O_2/day					298.2	mg COD/L	
							198.8	mg protein/L	
Mass of TMP applied to system/day	0.44	mg TMP as COD/day							
Oxygenase activity	41.22	mg O_2/day							
Based on analyses, Ox^+ C120 activity is higher than that required for complete oxidation of TMP									

Table II.11. Comparison of TMP mass loading and C23O activity for Ox^- cultures. Data relevant to Sections 4.2.8, 4.2.9 and Table 4.9.

Concentration (mg TMP as COD/L)	1.54	<-- This assumes complete oxidation of TMP to CO_2						
Flowrate (L/day)	0.29							
Mass applied/day (mg TMP as COD/day)	0.44							
For C230 reaction								
	Catechol		Oxygen		2-Hydroxy-*cis*,*cis*-muconate semialdehyde			
	$C_6H_6O_2$	+	O_2	-->	$C_6H_5O_4$	+	H_2O	
Stoichiometry of reaction	1		1.25		1		0.5	
MW (g/mol)	110.1		32		141.1		18	
MW (mg/umol)	0.1101							
Theoretical COD (g O_2/g catechol)	0.36							
C23O Activity for Ox^- cells	4.48E-03	umol catechol/mg protein-hr						
	4.93E-04	mg catechol/mg protein-hr						
	1.79E-04	mg O_2/mg protein-hr						
Assuming zero order reaction	0.07	mg O_2/hr			210	mg VSS/L		
kX	1.71	mg O_2/day			298.2	mg COD/L		
					198.8	mg protein/L		
Mass of TMP applied to system/day	0.44	mg TMP as COD/day						
Oxygenase activity	1.71	mg O_2/day						
Based on analyses, Ox^- C230 activity is higher than that required for complete oxidation of TMP								

Table II.12. Comparison of TMP mass loading and C23O activity for Ox^+ cultures. Data relevant to Sections 4.2.8, 4.2.9 and Table 4.9.

Concentration (mg TMP as COD/L)	1.54	<-- This assumes complete oxidation of TMP to CO_2						
Flowrate (L/day)	0.29							
Mass applied/day (mg TMP as COD/day)	0.44							
For C230 reaction								
	Catechol		Oxygen		2-Hydroxy-*cis*,*cis*-muconate semialdehyde			
	$C_6H_6O_2$	+	O_2	-->	$C_6H_5O_4$	+	H_2O	
Stoichiometry of reaction	1		1.25		1		0.5	
MW (g/mol)	110.1		32		141.1		18	
MW (mg/umol)	0.1101							
Theoretical COD (g O_2/g catechol)	0.36							
C23O Activity for Ox^- cells	0.10	umol catechol/mg protein-hr						
	1.15E-02	mg catechol/mg protein-hr						
	4.19E-03	mg O_2/mg protein-hr						
Assuming zero order reaction	1.66	mg O_2/hr			210	mg VSS/L		
kX	39.94	mg O_2/day			298.2	mg COD/L		
					198.8	mg protein/L		
Mass of TMP applied to system/day	0.44	mg TMP as COD/day						
Oxygenase activity	39.94	mg O_2/day						

Based on analyses, Ox^+ C230 activity is higher than that required for complete oxidation of TMP.

Table II.13. Comparison of TMP mass loading and Tod activity for Ox^+ cultures. Data relevant to Sections 4.2.8, 4.2.9 and Table 4.9.

Concentration (mg TMP as COD/L)	1.54	<-- This assumes complete oxidation of TMP to CO_2					
Flowrate (L/day)	0.29						
Mass applied/day (mg TMP as COD/day)	0.44						
Indole oxidation to indigo							
	Indole		Oxygen		Indigo		
	C_8H_7N	+	O_2	-->	$C_{16}H_{10}N_2O_2$	+	H_2O
Stoichiometry of reaction	2		2		1		2
MW (g/mol)	117.15		32		262.27		18
MW (mg/umol)	0.117				0.262		
Theoretical COD (g O_2/g indigo)	0.55				0.24		
Indigo activity	9.00E-05	mmol indigo/mg protein-hr			Biomass concentration		
	1.05E-05	mg indigo/mg protein-hr			210		mg VSS/L
					298.2		mg COD/L
Convert to indole oxidized	2.11E-05	mg indole oxidized/mg protein-hr			198.8		mg protein/L
	1.15E-05	mg O_2/mg protein-hr					
	2.29E-03	mg O_2/hr					
	5.50E-02	mg O_2/day					
Mass of TMP applied to system/day	0.44	mg TMP as COD/day					
Oxygenase activity	0.05	mg O_2/day					
Based on analyses, Ox^+ Tod activity is lower than that required for complete oxidation of TMP							

Table II.14. Comparison of TMP mass loading and AMO activity for AOB cultures. Data relevant to Section 4.2.9.

Concentration (mg TMP as COD/L)	1.54	<-- This assumes complete oxidation of TMP to CO_2												
Flowrate (L/day)	0.29													
Mass applied/day (mg TMP as COD/day)	0.44													
NH3 oxidation to nitrite (assuming no loss of electrons back to AMO)														
	NH_3	+	O_2	+	H^+	-->	NH_2OH	+	H_2O	-->	NO_2^-	+	H^+	
Stoichiometry of reaction	1		1		2		1		1		1		5	
MW (g/mol)	17		32		1		33		18		46		1	
MW (mg/umol)	0.017													
Theoretical COD (g O_2/g NH_3)	1.88													
Theoretical COD (g O_2/g NH_3-N)	2.29													
sNGR	142	mg NO_2^--N/g biomass as COD-day			Biomass concentration									
					90	mg VSS/L								
Convert to NH_3 oxidized	142	mg NH_3-N/g biomass as COD-day			127.8	mg COD/L								
	325	mg O_2/g COD-day			85.2	mg protein/L								
	41	mg O_2/hr												
Mass of TMP applied to system/day	0.44	mg TMP as COD/day												
Oxygenase activity	41	mg O_2/day												
Based on analyses, AMO activity is high than that required for complete oxidation of TMP														

II-4 Results from biotransformation experiments with Ox^-, Ox^+ and AOB chemostats.

Table II.15. Summary of ^{14}C mass balances on all reactors in this study. Data relevant to Section 4.2.6 to 4.2.9 and Figures 4-5 and 4-6.

	Standalone experiments					Sequential experiments					
	Ox^{-1}	Ox^{-2}	Ox^{-3}	Ox^{+4}	Ox^{+5}	AOB[6]	Ox^{-7}	Ox^{+8}	AOB[9]	Ox^{-10}	Ox^{+11}
Total activity input to experiment (μCi)	7.6	11.3	8.7	10.5	7.2	2.2	0.5	0.5	3.0	0.4	1.4
Total activity in traps (μCi)	4.9	6.7	5.6	6.1	4.0	0.0	0.1	0.2	0.0	0.1	0.4
Total activity in aqueous phase (μCi)	2.1	3.4	1.3	2.8	2.1	2.0	0.2	0.2	2.4	0.3	0.5
Total recovered activity without solids (μCi)	7.0	10.1	6.9	8.9	6.1	2.0	0.3	0.3	2.4	0.4	1.0
Percent recovery without solids (%)	**93**	**90**	**80**	**85**	**84**	**90**	**71**	**71**	**82**	**105**	**69**
Activity in solids (μCi)	0.9	1.8	1.6	1.1	1.1	0.0	0.1	0.1	0.0	0.1	0.2
Total recovered activity with solids (μCi)	8.0	11.9	8.5	10.0	7.1	2.0	0.4	0.4	2.4	0.5	1.1
Percent recovery with solids (%)	**105**	**106**	**98**	**95**	**99**	**90**	**83**	**85**	**82**	**118**	**83**
Percent contribution to total 14C added to experiments: Mineralization (%)	**65**	**60**	**64**	**58**	**55**	**0**	**25**	**33**	**0**	**37**	**30**
Percent contribution to total 14C added to experiments: Solids (%)	**12**	**16**	**18**	**10**	**15**	**0**	**13**	**14**	**0**	**13**	**14**
Percent contribution to total 14C added to experiments: Aqueous (%)	**28**	**30**	**15**	**27**	**29**	**90**	**46**	**38**	**82**	**68**	**39**

[1]Experiment performed in May 2007; [2]Experiment performed in July 2007; [3]Experiment performed in December 2008; [4]Experiment performed in July 2008; [5]Experiment performed in September 2008; [6]Experiment performed in November 2008; [7]Experiment performed in November 2008; [8]Experiment performed in November 2008; [9]Experiment performed in December 2008; [10]Experiment performed in December 2008; [11]Experiment performed in December 2008.

Table II.16. Summary of percent contribution of transformation products in Ox^-, Ox^+ and AOB chemostats.

Date of Sample	Total activity in experiment (uCi)	Total Activity in Effluent (uCi)	Total Activity in Trap (uCi)	Total activity in Solids (uCi)	Total activity recovered (uCi)	% Recovered	Activity in fraction (uCi)					% contribution to overall 14C activity							Avg % recovery
Ox- 1 (Data for Figure 4.5A)																			
							1 (4%)	**2 (3%)**	**3 (90%)**	**U1 (4%)**		**1**	**2**	**3**	**U1**	**CO2**	**Solids**		
4/9/2007	2.3	0.3	1.0	0.2	1.4	61.6	0.01	0.01	0.29	0.01		0.6	0.4	12.5	0.6	41.3	6.5		85.2
4/18/2007	5.3	0.9	2.8	0.5	4.3	80.6	0.04	0.03	0.85	0.04		0.7	0.5	16.0	0.7	52.9	10.0		26.2
4/22/2007	7.0	2.1	4.9	0.9	7.9	113.4	0.08	0.06	1.89	0.08		1.2	0.9	27.1	1.2	70.3	12.9		
											Avg	***0.8***	***0.6***	***18.5***	***0.8***	***54.8***	***9.8***		
											Stdev	***0.3***	***0.3***	***7.6***	***0.3***	***14.6***	***3.2***		
Ox+ 5 (Data for Figure 4.5B)																			
							1 (20%)	**3 (71%)**	**U2 (9%)**			**1**	**3**	**U2**	**CO2**	**Solids**			
9/15/2008	1.8	0.9	0.1	0.3	1.3	70.5	0.19	0.67	0.08			5.9	74.4	8.8	8.8	22.2			88.2
9/22/2008	4.4	2.3	0.5	0.9	3.7	82.6	0.46	1.62	0.21			2.1	26.1	3.1	3.1	21.5			21.1
9/30/2008	7.4	3.5	3.7	1.1	8.3	111.5	0.69	2.46	0.31			3.6	45.7	5.4	5.4	34.7			
											Avg	***3.8***	***48.7***	***5.8***	***5.8***	***26.2***			
											Stdev	***1.9***	***24.3***	***2.9***	***2.9***	***7.4***			
Ne 1 (Data for Figure 4.6A)																			
							1 (4%)	**2 (6%)**	**3 (77%)**	**4 (8%)**	**5 (5%)**	**1**	**2**	**3**	**4**	**5**	**CO2**	**Solids**	
11/6/2008	1.0	0.9			0.9	90.0	0.04	0.06	0.72	0.07	0.05	3.6	5.4	69.3	7.2	4.5	-	-	91.0
11/16/2008	2.5	1.9			1.9	75.9	0.08	0.11	1.47	0.15	0.10	3.0	4.6	58.5	6.1	3.8	-	-	15.6
11/20/2008	3.1	3.3			3.3	107.1	0.13	0.20	2.57	0.27	0.17	4.3	6.4	82.4	8.6	5.4	-	-	
											Avg	***3.6***	***5.5***	***70.1***	***7.3***	***4.5***	-	-	
											Stdev	***0.6***	***0.9***	***12.0***	***1.2***	***0.8***	-	-	
Ox- 10 (Data for Figure 4.6B)																			
							1 (14%)	**2 (13%)**	**3 (73%)**			**1**	**2**	**3**	**CO2**	**Solids**			
11/6/2008	0.1	0.1	0.0	0.0	0.1	83.7	0.01	0.01	0.04			7.5	7.0	39.2	9.2	20.8			79.8
11/16/2008	0.3	0.2	0.0	0.0	0.2	63.1	0.02	0.02	0.12			6.9	6.4	35.8	2.1	11.9			15.1
11/20/2008	0.4	0.2	0.1	0.1	0.4	92.5	0.03	0.03	0.16			7.1	6.6	37.2	27.8	13.9			
											Avg	***7.2***	***6.7***	***37.4***	***13.0***	***15.5***			
											Stdev	***0.3***	***0.3***	***1.7***	***13.2***	***4.7***			
Ox+ 8 (Data for Figure 4.6 C)																			

							1 (6%)	3 (76%)	5 (9%)	U1 (9%)		1	3	5	U1	CO2	Solids		
11/6/2008	0.1	0.1	0.0	0.0	0.1	140.9	0.01	0.07	0.01	0.01		5.9	74.4	8.8	8.8	22.2	20.8		104.5
11/18/2009	0.4	0.1	0.1	0.0	0.3	66.3	0.01	0.10	0.01	0.01		2.1	26.1	3.1	3.1	21.5	10.4		37.3
11/20/2008	0.4	0.3	0.2	0.1	0.5	106.4	0.02	0.20	0.02	0.02		3.6	45.7	5.4	5.4	34.7	11.6		
											Avg	***3.8***	***48.7***	***5.8***	***5.8***	***26.2***	***14.3***		
											Stdev	***1.9***	***24.3***	***2.9***	***2.9***	***7.4***	***5.7***		

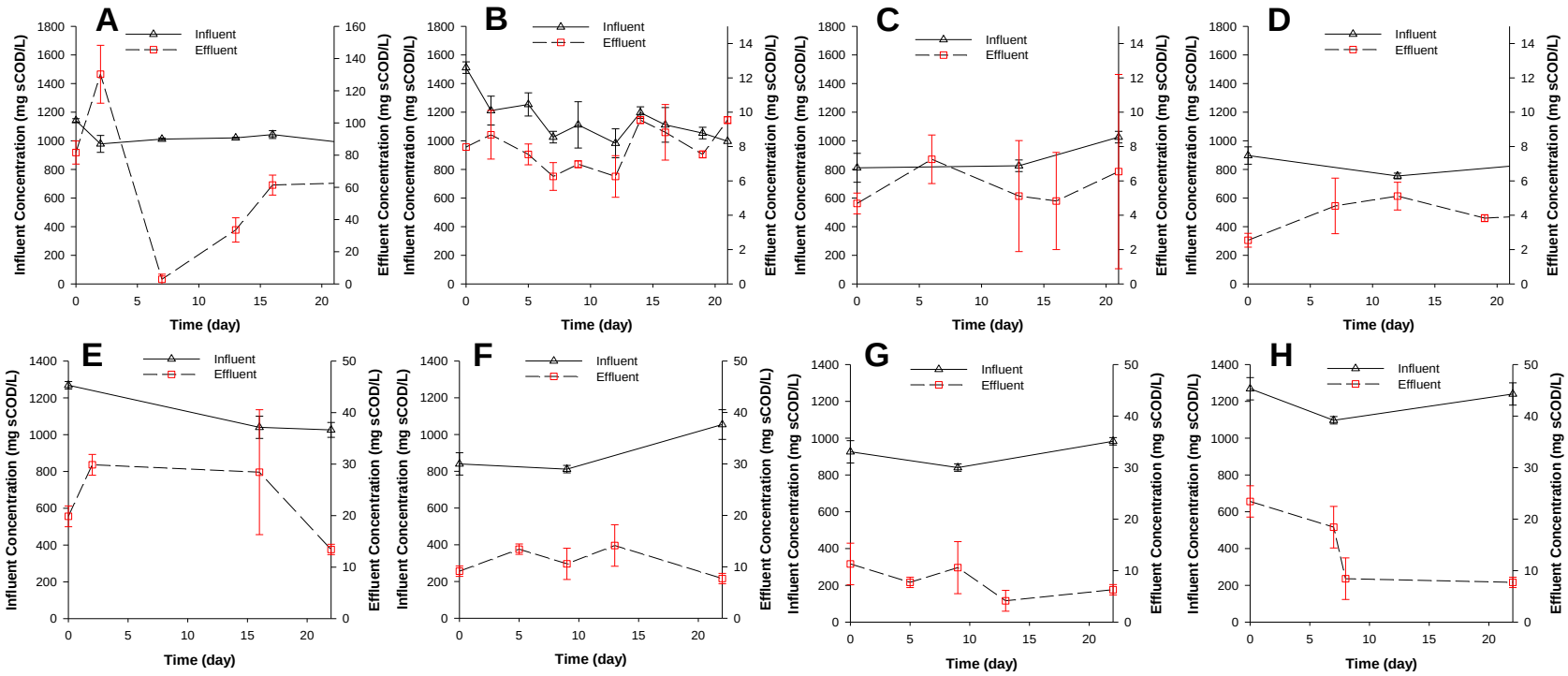

Figure II-2. Soluble COD profile for heterotrophic chemostat reactors from EE2 and TMP experiments. A: Ox^- reactors fed 1000 mg sCOD/L and 1.01 mg EE2/L, B: Ox^- reactors fed 1000 mg sCOD/L and 1 mg TMP/L, C: Ox^+ reactors fed 1000 mg sCOD/L and 1.01 mg EE2/L, D: Ox^+ reactors fed 1000 mg sCOD/L and 1 mg TMP/L, E: Ox^- reactors fed AOB reactor effluent from EE2 experiments supplemented with 1000 mg sCOD/L, E: Ox^- reactors fed AOB reactor effluent from TMP experiments supplemented with 1000 mg sCOD/L, G: Ox^+ reactors fed AOB reactor effluent from EE2 experiments supplemented with 1000 mg sCOD/L, H: Ox^+ reactors fed AOB reactor effluent from TMP experiments supplemented with 1000 mg sCOD/L. Error bars represent the relative mean difference of values obtained from duplicate reactors. Data relevant to Section 4.2.6 to 4.2.9 and Figures 4-5, 4-6, 4-7, 4-9.

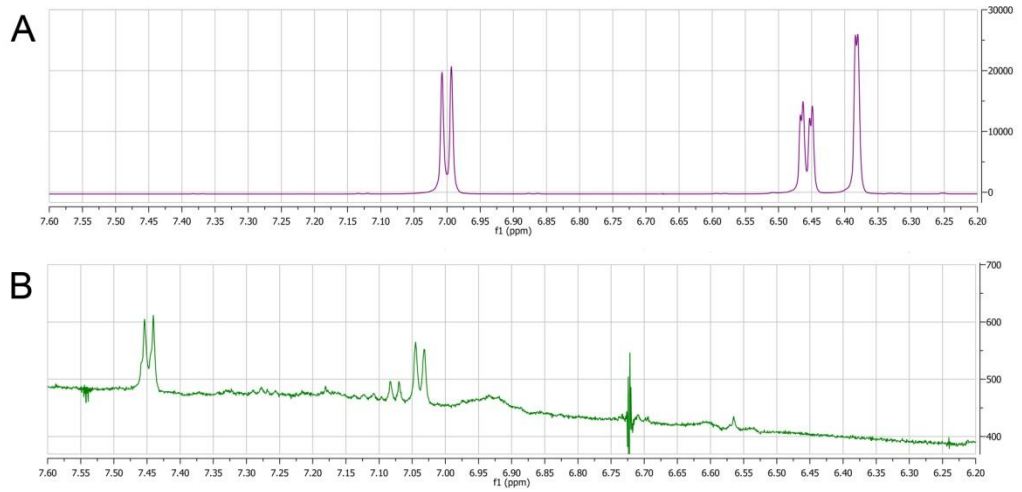

Figure II-3. 1H-NMR spectra of A: EE2 (m/z 295) and B: 4-OH-EE2 (m/z 311). Note doublet in B means that the aromatic protons are adjacent to each other. Data relevant to Section 4.2.6 Figures 4-5 and 4-6.

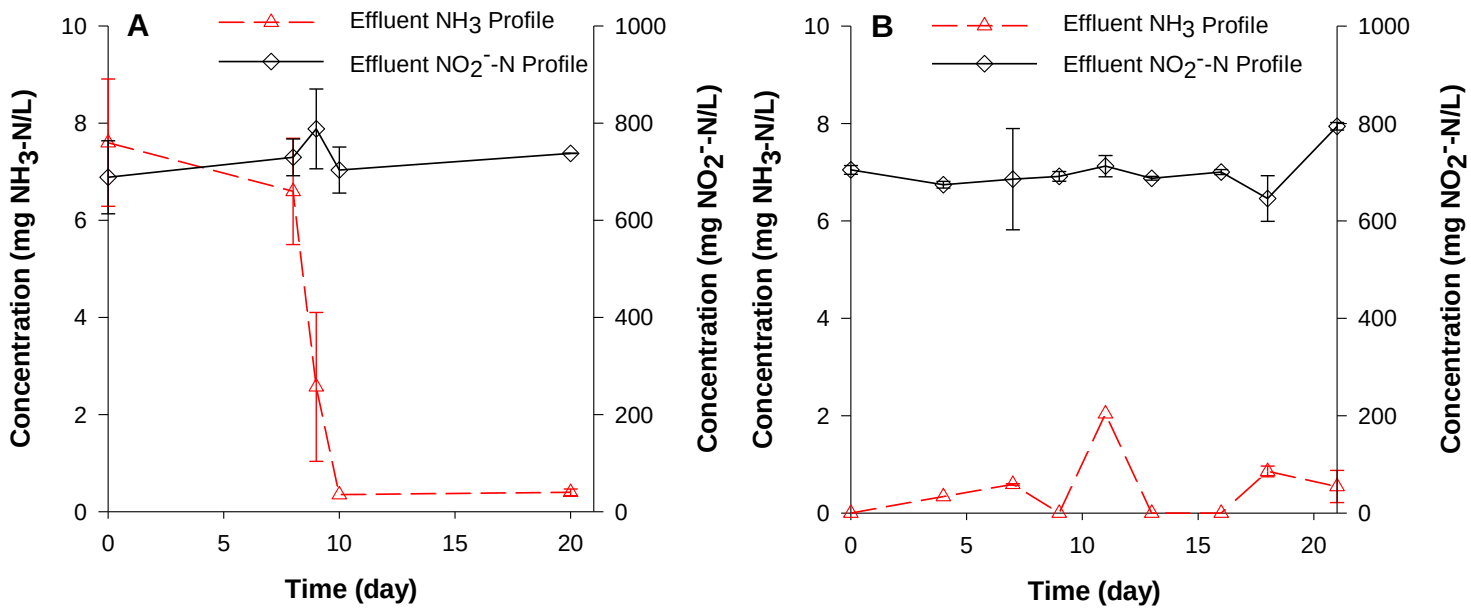

Figure II-4. Nitrogen profiles for AOB chemostats. A: AOB culture fed 1 mg/L EE2, B: AOB culture fed 1 mg/L TMP. Error bars represent the relative mean difference of values obtained from duplicate reactors. Data relevant to Section 4.2.7 and 4.2.9 and Figures 4-6 and 4-9.

II-4-a Estimation of pseudo-first order kinetic parameters.

Table II.17. Results from kinetic experiments with AOB cultures and EE2. Data relevant to Section 4.2.10 and Table 4.11.

Time (hr)	AOB Replicate 1					
	Exp. EE2 (mg EE2/L)	**Exp. EE2 (mg EE2 as COD/L)**	**Model EE2 (mg EE2 as COD/L)**	**Square of diff**	**$Y-Y_{bar}$**	**$(Y-Y_{bar})^2$**
0.0	0.193	0.523	0.523	0.00000	0.089	0.008
0.2	0.169	0.457	0.461	0.00001	0.026	0.001
0.5	0.141	0.383	0.381	0.00001	-0.054	0.003
1.0	0.131	0.356	0.322	0.00112	-0.112	0.013
		0.454 Y_{bar}		**0.000 SSE**		**0.011 SST**
					R^2	**0.998**

Time (hr)	AOB replicate 2					
	Exp. EE2 (mg EE2/L)	**Exp. EE2 (mg EE2 as COD/L)**	**Model EE2 (mg EE2 as COD/L)**	**Square of diff**	**$Y-Y_{bar}$**	**$(Y-Y_{bar})^2$**
0.0	0.247	0.670	0.670	0.00000	0.108	0.012
0.2	0.202	0.547	0.574	0.00072	0.011	0.000
0.5	0.173	0.470	0.454	0.00024	-0.108	0.012
		0.562 Y_{bar}		**0.001 SSE**		**0.023 SST**
					R^2	**0.959**

Table II.18. Results from kinetic experiments with Ox^+ cultures and EE2. Data relevant to Section 4.2.10 and Table 4.11.

Time (hr)	Ox^+ replicate 1					
	Exp. EE2 (mg EE2/L)	**Exp. EE2 (mg EE2 as COD/L)**	**Model EE2 (mg EE2 as COD/L)**	**Square of diff**	**$Y-Y_{bar}$**	**$(Y-Y_{bar})^2$**
0.0	0.250	0.677	0.677	0.00000	0.078	0.006
0.2	0.228	0.617	0.644	0.00074	0.045	0.002
0.5	0.217	0.587	0.586	0.00000	-0.013	0.000
1.0	0.190	0.515	0.506	0.00007	-0.093	0.009
		0.599		**0.001**		**0.017**
		Y_{bar}		**SSE**		**SST**
					R^2	**0.952**
Time (hr)	**Ox^+ replicate 2**					
	Exp. EE2 (mg EE2/L)	**Exp. EE2 (mg EE2 as COD/L)**	**Model EE2 (mg EE2 as COD/L)**	**Square of diff**	**$Y-Y_{bar}$**	**$(Y-Y_{bar})^2$**
0.0	0.281	0.761	0.761	0.00000	0.068	0.005
0.2	0.265	0.718	0.734	0.00024	0.040	0.002
0.5	0.248	0.671	0.682	0.00012	-0.011	0.000
1.0	0.230	0.623	0.612	0.00013	-0.082	0.007
		0.693		**0.000**		**0.013**
		Y_{bar}		**SSE**		**SST**
					R^2	**0.963**

Table II.19. Results from kinetic experiments with Ox^- cultures and EE2. Data relevant to Section 4.2.10 and Table 4.11.

Time (hr)	Ox^- replicate 1					
	Exp. EE2 (mg EE2/L)	**Exp. EE2 (mg EE2 as COD/L)**	**Model EE2 (mg EE2 as COD/L)**	**Square of diff**	**$Y-Y_{bar}$**	**$(Y-Y_{bar})^2$**
0.00	0.219	0.594	0.594	0.000	0.034	0.001
0.17	0.217	0.588	0.588	0.000	0.028	0.001
0.50	0.212	0.573	0.575	0.000	0.015	0.000
1.00	0.203	0.551	0.557	0.000	-0.003	0.000
3.00	0.182	0.492	0.490	0.000	-0.070	0.005
		0.560		**0.000**		**0.007**
		Y_{bar}		**SSE**		**SST**
					R^2	**0.994**
Time (hr)	Ox^- replicate 2					
	Model EE2 (mg EE2 as COD/L)	**Model EE2 (mg EE2 as COD/L)**	**Model EE2 (mg EE2 as COD/L)**	**Square of diff**	**$Y-Y_{bar}$**	**$(Y-Y_{bar})^2$**
0.0	0.250	0.677	0.677	0.00000	0.078	0.006
0.2	0.228	0.617	0.644	0.00073	0.045	0.002
0.5	0.217	0.587	0.585	0.00000	-0.014	0.000
1.0	0.190	0.515	0.506	0.00008	-0.093	0.009
		0.599		**0.001**		**0.017**
		Y_{bar}		**SSE**		**SST**
					R^2	**0.952**

Table II.20. Results from kinetic experiments with AOB and Ox^- mixed culture and EE2. Data relevant to Section 4.2.10 and Table 4.11.

Time (hr)	AOB and Ox^- replicate 1					
	Exp. EE2 (mg EE2/L)	**Exp. EE2 (mg EE2 as COD/L)**	**Model EE2 (mg EE2 as COD/L)**	**Square of diff**	**$Y-Y_{bar}$**	**$(Y-Y_{bar})^2$**
0.0	0.127	0.344	0.344	0.00000	0.344	0.118
0.3	0.120	0.324	0.298	0.00069	0.298	0.089
1.0	0.074	0.201	0.214	0.00017	0.214	0.046
1.5	0.074	0.201	0.168	0.00109	0.168	0.028
3.0	0.023	0.063	0.083	0.00037	0.083	0.007
4.0	0.016	0.044	0.051	0.00005	0.051	0.003
		0.196		**0.002**		**0.291**
		Y_{bar}		**SSE**		**SST**
					R^2	**0.992**

Time (hr)	AOB and Ox^- replicate 2					
	Exp. EE2 (mg EE2/L)	**Exp. EE2 (mg EE2 as COD/L)**	**Model EE2 (mg EE2 as COD/L)**	**Square of diff**	**$Y-Y_{bar}$**	**$(Y-Y_{bar})^2$**
0.0	0.124	0.337	0.337	0.00000	0.337	0.114
0.3	0.102	0.277	0.290	0.00017	0.290	0.084
0.5	0.108	0.293	0.262	0.00098	0.262	0.069
1.0	0.073	0.199	0.204	0.00002	0.204	0.041
1.5	0.061	0.166	0.158	0.00007	0.158	0.025
2	0.039	0.105	0.123	0.00033	0.123	0.015
3	0.029	0.080	0.074	0.00003	0.074	0.006
4	0.016	0.042	0.045	0.00001	0.045	0.002
		0.187		**0.002**		**0.355**
		Y_{bar}		**SSE**		**SST**
					R^2	**0.995**

Table II.21. Results from kinetic experiments with AOB and Ox^+ mixed culture and EE2. Data relevant to Section 4.2.10 and Table 4.11.

Time (hr)	AOB and Ox^+ replicate 1					
	Exp. EE2 (mg EE2/L)	**Exp. EE2 (mg EE2 as COD/L)**	**Model EE2 (mg EE2 as COD/L)**	**Square of diff**	**$Y-Y_{bar}$**	**$(Y-Y_{bar})^2$**
0.0	0.151	0.408	0.408	0.00000	0.408	0.166
0.3	0.123	0.334	0.349	0.00024	0.349	0.122
0.5	0.107	0.290	0.315	0.00064	0.315	0.099
1.0	0.103	0.280	0.243	0.00133	0.243	0.059
1.5	0.068	0.184	0.188	0.00001	0.188	0.035
2	0.046	0.125	0.145	0.00041	0.145	0.021
3	0.036	0.098	0.097	0.00000	0.097	0.009
4	0.025	0.067	0.052	0.00024	0.052	0.003
		0.223		**0.003**		**0.515**
		Y_{bar}		**SSE**		**SST**
					R^2	**0.994**

Time (hr)	AOB and Ox^+ replicate 2					
	Exp. EE2 (mg EE2/L)	**Exp. EE2 (mg EE2 as COD/L)**	**Model EE2 (mg EE2 as COD/L)**	**Square of diff**	**$Y-Y_{bar}$**	**$(Y-Y_{bar})^2$**
0.0	0.152	0.411	0.411	0.00000	0.411	0.169
0.3	0.133	0.359	0.355	0.00002	0.355	0.126
0.5	0.122	0.331	0.322	0.00008	0.322	0.104
1.0	0.090	0.245	0.253	0.00006	0.253	0.064
1.5	0.080	0.216	0.198	0.00032	0.198	0.039
2	0.045	0.123	0.155	0.00103	0.155	0.024
3	0.041	0.112	0.095	0.00027	0.095	0.009
4	0.023	0.062	0.059	0.00001	0.059	0.003
		0.232		**0.002**		**0.538**
		Y_{bar}		**SSE**		**SST**
					R^2	**0.997**

Table II.22. Results from kinetic experiments with Ox^+ culture and TMP. Data relevant to Section 4.2.10 and Table 4.11.

Time (hr)	Ox^+ replicate 1					
	Exp. TMP (mg TMP/L)	Exp. TMP (mg TMP as COD/L)	Model TMP (mg TMP as COD/L)	Square of diff	$Y-Y_{bar}$	$(Y-Y_{bar})^2$
0.00	0.72	1.116	1.116	0.00000	0.036	0.001
2.00	0.70	1.077	1.090	0.00019	0.010	0.000
4.00	0.71	1.087	1.065	0.00048	-0.015	0.000
6.00	0.68	1.040	1.041	0.00000	-0.039	0.002
		1.080		**0.001**		**0.003**
		Y_{bar}		**SSE**		**SST**
					R^2	**0.787**
Time (hr)	**Ox^+ replicate 2**					
	Exp. TMP (mg TMP/L)	**Exp. TMP (mg TMP as COD/L)**	**Model TMP (mg TMP as COD/L)**	**Square of diff**	**$Y-Y_{bar}$**	**$(Y-Y_{bar})^2$**
0.00	0.71	1.098	1.098	0.00000	0.026	0.001
1.00	0.70	1.079	1.077	0.00000	0.005	0.000
4.00	0.70	1.076	1.057	0.00037	-0.015	0.000
6.00	0.67	1.035	1.037	0.00000	-0.035	0.001
		1.072		**0.000**		**0.002**
		Y_{bar}		**SSE**		**SST**
					R^2	**0.822**
Time (hr)	**Ox^+ replicate 3**					
	Exp. TMP (mg TMP/L)	**Exp. TMP (mg TMP as COD/L)**	**Model TMP (mg TMP as COD/L)**	**Square of diff**	**$Y-Y_{bar}$**	**$(Y-Y_{bar})^2$**
0.50	0.72	1.101	1.101	0.00000	0.030	0.001
2.00	0.70	1.077	1.082	0.00002	0.002	0.000
6.00	0.67	1.035	1.033	0.00001	-0.047	0.002
		1.071		**0.000**		**0.003**
		Y_{bar}		**SSE**		**SST**
					R^2	**0.991**

Table II.23. Results from kinetic experiments with Ox^- culture and TMP. Data relevant to Section 4.2.10 and Table 4.11.

Time (hr)	Ox^- replicate 1					
	Exp. TMP	Exp. TMP	Model TMP	Square of diff	$Y-Y_{bar}$	$(Y-Y_{bar})^2$

	(mg TMP/L)	(mg TMP as COD/L)	(mg TMP as COD/L)			
0.00	0.71	1.093	1.093	0.00000	0.081	0.007
2.00	0.66	1.015	1.038	0.00056	0.027	0.001
4.00	0.65	0.999	0.987	0.00015	-0.025	0.001
6.00	0.61	0.941	0.937	0.00001	-0.075	0.006
		1.012		**0.001**		**0.014**
		Y_{bar}		**SSE**		**SST**
					R^2	**0.947**

Time (hr)	**Ox^- replicate 2**					
	Exp. TMP (mg TMP/L)	**Exp. TMP (mg TMP as COD/L)**	**Model TMP (mg TMP as COD/L)**	**Square of diff**	**$Y-Y_{bar}$**	**$(Y-Y_{bar})^2$**
0.00	0.70	1.071	1.071	0.00000	0.065	0.004
0.50	0.67	1.038	1.059	0.00043	0.053	0.003
4.00	0.63	0.976	0.977	0.00000	-0.029	0.001
6.00	0.61	0.938	0.933	0.00002	-0.073	0.005
		1.006		**0.000**		**0.013**
		Y_{bar}		**SSE**		**SST**
					R^2	**0.965**

Time (hr)	**Ox^- replicate 3**					
	Exp. TMP (mg TMP/L)	**Exp. TMP (mg TMP as COD/L)**	**Model TMP (mg TMP as COD/L)**	**Square of diff**	**$Y-Y_{bar}$**	**$(Y-Y_{bar})^2$**
0.00	0.71	1.093	1.093	0.00000	0.086	0.007
0.50	0.67	1.027	1.077	0.00253	0.069	0.005
4.00	0.64	0.990	0.970	0.00042	-0.038	0.001
6.00	0.60	0.919	0.913	0.00004	-0.094	0.009
		1.007		**0.003**		**0.022**
		Y_{bar}		**SSE**		**SST**
					R^2	**0.867**

Matlab code for equation 3-5

```
function [ds] = Monod_1(t,y,flag,qmax,Ks)

S = y(1);
%X =y(2);
ds = zeros(1,1);

%b = 0.24;
%Y = 0.55;
X = 747; %set biomass concentration to experimentally determined value

ds(1) = -(qmax)*(S)*X;
%ds(2) = ((umax*S)/(Ks+S))*X - b*X ;
```

Matlab code for solving equation using 4th order Runge Kutta

```
function [val]=SSE(k)

qmax = k(1);
%Ks =k(2);

t = [0.0
0.3
1.0
1.5
3.0
4.0
 ];

timespan = [t];

Sobs = [0.344
0.324
0.201
0.201
0.063
0.044
 ];

%Xobs = [200.01 200.02 200.02 200.03 200.03 200.05 200.05 200.05 200.06
200.07 200.07 200.06 200.07 200.08 200.09 200.09 200.10]';
y0 = [0.344];
[t ymodel] = ode45('Monod_1',timespan, y0, [], qmax);
resid = ymodel(:,1) - Sobs;
val1 = resid'*resid;
SST = ymodel(:,1)- (mean(Sobs));
val2 = SST'*SST;
val = (val1/val2)
```

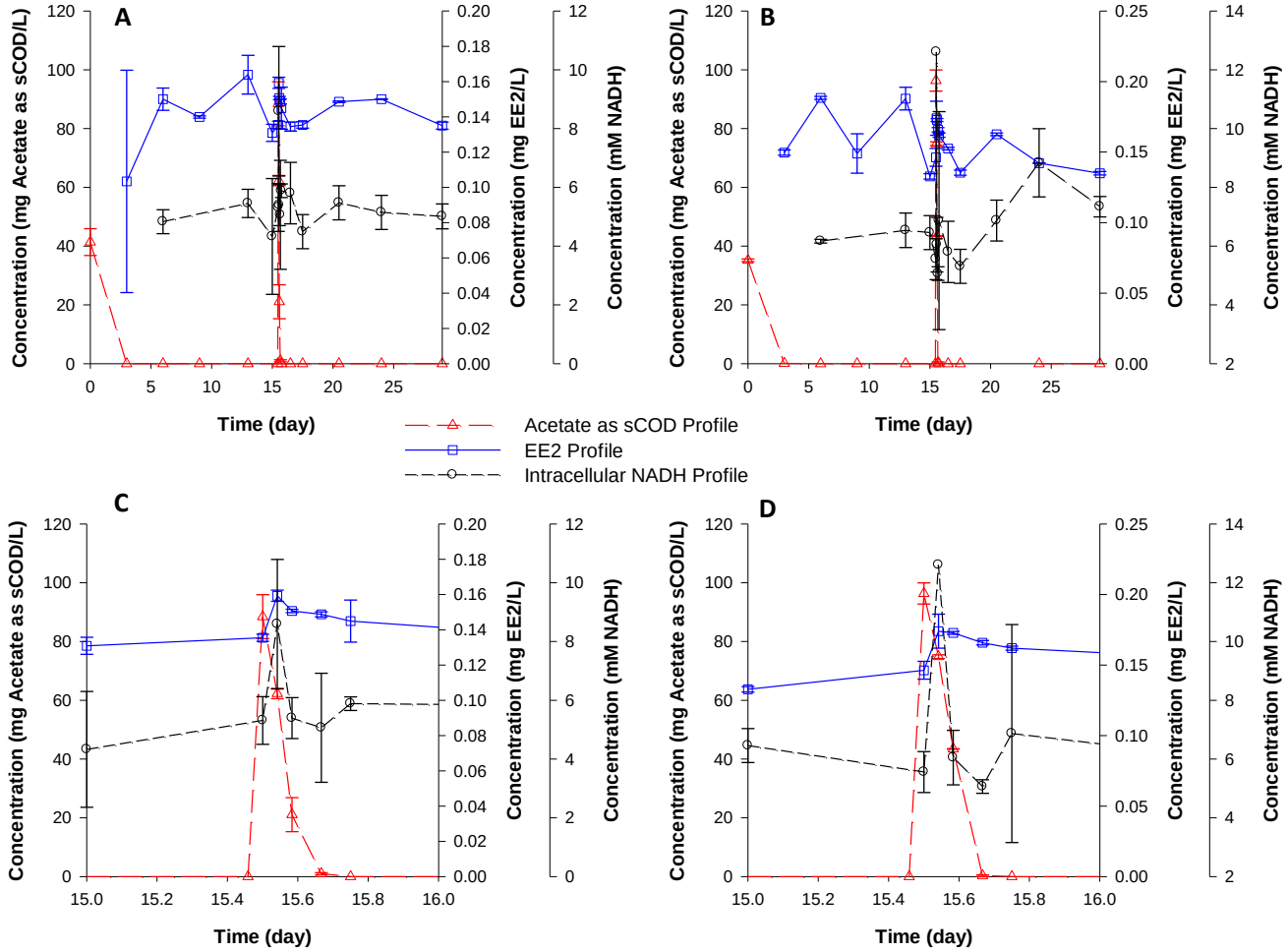

Figure II-5. Impact of rbCOD supplementation on Acetate, EE2 and Intracellular NADH concentrations in Ox^- chemostats. A: Ox^- reactor 1 EE2 profile over 28 days, A: Ox^- reactor 2 EE2 profile over 28 days, C: Ox^- reactor 1 EE2 profile immediately after acetate spike, C: Ox^- reactor 2 EE2 profile immediately after acetate spike. Data relevant to Section 4.3.2 and Figure 4-12.

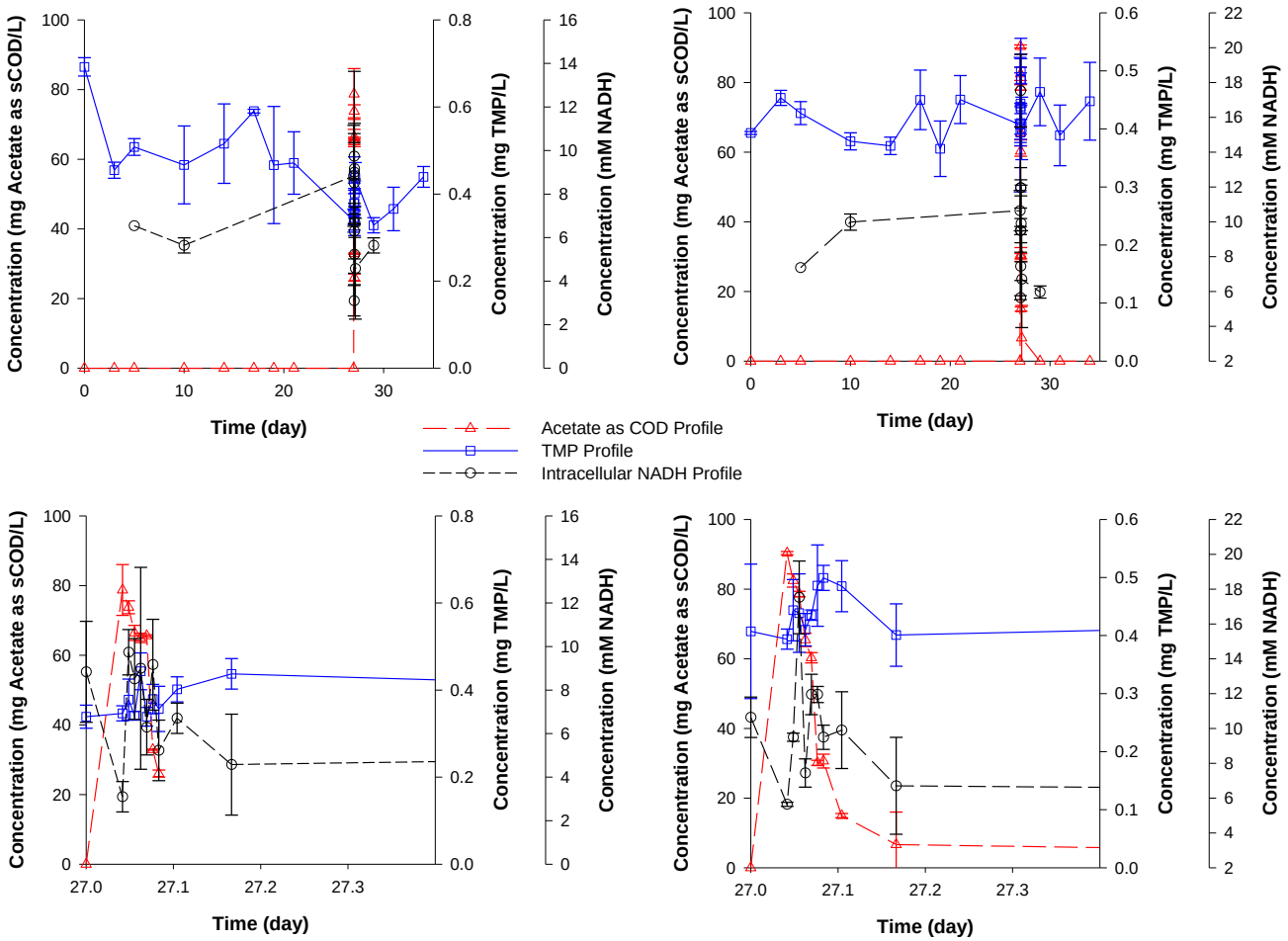

Figure II-6. Impact of rbCOD supplementation on Acetate, TMP and Intracellular NADH concentrations in Ox$^-$ chemostats. A: Ox$^-$ reactor 1 TMP profile over 34 days, B: Ox$^-$ reactor 2 TMP profile immediately 1 TMP profile over 34 days, C: Ox$^-$ reactor 1 TMP profile immediately after acetate spike, D: Ox$^-$ reactor 2 TMP profile immediately after acetate spike. Data relevant to Section 4.3.2 and Figure 4-12.

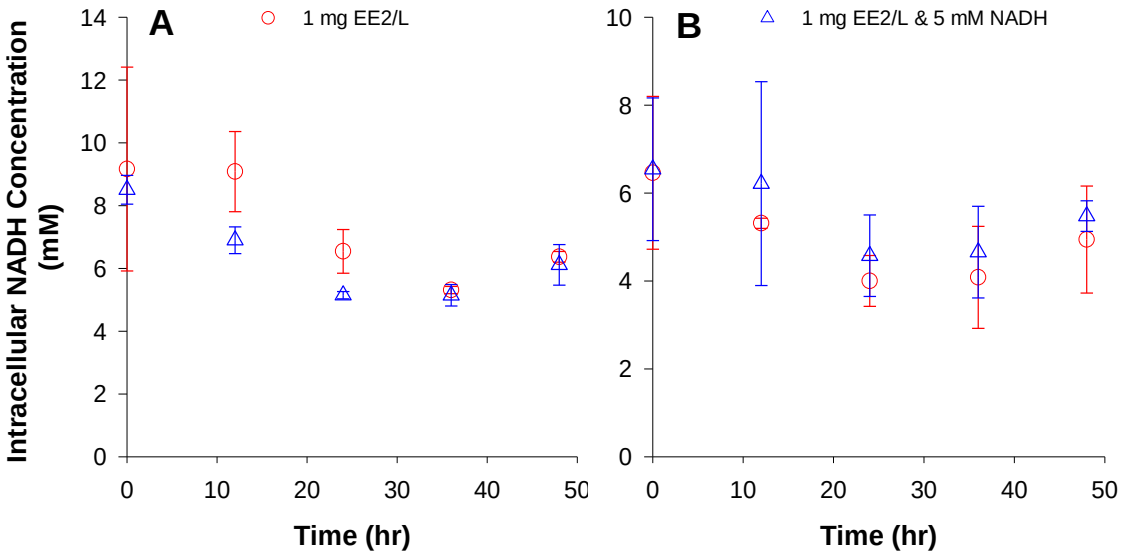

Figure II-7. Intracellular NADH profiles for short-term incubations. A: Ox^- culture, B: Ox^+ culture. Data relevant to Section 4.3.4 and Figure 4-13.

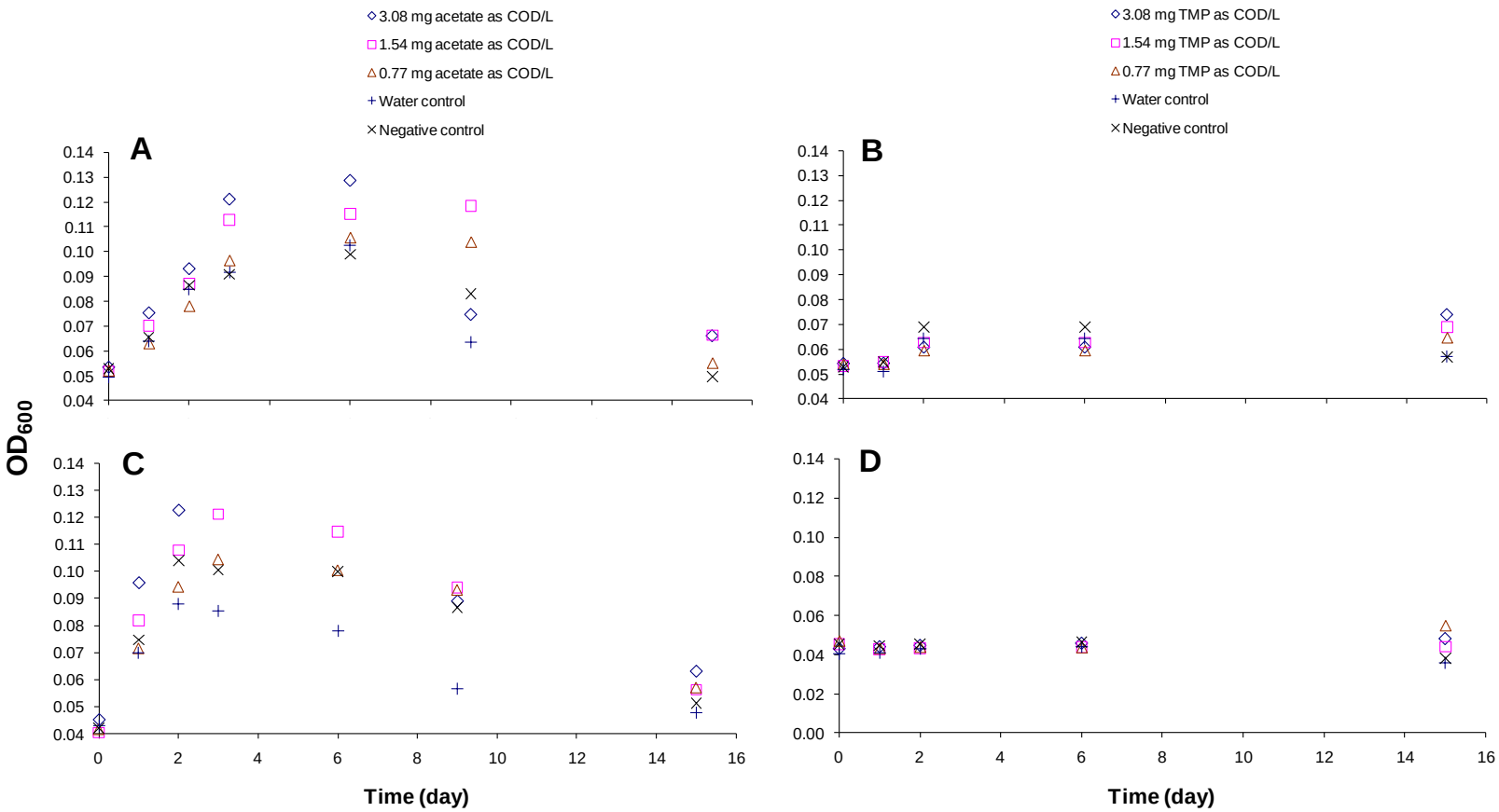

Figure II-8. Growth profile of Ox^- and Ox^+ cells incubated with various concentrations of acetate and TMP. A: Ox^- cells incubated with acetate only, B: Ox^- cells incubated with TMP only, C: Ox^+ cells incubated with acetate only, D: Ox^+ cells incubated with TMP only. Results are calculated from 9 replicates. Data relevant to Section 4.3.5.

II-5 Results from simple kinetic model.

Table II.24. Results from pseudo first order model simulation where sorption of EE2 was the only process considered. Data relevant to Section 4.3.7 and Figure 4-16.

Time (day)	Acetate (mg COD/L)	Model EE2 (mg COD/L)	Time (day)	Avg Exp. EE2 (mg COD/L)	DO (mg/L)	Biomass (mg COD/L)
0.0	1000.00	2.71	5.0		8.00	262.0
0.1	834.77	2.70	8.0	0.343	0.03	306.3
0.2	681.00	2.70	11.0	0.459	0.03	347.3
0.3	529.36	2.69	14.0	0.391	0.03	387.7
0.4	379.86	2.69	18.0	0.477	0.02	427.5
0.5	232.50	2.68	20.0	0.357	0.02	466.7
0.6	87.38	2.67	20.5	0.382	0.02	505.2
0.7	0.27	2.66	21.5	0.452	6.54	522.6
0.8	0.28	2.65	22.5	0.438	6.59	509.7
0.9	0.29	2.64	25.5	0.426	6.61	497.3
1.0	0.29	2.64	27.0	0.416	6.62	485.2
1.1	0.30	2.63	30.0	0.389	6.64	473.6
1.2	0.31	2.62	33.0	0.367	6.66	462.3
1.3	0.32	2.61	35.0	0.422	6.67	451.4
1.4	0.32	2.61	45.0	0.371	6.68	440.9
1.5	0.33	2.60	55.0	0.437	6.70	430.7
1.6	0.34	2.60			6.71	420.8
1.7	0.35	2.59			6.72	411.2
1.8	0.35	2.59			6.74	402.0
1.9	0.36	2.58			6.75	393.1
2.0	0.37	2.58			6.76	384.4
2.1	0.38	2.57			6.77	376.1
2.2	0.39	2.57			6.78	368.0
2.3	0.40	2.56			6.79	360.2
2.4	0.41	2.56			6.80	352.6
2.5	0.41	2.55			6.81	345.3
2.6	0.42	2.55			6.82	338.2
2.7	0.43	2.55			6.83	331.4
2.8	0.44	2.54			6.84	324.8
2.9	0.45	2.54			6.85	318.4
3.0	0.46	2.54			6.86	312.2
3.1	0.47	2.54			6.87	306.2
3.2	0.48	2.53			6.87	300.4
3.3	0.49	2.53			6.88	294.8
3.4	0.50	2.53			6.89	289.4
3.5	0.51	2.53			6.90	284.2
3.6	0.51	2.52			6.90	279.1
3.7	0.52	2.52			6.91	274.2
3.8	0.53	2.52			6.92	269.4
3.9	0.54	2.52			6.92	264.9
4.0	0.55	2.52			6.93	260.4
4.1	0.56	2.51			6.93	256.1
4.2	0.57	2.51			6.94	252.0

4.3	0.58	2.51			6.94	248.0
4.4	0.59	2.51			6.95	244.1
4.5	0.60	2.51			6.96	240.3
4.6	0.61	2.51			6.96	236.7
4.7	0.62	2.51			6.97	233.2
4.8	0.63	2.51			6.97	229.8
4.9	0.64	2.50			6.97	226.5
5.0	0.65	2.50			6.98	223.3
5.1	0.66	2.50			6.98	220.2
5.2	0.67	2.50			6.99	217.2
5.3	0.68	2.50			6.99	214.4
5.4	0.68	2.50			6.99	211.6
5.5	0.69	2.50			7.00	208.9
5.6	0.70	2.50			7.00	206.3
5.7	0.71	2.50			7.01	203.8
5.8	0.72	2.50			7.01	201.3
5.9	0.73	2.50			7.01	199.0
6.0	0.74	2.50			7.01	196.7
6.1	0.75	2.50			7.02	194.5
6.2	0.76	2.50			7.02	192.4
6.3	0.76	2.50			7.03	190.3
6.4	0.77	2.50			7.02	188.3
6.5	0.78	2.50			7.03	186.4
6.6	0.79	2.50			7.03	184.5
6.7	0.80	2.50			7.03	182.7
6.8	0.80	2.50			7.03	181.0
6.9	0.81	2.50			7.04	179.3
7.0	0.82	2.50			7.04	177.6
7.1	0.83	2.50			7.05	176.1
7.2	0.84	2.50			7.05	174.5
7.3	0.84	2.50			7.05	173.0
7.4	0.85	2.50			7.05	171.6
7.5	0.86	2.50			7.05	170.2
7.6	0.87	2.50			7.05	168.9
7.7	0.87	2.50			7.05	167.6
7.8	0.88	2.50			7.06	166.4
7.9	0.88	2.50			7.05	165.1
8.0	0.89	2.50			7.06	164.0
8.1	0.90	2.50			7.06	162.8
8.2	0.90	2.50			7.06	161.7
8.3	0.91	2.50			7.06	160.7
8.4	0.92	2.50			7.06	159.7
8.5	0.92	2.50			7.07	158.7
8.6	0.93	2.50			7.06	157.7
8.7	0.93	2.50			7.06	156.8
8.8	0.94	2.50			7.07	155.9
8.9	0.95	2.50			7.07	155.0
9.0	0.95	2.50			7.07	154.2
9.1	0.96	2.50			7.07	153.4
9.2	0.96	2.50			7.07	152.6

9.3	0.97	2.50			7.08	151.8
9.4	0.97	2.50			7.08	151.1
9.5	0.98	2.50			7.08	150.4
9.6	0.98	2.50			7.08	149.7
9.7	0.99	2.51			7.08	149.0
9.8	0.99	2.51			7.08	148.4
9.9	0.99	2.51			7.08	147.8
10.0	1.00	2.51			7.08	147.2
10.1	1.00	2.51			7.09	146.6
10.2	1.01	2.51			7.08	146.0
10.3	1.01	2.51			7.09	145.5
10.4	1.01	2.51			7.08	145.0
10.5	1.02	2.51			7.08	144.4
10.6	1.02	2.51			7.09	144.0
10.7	1.03	2.51			7.09	143.5
10.8	1.03	2.51			7.09	143.0
10.9	1.03	2.51			7.08	142.6
11.0	1.04	2.51			7.09	142.1
11.1	1.04	2.51			7.09	141.7
11.2	1.04	2.51			7.09	141.3
11.3	1.05	2.51			7.09	140.9
11.4	1.05	2.51			7.09	140.6
11.5	1.05	2.51			7.09	140.2
11.6	1.05	2.51			7.09	139.8
11.7	1.06	2.51			7.09	139.5
11.8	1.06	2.51			7.09	139.2
11.9	1.06	2.52			7.09	138.9
12.0	1.06	2.52			7.09	138.5
12.1	1.07	2.52			7.10	138.2
12.2	1.07	2.52			7.10	138.0
12.3	1.07	2.52			7.09	137.7
12.4	1.07	2.52			7.10	137.4
12.5	1.08	2.52			7.09	137.1
12.6	1.08	2.52			7.10	136.9
12.7	1.08	2.52			7.10	136.7
12.8	1.08	2.52			7.10	136.4
12.9	1.08	2.52			7.10	136.2
13.0	1.09	2.52			7.09	136.0
13.1	1.09	2.52			7.10	135.8
13.2	1.09	2.52			7.10	135.5
13.3	1.09	2.52			7.10	135.3
13.4	1.09	2.52			7.10	135.2
13.5	1.09	2.52			7.10	135.0
13.6	1.10	2.52			7.11	134.8
13.7	1.10	2.52			7.09	134.6
13.8	1.10	2.52			7.10	134.4
13.9	1.10	2.52			7.10	134.3
14.0	1.10	2.52			7.10	134.1
14.1	1.10	2.52			7.10	134.0
14.2	1.10	2.52			7.10	133.8

14.3	1.11	2.53			7.11	133.7
14.4	1.11	2.53			7.10	133.5
14.5	1.11	2.53			7.10	133.4
14.6	1.11	2.53			7.10	133.3
14.7	1.11	2.53			7.10	133.1
14.8	1.11	2.53			7.10	133.0
14.9	1.11	2.53			7.10	132.9
15.0	1.11	2.53			7.10	132.8
15.1	1.11	2.53			7.10	132.7
15.2	1.12	2.53			7.10	132.6
15.3	1.12	2.53			7.10	132.5
15.4	1.12	2.53			7.10	132.4
15.5	1.12	2.53			7.11	132.3
15.6	1.12	2.53			7.10	132.2
15.7	1.12	2.53			7.10	132.1
15.8	1.12	2.53			7.10	132.0
15.9	1.12	2.53			7.10	131.9
16.0	1.12	2.53			7.10	131.8
16.1	1.12	2.53			7.10	131.8
16.2	1.12	2.53			7.11	131.7
16.3	1.12	2.53			7.10	131.6
16.4	1.12	2.53			7.10	131.5
16.5	1.12	2.53			7.10	131.5
16.6	1.13	2.53			7.10	131.4
16.7	1.13	2.53			7.10	131.3
16.8	1.13	2.53			7.10	131.3
16.9	1.13	2.53			7.10	131.2
17.0	1.13	2.53			7.11	131.2
17.1	1.13	2.53			7.10	131.1
17.2	1.13	2.53			7.10	131.1
17.3	1.13	2.53			7.10	131.0
17.4	1.13	2.54			7.10	131.0
17.5	1.13	2.54			7.10	130.9
17.6	1.13	2.54			7.10	130.9
17.7	1.13	2.54			7.11	130.8
17.8	1.13	2.54			7.11	130.8
17.9	1.13	2.54			7.10	130.7
18.0	1.13	2.54			7.10	130.7
18.1	1.13	2.54			7.10	130.6
18.2	1.13	2.54			7.11	130.6
18.3	1.13	2.54			7.10	130.6
18.4	1.13	2.54			7.10	130.5
18.5	1.13	2.54			7.11	130.5
18.6	1.13	2.54			7.10	130.5
18.7	1.13	2.54			7.10	130.4
18.8	1.13	2.54			7.11	130.4
18.9	1.14	2.54			7.11	130.4
19.0	1.14	2.54			7.11	130.3
19.1	1.14	2.54			7.10	130.3
19.2	1.14	2.54			7.11	130.3

19.3	1.14	2.54			7.10	130.3
19.4	1.14	2.54			7.10	130.2
19.5	1.14	2.54			7.10	130.2
19.6	1.14	2.54			7.11	130.2
19.7	1.14	2.54			7.11	130.2
19.8	1.14	2.54			7.10	130.1
19.9	1.14	2.54			7.10	130.1
20.0	1.14	2.54			7.11	130.1
20.1	1.14	2.54			7.11	130.1
20.2	1.14	2.54			7.10	130.0
20.3	1.14	2.54			7.10	130.0
20.4	1.14	2.54			7.11	130.0
20.5	1.14	2.54			7.10	130.0
20.6	1.14	2.54			7.10	130.0
20.7	1.14	2.54			7.11	130.0
20.8	1.14	2.54			7.11	129.9
20.9	1.14	2.54			7.11	129.9
21.0	1.14	2.54			7.10	129.9
48.0	1.14	2.55			7.11	129.5

Table II.25. Results from pseudo first order model simulation where k_{EE2} = 6.22 L/g biomass as COD-day. Data relevant to Section 4.3.7 and Figure 4-16.

Time (day)	Acetate (mg COD/L)	Model EE2 (mg COD/L)	Time (day)	Avg Exp. EE2 (mg COD/L)	DO (mg/L)	Biomass (mg COD/L)
0	1000.00	2.71	5.0		8.00	262.0
0.1	834.77	2.27	8.0	0.343	0.03	306.3
0.2	681.00	1.87	11.0	0.459	0.03	347.3
0.3	529.36	1.50	14.0	0.391	0.03	387.7
0.4	379.86	1.18	18.0	0.477	0.02	427.5
0.5	232.50	0.92	20.0	0.357	0.02	466.7
0.6	87.38	0.70	20.5	0.382	0.02	505.2
0.7	0.27	0.54	21.5	0.452	6.54	522.6
0.8	0.28	0.42	22.5	0.438	6.59	509.7
0.9	0.29	0.34	25.5	0.426	6.61	497.3
1	0.29	0.28	27.0	0.416	6.62	485.2
1.1	0.30	0.24	30.0	0.389	6.64	473.6
1.2	0.31	0.21	33.0	0.367	6.66	462.3
1.3	0.32	0.19	35.0	0.422	6.67	451.4
1.4	0.32	0.18	45.0	0.371	6.68	440.9
1.5	0.33	0.17	55.0	0.437	6.70	430.7
1.6	0.34	0.16			6.71	420.8
1.7	0.35	0.16			6.72	411.2
1.8	0.35	0.15			6.74	402.0
1.9	0.36	0.15			6.75	393.1
2	0.37	0.15			6.76	384.4
2.1	0.38	0.15			6.77	376.1
2.2	0.39	0.16			6.78	368.0
2.3	0.40	0.16			6.79	360.2
2.4	0.41	0.16			6.80	352.6
2.5	0.41	0.16			6.81	345.3
2.6	0.42	0.16			6.82	338.2
2.7	0.43	0.17			6.83	331.4
2.8	0.44	0.17			6.84	324.8
2.9	0.45	0.17			6.85	318.4
3	0.46	0.17			6.86	312.2
3.1	0.47	0.18			6.87	306.2
3.2	0.48	0.18			6.87	300.4
3.3	0.49	0.18			6.88	294.8
3.4	0.50	0.19			6.89	289.4
3.5	0.51	0.19			6.90	284.2
3.6	0.51	0.19			6.90	279.1
3.7	0.52	0.20			6.91	274.2
3.8	0.53	0.20			6.92	269.4
3.9	0.54	0.20			6.92	264.9
4	0.55	0.20			6.93	260.4
4.1	0.56	0.21			6.93	256.1
4.2	0.57	0.21			6.94	252.0
4.3	0.58	0.21			6.94	248.0
4.4	0.59	0.22			6.95	244.1

4.5	0.60	0.22			6.96	240.3
4.6	0.61	0.22			6.96	236.7
4.7	0.62	0.23			6.97	233.2
4.8	0.63	0.23			6.97	229.8
4.9	0.64	0.23			6.97	226.5
5	0.65	0.24			6.98	223.3
5.1	0.66	0.24			6.98	220.2
5.2	0.67	0.24			6.99	217.2
5.3	0.68	0.25			6.99	214.4
5.4	0.68	0.25			6.99	211.6
5.5	0.69	0.25			7.00	208.9
5.6	0.70	0.25			7.00	206.3
5.7	0.71	0.26			7.01	203.8
5.8	0.72	0.26			7.01	201.3
5.9	0.73	0.26			7.01	199.0
6	0.74	0.27			7.01	196.7
6.1	0.75	0.27			7.02	194.5
6.2	0.76	0.27			7.02	192.4
6.3	0.76	0.27			7.03	190.3
6.4	0.77	0.28			7.02	188.3
6.5	0.78	0.28			7.03	186.4
6.6	0.79	0.28			7.03	184.5
6.7	0.80	0.29			7.03	182.7
6.8	0.80	0.29			7.03	181.0
6.9	0.81	0.29			7.04	179.3
7	0.82	0.29			7.04	177.6
7.1	0.83	0.30			7.05	176.1
7.2	0.84	0.30			7.05	174.5
7.3	0.84	0.30			7.05	173.0
7.4	0.85	0.30			7.05	171.6
7.5	0.86	0.31			7.05	170.2
7.6	0.87	0.31			7.05	168.9
7.7	0.87	0.31			7.05	167.6
7.8	0.88	0.31			7.06	166.4
7.9	0.88	0.32			7.05	165.1
8	0.89	0.32			7.06	164.0
8.1	0.90	0.32			7.06	162.8
8.2	0.90	0.32			7.06	161.7
8.3	0.91	0.32			7.06	160.7
8.4	0.92	0.33			7.06	159.7
8.5	0.92	0.33			7.07	158.7
8.6	0.93	0.33			7.06	157.7
8.7	0.93	0.33			7.06	156.8
8.8	0.94	0.33			7.07	155.9
8.9	0.95	0.34			7.07	155.0
9	0.95	0.34			7.07	154.2
9.1	0.96	0.34			7.07	153.4
9.2	0.96	0.34			7.07	152.6
9.3	0.97	0.34			7.08	151.8
9.4	0.97	0.35			7.08	151.1

9.5	0.98	0.35			7.08	150.4
9.6	0.98	0.35			7.08	149.7
9.7	0.99	0.35			7.08	149.0
9.8	0.99	0.35			7.08	148.4
9.9	0.99	0.35			7.08	147.8
10	1.00	0.36			7.08	147.2
10.1	1.00	0.36			7.09	146.6
10.2	1.01	0.36			7.08	146.0
10.3	1.01	0.36			7.09	145.5
10.4	1.01	0.36			7.08	145.0
10.5	1.02	0.36			7.08	144.4
10.6	1.02	0.36			7.09	144.0
10.7	1.03	0.37			7.09	143.5
10.8	1.03	0.37			7.09	143.0
10.9	1.03	0.37			7.08	142.6
11	1.04	0.37			7.09	142.1
11.1	1.04	0.37			7.09	141.7
11.2	1.04	0.37			7.09	141.3
11.3	1.05	0.37			7.09	140.9
11.4	1.05	0.37			7.09	140.6
11.5	1.05	0.38			7.09	140.2
11.6	1.05	0.38			7.09	139.8
11.7	1.06	0.38			7.09	139.5
11.8	1.06	0.38			7.09	139.2
11.9	1.06	0.38			7.09	138.9
12	1.06	0.38			7.09	138.5
12.1	1.07	0.38			7.10	138.2
12.2	1.07	0.38			7.10	138.0
12.3	1.07	0.38			7.09	137.7
12.4	1.07	0.38			7.10	137.4
12.5	1.08	0.39			7.09	137.1
12.6	1.08	0.39			7.10	136.9
12.7	1.08	0.39			7.10	136.7
12.8	1.08	0.39			7.10	136.4
12.9	1.08	0.39			7.10	136.2
13	1.09	0.39			7.09	136.0
13.1	1.09	0.39			7.10	135.8
13.2	1.09	0.39			7.10	135.5
13.3	1.09	0.39			7.10	135.3
13.4	1.09	0.39			7.10	135.2
13.5	1.09	0.39			7.10	135.0
13.6	1.10	0.39			7.11	134.8
13.7	1.10	0.39			7.09	134.6
13.8	1.10	0.39			7.10	134.4
13.9	1.10	0.39			7.10	134.3
14	1.10	0.40			7.10	134.1
14.1	1.10	0.40			7.10	134.0
14.2	1.10	0.40			7.10	133.8
14.3	1.11	0.40			7.11	133.7
14.4	1.11	0.40			7.10	133.5

14.5	1.11	0.40			7.10	133.4
14.6	1.11	0.40			7.10	133.3
14.7	1.11	0.40			7.10	133.1
14.8	1.11	0.40			7.10	133.0
14.9	1.11	0.40			7.10	132.9
15	1.11	0.40			7.10	132.8
15.1	1.11	0.40			7.10	132.7
15.2	1.12	0.40			7.10	132.6
15.3	1.12	0.40			7.10	132.5
15.4	1.12	0.40			7.10	132.4
15.5	1.12	0.40			7.11	132.3
15.6	1.12	0.40			7.10	132.2
15.7	1.12	0.40			7.10	132.1
15.8	1.12	0.40			7.10	132.0
15.9	1.12	0.40			7.10	131.9
16	1.12	0.40			7.10	131.8
16.1	1.12	0.40			7.10	131.8
16.2	1.12	0.40			7.11	131.7
16.3	1.12	0.40			7.10	131.6
16.4	1.12	0.41			7.10	131.5
16.5	1.12	0.41			7.10	131.5
16.6	1.13	0.41			7.10	131.4
16.7	1.13	0.41			7.10	131.3
16.8	1.13	0.41			7.10	131.3
16.9	1.13	0.41			7.10	131.2
17	1.13	0.41			7.11	131.2
17.1	1.13	0.41			7.10	131.1
17.2	1.13	0.41			7.10	131.1
17.3	1.13	0.41			7.10	131.0
17.4	1.13	0.41			7.10	131.0
17.5	1.13	0.41			7.10	130.9
17.6	1.13	0.41			7.10	130.9
17.7	1.13	0.41			7.11	130.8
17.8	1.13	0.41			7.11	130.8
17.9	1.13	0.41			7.10	130.7
18	1.13	0.41			7.10	130.7
18.1	1.13	0.41			7.10	130.6
18.2	1.13	0.41			7.11	130.6
18.3	1.13	0.41			7.10	130.6
18.4	1.13	0.41			7.10	130.5
18.5	1.13	0.41			7.11	130.5
18.6	1.13	0.41			7.10	130.5
18.7	1.13	0.41			7.10	130.4
18.8	1.13	0.41			7.11	130.4
18.9	1.14	0.41			7.11	130.4
19	1.14	0.41			7.11	130.3
19.1	1.14	0.41			7.10	130.3
19.2	1.14	0.41			7.11	130.3
19.3	1.14	0.41			7.10	130.3
19.4	1.14	0.41			7.10	130.2

19.5	1.14	0.41			7.10	130.2
19.6	1.14	0.41			7.11	130.2
19.7	1.14	0.41			7.11	130.2
19.8	1.14	0.41			7.10	130.1
19.9	1.14	0.41			7.10	130.1
20	1.14	0.41			7.11	130.1
20.1	1.14	0.41			7.11	130.1
20.2	1.14	0.41			7.10	130.0
20.3	1.14	0.41			7.10	130.0
20.4	1.14	0.41			7.11	130.0
20.5	1.14	0.41			7.10	130.0
20.6	1.14	0.41			7.10	130.0
20.7	1.14	0.41			7.11	130.0
20.8	1.14	0.41			7.11	129.9
20.9	1.14	0.41			7.11	129.9
21	1.14	0.41			7.10	129.9
48	1.14	0.41			7.11	129.5

Table II.26. Results from pseudo first order model simulation where k_{EE2} = 3.75 L/g biomass as COD-day. Data relevant to Section 4.3.7 and Figure 4-16.

Time (day)	Acetate (mg COD/L)	Model EE2 (mg COD/L)	Time (day)	Avg Exp. EE2 (mg COD/L)	DO (mg/L)	Biomass (mg COD/L)
0	1000.00	2.71	5.0		8.00	262.0
0.1	834.77	2.43	8.0	0.343	0.03	306.3
0.2	681.00	2.15	11.0	0.459	0.03	347.3
0.3	529.36	1.88	14.0	0.391	0.03	387.7
0.4	379.86	1.62	18.0	0.477	0.02	427.5
0.5	232.50	1.38	20.0	0.357	0.02	466.7
0.6	87.38	1.17	20.5	0.382	0.02	505.2
0.7	0.27	0.98	21.5	0.452	6.54	522.6
0.8	0.28	0.83	22.5	0.438	6.59	509.7
0.9	0.29	0.71	25.5	0.426	6.61	497.3
1	0.29	0.61	27.0	0.416	6.62	485.2
1.1	0.30	0.54	30.0	0.389	6.64	473.6
1.2	0.31	0.48	33.0	0.367	6.66	462.3
1.3	0.32	0.43	35.0	0.422	6.67	451.4
1.4	0.32	0.40	45.0	0.371	6.68	440.9
1.5	0.33	0.37	55.0	0.437	6.70	430.7
1.6	0.34	0.34			6.71	420.8
1.7	0.35	0.32			6.72	411.2
1.8	0.35	0.31			6.74	402.0
1.9	0.36	0.30			6.75	393.1
2	0.37	0.29			6.76	384.4
2.1	0.38	0.28			6.77	376.1
2.2	0.39	0.28			6.78	368.0
2.3	0.40	0.27			6.79	360.2
2.4	0.41	0.27			6.80	352.6
2.5	0.41	0.27			6.81	345.3
2.6	0.42	0.27			6.82	338.2
2.7	0.43	0.27			6.83	331.4
2.8	0.44	0.27			6.84	324.8
2.9	0.45	0.27			6.85	318.4
3	0.46	0.28			6.86	312.2
3.1	0.47	0.28			6.87	306.2
3.2	0.48	0.28			6.87	300.4
3.3	0.49	0.28			6.88	294.8
3.4	0.50	0.29			6.89	289.4
3.5	0.51	0.29			6.90	284.2
3.6	0.51	0.29			6.90	279.1
3.7	0.52	0.30			6.91	274.2
3.8	0.53	0.30			6.92	269.4
3.9	0.54	0.30			6.92	264.9
4	0.55	0.31			6.93	260.4
4.1	0.56	0.31			6.93	256.1
4.2	0.57	0.32			6.94	252.0
4.3	0.58	0.32			6.94	248.0
4.4	0.59	0.32			6.95	244.1

4.5	0.60	0.33			6.96	240.3
4.6	0.61	0.33			6.96	236.7
4.7	0.62	0.34			6.97	233.2
4.8	0.63	0.34			6.97	229.8
4.9	0.64	0.35			6.97	226.5
5	0.65	0.35			6.98	223.3
5.1	0.66	0.35			6.98	220.2
5.2	0.67	0.36			6.99	217.2
5.3	0.68	0.36			6.99	214.4
5.4	0.68	0.37			6.99	211.6
5.5	0.69	0.37			7.00	208.9
5.6	0.70	0.37			7.00	206.3
5.7	0.71	0.38			7.01	203.8
5.8	0.72	0.38			7.01	201.3
5.9	0.73	0.39			7.01	199.0
6	0.74	0.39			7.01	196.7
6.1	0.75	0.39			7.02	194.5
6.2	0.76	0.40			7.02	192.4
6.3	0.76	0.40			7.03	190.3
6.4	0.77	0.41			7.02	188.3
6.5	0.78	0.41			7.03	186.4
6.6	0.79	0.41			7.03	184.5
6.7	0.80	0.42			7.03	182.7
6.8	0.80	0.42			7.03	181.0
6.9	0.81	0.43			7.04	179.3
7	0.82	0.43			7.04	177.6
7.1	0.83	0.43			7.05	176.1
7.2	0.84	0.44			7.05	174.5
7.3	0.84	0.44			7.05	173.0
7.4	0.85	0.44			7.05	171.6
7.5	0.86	0.45			7.05	170.2
7.6	0.87	0.45			7.05	168.9
7.7	0.87	0.45			7.05	167.6
7.8	0.88	0.46			7.06	166.4
7.9	0.88	0.46			7.05	165.1
8	0.89	0.46			7.06	164.0
8.1	0.90	0.47			7.06	162.8
8.2	0.90	0.47			7.06	161.7
8.3	0.91	0.47			7.06	160.7
8.4	0.92	0.48			7.06	159.7
8.5	0.92	0.48			7.07	158.7
8.6	0.93	0.48			7.06	157.7
8.7	0.93	0.49			7.06	156.8
8.8	0.94	0.49			7.07	155.9
8.9	0.95	0.49			7.07	155.0
9	0.95	0.49			7.07	154.2
9.1	0.96	0.50			7.07	153.4
9.2	0.96	0.50			7.07	152.6
9.3	0.97	0.50			7.08	151.8
9.4	0.97	0.51			7.08	151.1

9.5	0.98	0.51			7.08	150.4
9.6	0.98	0.51			7.08	149.7
9.7	0.99	0.51			7.08	149.0
9.8	0.99	0.52			7.08	148.4
9.9	0.99	0.52			7.08	147.8
10	1.00	0.52			7.08	147.2
10.1	1.00	0.52			7.09	146.6
10.2	1.01	0.52			7.08	146.0
10.3	1.01	0.53			7.09	145.5
10.4	1.01	0.53			7.08	145.0
10.5	1.02	0.53			7.08	144.4
10.6	1.02	0.53			7.09	144.0
10.7	1.03	0.54			7.09	143.5
10.8	1.03	0.54			7.09	143.0
10.9	1.03	0.54			7.08	142.6
11	1.04	0.54			7.09	142.1
11.1	1.04	0.54			7.09	141.7
11.2	1.04	0.54			7.09	141.3
11.3	1.05	0.55			7.09	140.9
11.4	1.05	0.55			7.09	140.6
11.5	1.05	0.55			7.09	140.2
11.6	1.05	0.55			7.09	139.8
11.7	1.06	0.55			7.09	139.5
11.8	1.06	0.55			7.09	139.2
11.9	1.06	0.56			7.09	138.9
12	1.06	0.56			7.09	138.5
12.1	1.07	0.56			7.10	138.2
12.2	1.07	0.56			7.10	138.0
12.3	1.07	0.56			7.09	137.7
12.4	1.07	0.56			7.10	137.4
12.5	1.08	0.56			7.09	137.1
12.6	1.08	0.57			7.10	136.9
12.7	1.08	0.57			7.10	136.7
12.8	1.08	0.57			7.10	136.4
12.9	1.08	0.57			7.10	136.2
13	1.09	0.57			7.09	136.0
13.1	1.09	0.57			7.10	135.8
13.2	1.09	0.57			7.10	135.5
13.3	1.09	0.57			7.10	135.3
13.4	1.09	0.58			7.10	135.2
13.5	1.09	0.58			7.10	135.0
13.6	1.10	0.58			7.11	134.8
13.7	1.10	0.58			7.09	134.6
13.8	1.10	0.58			7.10	134.4
13.9	1.10	0.58			7.10	134.3
14	1.10	0.58			7.10	134.1
14.1	1.10	0.58			7.10	134.0
14.2	1.10	0.58			7.10	133.8
14.3	1.11	0.58			7.11	133.7
14.4	1.11	0.58			7.10	133.5

14.5	1.11	0.59			7.10	133.4
14.6	1.11	0.59			7.10	133.3
14.7	1.11	0.59			7.10	133.1
14.8	1.11	0.59			7.10	133.0
14.9	1.11	0.59			7.10	132.9
15	1.11	0.59			7.10	132.8
15.1	1.11	0.59			7.10	132.7
15.2	1.12	0.59			7.10	132.6
15.3	1.12	0.59			7.10	132.5
15.4	1.12	0.59			7.10	132.4
15.5	1.12	0.59			7.11	132.3
15.6	1.12	0.59			7.10	132.2
15.7	1.12	0.59			7.10	132.1
15.8	1.12	0.59			7.10	132.0
15.9	1.12	0.59			7.10	131.9
16	1.12	0.59			7.10	131.8
16.1	1.12	0.60			7.10	131.8
16.2	1.12	0.60			7.11	131.7
16.3	1.12	0.60			7.10	131.6
16.4	1.12	0.60			7.10	131.5
16.5	1.12	0.60			7.10	131.5
16.6	1.13	0.60			7.10	131.4
16.7	1.13	0.60			7.10	131.3
16.8	1.13	0.60			7.10	131.3
16.9	1.13	0.60			7.10	131.2
17	1.13	0.60			7.11	131.2
17.1	1.13	0.60			7.10	131.1
17.2	1.13	0.60			7.10	131.1
17.3	1.13	0.60			7.10	131.0
17.4	1.13	0.60			7.10	131.0
17.5	1.13	0.60			7.10	130.9
17.6	1.13	0.60			7.10	130.9
17.7	1.13	0.60			7.11	130.8
17.8	1.13	0.60			7.11	130.8
17.9	1.13	0.60			7.10	130.7
18	1.13	0.60			7.10	130.7
18.1	1.13	0.60			7.10	130.6
18.2	1.13	0.60			7.11	130.6
18.3	1.13	0.60			7.10	130.6
18.4	1.13	0.60			7.10	130.5
18.5	1.13	0.60			7.11	130.5
18.6	1.13	0.60			7.10	130.5
18.7	1.13	0.60			7.10	130.4
18.8	1.13	0.60			7.11	130.4
18.9	1.14	0.60			7.11	130.4
19	1.14	0.61			7.11	130.3
19.1	1.14	0.61			7.10	130.3
19.2	1.14	0.61			7.11	130.3
19.3	1.14	0.61			7.10	130.3
19.4	1.14	0.61			7.10	130.2

19.5	1.14	0.61			7.10	130.2
19.6	1.14	0.61			7.11	130.2
19.7	1.14	0.61			7.11	130.2
19.8	1.14	0.61			7.10	130.1
19.9	1.14	0.61			7.10	130.1
20	1.14	0.61			7.11	130.1
20.1	1.14	0.61			7.11	130.1
20.2	1.14	0.61			7.10	130.0
20.3	1.14	0.61			7.10	130.0
20.4	1.14	0.61			7.11	130.0
20.5	1.14	0.61			7.10	130.0
20.6	1.14	0.61			7.10	130.0
20.7	1.14	0.61			7.11	130.0
20.8	1.14	0.61			7.11	129.9
20.9	1.14	0.61			7.11	129.9
21	1.14	0.61			7.10	129.9
48	1.14	0.61			7.11	129.5

Table II.27. Results from pseudo first order model simulation where k_{EE2} = 3.11 L/g biomass as COD-day. Data relevant to Section 4.3.7 and Figure 4-16.

Time (day)	Acetate (mg COD/L)	Model EE2 (mg COD/L)	Time (day)	Avg Exp. EE2 (mg COD/L)	DO (mg/L)	Biomass (mg COD/L)
0	1000.00	2.71	5.0		8.00	262.0
0.1	834.77	2.48	8.0	0.343	0.03	306.3
0.2	681.00	2.24	11.0	0.459	0.03	347.3
0.3	529.36	2.00	14.0	0.391	0.03	387.7
0.4	379.86	1.77	18.0	0.477	0.02	427.5
0.5	232.50	1.55	20.0	0.357	0.02	466.7
0.6	87.38	1.34	20.5	0.382	0.02	505.2
0.7	0.27	1.16	21.5	0.452	6.54	522.6
0.8	0.28	1.00	22.5	0.438	6.59	509.7
0.9	0.29	0.88	25.5	0.426	6.61	497.3
1	0.29	0.78	27.0	0.416	6.62	485.2
1.1	0.30	0.69	30.0	0.389	6.64	473.6
1.2	0.31	0.63	33.0	0.367	6.66	462.3
1.3	0.32	0.57	35.0	0.422	6.67	451.4
1.4	0.32	0.52	45.0	0.371	6.68	440.9
1.5	0.33	0.49	55.0	0.437	6.70	430.7
1.6	0.34	0.45			6.71	420.8
1.7	0.35	0.43			6.72	411.2
1.8	0.35	0.41			6.74	402.0
1.9	0.36	0.39			6.75	393.1
2	0.37	0.38			6.76	384.4
2.1	0.38	0.37			6.77	376.1
2.2	0.39	0.36			6.78	368.0
2.3	0.40	0.35			6.79	360.2
2.4	0.41	0.34			6.80	352.6
2.5	0.41	0.34			6.81	345.3
2.6	0.42	0.34			6.82	338.2
2.7	0.43	0.34			6.83	331.4
2.8	0.44	0.34			6.84	324.8
2.9	0.45	0.34			6.85	318.4
3	0.46	0.34			6.86	312.2
3.1	0.47	0.34			6.87	306.2
3.2	0.48	0.34			6.87	300.4
3.3	0.49	0.34			6.88	294.8
3.4	0.50	0.34			6.89	289.4
3.5	0.51	0.35			6.90	284.2
3.6	0.51	0.35			6.90	279.1
3.7	0.52	0.35			6.91	274.2
3.8	0.53	0.36			6.92	269.4
3.9	0.54	0.36			6.92	264.9
4	0.55	0.36			6.93	260.4
4.1	0.56	0.37			6.93	256.1
4.2	0.57	0.37			6.94	252.0
4.3	0.58	0.37			6.94	248.0
4.4	0.59	0.38			6.95	244.1

4.5	0.60	0.38			6.96	240.3
4.6	0.61	0.39			6.96	236.7
4.7	0.62	0.39			6.97	233.2
4.8	0.63	0.40			6.97	229.8
4.9	0.64	0.40			6.97	226.5
5	0.65	0.40			6.98	223.3
5.1	0.66	0.41			6.98	220.2
5.2	0.67	0.41			6.99	217.2
5.3	0.68	0.42			6.99	214.4
5.4	0.68	0.42			6.99	211.6
5.5	0.69	0.43			7.00	208.9
5.6	0.70	0.43			7.00	206.3
5.7	0.71	0.44			7.01	203.8
5.8	0.72	0.44			7.01	201.3
5.9	0.73	0.45			7.01	199.0
6	0.74	0.45			7.01	196.7
6.1	0.75	0.45			7.02	194.5
6.2	0.76	0.46			7.02	192.4
6.3	0.76	0.46			7.03	190.3
6.4	0.77	0.47			7.02	188.3
6.5	0.78	0.47			7.03	186.4
6.6	0.79	0.48			7.03	184.5
6.7	0.80	0.48			7.03	182.7
6.8	0.80	0.48			7.03	181.0
6.9	0.81	0.49			7.04	179.3
7	0.82	0.49			7.04	177.6
7.1	0.83	0.50			7.05	176.1
7.2	0.84	0.50			7.05	174.5
7.3	0.84	0.50			7.05	173.0
7.4	0.85	0.51			7.05	171.6
7.5	0.86	0.51			7.05	170.2
7.6	0.87	0.52			7.05	168.9
7.7	0.87	0.52			7.05	167.6
7.8	0.88	0.52			7.06	166.4
7.9	0.88	0.53			7.05	165.1
8	0.89	0.53			7.06	164.0
8.1	0.90	0.54			7.06	162.8
8.2	0.90	0.54			7.06	161.7
8.3	0.91	0.54			7.06	160.7
8.4	0.92	0.55			7.06	159.7
8.5	0.92	0.55			7.07	158.7
8.6	0.93	0.55			7.06	157.7
8.7	0.93	0.56			7.06	156.8
8.8	0.94	0.56			7.07	155.9
8.9	0.95	0.56			7.07	155.0
9	0.95	0.57			7.07	154.2
9.1	0.96	0.57			7.07	153.4
9.2	0.96	0.57			7.07	152.6
9.3	0.97	0.58			7.08	151.8
9.4	0.97	0.58			7.08	151.1

9.5	0.98	0.58			7.08	150.4
9.6	0.98	0.58			7.08	149.7
9.7	0.99	0.59			7.08	149.0
9.8	0.99	0.59			7.08	148.4
9.9	0.99	0.59			7.08	147.8
10	1.00	0.59			7.08	147.2
10.1	1.00	0.60			7.09	146.6
10.2	1.01	0.60			7.08	146.0
10.3	1.01	0.60			7.09	145.5
10.4	1.01	0.60			7.08	145.0
10.5	1.02	0.61			7.08	144.4
10.6	1.02	0.61			7.09	144.0
10.7	1.03	0.61			7.09	143.5
10.8	1.03	0.61			7.09	143.0
10.9	1.03	0.62			7.08	142.6
11	1.04	0.62			7.09	142.1
11.1	1.04	0.62			7.09	141.7
11.2	1.04	0.62			7.09	141.3
11.3	1.05	0.63			7.09	140.9
11.4	1.05	0.63			7.09	140.6
11.5	1.05	0.63			7.09	140.2
11.6	1.05	0.63			7.09	139.8
11.7	1.06	0.63			7.09	139.5
11.8	1.06	0.63			7.09	139.2
11.9	1.06	0.64			7.09	138.9
12	1.06	0.64			7.09	138.5
12.1	1.07	0.64			7.10	138.2
12.2	1.07	0.64			7.10	138.0
12.3	1.07	0.64			7.09	137.7
12.4	1.07	0.64			7.10	137.4
12.5	1.08	0.65			7.09	137.1
12.6	1.08	0.65			7.10	136.9
12.7	1.08	0.65			7.10	136.7
12.8	1.08	0.65			7.10	136.4
12.9	1.08	0.65			7.10	136.2
13	1.09	0.65			7.09	136.0
13.1	1.09	0.66			7.10	135.8
13.2	1.09	0.66			7.10	135.5
13.3	1.09	0.66			7.10	135.3
13.4	1.09	0.66			7.10	135.2
13.5	1.09	0.66			7.10	135.0
13.6	1.10	0.66			7.11	134.8
13.7	1.10	0.66			7.09	134.6
13.8	1.10	0.66			7.10	134.4
13.9	1.10	0.66			7.10	134.3
14	1.10	0.67			7.10	134.1
14.1	1.10	0.67			7.10	134.0
14.2	1.10	0.67			7.10	133.8
14.3	1.11	0.67			7.11	133.7
14.4	1.11	0.67			7.10	133.5

14.5	1.11	0.67			7.10	133.4
14.6	1.11	0.67			7.10	133.3
14.7	1.11	0.67			7.10	133.1
14.8	1.11	0.67			7.10	133.0
14.9	1.11	0.67			7.10	132.9
15	1.11	0.68			7.10	132.8
15.1	1.11	0.68			7.10	132.7
15.2	1.12	0.68			7.10	132.6
15.3	1.12	0.68			7.10	132.5
15.4	1.12	0.68			7.10	132.4
15.5	1.12	0.68			7.11	132.3
15.6	1.12	0.68			7.10	132.2
15.7	1.12	0.68			7.10	132.1
15.8	1.12	0.68			7.10	132.0
15.9	1.12	0.68			7.10	131.9
16	1.12	0.68			7.10	131.8
16.1	1.12	0.68			7.10	131.8
16.2	1.12	0.68			7.11	131.7
16.3	1.12	0.68			7.10	131.6
16.4	1.12	0.68			7.10	131.5
16.5	1.12	0.69			7.10	131.5
16.6	1.13	0.69			7.10	131.4
16.7	1.13	0.69			7.10	131.3
16.8	1.13	0.69			7.10	131.3
16.9	1.13	0.69			7.10	131.2
17	1.13	0.69			7.11	131.2
17.1	1.13	0.69			7.10	131.1
17.2	1.13	0.69			7.10	131.1
17.3	1.13	0.69			7.10	131.0
17.4	1.13	0.69			7.10	131.0
17.5	1.13	0.69			7.10	130.9
17.6	1.13	0.69			7.10	130.9
17.7	1.13	0.69			7.11	130.8
17.8	1.13	0.69			7.11	130.8
17.9	1.13	0.69			7.10	130.7
18	1.13	0.69			7.10	130.7
18.1	1.13	0.69			7.10	130.6
18.2	1.13	0.69			7.11	130.6
18.3	1.13	0.69			7.10	130.6
18.4	1.13	0.69			7.10	130.5
18.5	1.13	0.69			7.11	130.5
18.6	1.13	0.69			7.10	130.5
18.7	1.13	0.69			7.10	130.4
18.8	1.13	0.69			7.11	130.4
18.9	1.14	0.69			7.11	130.4
19	1.14	0.69			7.11	130.3
19.1	1.14	0.69			7.10	130.3
19.2	1.14	0.70			7.11	130.3
19.3	1.14	0.70			7.10	130.3
19.4	1.14	0.70			7.10	130.2

19.5	1.14	0.70			7.10	130.2
19.6	1.14	0.70			7.11	130.2
19.7	1.14	0.70			7.11	130.2
19.8	1.14	0.70			7.10	130.1
19.9	1.14	0.70			7.10	130.1
20	1.14	0.70			7.11	130.1
20.1	1.14	0.70			7.11	130.1
20.2	1.14	0.70			7.10	130.0
20.3	1.14	0.70			7.10	130.0
20.4	1.14	0.70			7.11	130.0
20.5	1.14	0.70			7.10	130.0
20.6	1.14	0.70			7.10	130.0
20.7	1.14	0.70			7.11	130.0
20.8	1.14	0.70			7.11	129.9
20.9	1.14	0.70			7.11	129.9
21	1.14	0.70			7.10	129.9
48	1.14	0.70			7.11	129.5

Table II.28. Results from pseudo first order model simulation where sorption of TMP was the only process considered. Data relevant to Section 4.3.7 and Figure 4-17.

Time (day)	Acetate (mg COD/L)	Model TMP (mg COD/L)	Time (day)	Avg Exp. TMP (mg COD/L)	DO (mg/L)	Biomass (mg COD/L)
0	1000.00	1.54	5	0.835	8.00	262.0
0.1	834.77	1.53	8	0.699	0.03	306.3
0.2	681.00	1.51	10	0.720	0.03	347.3
0.3	529.36	1.49	15	0.651	0.03	387.7
0.4	379.86	1.47	19	0.683	0.02	427.5
0.5	232.50	1.44	22	0.780	0.02	466.7
0.6	87.38	1.41	24	0.641	0.02	505.2
0.7	0.27	1.38	26	0.710	6.54	522.6
0.8	0.28	1.35	32	0.574	6.59	509.7
0.9	0.29	1.32	33	0.570	6.61	497.3
1	0.29	1.30	34	0.633	6.62	485.2
1.1	0.30	1.28	35	0.600	6.64	473.6
1.2	0.31	1.26	36	0.657	6.66	462.3
1.3	0.32	1.24	37	0.596	6.67	451.4
1.4	0.32	1.22	38	0.666	6.68	440.9
1.5	0.33	1.21	39	0.659	6.70	430.7
1.6	0.34	1.19	40	0.683	6.71	420.8
1.7	0.35	1.18	41	0.645	6.72	411.2
1.8	0.35	1.17	42	0.610	6.74	402.0
1.9	0.36	1.16	43	0.581	6.75	393.1
2	0.37	1.15	44	0.683	6.76	384.4
2.1	0.38	1.14			6.77	376.1
2.2	0.39	1.14			6.78	368.0
2.3	0.40	1.13			6.79	360.2
2.4	0.41	1.13			6.80	352.6
2.5	0.41	1.12			6.81	345.3
2.6	0.42	1.12			6.82	338.2
2.7	0.43	1.11			6.83	331.4
2.8	0.44	1.11			6.84	324.8
2.9	0.45	1.11			6.85	318.4
3	0.46	1.11			6.86	312.2
3.1	0.47	1.11			6.87	306.2
3.2	0.48	1.11			6.87	300.4
3.3	0.49	1.11			6.88	294.8
3.4	0.50	1.11			6.89	289.4
3.5	0.51	1.11			6.90	284.2
3.6	0.51	1.11			6.90	279.1
3.7	0.52	1.11			6.91	274.2
3.8	0.53	1.12			6.92	269.4
3.9	0.54	1.12			6.92	264.9
4	0.55	1.12			6.93	260.4
4.1	0.56	1.12			6.93	256.1
4.2	0.57	1.13			6.94	252.0
4.3	0.58	1.13			6.94	248.0
4.4	0.59	1.13			6.95	244.1

4.5	0.60	1.14			6.96	240.3
4.6	0.61	1.14			6.96	236.7
4.7	0.62	1.15			6.97	233.2
4.8	0.63	1.15			6.97	229.8
4.9	0.64	1.15			6.97	226.5
5	0.65	1.16			6.98	223.3
5.1	0.66	1.16			6.98	220.2
5.2	0.67	1.17			6.99	217.2
5.3	0.68	1.17			6.99	214.4
5.4	0.68	1.18			6.99	211.6
5.5	0.69	1.18			7.00	208.9
5.6	0.70	1.19			7.00	206.3
5.7	0.71	1.19			7.01	203.8
5.8	0.72	1.20			7.01	201.3
5.9	0.73	1.20			7.01	199.0
6	0.74	1.21			7.01	196.7
6.1	0.75	1.21			7.02	194.5
6.2	0.76	1.22			7.02	192.4
6.3	0.76	1.22			7.03	190.3
6.4	0.77	1.23			7.02	188.3
6.5	0.78	1.23			7.03	186.4
6.6	0.79	1.24			7.03	184.5
6.7	0.80	1.24			7.03	182.7
6.8	0.80	1.25			7.03	181.0
6.9	0.81	1.26			7.04	179.3
7	0.82	1.26			7.04	177.6
7.1	0.83	1.27			7.05	176.1
7.2	0.84	1.27			7.05	174.5
7.3	0.84	1.28			7.05	173.0
7.4	0.85	1.28			7.05	171.6
7.5	0.86	1.29			7.05	170.2
7.6	0.87	1.29			7.05	168.9
7.7	0.87	1.30			7.05	167.6
7.8	0.88	1.30			7.06	166.4
7.9	0.88	1.31			7.05	165.1
8	0.89	1.31			7.06	164.0
8.1	0.90	1.32			7.06	162.8
8.2	0.90	1.32			7.06	161.7
8.3	0.91	1.33			7.06	160.7
8.4	0.92	1.33			7.06	159.7
8.5	0.92	1.34			7.07	158.7
8.6	0.93	1.34			7.06	157.7
8.7	0.93	1.35			7.06	156.8
8.8	0.94	1.35			7.07	155.9
8.9	0.95	1.36			7.07	155.0
9	0.95	1.36			7.07	154.2
9.1	0.96	1.37			7.07	153.4
9.2	0.96	1.37			7.07	152.6
9.3	0.97	1.38			7.08	151.8
9.4	0.97	1.38			7.08	151.1

9.5	0.98	1.39			7.08	150.4
9.6	0.98	1.39			7.08	149.7
9.7	0.99	1.40			7.08	149.0
9.8	0.99	1.40			7.08	148.4
9.9	0.99	1.41			7.08	147.8
10	1.00	1.41			7.08	147.2
10.1	1.00	1.41			7.09	146.6
10.2	1.01	1.42			7.08	146.0
10.3	1.01	1.42			7.09	145.5
10.4	1.01	1.43			7.08	145.0
10.5	1.02	1.43			7.08	144.4
10.6	1.02	1.44			7.09	144.0
10.7	1.03	1.44			7.09	143.5
10.8	1.03	1.44			7.09	143.0
10.9	1.03	1.45			7.08	142.6
11	1.04	1.45			7.09	142.1
11.1	1.04	1.46			7.09	141.7
11.2	1.04	1.46			7.09	141.3
11.3	1.05	1.46			7.09	140.9
11.4	1.05	1.47			7.09	140.6
11.5	1.05	1.47			7.09	140.2
11.6	1.05	1.47			7.09	139.8
11.7	1.06	1.48			7.09	139.5
11.8	1.06	1.48			7.09	139.2
11.9	1.06	1.48			7.09	138.9
12	1.06	1.49			7.09	138.5
12.1	1.07	1.49			7.10	138.2
12.2	1.07	1.49			7.10	138.0
12.3	1.07	1.50			7.09	137.7
12.4	1.07	1.50			7.10	137.4
12.5	1.08	1.50			7.09	137.1
12.6	1.08	1.51			7.10	136.9
12.7	1.08	1.51			7.10	136.7
12.8	1.08	1.51			7.10	136.4
12.9	1.08	1.52			7.10	136.2
13	1.09	1.52			7.09	136.0
13.1	1.09	1.52			7.10	135.8
13.2	1.09	1.52			7.10	135.5
13.3	1.09	1.53			7.10	135.3
13.4	1.09	1.53			7.10	135.2
13.5	1.09	1.53			7.10	135.0
13.6	1.10	1.54			7.11	134.8
13.7	1.10	1.54			7.09	134.6
13.8	1.10	1.54			7.10	134.4
13.9	1.10	1.54			7.10	134.3
14	1.10	1.55			7.10	134.1
14.1	1.10	1.55			7.10	134.0
14.2	1.10	1.55			7.10	133.8
14.3	1.11	1.55			7.11	133.7
14.4	1.11	1.55			7.10	133.5

14.5	1.11	1.56			7.10	133.4
14.6	1.11	1.56			7.10	133.3
14.7	1.11	1.56			7.10	133.1
14.8	1.11	1.56			7.10	133.0
14.9	1.11	1.57			7.10	132.9
15	1.11	1.57			7.10	132.8
15.1	1.11	1.57			7.10	132.7
15.2	1.12	1.57			7.10	132.6
15.3	1.12	1.57			7.10	132.5
15.4	1.12	1.58			7.10	132.4
15.5	1.12	1.58			7.11	132.3
15.6	1.12	1.58			7.10	132.2
15.7	1.12	1.58			7.10	132.1
15.8	1.12	1.58			7.10	132.0
15.9	1.12	1.58			7.10	131.9
16	1.12	1.59			7.10	131.8
16.1	1.12	1.59			7.10	131.8
16.2	1.12	1.59			7.11	131.7
16.3	1.12	1.59			7.10	131.6
16.4	1.12	1.59			7.10	131.5
16.5	1.12	1.59			7.10	131.5
16.6	1.13	1.60			7.10	131.4
16.7	1.13	1.60			7.10	131.3
16.8	1.13	1.60			7.10	131.3
16.9	1.13	1.60			7.10	131.2
17	1.13	1.60			7.11	131.2
17.1	1.13	1.60			7.10	131.1
17.2	1.13	1.61			7.10	131.1
17.3	1.13	1.61			7.10	131.0
17.4	1.13	1.61			7.10	131.0
17.5	1.13	1.61			7.10	130.9
17.6	1.13	1.61			7.10	130.9
17.7	1.13	1.61			7.11	130.8
17.8	1.13	1.61			7.11	130.8
17.9	1.13	1.61			7.10	130.7
18	1.13	1.62			7.10	130.7
18.1	1.13	1.62			7.10	130.6
18.2	1.13	1.62			7.11	130.6
18.3	1.13	1.62			7.10	130.6
18.4	1.13	1.62			7.10	130.5
18.5	1.13	1.62			7.11	130.5
18.6	1.13	1.62			7.10	130.5
18.7	1.13	1.62			7.10	130.4
18.8	1.13	1.62			7.11	130.4
18.9	1.14	1.63			7.11	130.4
19	1.14	1.63			7.11	130.3
19.1	1.14	1.63			7.10	130.3
19.2	1.14	1.63			7.11	130.3
19.3	1.14	1.63			7.10	130.3
19.4	1.14	1.63			7.10	130.2

19.5	1.14	1.63			7.10	130.2
19.6	1.14	1.63			7.11	130.2
19.7	1.14	1.63			7.11	130.2
19.8	1.14	1.63			7.10	130.1
19.9	1.14	1.63			7.10	130.1
20	1.14	1.63			7.11	130.1
20.1	1.14	1.64			7.11	130.1
20.2	1.14	1.64			7.10	130.0
20.3	1.14	1.64			7.10	130.0
20.4	1.14	1.64			7.11	130.0
20.5	1.14	1.64			7.10	130.0
20.6	1.14	1.64			7.10	130.0
20.7	1.14	1.64			7.11	130.0
20.8	1.14	1.64			7.11	129.9
20.9	1.14	1.64			7.11	129.9
21	1.14	1.64			7.10	129.9
48	1.14	1.67			7.11	129.5

Table II.29. Results from pseudo first order model simulation where k_{TMP} = 2.40 L/g biomass as COD-day. Data relevant to Section 4.3.7 and Figure 4-17.

Time (day)	Acetate (mg COD/L)	Model TMP (mg COD/L)	Time (day)	Avg Exp. TMP (mg COD/L)	DO (mg/L)	Biomass (mg COD/L)
0	1000.00	1.54	5	0.835	8.00	262.0
0.1	834.77	1.43	8	0.699	0.03	306.3
0.2	681.00	1.31	10	0.720	0.03	347.3
0.3	529.36	1.19	15	0.651	0.03	387.7
0.4	379.86	1.07	19	0.683	0.02	427.5
0.5	232.50	0.95	22	0.780	0.02	466.7
0.6	87.38	0.84	24	0.641	0.02	505.2
0.7	0.27	0.74	26	0.710	6.54	522.6
0.8	0.28	0.66	32	0.574	6.59	509.7
0.9	0.29	0.59	33	0.570	6.61	497.3
1	0.29	0.54	34	0.633	6.62	485.2
1.1	0.30	0.49	35	0.600	6.64	473.6
1.2	0.31	0.46	36	0.657	6.66	462.3
1.3	0.32	0.43	37	0.596	6.67	451.4
1.4	0.32	0.40	38	0.666	6.68	440.9
1.5	0.33	0.38	39	0.659	6.70	430.7
1.6	0.34	0.37	40	0.683	6.71	420.8
1.7	0.35	0.36	41	0.645	6.72	411.2
1.8	0.35	0.35	42	0.610	6.74	402.0
1.9	0.36	0.34	43	0.581	6.75	393.1
2	0.37	0.33	44	0.683	6.76	384.4
2.1	0.38	0.33			6.77	376.1
2.2	0.39	0.32			6.78	368.0
2.3	0.40	0.32			6.79	360.2
2.4	0.41	0.32			6.80	352.6
2.5	0.41	0.32			6.81	345.3
2.6	0.42	0.32			6.82	338.2
2.7	0.43	0.32			6.83	331.4
2.8	0.44	0.32			6.84	324.8
2.9	0.45	0.33			6.85	318.4
3	0.46	0.33			6.86	312.2
3.1	0.47	0.33			6.87	306.2
3.2	0.48	0.33			6.87	300.4
3.3	0.49	0.34			6.88	294.8
3.4	0.50	0.34			6.89	289.4
3.5	0.51	0.34			6.90	284.2
3.6	0.51	0.35			6.90	279.1
3.7	0.52	0.35			6.91	274.2
3.8	0.53	0.36			6.92	269.4
3.9	0.54	0.36			6.92	264.9
4	0.55	0.37			6.93	260.4
4.1	0.56	0.37			6.93	256.1
4.2	0.57	0.37			6.94	252.0
4.3	0.58	0.38			6.94	248.0
4.4	0.59	0.38			6.95	244.1

4.5	0.60	0.39			6.96	240.3
4.6	0.61	0.39			6.96	236.7
4.7	0.62	0.40			6.97	233.2
4.8	0.63	0.40			6.97	229.8
4.9	0.64	0.41			6.97	226.5
5	0.65	0.41			6.98	223.3
5.1	0.66	0.42			6.98	220.2
5.2	0.67	0.42			6.99	217.2
5.3	0.68	0.43			6.99	214.4
5.4	0.68	0.43			6.99	211.6
5.5	0.69	0.43			7.00	208.9
5.6	0.70	0.44			7.00	206.3
5.7	0.71	0.44			7.01	203.8
5.8	0.72	0.45			7.01	201.3
5.9	0.73	0.45			7.01	199.0
6	0.74	0.46			7.01	196.7
6.1	0.75	0.46			7.02	194.5
6.2	0.76	0.47			7.02	192.4
6.3	0.76	0.47			7.03	190.3
6.4	0.77	0.48			7.02	188.3
6.5	0.78	0.48			7.03	186.4
6.6	0.79	0.48			7.03	184.5
6.7	0.80	0.49			7.03	182.7
6.8	0.80	0.49			7.03	181.0
6.9	0.81	0.50			7.04	179.3
7	0.82	0.50			7.04	177.6
7.1	0.83	0.51			7.05	176.1
7.2	0.84	0.51			7.05	174.5
7.3	0.84	0.51			7.05	173.0
7.4	0.85	0.52			7.05	171.6
7.5	0.86	0.52			7.05	170.2
7.6	0.87	0.53			7.05	168.9
7.7	0.87	0.53			7.05	167.6
7.8	0.88	0.53			7.06	166.4
7.9	0.88	0.54			7.05	165.1
8	0.89	0.54			7.06	164.0
8.1	0.90	0.55			7.06	162.8
8.2	0.90	0.55			7.06	161.7
8.3	0.91	0.55			7.06	160.7
8.4	0.92	0.56			7.06	159.7
8.5	0.92	0.56			7.07	158.7
8.6	0.93	0.56			7.06	157.7
8.7	0.93	0.57			7.06	156.8
8.8	0.94	0.57			7.07	155.9
8.9	0.95	0.57			7.07	155.0
9	0.95	0.58			7.07	154.2
9.1	0.96	0.58			7.07	153.4
9.2	0.96	0.58			7.07	152.6
9.3	0.97	0.59			7.08	151.8
9.4	0.97	0.59			7.08	151.1

9.5	0.98	0.59			7.08	150.4
9.6	0.98	0.60			7.08	149.7
9.7	0.99	0.60			7.08	149.0
9.8	0.99	0.60			7.08	148.4
9.9	0.99	0.60			7.08	147.8
10	1.00	0.61			7.08	147.2
10.1	1.00	0.61			7.09	146.6
10.2	1.01	0.61			7.08	146.0
10.3	1.01	0.61			7.09	145.5
10.4	1.01	0.62			7.08	145.0
10.5	1.02	0.62			7.08	144.4
10.6	1.02	0.62			7.09	144.0
10.7	1.03	0.62			7.09	143.5
10.8	1.03	0.63			7.09	143.0
10.9	1.03	0.63			7.08	142.6
11	1.04	0.63			7.09	142.1
11.1	1.04	0.63			7.09	141.7
11.2	1.04	0.64			7.09	141.3
11.3	1.05	0.64			7.09	140.9
11.4	1.05	0.64			7.09	140.6
11.5	1.05	0.64			7.09	140.2
11.6	1.05	0.64			7.09	139.8
11.7	1.06	0.65			7.09	139.5
11.8	1.06	0.65			7.09	139.2
11.9	1.06	0.65			7.09	138.9
12	1.06	0.65			7.09	138.5
12.1	1.07	0.65			7.10	138.2
12.2	1.07	0.65			7.10	138.0
12.3	1.07	0.66			7.09	137.7
12.4	1.07	0.66			7.10	137.4
12.5	1.08	0.66			7.09	137.1
12.6	1.08	0.66			7.10	136.9
12.7	1.08	0.66			7.10	136.7
12.8	1.08	0.66			7.10	136.4
12.9	1.08	0.67			7.10	136.2
13	1.09	0.67			7.09	136.0
13.1	1.09	0.67			7.10	135.8
13.2	1.09	0.67			7.10	135.5
13.3	1.09	0.67			7.10	135.3
13.4	1.09	0.67			7.10	135.2
13.5	1.09	0.67			7.10	135.0
13.6	1.10	0.67			7.11	134.8
13.7	1.10	0.68			7.09	134.6
13.8	1.10	0.68			7.10	134.4
13.9	1.10	0.68			7.10	134.3
14	1.10	0.68			7.10	134.1
14.1	1.10	0.68			7.10	134.0
14.2	1.10	0.68			7.10	133.8
14.3	1.11	0.68			7.11	133.7
14.4	1.11	0.68			7.10	133.5

14.5	1.11	0.68			7.10	133.4
14.6	1.11	0.69			7.10	133.3
14.7	1.11	0.69			7.10	133.1
14.8	1.11	0.69			7.10	133.0
14.9	1.11	0.69			7.10	132.9
15	1.11	0.69			7.10	132.8
15.1	1.11	0.69			7.10	132.7
15.2	1.12	0.69			7.10	132.6
15.3	1.12	0.69			7.10	132.5
15.4	1.12	0.69			7.10	132.4
15.5	1.12	0.69			7.11	132.3
15.6	1.12	0.69			7.10	132.2
15.7	1.12	0.69			7.10	132.1
15.8	1.12	0.69			7.10	132.0
15.9	1.12	0.70			7.10	131.9
16	1.12	0.70			7.10	131.8
16.1	1.12	0.70			7.10	131.8
16.2	1.12	0.70			7.11	131.7
16.3	1.12	0.70			7.10	131.6
16.4	1.12	0.70			7.10	131.5
16.5	1.12	0.70			7.10	131.5
16.6	1.13	0.70			7.10	131.4
16.7	1.13	0.70			7.10	131.3
16.8	1.13	0.70			7.10	131.3
16.9	1.13	0.70			7.10	131.2
17	1.13	0.70			7.11	131.2
17.1	1.13	0.70			7.10	131.1
17.2	1.13	0.70			7.10	131.1
17.3	1.13	0.70			7.10	131.0
17.4	1.13	0.70			7.10	131.0
17.5	1.13	0.70			7.10	130.9
17.6	1.13	0.70			7.10	130.9
17.7	1.13	0.70			7.11	130.8
17.8	1.13	0.70			7.11	130.8
17.9	1.13	0.71			7.10	130.7
18	1.13	0.71			7.10	130.7
18.1	1.13	0.71			7.10	130.6
18.2	1.13	0.71			7.11	130.6
18.3	1.13	0.71			7.10	130.6
18.4	1.13	0.71			7.10	130.5
18.5	1.13	0.71			7.11	130.5
18.6	1.13	0.71			7.10	130.5
18.7	1.13	0.71			7.10	130.4
18.8	1.13	0.71			7.11	130.4
18.9	1.14	0.71			7.11	130.4
19	1.14	0.71			7.11	130.3
19.1	1.14	0.71			7.10	130.3
19.2	1.14	0.71			7.11	130.3
19.3	1.14	0.71			7.10	130.3
19.4	1.14	0.71			7.10	130.2

19.5	1.14	0.71			7.10	130.2
19.6	1.14	0.71			7.11	130.2
19.7	1.14	0.71			7.11	130.2
19.8	1.14	0.71			7.10	130.1
19.9	1.14	0.71			7.10	130.1
20	1.14	0.71			7.11	130.1
20.1	1.14	0.71			7.11	130.1
20.2	1.14	0.71			7.10	130.0
20.3	1.14	0.71			7.10	130.0
20.4	1.14	0.71			7.11	130.0
20.5	1.14	0.71			7.10	130.0
20.6	1.14	0.71			7.10	130.0
20.7	1.14	0.71			7.11	130.0
20.8	1.14	0.71			7.11	129.9
20.9	1.14	0.71			7.11	129.9
21	1.14	0.71			7.10	129.9
48	1.14	0.72			7.11	129.5

Table II.30. Results from pseudo first order model simulation where k_{TMP} = 1.20 L/g biomass as COD-day. Data relevant to Section 4.3.7 and Figure 4-17.

Time (day)	Acetate (mg COD/L)	Model TMP (mg COD/L)	Time (day)	Avg Exp. TMP (mg COD/L)	DO (mg/L)	Biomass (mg COD/L)
0	1000.00	1.54	5	0.835	8.00	262.0
0.1	834.77	1.48	8	0.699	0.03	306.3
0.2	681.00	1.41	10	0.720	0.03	347.3
0.3	529.36	1.33	15	0.651	0.03	387.7
0.4	379.86	1.25	19	0.683	0.02	427.5
0.5	232.50	1.17	22	0.780	0.02	466.7
0.6	87.38	1.09	24	0.641	0.02	505.2
0.7	0.27	1.01	26	0.710	6.54	522.6
0.8	0.28	0.94	32	0.574	6.59	509.7
0.9	0.29	0.88	33	0.570	6.61	497.3
1	0.29	0.83	34	0.633	6.62	485.2
1.1	0.30	0.78	35	0.600	6.64	473.6
1.2	0.31	0.74	36	0.657	6.66	462.3
1.3	0.32	0.71	37	0.596	6.67	451.4
1.4	0.32	0.68	38	0.666	6.68	440.9
1.5	0.33	0.65	39	0.659	6.70	430.7
1.6	0.34	0.63	40	0.683	6.71	420.8
1.7	0.35	0.61	41	0.645	6.72	411.2
1.8	0.35	0.60	42	0.610	6.74	402.0
1.9	0.36	0.58	43	0.581	6.75	393.1
2	0.37	0.57	44	0.683	6.76	384.4
2.1	0.38	0.56			6.77	376.1
2.2	0.39	0.55			6.78	368.0
2.3	0.40	0.55			6.79	360.2
2.4	0.41	0.54			6.80	352.6
2.5	0.41	0.54			6.81	345.3
2.6	0.42	0.53			6.82	338.2
2.7	0.43	0.53			6.83	331.4
2.8	0.44	0.53			6.84	324.8
2.9	0.45	0.53			6.85	318.4
3	0.46	0.53			6.86	312.2
3.1	0.47	0.53			6.87	306.2
3.2	0.48	0.53			6.87	300.4
3.3	0.49	0.53			6.88	294.8
3.4	0.50	0.53			6.89	289.4
3.5	0.51	0.54			6.90	284.2
3.6	0.51	0.54			6.90	279.1
3.7	0.52	0.54			6.91	274.2
3.8	0.53	0.54			6.92	269.4
3.9	0.54	0.55			6.92	264.9
4	0.55	0.55			6.93	260.4
4.1	0.56	0.56			6.93	256.1
4.2	0.57	0.56			6.94	252.0
4.3	0.58	0.56			6.94	248.0
4.4	0.59	0.57			6.95	244.1

4.5	0.60	0.57			6.96	240.3
4.6	0.61	0.58			6.96	236.7
4.7	0.62	0.58			6.97	233.2
4.8	0.63	0.59			6.97	229.8
4.9	0.64	0.59			6.97	226.5
5	0.65	0.60			6.98	223.3
5.1	0.66	0.60			6.98	220.2
5.2	0.67	0.61			6.99	217.2
5.3	0.68	0.61			6.99	214.4
5.4	0.68	0.62			6.99	211.6
5.5	0.69	0.62			7.00	208.9
5.6	0.70	0.63			7.00	206.3
5.7	0.71	0.64			7.01	203.8
5.8	0.72	0.64			7.01	201.3
5.9	0.73	0.65			7.01	199.0
6	0.74	0.65			7.01	196.7
6.1	0.75	0.66			7.02	194.5
6.2	0.76	0.66			7.02	192.4
6.3	0.76	0.67			7.03	190.3
6.4	0.77	0.67			7.02	188.3
6.5	0.78	0.68			7.03	186.4
6.6	0.79	0.68			7.03	184.5
6.7	0.80	0.69			7.03	182.7
6.8	0.80	0.69			7.03	181.0
6.9	0.81	0.70			7.04	179.3
7	0.82	0.70			7.04	177.6
7.1	0.83	0.71			7.05	176.1
7.2	0.84	0.72			7.05	174.5
7.3	0.84	0.72			7.05	173.0
7.4	0.85	0.73			7.05	171.6
7.5	0.86	0.73			7.05	170.2
7.6	0.87	0.74			7.05	168.9
7.7	0.87	0.74			7.05	167.6
7.8	0.88	0.75			7.06	166.4
7.9	0.88	0.75			7.05	165.1
8	0.89	0.75			7.06	164.0
8.1	0.90	0.76			7.06	162.8
8.2	0.90	0.76			7.06	161.7
8.3	0.91	0.77			7.06	160.7
8.4	0.92	0.77			7.06	159.7
8.5	0.92	0.78			7.07	158.7
8.6	0.93	0.78			7.06	157.7
8.7	0.93	0.79			7.06	156.8
8.8	0.94	0.79			7.07	155.9
8.9	0.95	0.80			7.07	155.0
9	0.95	0.80			7.07	154.2
9.1	0.96	0.80			7.07	153.4
9.2	0.96	0.81			7.07	152.6
9.3	0.97	0.81			7.08	151.8
9.4	0.97	0.82			7.08	151.1

9.5	0.98	0.82			7.08	150.4
9.6	0.98	0.82			7.08	149.7
9.7	0.99	0.83			7.08	149.0
9.8	0.99	0.83			7.08	148.4
9.9	0.99	0.83			7.08	147.8
10	1.00	0.84			7.08	147.2
10.1	1.00	0.84			7.09	146.6
10.2	1.01	0.85			7.08	146.0
10.3	1.01	0.85			7.09	145.5
10.4	1.01	0.85			7.08	145.0
10.5	1.02	0.86			7.08	144.4
10.6	1.02	0.86			7.09	144.0
10.7	1.03	0.86			7.09	143.5
10.8	1.03	0.87			7.09	143.0
10.9	1.03	0.87			7.08	142.6
11	1.04	0.87			7.09	142.1
11.1	1.04	0.87			7.09	141.7
11.2	1.04	0.88			7.09	141.3
11.3	1.05	0.88			7.09	140.9
11.4	1.05	0.88			7.09	140.6
11.5	1.05	0.89			7.09	140.2
11.6	1.05	0.89			7.09	139.8
11.7	1.06	0.89			7.09	139.5
11.8	1.06	0.89			7.09	139.2
11.9	1.06	0.90			7.09	138.9
12	1.06	0.90			7.09	138.5
12.1	1.07	0.90			7.10	138.2
12.2	1.07	0.90			7.10	138.0
12.3	1.07	0.91			7.09	137.7
12.4	1.07	0.91			7.10	137.4
12.5	1.08	0.91			7.09	137.1
12.6	1.08	0.91			7.10	136.9
12.7	1.08	0.92			7.10	136.7
12.8	1.08	0.92			7.10	136.4
12.9	1.08	0.92			7.10	136.2
13	1.09	0.92			7.09	136.0
13.1	1.09	0.92			7.10	135.8
13.2	1.09	0.93			7.10	135.5
13.3	1.09	0.93			7.10	135.3
13.4	1.09	0.93			7.10	135.2
13.5	1.09	0.93			7.10	135.0
13.6	1.10	0.93			7.11	134.8
13.7	1.10	0.94			7.09	134.6
13.8	1.10	0.94			7.10	134.4
13.9	1.10	0.94			7.10	134.3
14	1.10	0.94			7.10	134.1
14.1	1.10	0.94			7.10	134.0
14.2	1.10	0.94			7.10	133.8
14.3	1.11	0.95			7.11	133.7
14.4	1.11	0.95			7.10	133.5

14.5	1.11	0.95			7.10	133.4
14.6	1.11	0.95			7.10	133.3
14.7	1.11	0.95			7.10	133.1
14.8	1.11	0.95			7.10	133.0
14.9	1.11	0.95			7.10	132.9
15	1.11	0.95			7.10	132.8
15.1	1.11	0.96			7.10	132.7
15.2	1.12	0.96			7.10	132.6
15.3	1.12	0.96			7.10	132.5
15.4	1.12	0.96			7.10	132.4
15.5	1.12	0.96			7.11	132.3
15.6	1.12	0.96			7.10	132.2
15.7	1.12	0.96			7.10	132.1
15.8	1.12	0.96			7.10	132.0
15.9	1.12	0.97			7.10	131.9
16	1.12	0.97			7.10	131.8
16.1	1.12	0.97			7.10	131.8
16.2	1.12	0.97			7.11	131.7
16.3	1.12	0.97			7.10	131.6
16.4	1.12	0.97			7.10	131.5
16.5	1.12	0.97			7.10	131.5
16.6	1.13	0.97			7.10	131.4
16.7	1.13	0.97			7.10	131.3
16.8	1.13	0.97			7.10	131.3
16.9	1.13	0.97			7.10	131.2
17	1.13	0.98			7.11	131.2
17.1	1.13	0.98			7.10	131.1
17.2	1.13	0.98			7.10	131.1
17.3	1.13	0.98			7.10	131.0
17.4	1.13	0.98			7.10	131.0
17.5	1.13	0.98			7.10	130.9
17.6	1.13	0.98			7.10	130.9
17.7	1.13	0.98			7.11	130.8
17.8	1.13	0.98			7.11	130.8
17.9	1.13	0.98			7.10	130.7
18	1.13	0.98			7.10	130.7
18.1	1.13	0.98			7.10	130.6
18.2	1.13	0.98			7.11	130.6
18.3	1.13	0.98			7.10	130.6
18.4	1.13	0.98			7.10	130.5
18.5	1.13	0.99			7.11	130.5
18.6	1.13	0.99			7.10	130.5
18.7	1.13	0.99			7.10	130.4
18.8	1.13	0.99			7.11	130.4
18.9	1.14	0.99			7.11	130.4
19	1.14	0.99			7.11	130.3
19.1	1.14	0.99			7.10	130.3
19.2	1.14	0.99			7.11	130.3
19.3	1.14	0.99			7.10	130.3
19.4	1.14	0.99			7.10	130.2

19.5	1.14	0.99			7.10	130.2
19.6	1.14	0.99			7.11	130.2
19.7	1.14	0.99			7.11	130.2
19.8	1.14	0.99			7.10	130.1
19.9	1.14	0.99			7.10	130.1
20	1.14	0.99			7.11	130.1
20.1	1.14	0.99			7.11	130.1
20.2	1.14	0.99			7.10	130.0
20.3	1.14	0.99			7.10	130.0
20.4	1.14	0.99			7.11	130.0
20.5	1.14	0.99			7.10	130.0
20.6	1.14	0.99			7.10	130.0
20.7	1.14	0.99			7.11	130.0
20.8	1.14	0.99			7.11	129.9
20.9	1.14	0.99			7.11	129.9
21	1.14	0.99			7.10	129.9
48	1.14	1.00			7.11	129.5

Table II.31. Results from zero order model simulation where k_{EE2} = 2.6 mg EE2/g biomass as COD-day. Data relevant to Section 4.3.7.

Time (day)	Acetate (mg COD/L)	Model EE2 (mg COD/L)	Time (day)	Avg Exp. EE2 (mg COD/L)	DO (mg/L)	Biomass (mg COD/L)
0	1000.00	2.710	5		8.00	262.0
0.1	834.77	2.631	8	0.343	0.03	306.3
0.2	681.00	2.542	11	0.459	0.03	347.3
0.3	529.36	2.444	14	0.391	0.03	387.7
0.4	379.86	2.336	18	0.477	0.02	427.5
0.5	232.50	2.219	20	0.357	0.02	466.7
0.6	87.38	2.093	21	0.382	0.02	505.2
0.7	0.27	1.961	22	0.452	6.54	522.6
0.8	0.28	1.832	23	0.438	6.59	509.7
0.9	0.29	1.708	26	0.426	6.61	497.3
1	0.29	1.590	27	0.416	6.62	485.2
1.1	0.30	1.478	30	0.389	6.64	473.6
1.2	0.31	1.370	33	0.367	6.66	462.3
1.3	0.32	1.267	35	0.422	6.67	451.4
1.4	0.32	1.169	45	0.371	6.68	440.9
1.5	0.33	1.075	55	0.437	6.70	430.7
1.6	0.34	0.986			6.71	420.8
1.7	0.35	0.901			6.72	411.2
1.8	0.35	0.819			6.74	402.0
1.9	0.36	0.741			6.75	393.1
2	0.37	0.667			6.76	384.4
2.1	0.38	0.597			6.77	376.1
2.2	0.39	0.530			6.78	368.0
2.3	0.40	0.466			6.79	360.2
2.4	0.41	0.405			6.80	352.6
2.5	0.41	0.347			6.81	345.3
2.6	0.42	0.291			6.82	338.2
2.7	0.43	0.239			6.83	331.4
2.8	0.44	0.189			6.84	324.8
2.9	0.45	0.142			6.85	318.4
3	0.46	0.097			6.86	312.2
3.1	0.47	0.054			6.87	306.2
3.2	0.48	0.014			6.87	300.4
3.3	0.49	-0.024			6.88	294.8
3.4	0.50	-0.061			6.89	289.4
3.5	0.51	-0.095			6.90	284.2
3.6	0.51	-0.127			6.90	279.1
3.7	0.52	-0.158			6.91	274.2
3.8	0.53	-0.187			6.92	269.4
3.9	0.54	-0.214			6.92	264.9
4	0.55	-0.239			6.93	260.4
4.1	0.56	-0.263			6.93	256.1
4.2	0.57	-0.286			6.94	252.0
4.3	0.58	-0.307			6.94	248.0
4.4	0.59	-0.327			6.95	244.1

4.5	0.60	-0.346			6.96	240.3
4.6	0.61	-0.363			6.96	236.7
4.7	0.62	-0.379			6.97	233.2
4.8	0.63	-0.394			6.97	229.8
4.9	0.64	-0.408			6.97	226.5
5	0.65	-0.421			6.98	223.3
5.1	0.66	-0.433			6.98	220.2
5.2	0.67	-0.443			6.99	217.2
5.3	0.68	-0.453			6.99	214.4
5.4	0.68	-0.463			6.99	211.6
5.5	0.69	-0.471			7.00	208.9
5.6	0.70	-0.478			7.00	206.3
5.7	0.71	-0.485			7.01	203.8
5.8	0.72	-0.491			7.01	201.3
5.9	0.73	-0.496			7.01	199.0
6	0.74	-0.501			7.01	196.7
6.1	0.75	-0.505			7.02	194.5
6.2	0.76	-0.508			7.02	192.4
6.3	0.76	-0.511			7.03	190.3
6.4	0.77	-0.513			7.02	188.3
6.5	0.78	-0.514			7.03	186.4
6.6	0.79	-0.516			7.03	184.5
6.7	0.80	-0.516			7.03	182.7
6.8	0.80	-0.516			7.03	181.0
6.9	0.81	-0.516			7.04	179.3
7	0.82	-0.515			7.04	177.6
7.1	0.83	-0.514			7.05	176.1
7.2	0.84	-0.513			7.05	174.5
7.3	0.84	-0.511			7.05	173.0
7.4	0.85	-0.509			7.05	171.6
7.5	0.86	-0.506			7.05	170.2
7.6	0.87	-0.504			7.05	168.9
7.7	0.87	-0.501			7.05	167.6
7.8	0.88	-0.497			7.06	166.4
7.9	0.88	-0.494			7.05	165.1
8	0.89	-0.490			7.06	164.0
8.1	0.90	-0.486			7.06	162.8
8.2	0.90	-0.481			7.06	161.7
8.3	0.91	-0.477			7.06	160.7
8.4	0.92	-0.472			7.06	159.7
8.5	0.92	-0.467			7.07	158.7
8.6	0.93	-0.462			7.06	157.7
8.7	0.93	-0.457			7.06	156.8
8.8	0.94	-0.451			7.07	155.9
8.9	0.95	-0.446			7.07	155.0
9	0.95	-0.440			7.07	154.2
9.1	0.96	-0.434			7.07	153.4
9.2	0.96	-0.428			7.07	152.6
9.3	0.97	-0.422			7.08	151.8
9.4	0.97	-0.416			7.08	151.1

9.5	0.98	-0.410			7.08	150.4
9.6	0.98	-0.404			7.08	149.7
9.7	0.99	-0.397			7.08	149.0
9.8	0.99	-0.391			7.08	148.4
9.9	0.99	-0.385			7.08	147.8
10	1.00	-0.378			7.08	147.2
10.1	1.00	-0.371			7.09	146.6
10.2	1.01	-0.365			7.08	146.0
10.3	1.01	-0.358			7.09	145.5
10.4	1.01	-0.351			7.08	145.0
10.5	1.02	-0.345			7.08	144.4
10.6	1.02	-0.338			7.09	144.0
10.7	1.03	-0.331			7.09	143.5
10.8	1.03	-0.324			7.09	143.0
10.9	1.03	-0.317			7.08	142.6
11	1.04	-0.311			7.09	142.1
11.1	1.04	-0.304			7.09	141.7
11.2	1.04	-0.297			7.09	141.3
11.3	1.05	-0.290			7.09	140.9
11.4	1.05	-0.283			7.09	140.6
11.5	1.05	-0.276			7.09	140.2
11.6	1.05	-0.270			7.09	139.8
11.7	1.06	-0.263			7.09	139.5
11.8	1.06	-0.256			7.09	139.2
11.9	1.06	-0.249			7.09	138.9
12	1.06	-0.242			7.09	138.5
12.1	1.07	-0.236			7.10	138.2
12.2	1.07	-0.229			7.10	138.0
12.3	1.07	-0.222			7.09	137.7
12.4	1.07	-0.216			7.10	137.4
12.5	1.08	-0.209			7.09	137.1
12.6	1.08	-0.203			7.10	136.9
12.7	1.08	-0.196			7.10	136.7
12.8	1.08	-0.190			7.10	136.4
12.9	1.08	-0.183			7.10	136.2
13	1.09	-0.177			7.09	136.0
13.1	1.09	-0.170			7.10	135.8
13.2	1.09	-0.164			7.10	135.5
13.3	1.09	-0.158			7.10	135.3
13.4	1.09	-0.152			7.10	135.2
13.5	1.09	-0.145			7.10	135.0
13.6	1.10	-0.139			7.11	134.8
13.7	1.10	-0.133			7.09	134.6
13.8	1.10	-0.127			7.10	134.4
13.9	1.10	-0.121			7.10	134.3
14	1.10	-0.115			7.10	134.1
14.1	1.10	-0.109			7.10	134.0
14.2	1.10	-0.103			7.10	133.8
14.3	1.11	-0.098			7.11	133.7
14.4	1.11	-0.092			7.10	133.5

14.5	1.11	-0.086			7.10	133.4
14.6	1.11	-0.081			7.10	133.3
14.7	1.11	-0.075			7.10	133.1
14.8	1.11	-0.070			7.10	133.0
14.9	1.11	-0.064			7.10	132.9
15	1.11	-0.059			7.10	132.8
15.1	1.11	-0.053			7.10	132.7
15.2	1.12	-0.048			7.10	132.6
15.3	1.12	-0.043			7.10	132.5
15.4	1.12	-0.037			7.10	132.4
15.5	1.12	-0.032			7.11	132.3
15.6	1.12	-0.027			7.10	132.2
15.7	1.12	-0.022			7.10	132.1
15.8	1.12	-0.017			7.10	132.0
15.9	1.12	-0.012			7.10	131.9
16	1.12	-0.007			7.10	131.8
16.1	1.12	-0.003			7.10	131.8
16.2	1.12	0.002			7.11	131.7
16.3	1.12	0.007			7.10	131.6
16.4	1.12	0.012			7.10	131.5
16.5	1.12	0.016			7.10	131.5
16.6	1.13	0.021			7.10	131.4
16.7	1.13	0.025			7.10	131.3
16.8	1.13	0.030			7.10	131.3
16.9	1.13	0.034			7.10	131.2
17	1.13	0.039			7.11	131.2
17.1	1.13	0.043			7.10	131.1
17.2	1.13	0.047			7.10	131.1
17.3	1.13	0.051			7.10	131.0
17.4	1.13	0.055			7.10	131.0
17.5	1.13	0.060			7.10	130.9
17.6	1.13	0.064			7.10	130.9
17.7	1.13	0.068			7.11	130.8
17.8	1.13	0.072			7.11	130.8
17.9	1.13	0.076			7.10	130.7
18	1.13	0.079			7.10	130.7
18.1	1.13	0.083			7.10	130.6
18.2	1.13	0.087			7.11	130.6
18.3	1.13	0.091			7.10	130.6
18.4	1.13	0.094			7.10	130.5
18.5	1.13	0.098			7.11	130.5
18.6	1.13	0.102			7.10	130.5
18.7	1.13	0.105			7.10	130.4
18.8	1.13	0.109			7.11	130.4
18.9	1.14	0.112			7.11	130.4
19	1.14	0.115			7.11	130.3
19.1	1.14	0.119			7.10	130.3
19.2	1.14	0.122			7.11	130.3
19.3	1.14	0.125			7.10	130.3
19.4	1.14	0.129			7.10	130.2

19.5	1.14	0.132			7.10	130.2
19.6	1.14	0.135			7.11	130.2
19.7	1.14	0.138			7.11	130.2
19.8	1.14	0.141			7.10	130.1
19.9	1.14	0.144			7.10	130.1
20	1.14	0.147			7.11	130.1
20.1	1.14	0.150			7.11	130.1
20.2	1.14	0.153			7.10	130.0
20.3	1.14	0.156			7.10	130.0
20.4	1.14	0.159			7.11	130.0
20.5	1.14	0.161			7.10	130.0
20.6	1.14	0.164			7.10	130.0
20.7	1.14	0.167			7.11	130.0
20.8	1.14	0.169			7.11	129.9
20.9	1.14	0.172			7.11	129.9
21	1.14	0.175			7.10	129.9
48	1.14	0.348			7.11	129.5

Table II.32. Results from zero order model simulation where k_{TMP} = 10 mg TMP/g biomass as COD-day. Data relevant to Section 4.3.7.

Time (day)	Acetate (mg COD/L)	Model TMP (mg COD/L)	Time (day)	Avg Exp. TMP (mg COD/L)	DO (mg/L)	Biomass (mg COD/L)
0	1000.00	1.540	5	0.835	8.00	262.0
0.1	834.77	1.499	8	0.699	0.03	306.3
0.2	681.00	1.450	10	0.720	0.03	347.3
0.3	529.36	1.396	15	0.651	0.03	387.7
0.4	379.86	1.336	19	0.683	0.02	427.5
0.5	232.50	1.271	22	0.780	0.02	466.7
0.6	87.38	1.202	24	0.641	0.02	505.2
0.7	0.27	1.131	26	0.710	6.54	522.6
0.8	0.28	1.063	32	0.574	6.59	509.7
0.9	0.29	1.001	33	0.570	6.61	497.3
1	0.29	0.944	34	0.633	6.62	485.2
1.1	0.30	0.892	35	0.600	6.64	473.6
1.2	0.31	0.843	36	0.657	6.66	462.3
1.3	0.32	0.799	37	0.596	6.67	451.4
1.4	0.32	0.758	38	0.666	6.68	440.9
1.5	0.33	0.721	39	0.659	6.70	430.7
1.6	0.34	0.686	40	0.683	6.71	420.8
1.7	0.35	0.655	41	0.645	6.72	411.2
1.8	0.35	0.626	42	0.610	6.74	402.0
1.9	0.36	0.600	43	0.581	6.75	393.1
2	0.37	0.575	44	0.683	6.76	384.4
2.1	0.38	0.553			6.77	376.1
2.2	0.39	0.533			6.78	368.0
2.3	0.40	0.515			6.79	360.2
2.4	0.41	0.499			6.80	352.6
2.5	0.41	0.484			6.81	345.3
2.6	0.42	0.471			6.82	338.2
2.7	0.43	0.459			6.83	331.4
2.8	0.44	0.448			6.84	324.8
2.9	0.45	0.439			6.85	318.4
3	0.46	0.431			6.86	312.2
3.1	0.47	0.424			6.87	306.2
3.2	0.48	0.417			6.87	300.4
3.3	0.49	0.412			6.88	294.8
3.4	0.50	0.408			6.89	289.4
3.5	0.51	0.404			6.90	284.2
3.6	0.51	0.401			6.90	279.1
3.7	0.52	0.399			6.91	274.2
3.8	0.53	0.398			6.92	269.4
3.9	0.54	0.397			6.92	264.9
4	0.55	0.397			6.93	260.4
4.1	0.56	0.397			6.93	256.1
4.2	0.57	0.398			6.94	252.0
4.3	0.58	0.400			6.94	248.0
4.4	0.59	0.402			6.95	244.1
4.5	0.60	0.404			6.96	240.3

4.6	0.61	0.407			6.96	236.7
4.7	0.62	0.410			6.97	233.2
4.8	0.63	0.413			6.97	229.8
4.9	0.64	0.417			6.97	226.5
5	0.65	0.421			6.98	223.3
5.1	0.66	0.425			6.98	220.2
5.2	0.67	0.429			6.99	217.2
5.3	0.68	0.434			6.99	214.4
5.4	0.68	0.439			6.99	211.6
5.5	0.69	0.444			7.00	208.9
5.6	0.70	0.450			7.00	206.3
5.7	0.71	0.455			7.01	203.8
5.8	0.72	0.461			7.01	201.3
5.9	0.73	0.467			7.01	199.0
6	0.74	0.473			7.01	196.7
6.1	0.75	0.479			7.02	194.5
6.2	0.76	0.486			7.02	192.4
6.3	0.76	0.492			7.03	190.3
6.4	0.77	0.499			7.02	188.3
6.5	0.78	0.505			7.03	186.4
6.6	0.79	0.512			7.03	184.5
6.7	0.80	0.518			7.03	182.7
6.8	0.80	0.525			7.03	181.0
6.9	0.81	0.532			7.04	179.3
7	0.82	0.539			7.04	177.6
7.1	0.83	0.546			7.05	176.1
7.2	0.84	0.553			7.05	174.5
7.3	0.84	0.560			7.05	173.0
7.4	0.85	0.567			7.05	171.6
7.5	0.86	0.574			7.05	170.2
7.6	0.87	0.581			7.05	168.9
7.7	0.87	0.588			7.05	167.6
7.8	0.88	0.595			7.06	166.4
7.9	0.88	0.602			7.05	165.1
8	0.89	0.609			7.06	164.0
8.1	0.90	0.616			7.06	162.8
8.2	0.90	0.622			7.06	161.7
8.3	0.91	0.629			7.06	160.7
8.4	0.92	0.636			7.06	159.7
8.5	0.92	0.643			7.07	158.7
8.6	0.93	0.650			7.06	157.7
8.7	0.93	0.657			7.06	156.8
8.8	0.94	0.664			7.07	155.9
8.9	0.95	0.670			7.07	155.0
9	0.95	0.677			7.07	154.2
9.1	0.96	0.684			7.07	153.4
9.2	0.96	0.690			7.07	152.6
9.3	0.97	0.697			7.08	151.8
9.4	0.97	0.703			7.08	151.1
9.5	0.98	0.710			7.08	150.4

9.6	0.98	0.716			7.08	149.7
9.7	0.99	0.722			7.08	149.0
9.8	0.99	0.728			7.08	148.4
9.9	0.99	0.735			7.08	147.8
10	1.00	0.741			7.08	147.2
10.1	1.00	0.747			7.09	146.6
10.2	1.01	0.753			7.08	146.0
10.3	1.01	0.759			7.09	145.5
10.4	1.01	0.765			7.08	145.0
10.5	1.02	0.771			7.08	144.4
10.6	1.02	0.776			7.09	144.0
10.7	1.03	0.782			7.09	143.5
10.8	1.03	0.788			7.09	143.0
10.9	1.03	0.793			7.08	142.6
11	1.04	0.799			7.09	142.1
11.1	1.04	0.804			7.09	141.7
11.2	1.04	0.809			7.09	141.3
11.3	1.05	0.815			7.09	140.9
11.4	1.05	0.820			7.09	140.6
11.5	1.05	0.825			7.09	140.2
11.6	1.05	0.830			7.09	139.8
11.7	1.06	0.835			7.09	139.5
11.8	1.06	0.840			7.09	139.2
11.9	1.06	0.845			7.09	138.9
12	1.06	0.850			7.09	138.5
12.1	1.07	0.855			7.10	138.2
12.2	1.07	0.859			7.10	138.0
12.3	1.07	0.864			7.09	137.7
12.4	1.07	0.869			7.10	137.4
12.5	1.08	0.873			7.09	137.1
12.6	1.08	0.878			7.10	136.9
12.7	1.08	0.882			7.10	136.7
12.8	1.08	0.886			7.10	136.4
12.9	1.08	0.890			7.10	136.2
13	1.09	0.895			7.09	136.0
13.1	1.09	0.899			7.10	135.8
13.2	1.09	0.903			7.10	135.5
13.3	1.09	0.907			7.10	135.3
13.4	1.09	0.911			7.10	135.2
13.5	1.09	0.914			7.10	135.0
13.6	1.10	0.918			7.11	134.8
13.7	1.10	0.922			7.09	134.6
13.8	1.10	0.926			7.10	134.4
13.9	1.10	0.929			7.10	134.3
14	1.10	0.933			7.10	134.1
14.1	1.10	0.936			7.10	134.0
14.2	1.10	0.940			7.10	133.8
14.3	1.11	0.943			7.11	133.7
14.4	1.11	0.947			7.10	133.5
14.5	1.11	0.950			7.10	133.4

14.6	1.11	0.953			7.10	133.3
14.7	1.11	0.956			7.10	133.1
14.8	1.11	0.959			7.10	133.0
14.9	1.11	0.962			7.10	132.9
15	1.11	0.965			7.10	132.8
15.1	1.11	0.968			7.10	132.7
15.2	1.12	0.971			7.10	132.6
15.3	1.12	0.974			7.10	132.5
15.4	1.12	0.977			7.10	132.4
15.5	1.12	0.980			7.11	132.3
15.6	1.12	0.982			7.10	132.2
15.7	1.12	0.985			7.10	132.1
15.8	1.12	0.988			7.10	132.0
15.9	1.12	0.990			7.10	131.9
16	1.12	0.993			7.10	131.8
16.1	1.12	0.995			7.10	131.8
16.2	1.12	0.998			7.11	131.7
16.3	1.12	1.000			7.10	131.6
16.4	1.12	1.002			7.10	131.5
16.5	1.12	1.005			7.10	131.5
16.6	1.13	1.007			7.10	131.4
16.7	1.13	1.009			7.10	131.3
16.8	1.13	1.011			7.10	131.3
16.9	1.13	1.014			7.10	131.2
17	1.13	1.016			7.11	131.2
17.1	1.13	1.018			7.10	131.1
17.2	1.13	1.020			7.10	131.1
17.3	1.13	1.022			7.10	131.0
17.4	1.13	1.024			7.10	131.0
17.5	1.13	1.026			7.10	130.9
17.6	1.13	1.027			7.10	130.9
17.7	1.13	1.029			7.11	130.8
17.8	1.13	1.031			7.11	130.8
17.9	1.13	1.033			7.10	130.7
18	1.13	1.035			7.10	130.7
18.1	1.13	1.036			7.10	130.6
18.2	1.13	1.038			7.11	130.6
18.3	1.13	1.040			7.10	130.6
18.4	1.13	1.041			7.10	130.5
18.5	1.13	1.043			7.11	130.5
18.6	1.13	1.044			7.10	130.5
18.7	1.13	1.046			7.10	130.4
18.8	1.13	1.047			7.11	130.4
18.9	1.14	1.049			7.11	130.4
19	1.14	1.050			7.11	130.3
19.1	1.14	1.052			7.10	130.3
19.2	1.14	1.053			7.11	130.3
19.3	1.14	1.054			7.10	130.3
19.4	1.14	1.056			7.10	130.2
19.5	1.14	1.057			7.10	130.2

19.6	1.14	1.058			7.11	130.2
19.7	1.14	1.059			7.11	130.2
19.8	1.14	1.061			7.10	130.1
19.9	1.14	1.062			7.10	130.1
20	1.14	1.063			7.11	130.1
20.1	1.14	1.064			7.11	130.1
20.2	1.14	1.065			7.10	130.0
20.3	1.14	1.066			7.10	130.0
20.4	1.14	1.067			7.11	130.0
20.5	1.14	1.068			7.10	130.0
20.6	1.14	1.069			7.10	130.0
20.7	1.14	1.070			7.11	130.0
20.8	1.14	1.071			7.11	129.9
20.9	1.14	1.072			7.11	129.9
21	1.14	1.073			7.10	129.9
48	1.14	1.117			7.11	129.5

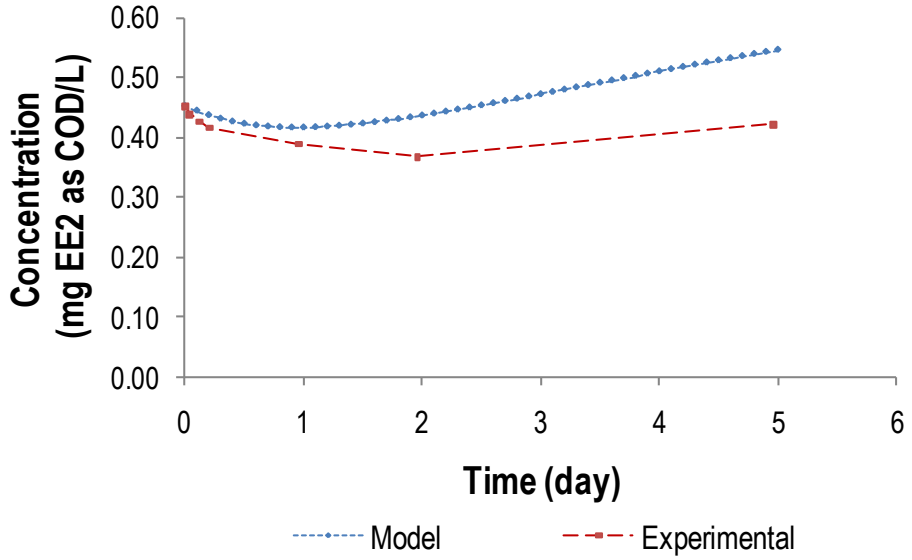

Figure II-9. Comparison of experimental data and model results describing EE2 removal from Ox^- chemostat after acetate supplementation. Data relevant to Section 4.3.8 and Figure 4-18.

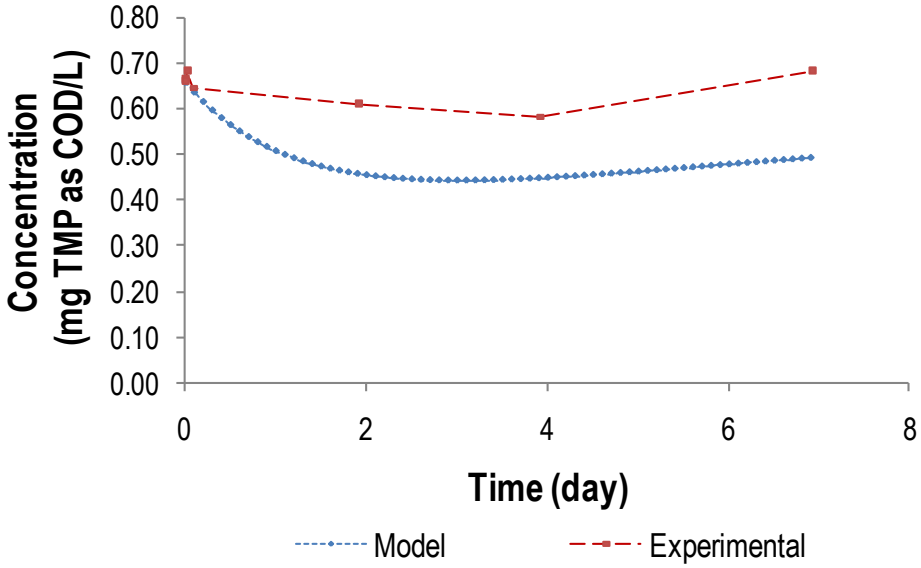

Figure II-10. Comparison of experimental data and model results describing TMP removal from Ox^- chemostat after acetate supplementation. Data relevant to Section 4.3.8 and Figure 4-19.

Table II.33. Results from simulation of EE2 fate after supplementation of acetate into Ox^- reactors. Data relevant to Section 4.3.8 and Figure 4-18.

Time (day)	Acetate (mg COD/L)	Model EE2 (mg COD/L)	Time (day)	Exp. EE2 (mg COD/L)
0	100	0.452	0.00	0.452
0.1	0.498	0.444	0.04	0.438
0.2	0.507	0.437	0.13	0.426
0.3	0.517	0.431	0.21	0.416
0.4	0.526	0.426	0.96	0.389
0.5	0.535	0.423	1.96	0.367
0.6	0.545	0.420	4.96	0.422
0.7	0.555	0.418		
0.8	0.564	0.417		
0.9	0.574	0.417		
1	0.583	0.417		
1.1	0.593	0.417		
1.2	0.602	0.418		
1.3	0.611	0.419		
1.4	0.621	0.421		
1.5	0.631	0.423		
1.6	0.640	0.425		
1.7	0.649	0.428		
1.8	0.658	0.431		
1.9	0.668	0.433		
2	0.677	0.436		
2.1	0.686	0.440		
2.2	0.695	0.443		
2.3	0.704	0.446		
2.4	0.713	0.450		
2.5	0.722	0.453		
2.6	0.732	0.457		
2.7	0.739	0.460		
2.8	0.748	0.464		
2.9	0.757	0.468		
3	0.765	0.472		
3.1	0.774	0.475		
3.2	0.782	0.479		
3.3	0.790	0.483		
3.4	0.799	0.487		
3.5	0.806	0.491		
3.6	0.814	0.494		
3.7	0.822	0.498		

3.8	0.829	0.502		
3.9	0.837	0.506		
4	0.845	0.509		
4.1	0.852	0.513		
4.2	0.859	0.517		
4.3	0.866	0.521		
4.4	0.874	0.524		
4.5	0.880	0.528		
4.6	0.887	0.531		
4.7	0.893	0.535		
4.8	0.900	0.538		
4.9	0.905	0.542		
5	0.912	0.545		

Table II.34. Results from simulation of TMP fate after supplementation of acetate into Ox^- reactors. Data relevant to Section 4.3.8 and Figure 4-19.

Time (day)	Acetate (mg COD/L)	Model TMP (mg COD/L)	Time (day)	Exp. TMP (mg COD/L)
0	100	0.657	0.00	0.666
0.1	0.498	0.635	0.01	0.659
0.2	0.507	0.615	0.03	0.683
0.3	0.517	0.596	0.09	0.645
0.4	0.526	0.579	1.92	0.610
0.5	0.535	0.564	3.92	0.581
0.6	0.545	0.550	6.92	0.683
0.7	0.555	0.537		
0.8	0.564	0.526		
0.9	0.574	0.516		
1	0.583	0.507		
1.1	0.593	0.498		
1.2	0.602	0.491		
1.3	0.611	0.484		
1.4	0.621	0.478		
1.5	0.631	0.472		
1.6	0.640	0.468		
1.7	0.649	0.463		
1.8	0.658	0.460		
1.9	0.668	0.456		
2	0.677	0.453		
2.1	0.686	0.451		
2.2	0.695	0.449		
2.3	0.704	0.447		
2.4	0.713	0.445		
2.5	0.722	0.444		
2.6	0.732	0.443		
2.7	0.739	0.443		
2.8	0.748	0.442		
2.9	0.757	0.442		
3	0.765	0.442		
3.1	0.774	0.442		
3.2	0.782	0.442		
3.3	0.790	0.442		
3.4	0.799	0.443		
3.5	0.806	0.443		
3.6	0.814	0.444		
3.7	0.822	0.445		

3.8	0.829	0.446		
3.9	0.837	0.447		
4	0.845	0.448		
4.1	0.852	0.449		
4.2	0.859	0.450		
4.3	0.866	0.451		
4.4	0.874	0.453		
4.5	0.880	0.454		
4.6	0.887	0.455		
4.7	0.893	0.457		
4.8	0.900	0.458		
4.9	0.905	0.460		
5	0.912	0.461		

II-6 – Matlab code

Matlab code for equations 4-3 to 4-6.

```
function [ds] = FirstorderEE2_simple(t,y,flag,k)

A = y(1);
E = y(2);
O = y(3);
X = y(4);
%Xi =y(8);
ds = zeros(4,1);

%Initialize constants
% Reactor hydraulics and O2 supply
Q = 0.288; %L/day
V = 2; %L
KLa = 140; %1/day from Laspidou paper

% Heterotrophic culture parameters
Yh = 0.3; % mg COD/mg COD: From GDL
fi = 0.2; % mg COD/mg COD for endogenous: From GDL assuming traditional
lysis/regrowth
bh = 0.24; % 1/day: From GDL assuming traditional lysis regrowth
umaxh = 6.25; % 1/day: From Hiatt
Ksa = 20; % mg COD/L: From Hiatt
Kso = 0.1; % mg O2/L: From Hiatt

% EE2 parameters
qmaxe = 0.00611; % L/mg COD-day for EE2
kd1 = 0.00047; %L/mg biomass-COD for EE2
%kd2 = 0.00027;

% TMP Parameters
%qmaxe = 0.001; % L/mg COD-day for EE2
%kd = 0.0046; %L/mg biomass-COD for EE2
%kf = 0.000355; (L/mg biomass-COD^
```

```
%n = 1.11; % Freundlich dimensionless constant of linearity

%Initial Concentrations
A0 = 1000; % mg acetate-COD/L
E0 = 2.71; %mg EE2-COD/L
O0 = 8; % mg O2/L
%X0 = 252; %mg biomass-COD/L
%Xi = 20.9; % mg biomass-COD/L

% Mass balance on Acetate
ds(1) = ((Q/V)*A0)-((Q/V)*A)- (umaxh/Yh)*(A/(Ksa+A))*(O/(Kso+O))*X ; %OK
% Mass balance on EE2
ds(2) = ((Q/V)*E0) -((Q/V)*E) - kd1*E*X*(Q/V) -(qmaxe*E*X);
%kd1*E*X*(Q/V);
%- kd2*E*EPS*(Q/V); %OK
%Mass balance on oxygen
ds(3) = (KLa*(O0-O))- (1-Yh)*((umaxh/Yh)*(A/(Ksa+A))*(O/(Kso+O))*X) - (1-
fi)*(bh)*(X)*(O/(Kso+O)); %OK I think
%Mass balance on heterotrophic biomass
ds(4) = ((-Q/V)*X) - (1-fi)*(bh)*(X)*(O/(Kso+O)) +
(umaxh)*(A/(Ksa+A))*(O/(Kso+O))*X ;
%Mass balance on inert debris
%ds(8) = ((-Q/V)*Xi) -(fi)*(bh)*(O/(Kso+O))*X;

%ds(1) = ((Q/V)*A0)-((Q/V)*A)- (umaxh/Yh)*(A/(Ksa+A))*X;
%ds(2) = ((Q/V)*E0)-((Q/V)*E)-(qmaxe*E*X) - kd*E*X*(Q/V);
%ds(3) = (KLa*(O0-O))-(1-((fi*bh)/(bh*(1-(Yh*(1-fi))))))*(bh*(1-(Yh*(1-
fi))))*(O/(Kso+O))*X - ((1-Yh)/Yh)*(umaxh)*(A/(Ksa+A))*(O/(Kso+O))*X;
%ds(3) = ((-Q/V)*X)+(umaxh)*(A/(Ksa+A))*X - (bh*(1-(Yh*(1-fi))))*X;
```

Matlab code to simultaneously solve equations 4-3 to 4-6.

```
function [out] = Solutionfirstorder(T,Y)

timespan = [0:0.1:48];

[T,Y] = ode45('FirstorderEE2_simple',timespan, [1000; 2.71; 8; 262]);
figure(1)
plot(T,Y(:,1),'r')
title('Acetate Profile')
xlabel('Time')
ylabel('Acetate Concentration')

figure(2)
plot(T,Y(:,2),'b')
title('EE2 Profile')
xlabel('Time')
ylabel('EE2 Concentration')

figure(4)
plot(T,Y(:,4),'o')
title('DO Profile')
xlabel('Time')
ylabel('DO concentration')
```

```
figure(4)
plot(T,Y(:,4),'+')
title('Biomass Profile')
xlabel('Time')
ylabel('Biomass Concentration')

%figure(8)
%plot(T,Y(:,8),'+')
%title('Inert Profile')
%xlabel('Time')
%ylabel('Inert Concentration')

%figure(5)
%plot(T,Y(:,5),'g')
%title('Power Profile')
%xlabel('Time')
%ylabel('Power')

out = [T,Y];

dlmwrite('Ox- 6.22 single kd.csv',[T,Y], ';')% write results to comma
delimited file
```

II-7 Reference

1. Klein, C. Degradation of 17α-ethinylestradiol in Wastewater Treatment Systems. State University of New York at Buffalo, Buffalo, 2007.

APPENDIX III

Protocols used for liquid scintillation counting were optimized as described below. Results from these optimization procedures are presented. Data in this section is most relevant to the method outlined in **Section 3.13.5**. Data acquired in subsequent experiments where radiolabeled isotopes were used are discussed in **sections 4.1, 4.2** and **4.3**.

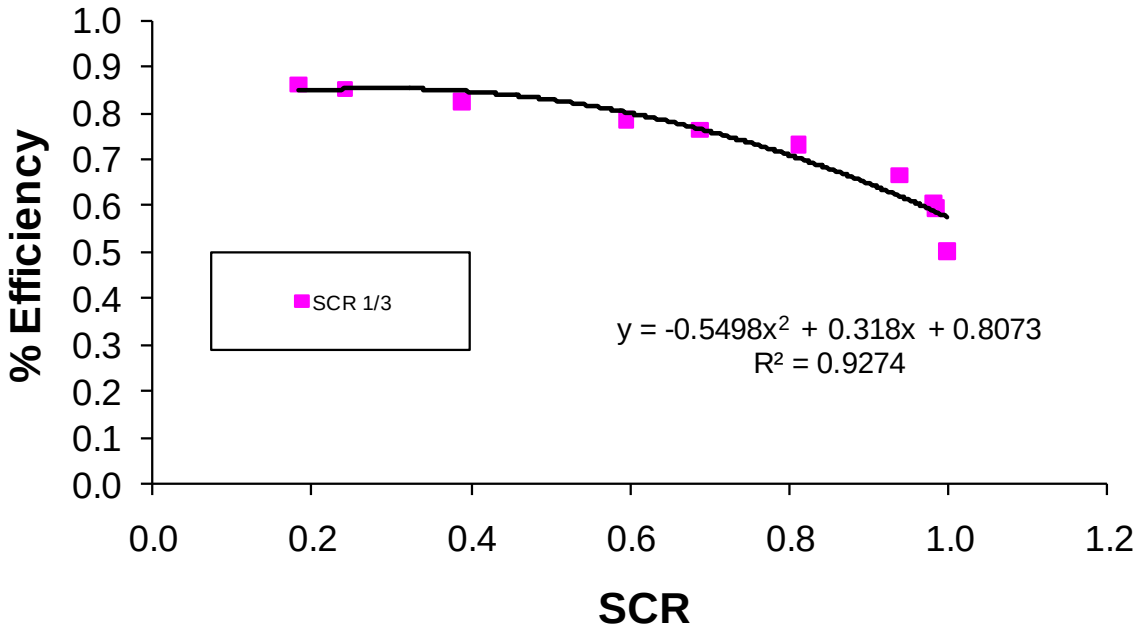

Figure III-1. Example of quench curve used to correct liquid scintillation counts. Quench curve was constructed from data in Table III.1.

Table III.1. Data obtained from liquid scintillation counts of Beckman quench set.

Std Activity	Measured Activity			% Efficiency		SCR	
	Chan 1	Chan 2	Chan 3	Chan 2	Chan 3	1/2	1/3
150000	23738	105046	129267	0.70	0.86	0.23	0.18
150000	30921	96911	127841	0.65	0.85	0.32	0.24
150000	48006	75855	123867	0.51	0.83	0.63	0.39
150000	70145	47767	117918	0.32	0.79	1.47	0.59
150000	78762	35887	114653	0.24	0.76	2.19	0.69
150000	89081	20624	109711	0.14	0.73	4.32	0.81
150000	93766	6126	99895	0.04	0.67	15.31	0.94
150000	89451	1686	91138	0.01	0.61	53.07	0.98
150000	88008	1300	89312	0.01	0.60	67.70	0.99
150000	75206	124	75334	0.00	0.50	608.12	1.00

The quenching agents in the calibration set were toluene and chloroform.

III-1 Determination of the optimum sample to scintillant ratio for use in liquid scintillation counts of radiolabeled aqueous solutions and caustic solutions.

Radiolabeled sodium bicarbonate ($NaH^{14}CO_3$) was supplemented into Nanopure™ water and mixed thoroughly to achieve a final activity of 0.25 μCi/L. Samples from this mixture were counted using various sample to scintillant (ScintiVerse I cocktail) ratios (1:1, 1:2, 1:5, 1:10) using a Beckman LS1800 liquid scintillation counter. Counts were obtained across all three channels as follows:
Channel 1 was set to measure between 0 and 400,
Channel 2 was set to measure between 150 to 670
Channel 3 was set to measure between 0 to 1000.

Sample to channel ratios (SCRs) were determined by dividing the counts per minute (cpm) obtained from the different channels, i.e. SCR 1 to 2 = Channel 1 cpm/ Channel 2 cpm. These SCRs were then used to calculate the corresponding disintegrations per minute using the quench curve (**Figure III-1**) and the following formula:

$$dpm = \frac{cpm\,(measured)}{\%E\ \ (quench\,curve)} \qquad \text{(III-1)}$$

Table III.2. Percent recovery of $NaH^{14}CO_3$ in aqueous samples

Dilution of samples	Sample:Scintillant Ratio[a]			
	1:5	**1:20**	**1:50**	**1:100**
No dilution	92	n/a	n/a	n/a
1:2	n/a	93	88	44
1:5	n/a	53	33	-147
1:10	n/a	42	-105	-444

[a]Results are average over 6 replicates.

No dilution of aqueous samples was necessary. Sufficient recovery was achieved using a 1:5 ratio of undiluted sample to scintillant. In cases where extremely high activities were present, 1:2 dilution of samples followed by 1:20 or 1:50 application of diluted sample to scintillant was also appropriate. All subsequent counts of radiolabeled aqueous solutions utilized these protocols.

III-2 Determination of the optimum sample to scintillant ratio for use in liquid scintillation counts of radiolabeled aqueous solutions and caustic solutions.

Radiolabeled sodium bicarbonate ($NaH^{14}CO_3$) was supplemented into a 5N sodium hydroxide solution and mixed thoroughly to achieve a final activity of 0.25 μCi/L. Samples from this suspension were diluted using Nanopure™ water and then combined at various sample to scintillant ratios (1:1, 1:2, 1:5, 1:10). Counting was performed using a Beckman LS1800 liquid scintillation counter as described in **Section III-1**.

Table III.3. Percent recovery of $NaH^{14}CO_3$ in caustic solutions.

Dilution of samples	Sample:Scintillant Ratio[a]			
	1:5	**1:20**	**1:50**	**1:100**
No dilution	30	89	105	87
1:2	n/a	94	115	85
1:5	n/a	100	114	87
1:10	n/a	79	85	131

[a]Results are average over 6 replicates.

These results indicated that dilution of caustic samples increased recovery of radioactivity. Sufficient recovery was achieved using a 1:5 dilution of samples followed by application of 1:20 sample to scintillant ratio. In cases where sample volumes and activities were sufficiently high, 1:2 dilutions followed by application of 1:20 or 1:50 sample to scintillant ratio was also appropriate. All subsequent counts of radiolabeled caustic solutions utilized these protocols.